SOURCE APPORTIONMENT OF SULPHATE AEROSOLS AND GASEOUS SULPHUR DIOXIDE OVER THE NW ATLANTIC DURING THE SPRING SABINA CRUISE 2003 USING STABLE SULPHUR ISOTOPES

SARAH JANE EATON

Source Apportionment of Sulphate Aerosols and Gaseous Sulphur Dioxide over the NW Atlantic during the Spring SABINA Cruise 2003 using Stable Sulphur Isotopes

By

© Sarah Jane Eaton

A thesis submitted to the
School of Graduate Studies
in partial fulfillment of the requirements for the degree of
Masters of Science

Department of Earth Science
Memorial University of Newfoundland
St. John's, Canada

September 2006

Abstract

Sulphate aerosols have the potential to alter climate, reducing the effect of increasing greenhouse gas emissions by scattering incident solar radiation back to space. Dimethylsulphide (DMS) is emitted from the surface ocean, and oxidized into methanesulphonic acid (MSA) aerosols, or gaseous sulphur dioxide (SO_2) in the atmosphere. Sulphur dioxide is further oxidized forming new sulphate aerosols. During the spring (2003) cruise of the NW Atlantic as part of the Canadian-Surface Ocean Lower Atmosphere Study (C-SOLAS), size segregated and total particulate sulphate aerosols and gaseous SO_2 samples were collected. Samples were collected diurnally using mass flow-controlled, high-volume air samplers. The cruise consisted of a Lagrangian study, following a phytoplankton bloom and a Transect study from 36°N to 54°N. Sulphur isotope abundance analyses were conducted on both the aerosol and SO_2 samples, while chemical characterisation of anions, cations, and MSA was conducted using ion chromatography.

The Lagrangian study revealed relatively constant biogenic SO_2 concentrations, with variable anthropogenic SO_2 concentrations. Biogenic sulphate concentrations ranged from 0 to 1720ngm^{-3} with the largest average concentrations in the total particulate and 0.49μm size fraction. These were not coincident with higher than average biogenic SO_2 concentrations. Anthropogenic sulphate dominated the smaller size fractions, and concentrations were generally larger than the biogenic concentrations with the exception of the 3.0-1.5μm size fraction. The isotope data indicated that the smaller size fractions

were dominated by anthropogenic emissions, likely derived from the ships emissions. Negative $\delta^{34}S_{NSS}$ values were present in the data set and are potentially linked to the combustion of Middle Eastern oil at a refinery in Newfoundland or H_2S flaring from the Sable Island gas fields.

Acknowledgements

This thesis is dedicated to my supervisor Dr. Moire Wadleigh who passed away November 2004. Her patience was astounding and her dedication to science, and me as a student was overwhelming. At times when others would have quit, Moire persevered, and I treasure the discussions we had and the time we spent together. I would have enjoyed working with her on the discussion of the results and listening to her insights regarding the source apportionment. Moire was not only a supervisor, but a friend; a friend who is missed.

I want to thank my co-supervisors Dr. Ann-Lise Norman and Dr. Robyn Jamieson and committee members Dr. Mark Wilson and Dr. Ali Aksu. Robyn and Ann-Lise both provided incredible insight and knowledge regarding aerosols, the sulphur cycle and life in general. Communicating with Ann-Lise over email, fax and phone seemed daunting, but it worked amazing well. I can honestly say that without the guidance of my co-supervisors this thesis would never have been completed. This work was improved by comments from two anonymous reviewers.

The lab work associated with characterizing the sources of sulphate aerosols is very time consuming. The assistance of Wing Tang, Tiffany Zwarich, Nenita Lozano, Jesusa Overend-Pontoy, Astrid Sanusi, Michelle Seguin and Steve Taylor from the Isotope Sciences Laboratory at the University of Calgary was instrumental and without their help

I am sure I would still be preparing samples. Alison Pye conducted the isotopic analysis at Memorial, and assisted me with ion chromatography. Her expertise was appreciated, more than she knows. Carolyn Burridge, my shipmate and office-mate was a great help with sample collection and preparing for the cruise. The captain and crew of the CCGS Hudson supplied a safe, fun and positive working environment and my gratitude is extended to them. The entire C-SOLAS research network has not only provided valuable insight, peer review and collaborations, but also friendship.

The support of fellow graduate students is paramount in the successful completion of this thesis. Kim, Michelle, Angie, Erin, Vic, Jackie and Laura provided much guidance and many good times throughout the past two years. Finally I must thank Chris, my family and friends for listening to my continual chatter about aerosols and their climatic implications.

Table of Contents

List of Tables

List of Figures

List of Acronyms

C-SOLAS -	Canadian-Surface Ocean Lower Atmosphere Study
CCN -	Cloud Condensation Nuclei
CDT -	Conductivity-Temperature-Depth Recorder
V-CDT -	Vienna-Canyon Diablo Troilite
DMS -	Dimethylsulphide
HYSPLIT -	Hybrid Single-Particle Lagrangian Integrated Trajectory
MSA -	Methanesulphonic Acid
NOAA -	National Oceanic and Atmospheric Administration
NODEM -	Northern Oceans DMS Emission Model Programme
NPRI -	National Pollutant Release Inventory
NRCC -	National Research Council of Canada
SABINA -	Study of the Air-Sea Biogeochemical Interactions in the Northwest Atlantic
SERIES -	Sub-arctic Ecosystem Response to Iron Enrichment Study
SOLAS -	Surface Ocean Lower Atmosphere Study

Chapter One: Introduction

1.1 Introduction

Scientists began pondering whether the Earth could regulate its climate through positive and negative feedback loops in the early 1970's. Lovelock and Margulis (1974) hypothesized that the Earth could regulate its climate through the interactions of the hydrosphere, atmosphere and biosphere. This hypothesis was named after the early Earth goddess, the "Gaia hypothesis". Lovelock and Margulis (1974) proposed that the Earth, through its surface environments and biota, could regulate itself and correct any imbalances, keeping the Earth at a steady state. The control of atmospheric CO_2 is one of the climate stabilization mechanisms discussed in the Gaia hypothesis (Shaw 1983).

The CLAW hypothesis was named after authors, *C*harlson, *L*ovelock, *A*ndreae, and *W*arren, and is an extension of the Gaia hypothesis. CLAW was based upon the premise that dimethylsulphide (DMS) produced in association with phytoplankton and emitted into the atmosphere is oxidized into sulphate particles which could act as cloud condensation nuclei (CCN) for marine clouds. As the number of CCN increase, the albedo of the clouds increases, thus altering the Earth's climate (Charlson *et al.* 1987). The ability of clouds to reflect incoming solar radiation is dependent on the number of CCN, and clouds with a higher albedo reflect more shortwave radiation. DMS can also be oxidized into methanesulphonic acid (MSA) which does not create new CCN but rather adds mass to pre-existing aerosols. Charlson *et al.* (1987) proposed that an increase in ocean surface temperature would

result in an increase in phytoplanktonic algal growth, zooplankton grazing, and increase in bacterial utilization of DMS. They argued that the combined effect would result in an increase in both DMS production and emission into the atmosphere. Increased DMS emissions would result in an increase in the total number of aerosols present in the atmosphere, increasing the albedo of the Earth. The initial global temperature change would therefore be thwarted by increased albedo. The CLAW hypothesis is an example of a negative feedback loop where biota reacts to counteract the initial change, and return the Earth to a steady state.

Sulphate aerosols are important climatically as they alter the Earth's albedo directly by scattering incoming solar radiation and indirectly by forming CCN and adding mass to the pre-existing CCN. Sulphate aerosols are formed through oxidation processes and can have natural sources (e.g. DMS, sea salt sulphate) and anthropogenic sources (e.g. fossil fuel combustion). DMS is an important climate change gas as it is oxidized to form sulphate particles which have the ability to alter the albedo of clouds in the marine atmosphere. Russell *et al.* (1994) and Charlson *et al.* (1987) proposed that aerosols could reflect as much incoming solar radiation as is currently causing global warming from fossil fuel combustion. A 30% increase in aerosols which act as CCN could decrease the global temperatures by 1.3°C (Malin and Kirst 1997). As aerosols have the ability to alter the climate, the importance of apportioning sources of sulphate aerosols in the remote marine atmosphere, and in particular those unaffected by human management practices, helps quantify the importance of DMS oxidation products in that region.

1.2 SOLAS

The SOLAS (Surface Ocean Lower Atmosphere Study) science programme is an international program that deals with all aspects of the ocean-atmosphere interaction. Examples of projects conducted by SOLAS members include: iron fertilization experiments in the Pacific (SERIES, SEEDS I, II and III) transect studies of the Atlantic (SABINA , Atlantic Meridional Transect), land and sea observatories, modelling, cold climate experiments and aircraft studies. All of these projects assist in the understanding and completion of the central goal of SOLAS: "to achieve quantitative understanding of the key biogeochemical physical interactions and feedbacks between the ocean and the atmosphere, and how this coupled system affects and is affected by climate and environmental change" (http://csolas.dal.ca). Canadian-SOLAS (C-SOLAS) is a part of the international SOLAS research initiative. Canadian involvement in the SOLAS program included initiating the SERIES (Sub-Arctic Enrichment Iron Enrichment Study) and SABINA (Study of the Air-Sea Biogeochemical Interactions in the Northwest Atlantic) projects.

Within C-SOLAS over 50 researchers from across Canada work to understand and quantify the central hypothesis: "marine production and emissions of climatically-active trace gases in surface oceans have a significant effect on the chemistry and physics of the overlying atmosphere and on climate" (http://csolas.dal.ca). Two main research objectives were implemented in an attempt to answer the hypothesis. The first was an artificially induced phytoplankton bloom, created by the addition of iron in the North East Pacific Ocean (SERIES). The iron fertilization experiment took

place at Station Papa in the NE Pacific in July 2001. Iron fertilization experiments in High Nutrient, Low Chlorophyll (HNLC) regions of the world's oceans have been conducted to study the effects of adding limiting nutrients on ocean biogeochemistry, and it is believed that phytoplankton blooms induced by adding soluble iron could potentially sequester atmospheric CO_2 (Boyd *et al.* 2000; Landry *et al.* 2000; Boyd *et al.* 2004). The second theme was a detailed study of the dynamics of phytoplankton blooms in the NW Atlantic, and their seasonality. This objective required three cruises (spring, summer and fall) to study the ocean - atmosphere dynamics during the different seasons. The spring SABINA cruise incorporated a Lagrangian study at the site of a declining phytoplankton bloom, along with a Transect study from 39°N to 54°N. The summer and fall SABINA cruises only conducted Transect studies. The spring SABINA cruise is the topic of this thesis and is of importance and significance as very few studies have collected atmospheric data while following a phytoplankton bloom which is experiencing a rapid decline in biomass. Wadleigh (2004) collected aerosol samples in the location of a phytoplankton bloom, but did not follow the bloom as it declined, thus the Lagrangian study is the first to follow a phytoplankton bloom in the productive North Atlantic.

The SABINA spring cruise took place from April 23, 2003 to May 16, 2003, aboard the Canadian Coast Guard Ship Hudson (CCGS Hudson). The spring cruise data are exciting as the progression of a phytoplankton bloom which experiences a rapid decline in phytoplankton biomass was recorded, and also because it involves samples collected in warm (21°C) and cold (1°C) air temperatures. The Transect study was a

temporal study of atmospheric DMS, as concentrations varied (Wadleigh *et al.* 2004) with changes in latitude and air temperature so that oxidation patterns could be investigated. The North Atlantic has been shown to be impacted by continental emissions in clean air (background) conditions (Savoie *et al.* 1989; Pszenny *et al.* 1990; Berresheim *et al.* 1991). This remained true in this study; though we attempt to define the contribution from biogenic emissions to aerosol sulphate loads using isotope techniques.

1.3 Atmospheric Sulphur

Sulphur (S) is found naturally in the hydrosphere, atmosphere, biosphere and lithosphere. Sources include volcanic emissions, sea spray, biogenic gas emissions, anthropogenic sources and Aeolian deposition (*Figure 1-1*). Sinks of sulphur consist of wet and dry deposition over the ocean (with sulphate (SO_4^{2-}) as the most prevalent form), and the continents. The atmosphere is not a sink for sulphur; sulphur passes in and out of the atmosphere, with a short residence time ranging between <1day to 2 weeks (Nguyen *et al.* 1978; Schlesinger 1997).

Sulphur can be found in varying oxidation states between -2 (sulphides) to +6 (SO_4^{2-}). Sulphate can be reduced by two biochemical pathways: assimilatory and dissimilatory reduction. Assimilatory reduction is when sulphate is reduced and synthesized into organic sulphur compounds used in the cell (e.g. amino acids).

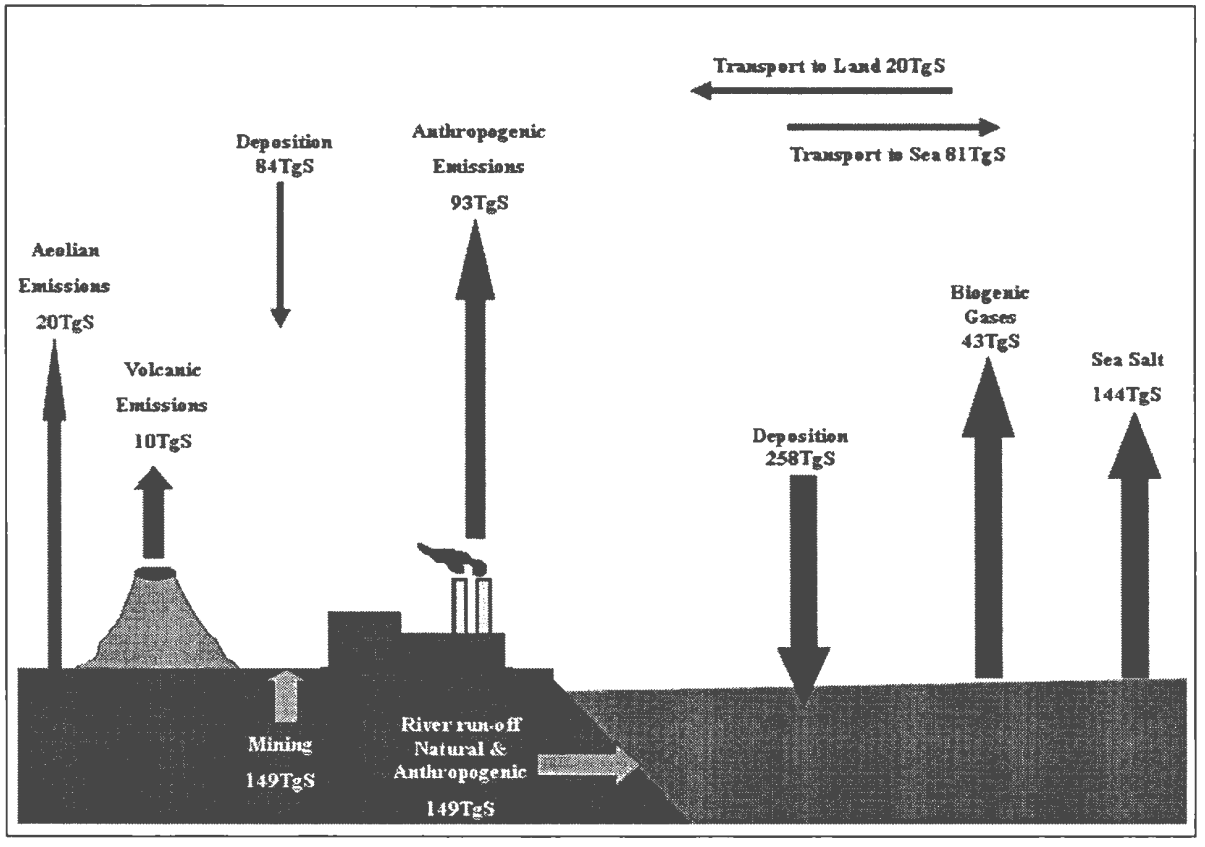

Figure 1-1 - Global sulphur cycle including anthropogenic and natural sources and sinks of sulphur (TgS = 10^{12}g of sulphur) (modified from Brimblecombe *et al.* 1989).

Sulphur is fixed within organic matter in the cell, and becomes volatile when organisms die and microbial degradation occurs. Dissimilatory sulphate reduction refers to instances when sulphate is used as an electron acceptor to support respiration when oxygen is not readily available. Some sulphate reducing bacteria are strict anaerobes, but others can function in the presence of O_2. Dissimilatory sulphate reduction occurs in sediments throughout the ocean but it is most common in shallow ocean basins near coastal regions where, because of a lack of circulation, there is a significant depletion of oxygen, but sulphate is available in excess (Jannasch 1983).

1.3.1 Sulphur Compounds

The natural sources of atmospheric sulphur consist of volcanic emissions, biogenic emissions from both terrestrial and oceanic sources, dust and sea salt. Sulphur in the atmosphere occurs in the following forms: H_2S (hydrogen sulphide), DMS, SO_2, MSA, SO_4^{2-} and COS (carbonyl sulphide). Some of these sulphur compounds (H_2S, DMS, SO_2, COS) are important climatically as they can be oxidized to produce fine sulphate aerosols which can increase backscattering and reduce the amount of incoming solar radiation. However, as discussed by Charlson et al. (1987), H_2S and COS contribute relatively small amounts of sulphur to the atmospheric sulphur reservoir relative to DMS. Wetlands, anaerobic soils, and the ocean emit H_2S, MSA, DMS and COS (Andreae 1990). These biogenic emissions are oxidized into SO_4^{2-}, and re-deposited, contributing to the natural sulphur cycle (Newman *et al.* 1991). Nriagu *et al.* (1987) estimated that the annual biogenic sulphur emissions from continental sites in Canada ranged from 0.25 to 0.1TgSyear^{-1}. Sea salt aerosols also

add sulphur to the atmosphere, as SO_4^{2-} is an important constituent of the ocean. Andreae and Jaeschke (1992) reported that approximately 90% of the sea salt sulphate emitted into the marine atmosphere is re-deposited into the ocean, with the remaining 10% deposited on the nearest 100km of land. The relative importance of each of these sulphur components to the atmospheric reservoir is described in the sections below.

1.3.1.1 Dimethylsulphide (DMS)

Dimethylsulphide (DMS, CH_3SCH_3) is the most common volatile sulphur species over the ocean (Andreae 1990, Newman *et al.* 1991), with an annual flux of approximately $8.0\pm0.5 TgSyear^{-1}$ (Bates *et al.* 1992). It is concentrated in the upper layers of the ocean, with maximum concentrations found on continental shelves and in highly productive regions (Andreae and Barnard 1984). Production occurs through enzymatic cleavage of dimethylsulphoniopropionate (DMSP), an algal component of the cell (equation 1) (Challenger and Simpson 1948).

$$(CH_3)_2SCH_2CH_2COOH \rightarrow (CH_3)_2S + CH_2CHCOOH \quad (1)$$
$$(DMSP) \rightarrow (DMS) + (Acrylic\ Acid)$$

It has been postulated that DMSP regulates osmotic pressure in phytoplankton, and isn't always converted into DMS, as it is used in the food web (Vairavamurthy et al, 1985). External events such as atmospheric exposure of tidal flats or a turbulent sea state result in an increase in DMS production, and emission (Andreae 1990). Oceanic DMS concentrations are dependent on phytoplankton species. Species with the highest DMSP concentrations are: dinoflagellates, prymnesiophytes (primarily

coccolithophores) and chrysophytes (Keller *et al.* 1989). Chlorophytes, cryptomonads, diatoms and cyanobacteria contain only small amounts of DMSP cell quota (Keller *et al.* 1989).

Dimethylsulphide is oxidized to SO_2 and MSA upon emission into the atmosphere (*Figure 1-2*), with a residence time of approximately one day (Newman *et al.* 1991). Much of the SO_4^{2-} derived from DMS oxidation is deposited back into the ocean through wet and dry deposition (Schlesinger 1997) due to the rapid oxidation of DMS and growth of fine aerosols in an environment with high humidity.

1.3.1.2 Sulphur Dioxide

Sulphur dioxide is produced naturally in the atmosphere from the oxidation of DMS and is also emitted through fossil fuel combustion (*Figure 1-2*). Sulphur dioxide is a colorless gas, with a residence time of approximately 12 hours in northern Europe (Nordlund 1983) and 32 days in the Arctic (Barrie and Hoff 1984). As a gas, SO_2 is oxidized by OH to produce sulphate aerosols, and is also dissolved in liquids on the surface of aerosols where it undergoes aqueous oxidation, increasing the sulphate content of pre-existing aerosols (De Bruyn *et al.* 1994; Russell *et al.* 1994; Andreae and Crutzen 1997). When SO_2 is dissolved in liquids on the surface of aerosols, it can be oxidized by hydrogen peroxide (H_2O_2), ozone (O_3) and molecular oxygen (O_2), in the presence of metal catalysts such as Mn^{2+} and Fe^{3+} (Wojcik and Chang 1997).

Forrest and Newman (1977) studied the oxidation times of gaseous SO_2 from a nickel smelter and found that oxidation occurred at an average rate of 1% per hour. As SO_2 is oxidized it can also be removed from the atmosphere through dry and wet deposition. It is estimated that 50% of SO_2 emitted is dry deposited, whereas the remaining 50% is oxidized into SO_4^{2-} particles (Möller 1980).

1.3.1.3 Hydrogen Sulphide

Hydrogen sulphide (H_2S) was originally thought to be the primary biogenic sulphur gas in the atmosphere over oceans (e.g.: Rasmussen 1974; Galloway and Whelpdale 1987; Aneja and Cooper 1989). It is now known that DMS is the primary biogenic sulphur gas. Hydrogen sulphide is a biogenic sulphur product, produced through dissimilatory sulphate reduction, which can be oxidized in hours in oxygenated seawater with a residence time of approximately one day in the atmosphere (Newman et al. 1991). Cutter and Krahforst (1988) reported surface water H_2S concentrations for the Atlantic Ocean, off the coast of South Carolina. Concentrations ranged between 3.8ngL^{-1} in near shore environments to 1.62ngL^{-1} in offshore waters, with maxima before sunrise. Higher concentrations (>230ngm^{-3}) were reported from wetlands and in coastal regions whereas low concentrations were found in open ocean areas (Junge 1960).

1.3.1.4 Carbonyl Sulphide

The average carbonyl sulphide (COS) concentration in the remote troposphere is approximately 127mgm^{-3}; making it the most abundant sulphur compound in the

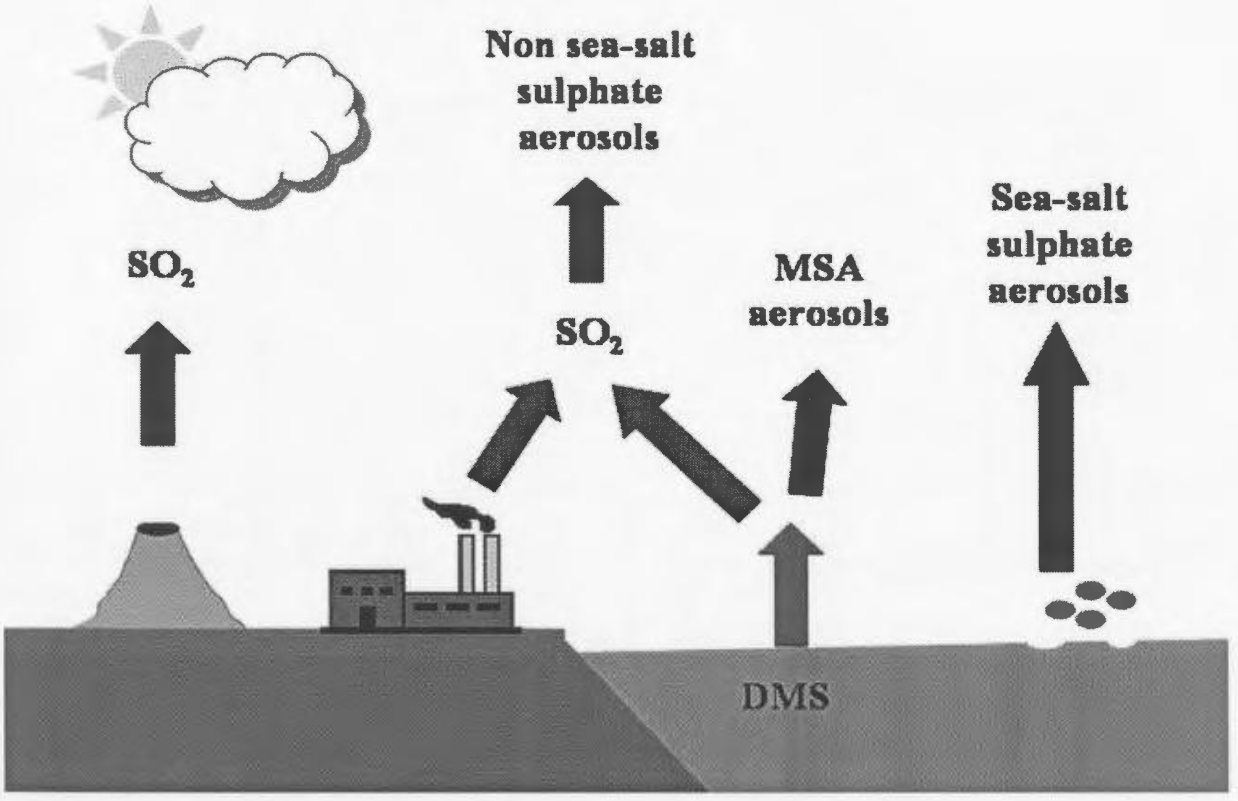

Figure 1-2 – Oxidation pathways of DMS and SO_2.

remote atmosphere (Mihalopoulos *et al.* 1992). The global emission of COS is approximately $2Tgyear^{-1}$, with a residence time of approximately 2 years (Khalil and Rasmussen 1984). Sources of COS include: wetlands, soils, volcanoes, biomass burning, anthropogenic emissions, the ocean (Khalil and Rasmussen 1984) and photo-oxidation of CS_2 by UV-B radiation (Andreae and Crutzen 1997). The largest oceanic concentrations reported are from coastal areas (Mihalopoulos *et al.* 1992), with a diurnal pattern with the maximum occurring at mid-day. Carbonly sulphide is basically un-reactive and thus can be transported into the stratosphere, ultimately being oxidized into stratospheric sulphate aerosols.

1.3.1.5 Sulphate

1.3.1.5.1 Sea Salt Sulphate

Sea salt is another important source of sulphate to the marine atmosphere. Sulphate is one of the most common constituents in ocean water and as waves break, bubbles are created, bursting at the ocean surface releasing sea salt aerosols into the atmosphere. Sea salt aerosols are composed of the main constituents of seawater, namely sodium (Na^+), chlorine (Cl^-), potassium (K^+), magnesium (Mg^{2+}), calcium (Ca^{2+}) and SO_4^{2}. Sea salt aerosols are generally large in size, ranging from 0.3 to 300μm (Katoshevski *et al.* 1999). Larger aerosols are produced when wind stress is high, and oceanic aerosols <3.0μm can have in excess of 50% sea salt. Sea salt aerosols are important over the remote marine atmosphere for increasing the number of available CCN.

1.3.1.5.2 Anthropogenic Sulphate

Anthropogenic emissions contribute 93TgSyear^{-1} to the atmosphere (Brimblecombe *et al.* 1989). This is comparable to the input of sulphate to the marine atmosphere from sea spray sulphate aerosols, but the aerosols produced from anthropogenic activity are fine and can travel greater distances than sea spray aerosols (Shaw 1983). The two largest anthropogenic sulphur sources are fossil fuel combustion and refining, and smelting of metals (Möller 1984; Wojcik and Chang 1997). Much of the sulphur added to the atmosphere is in the form of SO_2, which is oxidized to sulphate from the combustion of fossil fuels. Prospero *et al.* (1983) estimated the anthropogenic input of sulphur into the global atmospheric sulphur cycle to be approximately 35%, with 90% of the total SO_4^{2-} loading on the atmospheric sulphur cycle above North America and Europe from anthropogenic sources (Chin and Jacob 1996).

1.3.2 Sulphur and the North Atlantic

The Northern hemisphere contains large land masses, and a large percentage of the industrialized nations relying on S-bearing fossil fuels, resulting in increased anthropogenic sulphur emissions compared to the Southern hemisphere (Shinn and Lynn 1979). The Northern hemisphere receives approximately 90% of global anthropogenic inputs into the atmosphere (Houghton *et al.* 1995). In the eastern United States, the anthropogenic loading results in a net transport of 4.3TgSyear^{-1} to the ocean, and 2.0TgSyear^{-1} to eastern Canada (Galloway and Whelpdale 1980; 1987). In 2000, $2.4*10^{-3}$TgSyear^{-1} of SO_2 was emitted into the atmosphere in Canada

(Environment Canada 2004), while the USA emitted $13.9*10^{-3}TgSyear^{-1}$, (Environmental Protection Agency 2004). Of the anthropogenic emissions in the US, 50% are deposited in the region producing the emissions and, the remaining 50% are transported to Canada and the North Atlantic Ocean, due to the predominantly south-westerly wind directions (Galloway and Whelpdale 1980). Average concentrations of SO_2 are higher above the North Atlantic than the average background for the Pacific and Antarctic due in part to anthropogenic emissions from the North American continent (Mészãros 1978).

Numerous studies have been conducted in the Atlantic Ocean studying the concentrations of SO_2 and SO_4^{2-} in attempts to define the North Atlantic sulphur cycle (e.g.: Savoie *et al.* 1989; Pszenny *et al.* 1990; Berresheim *et al.* 1991; Wadleigh 2004). Sulphur concentrations are dependent on the history of the air mass sampled. Pszenny *et al.* (1990) reported SO_2 concentrations ranging between 32 to $301ngm^{-3}$ during a month long cruise in the north and south Atlantic, while previously Berresheim (1987) found SO_2 concentrations ranging from 5.4 to $22.4ngm^{-3}$.

Total SO_4^{2-} was often reported in earlier studies and later with advances in scientific understanding and technical abilities, non sea-salt sulphate ($NSS\text{-}SO_4^{2-}$) was also reported, which does not include sea spray sulphate ($SS\text{-}SO_4^{2-}$). Gravenhorst (1977) first reported total SO_4^{2-} concentrations for the Atlantic Ocean atmosphere following a summer long shipboard sampling program in 1977 and found a concentration of $1200ngm^{-3}$ in background conditions. Patris *et al.* (2000) reported an average total

SO_4^{2-} concentration of 375ngm^{-3} from shipboard measurements of the north and south Atlantic in October and November 1996. McGovern *et al.* (1999) looked at total SO_4^{2-} at the Canary Islands at a remote sampling station and found concentrations were less than 1000ngm^{-3} in clean, background conditions, but during pollution periods the concentrations increased to 3200 to 5500ngm^{-3}. NSS-SO_4^{2-} concentrations vary depending on the location of the sample, and whether the aerosols were collected in background or pollution periods. Savoie *et al.* (1989) reported a mean NSS-SO_4^{2-} concentration of 751 (SD = 602ngm^{-3}) from 1984 to 1987 from a sampling site in Bermuda, while Pszenny *et al.* (1990) found a range between 33.6 to 1152ngm^{-3} from shipboard measurements, which included both marine and continental air masses. Berresheim *et al.* (1991) studied NSS-SO_4^{2-} in both continental and marine air masses on a cruise of the NW Atlantic between September 1985 and 1986 and found a continental average of 201.6 (SD = 69.9ngm^{-3}) and a marine average of 48.9 (SD = 28.1ngm^{-3}). Wadleigh (2004) reported an average NSS-SO_4^{2-} concentration of 416ngm^{-3} from a 3 week cruise of the North Atlantic in spring, 1998; sampling both marine and continental air masses. The wide range of SO_2 and total-SO_4^{2-} concentrations indicate that the source of the sulphur cannot be completely determined from the concentrations, but generally higher concentrations were found in polluted air masses, and lower concentrations in background concentrations.

1.4 Aerosols

1.4.1 Aerosols and Climate

Aerosols cool the Earth both directly and indirectly (*Figure 1-3*). Aerosols directly absorb sunlight, which prevents a portion of solar radiation from reaching the Earth surface. Direct radiation scattering by aerosols also affects albedo by changing the angle of the incoming solar radiation, scattering some of the incoming solar radiation back to space. Indirect cooling of the Earth occurs due to increased cloud cover. The indirect effect results from the impact aerosols have on cloud formation, precipitation events and changes in cloud properties. Aerosols can act as CCN, or add mass to pre-existing CCN, which are integral parts of cloud formation. As more fine aerosols are created, more clouds are created, and the concentration of CCN increases, increasing the albedo of the Earth. Aerosols between 0.08 and 1.0μm are important to climate forcing as they scatter radiation most efficiently, and remain in the atmosphere for the longest time (Shaw 1983; Murphy *et al.* 1998).

1.4.2 Aerosol Classification and Formation

Aerosols can be classified as "primary" particles, which are emitted directly to the atmosphere; or "secondary" particles, which form as a result of chemical and physical reactions in the atmosphere. They are also classified by size, composition, production type and source. Aerosols can be classed according to their type of origin: point sources, widespread surface sources, area sources, and spatial sources. Examples of point sources are volcanoes and power plants, whereas dry lakebeds and the ocean are examples of widespread sources. Area sources such as localized industry affect both

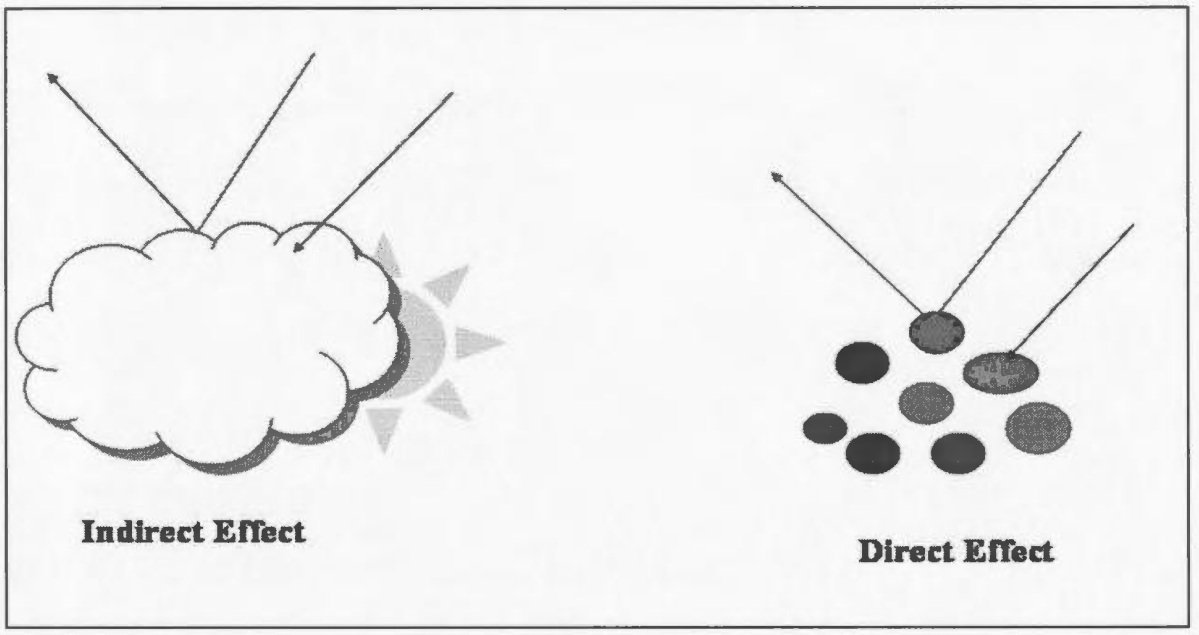

Figure 1-3 – Illustrations of both the direct and indirect effect of aerosol sulphate on incoming radiation.

regional and local scales. Spatial sources are gas to particle conversion and cloud processes.

Three modes of particles are identified in the lower atmosphere: transient or Aitken nuclei (<0.1μm diameter), accumulation (>0.1 to <2.0μm diameter) and coarse (>2.0μm diameter). Aiken nuclei aerosols coagulate and coalescence to become accumulation mode aerosols, and are generally composed of sulphates, nitrates, ammonium, lead, bromine, carbon and organic matter (National Research Council of Canada (NRCC) 1982; Prospero *et al.* 1983). Both Aitken nuclei and accumulation mode aerosols are classified as "fine" particles. Fine aerosols are less than 2μm in diameter and are commonly formed from condensation of precursor gases. Coarse aerosols are >2μm in diameter and are generally produced by mechanical processes such as bubbles bursting at the ocean surface, or soil dust entrainment. Coarse aerosols are not buoyant in the atmosphere due to their weight, except with high wind speeds, and they lack long atmospheric lifetimes (~1 day) (Kaufman *et al.* 2002).

Gases are exchanged from the ocean into the atmosphere, and the amount of gas exchange from the ocean is dependent on wind speed. Increased gas exchange results from stronger winds and large waves. As the waves break, bubbles are produced in the surface waters and as the bubbles rise to the surface they burst. Turbulent diffusion transports sea salt particles and DMS from the ocean into the atmosphere. As the aerosols are transported upwards into the atmosphere, the heavier aerosols are removed by gravitational fallout (Petelski 2003). Once an aerosol is entrained in the

atmosphere it undergoes Brownian diffusion and coagulation (Prospero *et al.* 1983). Coalescence can give rise to larger particles. As the particles fall due to gravitational forces, or when particles collide, they combine to create larger particles (Andreae *et al.* 1986).

Three gas-to-particle conversion processes have been identified: homogenous homomolecular nucleation; homogenous heteromolecular nucleation; and heterogenous heteromolecular nucleation. The formation of new liquid or solid particles from the gas phase is known as homogeneous, homomolecular nucleation (Prospero *et al.* 1983), and is the production of a stable particle from a single gaseous species. Homogenous heteromolecular (two or more species) nucleation is the growth of particles by molecule deposition from the gas phase, with water as one of the gaseous molecules (Andreae and Crutzen 1997). High super-saturation levels are required for homogenous nucleation to occur. Heterogenous, heteromolecular condensation is the growth of pre-existing particles by deposition of molecules from the gaseous phase (Andreae and Crutzen 1997). Sulphur dioxide oxidation to H_2SO_4 can result from heteromolecular condensation, and is a method of MSA production. Ozone and OH are important in gas to particle conversion, and as they are products of photochemistry, gas to particle conversions can show a diurnal pattern (Prospero *et al.* 1983). Sulphur dioxide can react with either OH or O_3 (and water) to produce H_2SO_4 aerosols. Aerosols formed by gas to particle conversion tend to be more volatile than sea salt aerosols (Fitzgerald 1991).

1.4.3 Aerosol Lifetime and Removal

Aerosol residence time is dependent on size. Aerosols larger than 1μm are believed to be removed by dry deposition, while fine aerosols are removed by scavenging processes, such as precipitation (Bonsang *et al.* 1980). Aerosols remain in clouds until a precipitation event, and if the cloud does not yield precipitation, aerosols can pass in and out of different clouds before being deposited (Prospero *et al.* 1983) (*Figure 1-4*). In the absence of precipitation, fine aerosols can be transported over 1000km by diffusion and advection. Coarse aerosols (>2μm) can be transported over 100km in circumstances, as is the case in volcanic eruptions, but generally their large size does not allow an atmospheric residence time of greater than a day and they are generally removed by sedimentation (Bonsang *et al.* 1980). Aerosols with diameters between 0.1μm and 2μm have a residence time of approximately one week in the troposphere (Prospero *et al.* 1983).

1.4.4 Aerosol Composition

1.4.4.1 Natural Aerosols

Aerosol composition is primarily determined by the source of the aerosol. Natural aerosols include sea spray, dust, volcanic ejecta, biogenic materials, biomass burning products, and natural gas to particle conversions. Airborne soil can form aerosols when winds carry soil particles aloft: 90% are larger than 1.0μm. Dry lake beds in the Saharan desert are the source of large amounts of sediment (Kaufman *et al.* 2002), and it is unknown how much is transported over the Atlantic Ocean and the continents. Deserts often contain large gypsum ($CaSO_4 \cdot 2H_2O$) deposits, and the

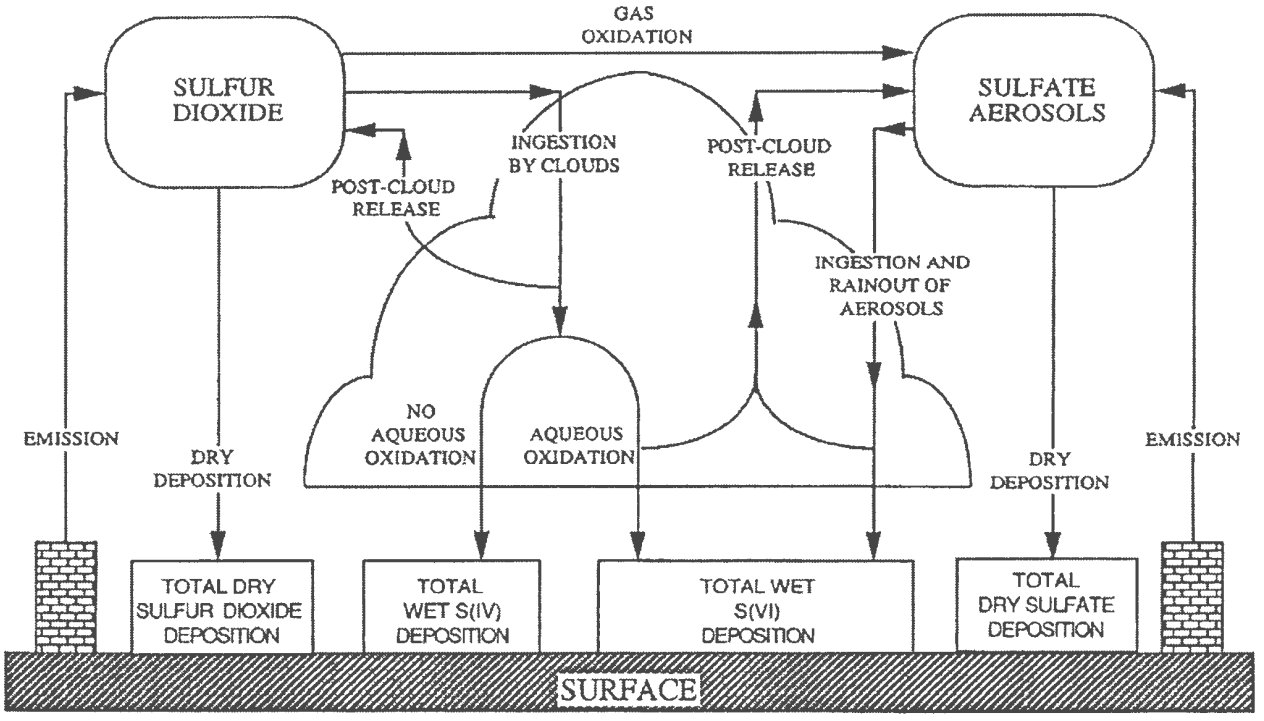

Figure 1-4 – Removal mechanisms and pathways of atmospheric SO_2 and SO_4^{2-} aerosols, with oxidation states in parenthesis (Wojcik and Chang 1997).

gypsum is carried by wind action into the atmosphere and deposited by dry and wet deposition.

Biomass burning produces aerosols composed of carbon, minerals and sometimes benzene (NRCC 1982). Eighty percent of the aerosols produced from biomass burning are smaller than 1.0μm (NRCC 1982). Sea salt aerosols are generally larger than 1.0μm, and are composed of ocean water constituents. Volcanic emissions are another natural source of aerosols to the atmosphere, and the aerosols created range from 0.01μm to >60μm. The chemical composition of the volcanic aerosol is wide ranging and dependent on the volcano's composition. When volcanic ejecta are released into the atmosphere, the finer aerosols produced from SO_2 oxidation can persist for weeks.

1.4.4.2 Anthropogenic Aerosols

Anthropogenic aerosols account for 10% of the global mass of aerosols (Kahn 2003), and include soot, road dust, smoke, and conversion products from anthropogenic gases. Aerosols can be directly emitted into the atmosphere, as is the case with dust from unpaved roads, wind erosion from storage piles, and particulate matter from smoke stacks, but many of the anthropogenic aerosols are created by gas phase reactions with SO_2 and NO_3.

Urban haze is an example of the effect of anthropogenic aerosols, and is the result of fine hygroscopic aerosols downwind of populated regions, or heavily industrialized

areas. Polluted areas have more particles than non-polluted areas, and the high concentration of particles can increase cloud reflectance by 25% and reduce the size of the cloud droplets by 20-30% (Kaufman *et al.* 2002). Clouds with smaller droplets are less efficient at producing precipitation, thus the greater numbers of aerosols may ultimately affect the precipitation pattern in a given area (Kaufman *et al.* 2002).

1.4.5 Sulphate Aerosol Formation

Sulphate is formed from the oxidation of DMS, SO_2 and H_2S (to a lesser extent). *Figure 1-5* highlights the DMS oxidation pathways including oxidizing species. Upon emission into the atmosphere DMS is oxidized by both OH and NO_3, to produce MSA, H_2SO_4 aerosols and SO_2. Andreae (1990) reported that the OH pathway is predominant, but in moderate to highly polluted atmospheres, the concentration of NO_x and O_3 are adequate to produce NO_3 at night, which allows NO_3 to be an important oxidant of DMS in polluted atmospheres over the NW Atlantic. Dimethylsulphide is oxidized by OH during daylight hours, and DMS concentrations are believed to decrease as OH concentrations increase, resulting in a DMS minimum in late afternoon. As the OH concentrations fall during the night, DMS exhibits a maximum concentration in the early morning. Sulphur Dioxide has the inverse relationship, showing increases with increasing OH concentrations and vice versa. De Bruyn *et al.* (2002) reported a diurnal cycle of DMS and SO_2 when clean air masses were sampled. Polluted air masses alter this diurnal cycle with the presence of NO_3 which acts as an oxidant at night.

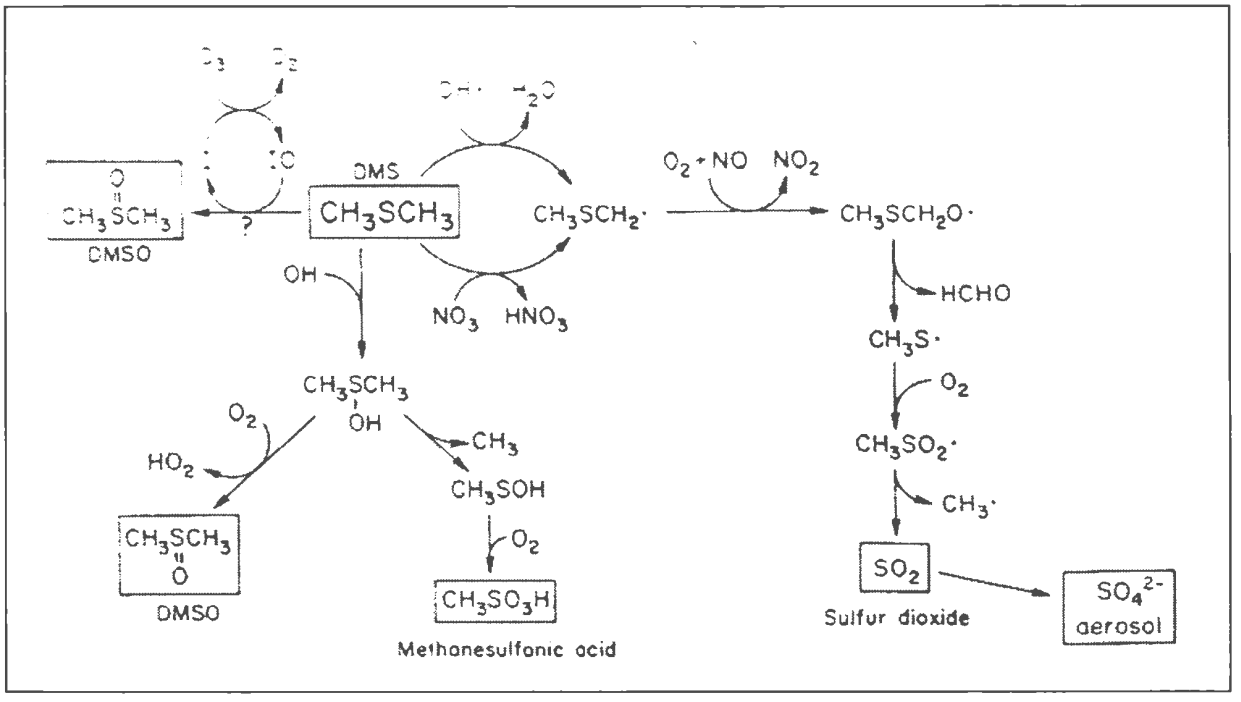

Figure 1-5 – DMS oxidation pathways (Andreae 1990).

Methanesulphonic acid (MSA, CH_3SO_3H) is the end product of OH addition reaction, while SO_2 is possibly the result of H abstraction reactions (Berresheim *et al.* 1990). Addition reactions are the addition of OH to the sulphur atom, while abstraction reactions are the result of the subtraction of an H atom (Fitzgerald 1991). Below 12°C, the addition pathway dominates, while above 12°C, the abstraction pathway is dominant (Berresheim *et al.*1990). This may indicate that below 12°C MSA may be the dominant oxidation product, and above 12°C SO_2 would be the dominant oxidation product of DMS. Nitrate and HNO_3 are important in the formation of SO_2, as they are used as oxidants of DMS. Dimethylsulphide reacts with HNO_3 and/or NO_3 to produce $CH_3SCH_2^{\cdot}$, which is further oxidized by NO_2 to eventually produce SO_2, and can be further oxidized into SO_4^{2-} aerosols. Oxidation of DMS can also occur by iodine oxide (IO) to produce DMSO, but this is not believed to be of great importance, as the reaction rate is believed to be slow and IO concentrations are low (O'Dowd *et al.* 2002).

When atmospheric SO_2 is in the aqueous phase it has an oxidation state of IV, which can be oxidized into sulphur (VI) by H_2O_2, O_3 and O_2 in the presence of metal catalysts, and as it is incorporated by the cloud it can be removed by precipitation in oxidation states of IV and VI (Wojcik and Chang 1997). *Figure1-6* illustrates the pathways that SO_2, DMS, MSA and sulphate aerosols encounter once entrained into the atmosphere.

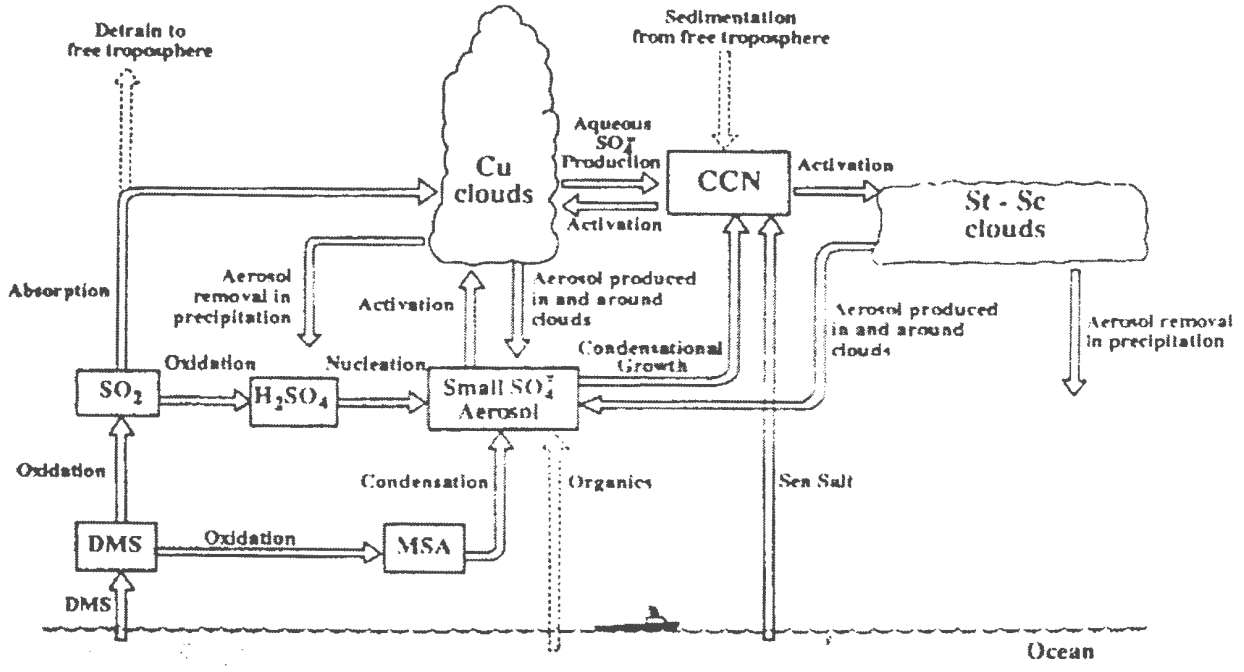

Figure 1-6 – Sources and sinks of marine sulphate aerosols (Hobbs 1993). Note: Cu – cumulus, St – stratus and Sc – stratocumulus.

1.5 Sulphur Isotopes

Stable isotopes of an element are atoms with different numbers of neutrons in their nuclei, which do not undergo radioactive decay. Sulphur has four stable isotopes, $^{32, 33, 34, 36}S$ with abundances of 95%, 0.77%, 4.2% and 0.017% respectively. ^{32}S and ^{34}S are more abundant and thus studied more often. Vienna-Canyon Diablo Troilite (V-CDT) is the standard used to compare ^{34}S to ^{32}S abundance ratios. V-CDT is a synthetic standard formulated to imitate the isotopic composition of troilite (FeS) in the Canyon Diablo meteorite. The standard, V-CDT is assigned a value of 0‰, and deviations from the ratio of the number of atoms of ^{34}S to that of ^{32}S of V-CDT are expressed using the per mil (‰) notation (equation 2).

$$\delta^{34}S = \left[\frac{\left({}^{34}S / {}^{32}S \right)sample}{\left({}^{34}S / {}^{32}S \right)std} - 1 \right] \times 1000 \qquad (2)$$

1.5.1 Natural Isotopic Abundances

Sulphur isotope abundance ratios are important tools, as sources can have specific isotope compositions, and many natural processes are isotopically selective. The average $\delta^{34}S$ isotopic value of seawater is presently +21‰, with sea spray having the same isotopic composition (Rees 1978).

Dimethylsulphide ranges isotopically between +15 and +21‰ due to fractionation, with an average of +18‰ (Calhoun *et al.* 1991). The $\delta^{34}S$ value of MSA has recently been determined to be ~+18‰ (Sanusi *et al.* 2006). Desert dust composed of sulphate has an isotopic range of -35 to +13‰; depending on the plant types from which the dust was formed (*Figure 1-7*) (Schlesinger and Peterjohn 1988). Maritime

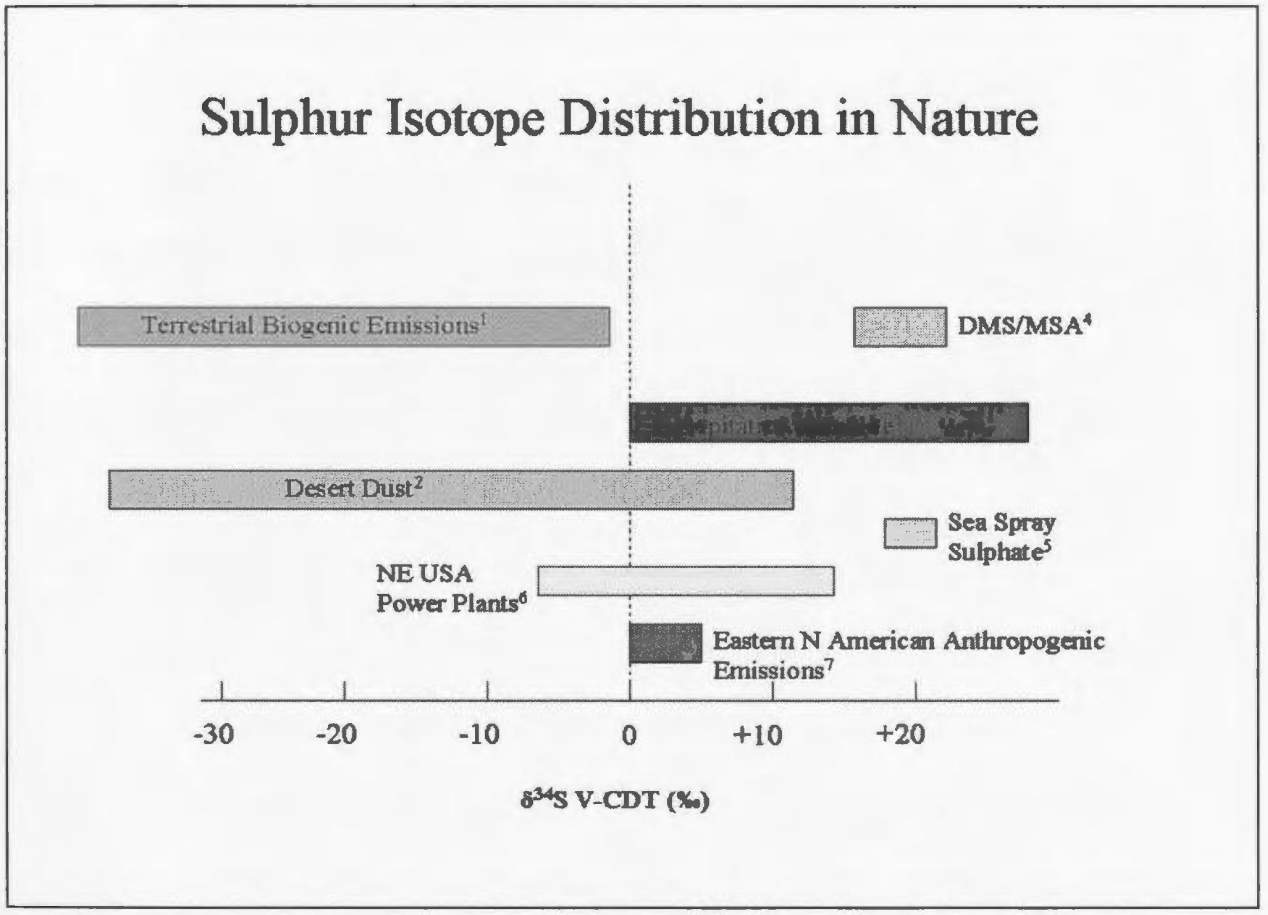

Figure 1-7 – Sulphur isotopic distribution (‰) found naturally on Earth (Rees 1978[(5)]; Schlesinger and Peterjohn 1988[(1, 2)]; Caron *et al.* 1986[(3)], Newman *et al.* 1991[(1, 3)], Krouse *et al.* 1991[(1, 3, 6, 7)]; Calhoun *et al.* 1991[(4)]; Jamieson and Wadleigh 1996[(3)]; Wadleigh 2004[(7)]; Sanusi *et al.* 2006[(4)]).

Saharan dust aerosols have an isotopic composition of +13‰, though no sea salt correction was applied (Gravenhorst 1977). Middle Eastern crude oil ranges isotopically between -3 and -10‰ (Thode and Monster 1970). Precipitation sulphate can range between +18‰ and -2‰, but the isotopic composition is dependent on the localization of the system (Wadleigh *et al.* 1996).

1.5.2 Sulphur Isotope Fractionation

The stable isotopic composition of elements in a compound may preserve a record of the environmental conditions under which the compound was formed. Isotope fractionation is the alteration of isotopic composition during a chemical, physical or biogenic transformation. Fractionation of isotopes is caused by isotope exchange reactions and mass dependent chemical, biological and physical reactions. Fractionation (α) between two substances or phases, A and B are defined (equation 3), where R is the ratio of the heavy to light isotope abundances.

$$\alpha_{AB} = R_A / R_B \qquad (3)$$

Chemical and biological reactions produce the most significant fractionations on Earth. The extent of fractionation is dependent on the differences between the masses of the isotopes; the temperatures at which the compound was formed; and the types of chemical bonds that exist within the compound. Fractionation is also dependent on the process from which the compound is formed. Two important types of isotope fractionation can occur: kinetic isotope effects and isotope exchange. Isotope

exchange can occur among molecules or phases of one compound. Isotopic equilibrium may be attained in which case an equilibrium constant can be defined. Kinetic fractionation occurs in unidirectional reactions and the term "kinetic isotope effect" refers to the ratio of isotopic rate constants at one step in a reaction. Environmental conditions regulate kinetic fractionation (Krouse and McCready 1974). An example of kinetic fractionation is dissimilatory bacterial sulphate reduction. The fractionation involved in this reaction results in total product S^{2-} ranging from very negative to zero with respect to the initial SO_4^{2-}, and α can exceed 1.05 (Krouse and McCready 1974).

Dimethylsulphide is produced by assimilatory sulphate reduction, with minimal fractionation (+1 to +4‰) (Kaplan and Rittenberg 1964; Chambers and Trudinger 1979). As DMS is emitted into the atmosphere and oxidized into SO_2 and MSA, only small isotope fractionations are expected. Calhoun and Bates (1989) estimate a fractionation between -4 and 0‰, for oxidation of DMS to SO_4^{2-}, with the range due to the two different ways SO_4^{2-} can be formed. When SO_4^{2-} is formed from gaseous oxidation, it is believed to be isotopically lighter than SO_2, but when SO_4^{2-} is formed from aqueous oxidation the resulting SO_4^{2-} is isotopically heavier (Saltzman *et al.* 1983). No isotopic fractionation is associated with the production of sea spray particles, thus they have an isotopic composition of ~+21‰ (Rees 1978).

1.5.3 Source Apportionment of Sulphate Aerosols

There are many assumptions involved when determining sources of sulphur from isotope composition measurements. These are present in the calculation of NSS-SO_4^{2-}, SS-SO_4^{2-}, $\delta^{34}S_{NSS}$ (*Appendix I.1*), anthropogenic and biogenic concentrations. Percent sea salt is calculated (equation 4) using Mg^{2+} as the conservative sea salt tracer, where 2.10 is the average mass ratio of SO_4/Mg in ocean water, and SO_4/Mg_{sample} refers to the ratio of the concentrations of SO_4^{2-} and Mg^{2+} in the sample as determined by ion chromatography.

$$\% \text{ Sea Salt Sulphate} = 2.10 / (SO_4 / Mg)_{sample} \times 100 \quad (4)$$

The sea salt correction assumes that the ratio of bulk seawater is the same in sea spray, and that the SO_4/Mg ratio is relatively constant throughout world oceans (Keene *et al.* 1986). Equation 4 also assumes that all Mg^{2+} is from sea salt contributions, which is not necessarily correct, as Mg^{2+} has been shown to have Saharan dust origin (Galloway and Whelpdale 1987; Savoie *et al.* 1989). The sea salt correction presumes that there is no fractionation of the SO_4^{2-} to Mg^{+} ratio as sea spray is injected into the atmosphere and assimilated into aerosols. This is not unreasonable given that the mechanical transport of sea salt to the atmosphere through sea spray is a macroscopic process which is very unlikely to be altered by chemical fractionation. Previously (e.g. Wadleigh *et al.* 1996) Cl^- was used as the conservative tracer, but it was found to be volatile in the marine atmosphere as HCl, which invalidates the assumptions previously discussed. Sodium can also be used as a tracer, but for this study, resulted in a large number of samples having a % sea salt

greater than 100%. When Mg^{2+} resulted in erroneous (>100% or <0%) values, Na^{+} was used (n=13). In instances where Na^{+} was used in place of sea spray Mg^{2+}, a distinguishing note is added to identify the sample. If percent sea salt values were >90%, the resulting $\delta^{34}S_{NSS}$, NSS-SO_4^{2-} and SS-SO_4^{2-} concentrations were associated with a very large uncertainty (>±5‰) and thus were omitted. The calculation of $\delta^{34}S_{NSS}$, concentrations of NSS-SO_4^{2-}, SS-SO_4^{2-}, fractions of non sea salt, and sea salt are dependent on equation 4, and thus involve the same assumptions.

The biogenic fraction was calculated by mass balance as illustrated by equation 5 (*Appendix I.2*). Using equation 5 involves assumptions about the $\delta^{34}S$ values of sea salt, anthropogenic sulphate and biogenic sulphate. $\delta^{34}S_{anthropogenic}$ (δ_a) is set at +3‰ (Wadleigh 2004), which is believed to be the average value for Eastern North American emissions (e.g. Norman *et al.* 1999, Wadleigh 2004). $\delta^{34}S_{sea\ salt}$ (δ_{ss}) is constant at +21‰, while $\delta^{34}S_{biogenic}$ (δ_b) is +15 to 19‰ (Calhoun *et al.* 1991). The fraction of sea salt, $f_{sea\ salt}$, is determined from equation 4, and f_{total} is 1. Assumptions involved in the determination of the biogenic fraction are associated with constancy of the $\delta^{34}S$ values for sea salt, anthropogenic and biogenic fractions. Sea spray $\delta^{34}S$ is very constant throughout the globe (Rees 1978). δ_a assumes that anthropogenic sulphur is from Eastern North America and that the average $\delta^{34}S$ value of +3‰ is appropriate for background air over the North Atlantic. To calculate the propagated error of f_b the errors associated with each variable in equation 5 must be known. The errors are then added or subtracted through mathematical equations as outlined in common Chemistry lab manuals. The propagated uncertainty for f_b and subsequently

the biogenic and anthropogenic concentrations of sulphate are presented in figure captions throughout Chapter 5.

$$f_b = \frac{(\delta_t f_t - \delta_{ss} f_{ss} - \delta_a f_t + \delta_a f_{ss})}{(\delta_b - \delta_a)} \quad (5)$$

1.6 Previous Studies

Aerosols are interesting to study because of their climatic implications and the ability to determine sources using chemical and isotopic properties. Before isotopic analysis became prevalent within the atmospheric community, researchers analysed concentrations of sulphur and other ions that impacted on filter paper using flow-through technologies. The first aerosol studies using isotopes of sulphur began in the 1970's (Gravenhorst 1977). Large scale studies, similar to this project have been completed in the Atlantic, Pacific, Arctic and Southern Oceans and recent scientific advances have allowed the determination of the isotopic composition of DMS, SS-SO_4^{2-}, NSS-SO_4^{2-}, and most recently MSA (e.g.: Saltzman *et al.* 1983; Prospero *et al.* 1983; Savoie and Prospero 1989; Nriagu *et al.* 1991; Berresheim *et al.* 1991; Patris *et al.* 2000; Wadleigh 2004; Sanusi *et al.* 2005).

1.6.1 Precipitation Sulphate

Precipitation studies of sulphate can be used in association with aerosol studies, as both collect atmospheric components. Precipitation sulphate shows a wide range of $\delta^{34}S$ values (0 to +20‰) (*Figure 1-7*), but most North American precipitation samples fall between +1 and +30‰ (e.g.: Caron *et al.* 1986; Wadleigh *et al.* 1996; Nriagu *et al.* 1991, Newman *et al.* 1991, Krouse *et al.* 1991). Precipitation and

aerosol samples collected from Eastern North American anthropogenic emissions (excluding NE USA power plants) range between 0 to +14‰, averaging ~+3‰ (Saltzman *et al.* 1983; Caron *et al.* 1986; Barrie *et al.* 1992; Nriagu *et al.* 1991; Jamieson and Wadleigh 1999; Wadleigh 2004). Northeastern USA power plants range between -5 to 14‰ (Newman *et al.* 1991). Nriagu *et al.* (1987) studied the isotopic values of rain in weekly bulk precipitation samples for a four year period in the Great Lakes region and found a seasonal variation, with winter values ranging between +4.5 to +5.3‰, and summer values ranging from +1.9 to +3.4‰ (but lacking statistically significance; t-test p=0.11). Lower summer values were attributed to increased biogenic emissions from continental wetlands. Further east, Wadleigh *et al.* (1996) found heavier (+13.6‰) isotopic ratios in the winter months compared to the summer values (+4.9‰) from a sampling site in Nova Scotia with both continental and marine influences. Jamieson and Wadleigh (1999) collected precipitation samples from two coastal sites in Newfoundland. The coastal sites ranged isotopically between +6.8‰ and +10.0‰. For both of the sites the $\delta^{34}S_{NSS}$ values were essentially the same (+4.1‰ and +4.3‰), indicating local and long range anthropogenic sulphur contributions (Jamieson and Wadleigh 1999).

1.6.2 Apportionment of Sulphate Aerosols over the NW Atlantic

Savoie *et al.* (1989) collected over 1100 bulk aerosol samples from 1984 to 1987 at Barbados. They found that the NSS-SO_4^{2-} concentration had a mean of 751, SD = 602ngm^{-3}, while the MSA mean was 20.7, SD = 9.3ngm^{-3} and NO_3^- mean was 509, SD = 389ngm^{-3}. Non sea salt -SO_4^{2-} and NO_3^- average concentrations were higher

than previously reported for remote marine locations (Prospero *et al.* 1983) and a seasonal relationship was found between NO_3^- and NSS-SO_4^{2-} for the winter and summer. The winter correlation between NO_3^- and NSS-SO_4^{2-} was more dramatic which may be due to an increase in NO_3^- from continental sources. Savoie *et al.* (1989) determined that 40% of the NSS-SO_4^{2-} was not related to African dust events, and could potentially be from biogenic sulphur.

Pszenny *et al.* (1990) reported SO_2, MSA, NH_4^+, NO_3^- and NSS-SO_4^{2-} concentrations in aerosol samples from shipboard sampling of the North Atlantic in the summer of 1989. Due to the effects of continental sulphur, higher concentrations of MSA and biogenic NSS-SO_4^{2-} were only found at higher latitudes when continental influence was less.

Berresheim *et al.* (1991) studied gaseous SO_2, DMS, and the chemical composition of aerosols collected during 4 cruises between September 1985 and September 1986 in the NW Atlantic. Cruise II was conducted during the spring, between 70°W and the east coast of North America, collecting aerosols <1.5μm and >2.0μm. Samples collected in continental air masses had 97% of the sulphur from these continental sources. Continental air masses had concentrations of NSS-SO_4^{2-} with a mean of 2456.8±730ngm^{-3}, compared to marine air masses (mean = 595±342.5ngm$^{-3)}$. Sulphur dioxide, NO_3^- and NH_4^+ concentrations all showed the same trend, with increased concentrations in continental air masses while MSA had the inverse trend. Nitrate concentrations were 4-5 times higher than Savoie and Prospero (1989) had

previously reported for the Pacific, indicating that the NW Atlantic had higher background concentrations due to anthropogenic loading of the atmosphere. Sulphur dioxide concentrations were at a minimum during the spring cruise, due to the decrease in fossil fuel combustion after the winter months. The fine aerosols in continental air masses had higher concentrations of MSA and NO_3^-, which the authors attribute to higher scavenging rates of gaseous MSA and HNO_3 in the marine air mass. Sampling occurred on a diurnal basis, but no statistical significance was found between day and night sampling. Berresheim *et al.* (1991) concluded that the atmosphere above the western North Atlantic Ocean was continually impacted by North American continental pollution.

1.6.3 MSA/NSS-SO_4 Ratios

Molar MSA/NSS-SO_4^{2-} ratios are used to determine the relative contributions of DMS-SO_4^{2-} to NSS-SO_4^{2-} in the remote marine atmosphere. Methanesulphonic acid has only marine sources, whereas NSS-SO_4^{2-} can be natural or anthropogenic in origin. The physical and chemical properties of MSA and NSS-SO_4^{2-} are similar and it is thought that they could be removed from the atmosphere in similar ways. The ratios are often presented as percentages of MSA/NSS-SO_4^{2-}. MSA/NSS-SO_4^{2-} ratios are not constant, and vary with latitude, with higher ratios found at higher latitudes (e.g. Berresheim 1987; Calhoun 1990; Bates *et al.* 1992). The variance in the ratio is believed to be due to the temperature dependence of MSA or SO_2 formation from DMS oxidation (Bates *et al.* 1992). Higher ratios are expected in areas with higher than average atmospheric DMS concentrations.

Savoie *et al.* (1989) reported MSA/NSS-SO_4^{2-} ratios from the North Atlantic and found a mean of 0.03, or 3%, and this value is currently used as an average for the region. Berresheim *et al.* (1991) reported MSA/NSS-SO_4^{2-} (as a %) ratios in continental and marine air masses. They found that mean daytime MSA/NSS-SO_4^{2-} ratios in marine air masses were five times higher (3.7± 2.6%), compared to continental air masses (0.8± 0.4%). Night ratios showed the same trend, with higher ratios in the marine air mass. The higher ratio was the result of lower NSS-SO_4^{2-} values, rather than higher MSA concentrations. The highest MSA/NSS-SO_4^{2-} ratio was found 0.5 days after an atmospheric DMS maximum concentration, indicating that the increase was due to the oxidation of DMS into MSA.

Wadleigh (2004) sampled aerosols over the North Atlantic in 1998 and 1999 and MSA/NSS-SO_4^{2-} (%) ratios were reported. For the spring cruise (1998) the range was low (0 to 6.8%) illustrating no size dependence, whereas for the fall cruise (1999) the range increased (0 to 98%), with the largest values found in the 3.0-0.95μm size fraction. The largest MSA/NSS-SO_4^{2-} ratios corresponded with two phytoplankton blooms. Wadleigh (2004) proposed that the phytoplankton production of DMS and its future oxidation lead to MSA condensing on pre-existing NSS-SO_4^{2-} particles, and the higher ratios in 1999 were attributed to Northerly stations sampled.

1.6.4 Review of Isotopic Studies of Aerosols over the North Atlantic

Gravenhorst (1977) conducted both laboratory and field studies in the North Atlantic in an attempt to determine sulphate sources. This was one of the earliest isotopic

studies of aerosols over the Atlantic with analysis of size fractions and total particulate aerosol samples. The cruise began in Germany and returned via the Canary Islands. The average SO_4^{2-} concentration was 1200ngm^{-3} in background conditions, and 2800ngm^{-3} when the aerosols were collected under the influence of Saharan dust. Ammonium concentrations were dependent on the aerosol size, with the highest concentrations found in the smallest size fractions. Aerosols collected were also analysed for sulphur isotopic composition. Two aerosols were collected during continental influence, with $\delta^{34}S_{NSS}$ values of +7 and +9‰, while the total $\delta^{34}S$ values were +10 and +12‰. Over the SW Atlantic, there was a wider range for $\delta^{34}S_{NSS}$ (-12 and +10‰) and for $\delta^{34}S_{total}$ (+2 and +14‰). A total particulate aerosol sample collected on a frequently used seaway had a $\delta^{34}S_{NSS}$ value of +11‰, while $\delta^{34}S_{total}$ was +13‰.

McArdle and Liss (1995) studied aerosol sulphate from Mace Head, Ireland and Ny lesund, Spitsberg en, two coastal sites with high biologic activity. $\delta^{34}S$ was measured, and a range between +5 to +23‰ was found. The higher $\delta^{34}S$ values were found in the summer, despite less sea salt influence, indicating that DMS oxidation is an important source of sulphur to the remote marine atmosphere. Biogenic contributions were ~20% at Mace Head in the winter, and rose to 30% in the summer. At Ny l esund biogenic contributions ranged from 15% in the winter to 30% in the summer. MSA concentrations showed a seasonal cycle, with summer highs (~170ng·m^{-3}) and winter lows (below detection).

Patris *et al.* (2000) measured the sulphur isotopic compositions of size segregated aerosols while transiting through the South and North Atlantic in October and November 1996. Nitrate values were among the lowest reported for the Atlantic and concentrations increased with decreasing size, indicating anthropogenic contributions in the smaller size fractions. Two bulk aerosol samples were collected, with a $\delta^{34}S$ value of +20.8‰ from a marine air mass and +13.8‰ (calculated $\delta^{34}S_{NSS}$ = +9.4±2.6‰) from an air mass originating off the coast of Africa. Size segregated samples were also collected and for the coarse (>1.5μm) size fraction; ~80% of the total sulphate was sea salt derived, with relatively constant isotopic compositions (~19‰). Aerosols <1.5μm were more sensitive to local and regional sources, and the $\delta^{34}S_{NSS}$ of the 1.5-0.49μm size fractions had an average isotopic composition of ~+11‰, with variation from the mean increasing as the size decreased. Aerosols <0.49μm had sea salt fractions <16%, with distinctive isotopic compositions from continental sources, ranging from +0.3± 6.8‰ to +11.1±1.1‰. Biogenic contributions were smaller in the North Atlantic (<35%) compared to the South Atlantic (50 to 90%).

Turkeian *et al.* (2001) studied the isotopic compositions of size segregated aerosols to determine the contributions of biogenic and anthropogenic sulphur in westerly winds in the spring of 1998 at Bermuda. The range of $\delta^{34}S$ values was +2.1 to +5.1‰ (mean = +3.8‰), consistent with sulphurous emissions from the combustion of fossil fuels. Submicron NSS-SO_4^{2-} concentrations ranged from 720 to 1250ng·m^{-3} (mean = 1100ngm^{-3}) but the average marine biogenic contribution to NSS-SO_4^{2-} was an order

of magnitude smaller (19.2±14.4ngm^{-3}), with 0 to 29% biogenic contribution to total NSS-SO_4^{2-}.

Wadleigh (2004) participated in two cruises of the NW Atlantic in spring 1998 and fall 1999, collecting size segregated aerosols. Isotopic analyses displayed a general trend of decreasing $\delta^{34}S$ values with decreasing aerosol size (~+20‰ in the large size fractions to ~+8‰ in the small size fractions). Methanesulphonic acid, NSS-SO_4^{2-} and NO_3^- concentrations were higher during the spring cruise than the fall, with means of 15.8, 624 and 462ngm^{-3} respectively.

1.7 Objectives

The objectives of this thesis were (1) to measure the isotopic and chemical composition of sulphate aerosols and gaseous sulphur dioxide from the spring SABINA C-SOLAS cruise of the Northwest Atlantic Ocean in 2003 and (2) to identify aerosol sulphate and sulphur dioxide sources using apportionment techniques, and (3) to examine concentration differences of DMS oxidation products (MSA and sulphate) as a function of latitude and temperature.

This study was part of a larger seasonal study of DMS and its oxidation products over the North Atlantic. The spring, summer and fall cruises of 2003 spanned the entire seasonal cycle of aerosols and gaseous sulphur dioxide over the NW Atlantic and this study reports results from the spring cruise. The springtime Lagrangian study was the first to follow a phytoplankton bloom's progression, while collecting atmospheric

samples in the vicinity of the bloom. Atmospheric samples represent much larger scales than those characterized by oceanographers studying bloom progressions. However, aerosols and gaseous sulphur dioxide collected throughout the Lagrangian study could be used to determine if local processes such as phytoplankton blooms had a discernable effect on local atmospheric sulphur chemistry, particularly with respect to sulphur dioxide and sulphate and MSA aerosols.

Aerosols and SO_2 were collected on a diurnal cycle, with daytime and night-time samples. Due to the differing oxidation mechanisms in the day and at night it is hypothesized that day/night differences in aerosol and SO_2 concentrations and isotopic compositions will be observed and will relate to oxidation of biogenic sulphur. Validating the above hypotheses by comparing size segregated and total aerosol samples with the amount of MSA and biogenic SO_2 will aid in determining

1. Whether the amounts and proportion of biogenic SO_2 and aerosol sulphate present in the atmosphere was a function of latitude and/or temperature,
2. Whether MSA concentrations were related to biogenic SO_2 or sulphate, and whether this changed with latitude and/or temperature,
3. Whether diurnal variations in biogenic SO_2, sulphate, and MSA concentrations exist,
4. Whether biogenic aerosols are associated with smaller size fractions.

The results from this study are useful to the larger research community and will provide data that can be used to test various oxidation mechanisms for DMS in the remote marine atmosphere, and potentially define the importance of NO_x oxidation.

There is a distinct deficiency in the number of SO_2 measurements in the NW Atlantic and this study adds important data to the global data base. This was the first study of the NW Atlantic to examine the concentrations of anthropogenic and biogenic sulphate and sulphur dioxide concurrently on a diurnal cycle. The measurements of both anthropogenic and biogenic SO_2 can be further used by modellers to model DMS climate interactions.

Chapter Two: Methods and Cruise Description

2.1 Cruise Location

The Spring SABINA cruise took place from April 23rd to May 16th, 2003 (Julian Days 103-135). Seven oceanographic stations were sampled, with a Lagrangian study at station L1, followed by a Transect study ranging from 36^0N to 54^0N (*Figure 2-1*). The oceanographic stations were selected from biogeochemical provinces identified by Longhurst (1998) (Section 2.2). The Lagrangian study followed a water mass that was identified from satellite images (high chlorophyll content in surface waters) as having a phytoplankton bloom. Once the phytoplankton bloom was established through oceanographic measurements using CTD data, an ocean drifter was used to track the water mass and ensure that the same water mass was sampled each day. The ocean drifter consisted of a float, cable and a drogue. The drogue helps the drifter move with the water flow. The Lagrangian study ended when the drogue could not be found; presumably it became entangled in a passing vessel and the water mass could not be re-located. The cruise time line is presented in *Appendix II.1.* Fifteen day and night sample sets were collected and daily average air temperatures ranging from ~5^0C to ~20^0C.

2.2 Biogeochemical Provinces

The biogeochemical provinces of the North Atlantic were originally identified by Longhurst (1998) using remote sensing, ocean surface temperature climatology and nutrient concentrations. The overall goal of the C-SOLAS programme during the transect study was to sample different biogeochemical provinces, and the stations

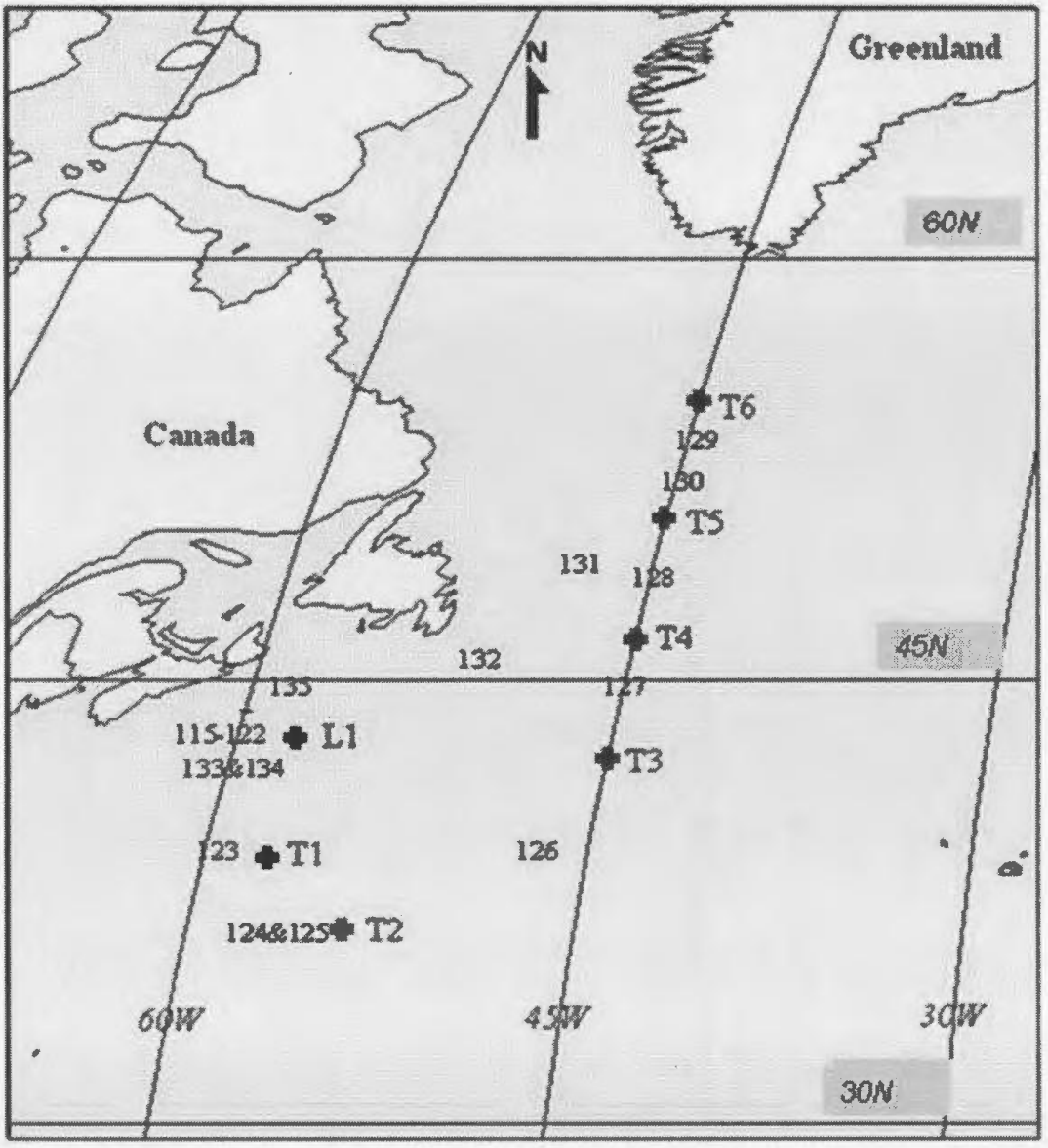

Figure 2-1 – Cruise track from Spring SABINA cruise. Crosses indicate the stations where the oceanographic measurements were made, and the Julian Day indicates the day and approximate location where the sample was collected.

were set according to provinces determined by Longhurst (1998). The biogeochemical provinces are not stationary and move with the seasons, air and sea temperature, wind direction and intensity. Devred and Roy (2005) used satellite derived data and real-time data (salinity, temperature, chlorophyll data and photic zone depth) to determine the biogeochemical provinces during the cruise (*Figure 2-2*). A new province, "Slope Water" was added by Devred and Roy (2005). The new province determination was necessary as the water mass did not match any of the criteria defined by Longhurst (1998).

2.3 Aerosol and Sulphur Dioxide Sample Collection

Sulphate aerosol and SO_2 samples were collected using four high-volume, flow-controlled air sampling units. The samplers were secured aboard the CCGS Hudson at the front of the ship, on the deck above the bridge, at a height of approximately 30 meters above sea level. Two samplers were designated for daytime sampling, and two for night-time sampling (*Figure 2-3*). The daytime samplers were used from sunrise to sunset, the night samplers were turned on after sunset. Day and night samplers were never used concurrently. The daytime samplers were provided by the University of Calgary (Sierra Miscu); the night samplers were provided by Memorial University (Anderson Sierra) and were equipped with PM_{10} heads. The PM_{10} heads allow only aerosols with a diameter $\leq 10\mu m$ to enter the sampling unit.

The daytime and night sampling units perform and operate in the same fashion. One sampler for both day and night sampling was equipped with a cascade impactor, and a back-up filter (*Figure 2-4*). The other sampling unit was equipped with a total

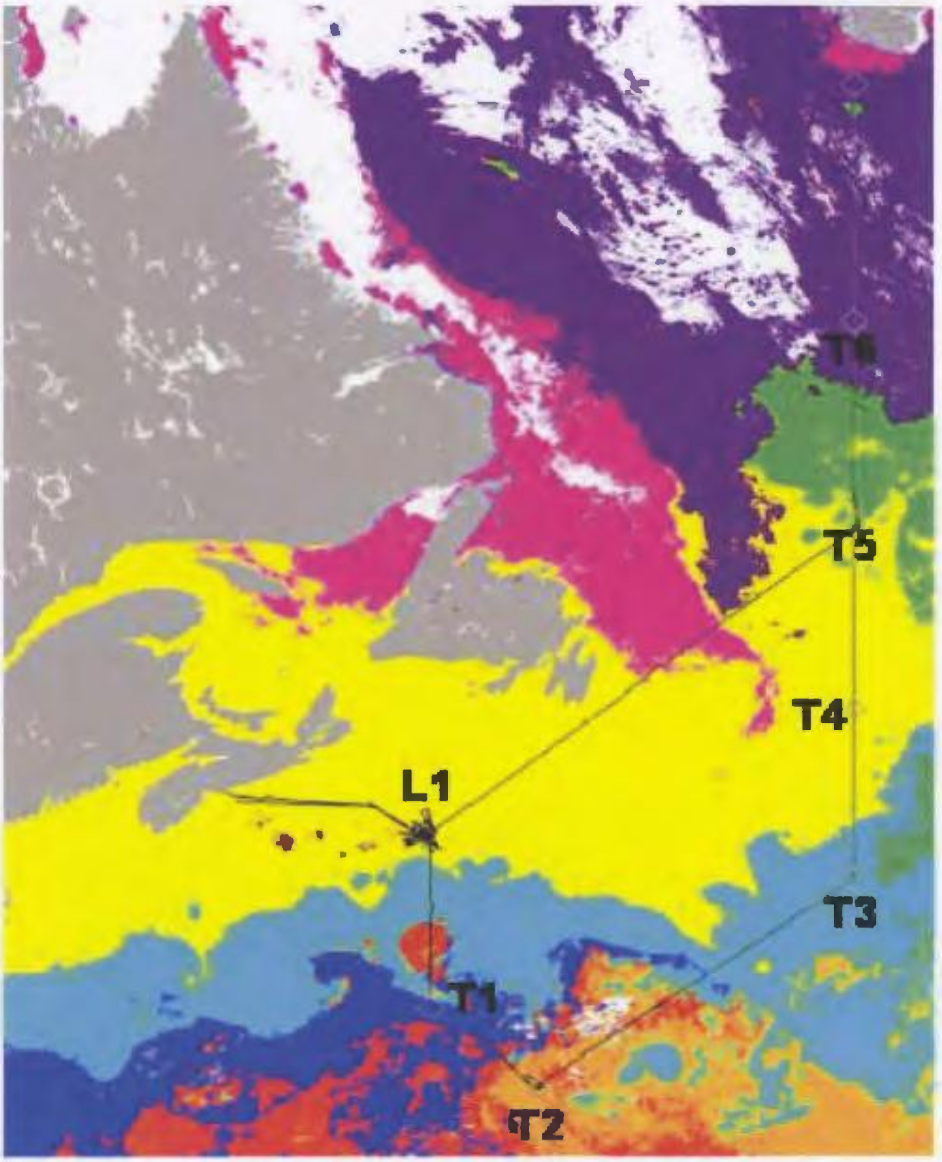

Station	Color	Biogeochemical Province
L1	Yellow	North West Continental Shelf
T1	Blue	Gulf Stream
T2	Orange	Subtropical Gyre East
T3	Pale Blue	Slope Waters
T4	Yellow	North West Continental Shelf
T5	Green	North Atlantic Drift
T6	Purple	Arctic Water

Figure 2-2 – Biogeochemical province determination by Devred and Roy (2005).

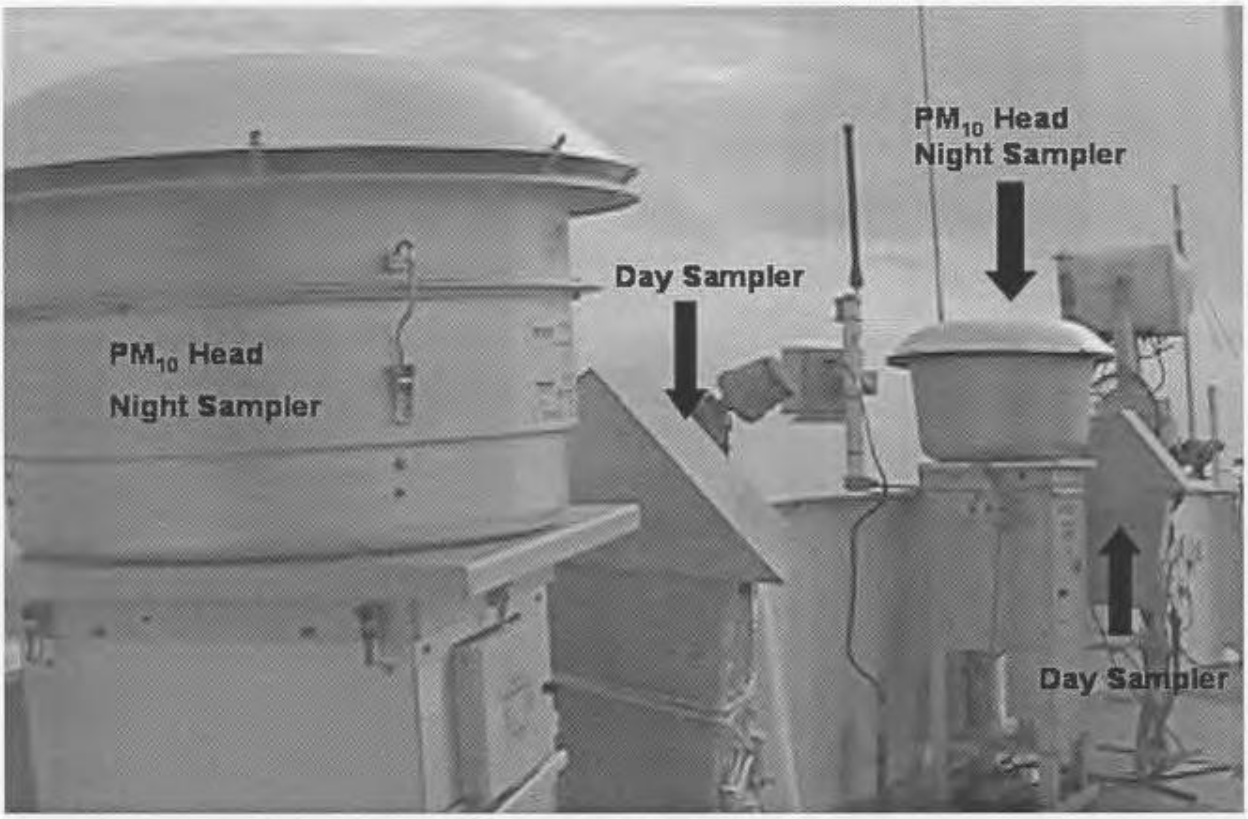

Figure 2-3 – Day and night samplers on the deck of the CCGS Hudson.

particulate filter, along with a SO_2 filter (*Figure 2-5*). Diurnal sampling took place to allow the examination of the difference between the aerosols and SO_2 collected during the day and night. The PM_{10} samplers were only used for night sampling only (April 25th to May 5th) and therefore the total particulate samples from the daytime (<100um) and night-time (PM10) samples from this time period were not directly comparable. Differences between the two sample sets were restricted to trends. The SO_2 filters and size segregated aerosols <7.2μm were not affected.

A rain storm on May 5th soaked the motor of the total particulate and SO_2 PM_{10} samplers. All total particulate and SO_2 samples were collected with a sampler collecting all size fractions (<100μm). Therefore it is possible to compare the day/night differences in these samples for the total particulate size fractions for samples collected after May 5th. .

Sampling time ranged from 5 to 19 hours. Samples were taken in dry conditions, and the samplers were turned off during heavy rain events, or periods of continuous rain. Every attempt was made to reduce the contamination from the ships own emissions which contain SO_2 and other sulphur compounds from fuel combustion. The samplers were turned off if the prevailing winds were from the rear of the ship, causing the emissions from the stack to blow over the front of the ship where the samplers were located. The samplers were also turned off when the ship was motionless, as the possibility of the ships stack emissions reaching the samplers was increased.

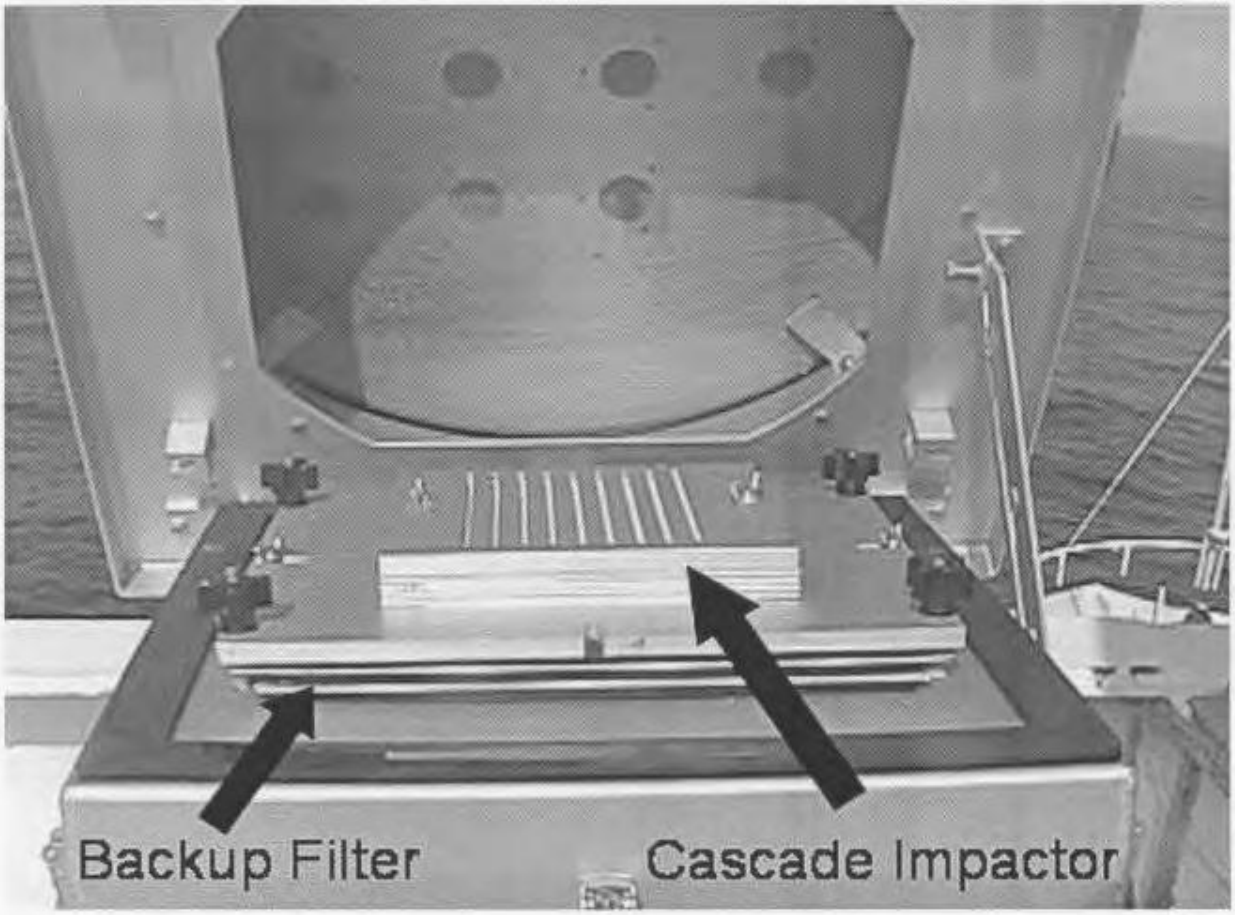

Figure 2-4 – Cascade impactor and back-up filter secured on the high volume sampler.

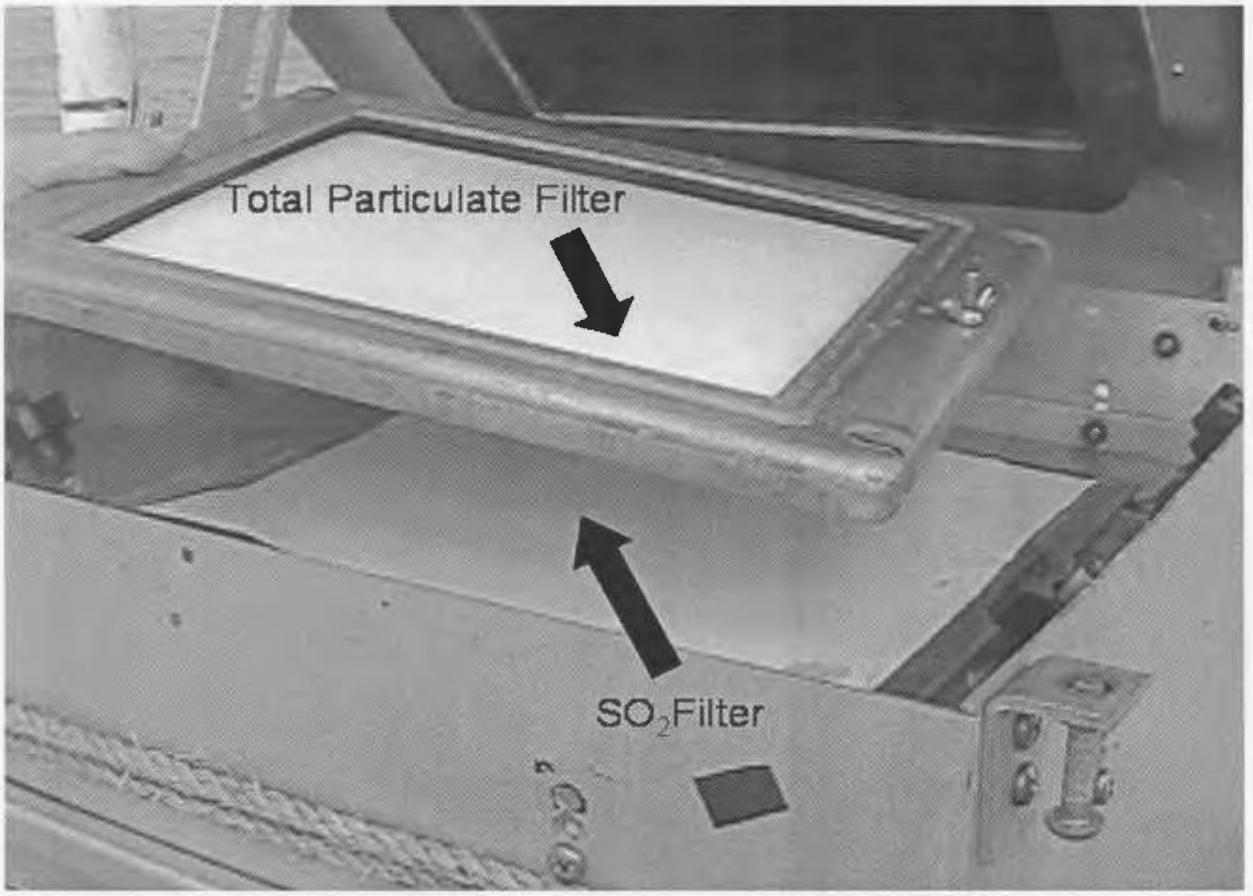

Figure 2-5 – Total particulate filter and SO_2 filter on the high volume sampler.

2.3.1 Size Segregated Sample Collection

The size segregated samples were collected using Graseby 320 five-stage cascade impactors. The top five stages in the cascade impactor were slotted, with the slots one half inch apart. As the aerosols travelled through the cascade impactor, they were trapped within the mesh of the quartz filter paper, according to aerodynamic size (*Table 2-1*). The width between the slots becomes smaller as the aerosols travel through the impactor. As the width between the slots decreases, larger aerosols become entrained in the lattice of the filter (Tisch Environmental Operators Manual). Smaller aerosols travel through the slots until they too become entrained. The 6^{th} stage, or back-up filter, catches all particles smaller than stage 5 (<0.49μm). The slotted filters measure 0.143m by 0.149m, and their small size allows only minimal amounts of gaseous pollutants to be absorbed (Tisch Environmental Operators Manual). The aerosols were collected onto Whatman quartz microfibre filters. Quartz filters were used instead of cellulose filters as the particles are retained in the lattice of the quartz filter, and due to the low concentration of alkaline earth metals in the filter fibres, no products from SO_2 and NO_2 were created (Tisch Environmental Operators Manual; Whatman 2005).

After the samples had been collected, they were removed from the samplers, placed in a clean plastic carrying case, and returned to the clean lab aboard the CCGS Hudson. While wearing latex gloves, the aerosol samples were removed from the filter casings, wrapped in aluminium foil and placed in a clean, labelled Ziploc bag.

Table 2-1 – Aerosol diameter cut-off ranges for the cascade impactor.

Stage	Aerodynamic Size Collected
Stage 1	100-7.2μm (no PM_{10} head) 10 to 7.2μm (PM_{10} head)
Stage 2	7.2 to 3.0μm
Stage 3	3.0 to 1.5μm
Stage 4	1.5 to 0.95μm
Stage 5	0.95 to 0.49μm
Stage 6 (Back-up Filter)	< 0.49 μm

Note: Flow was constant at 1.13m^3 per minute.

The filter casings were then cleaned with distilled, deionized water to remove any possible contamination before filters for the next sample were loaded.

2.3.2 Total Particulate Sample Collection

Total particulate samples were also collected using Whatman quartz microfibre filters. The size of the total particulate filter was 0.203m by 0.254m. Daytime samplers were not equipped with PM_{10} heads, so all size fractions $\leq$100μm were collected. Night-time samplers were equipped with PM_{10} heads, thus only aerosols with a diameter $\leq$10μm were collected. The samples were packaged in the same manner as the size segregated samples.

2.3.3 Sulphur Dioxide Collection

Filters used to collect SO_2 were placed beneath the total particulate filter. These filters were composed of cellulose acetate (S&S Biopath Inc. #410) and were treated with a KCO_3/glycerol solution to form an adduct with SO_2, trapping it. Filters were removed from the sampler and placed in a labelled Ziploc bag at the end of each sampling period. *Tables 2-2* and *2-3* display the specific details regarding both the day and night samples, including the date the sample was taken, the location where the sample was collected, the duration of sampling, and any problems or irregularities encountered during sampling.

Table 2-2 – Daytime sample descriptions.

Dates Sampled (2003)	Julian Day (2003)	Sampling Time (minutes)	Location	Latitude (Start of sampling)	Longitude (Start of sampling)	Average Temp (^{0}C)	Average Wind Speed (km/hr)	Note
April 25th & 26th	115&116	765	L1	43°23'.9N	57°42'.9W	4.5	24.3	Sable Island visible.
April 27th & 28th	117&118	900	L1	43°20.8N	57°33'.7W	6.0	39.3	
April 29th & 30th	119&120	720	L1	43°33'.5N	57°25'.9W	6.7	38.5	2 ships in distance.
May 1 & 2nd	121&122	710	L1	43°40'.8N	57°30'.5W	8.1	24.4	Sesimic ship <10km away
May 3rd	123	480	T1	39°02'N	57°14'.2W	21.9	81.5	
May 4th & 5th	124&125	675	T2	36°54'.3N	54°30'.7W	19.0	31.7	
May 6th	126	615	T3+	39°23'.1N	50°15'W	16.7	30.7	
May 7th	127	645	T4+	42°05'.4N	45°25'.9W	14.0	50.9	Stormy weather.
May 8th	128	585	T5+	46°04'.5N	44°59'.9W	5.9	24.6	
May 9th	129	510	T6+	50°23'.7N	45°00'.1W	7.5	16.3	
May 10th	130	690	T5+	54°31'.6N	44°59'.8W	4.6	23.2	
May 11th	131	490	L1+	50°32'.8N	44°52'.6W	9.0	52.0	
May 12th	132	630	L1+	47°41'.3N	50°18'W	7.6	29.3	
May 13th	133	570	L1	44°17'.5N	56°11'.8W	7.4	31.9	
May 14th	134	365	L1	43°36'.8N	58°09'.8W	9.0	15.2	
May 15th	135	465	Halifax+	43°23'.9N	57°47'.9W	6.0	23.2	

Note: + is used to denote samples collected while transiting to the next station.

Temperature and wind speed are averaged over the length of the sampling time.

Table 2-3 – Night-time sample descriptions.

Dates Sampled	Julian Day (2003)	Sampling Time (minutes)	Location	Latitude (Start of sampling)	Longitude (Start of sampling)	Average Temp (^{0}C)	Average Wind Speed (km/hr)	Note
April 26th & 27th	116 & 117	910	L1	43°27'.7N	57°39'.4W	2.5	38.3	
April 28th - 30th	118-120	1125	L1	43°29'.0N	57°50'.6W	4.0	33.2	
May 1st & 2nd	121&122	825 900 (SO_2 & Total)	L1 & T1$^+$	43°34'.3N	57°36'.1W	19.9	36.1	
May 4th	124	540	T2	37°05'.6N	54°48'.5W	19.2	18.3	Stormy Weather.
May 5th	125	300	T3$^+$	37°58'.9N	53°40'.4W	19.8	40.2	PM_{10} Total & SO_2 sampler malfunctions.
May 6th	126	585	T3$^+$	41°00'.2N	47°23'.7W	13.5	59.3	No Total & SO_2 sample collected
May 7th	127	600	T4v	43°56'.6N	44°59'.9W	8.6	32.4	*
May 8th	128	570	T5$^+$	48°17'.3N	45°00'.9W	6.6	20.0	*
May 9th	129	600	T6$^+$	52°22'.4N	44°59'.4W	4.0	21.9	*
May 10th	130	450	T5$^+$	52°42'.9N	44°59'.8W	8.0	39.4	*
May 11th	131	525	L1$^+$	49°03'N	47°49'.8W	4.0	35.6	*
May 12th	132	300	L1$^+$	45°18'.5N	54°27'.9W	4.7	25.6	*
May 13th	133	330	L1	43°25'.4N	57°40'.1W	7.3	28.5	*
May 14th	134	420	L1	43°29'.1N	57°32'.6W	5.0	20.9	*
May 15th	135	435	Halifax$^+$	44°11'.8N	60°28'.7W	4.0	29.8	*

Note: $^+$ is used to denote samples collected while transiting to the next station. * indicates that the daytime sampler (no PM_{10} head) was used in place of the night sampler. Temperature and wind speed are averaged over the length of the sampling time.

2.4 Fuel and Oil Collection

Approximately 500mL of diesel fuel and oil used on the CCGS Hudson were collected while aboard the vessel. The fuel and oil samples were analyzed for $\delta^{34}S$ to determine the isotope composition. It was expected that the fuel and oil would have isotopic values similar to Eastern North American emissions (*Figure 1-7*).

2.5 Filter Preparation for Isotopic Analysis

2.5.1 Aerosol Sulphate Preparation

Filter paper containing the aerosol samples was torn into small pieces approximately $30cm^2$, and placed into a clean, labeled 600mL Pyrex beaker. In preparing total particulate filters, 200mL of deionized-distilled (DD) water (18 megaOhmm) was added, ensuring that the sample was completely submerged. Less DD water was needed to submerge the smaller size segregated filters (75mL). The beaker containing the sample was then placed in a Branson 8200 ultrasonic bath for 30 minutes. After sonication the solution was filtered using a vacuum filter apparatus equipped with a 47mm diameter, 0.45μm pore size Millipore filter to remove quartz filter fibres. Two 10mL aliquots of the filtrate were collected in 12mL screw cap VWR Scientific glass vials for ion chromatography analysis. Environmental Grade 10% $BaCl_2$ was added in excess to the remainder of the solution and mixed well to form $BaSO_4$. Three M HCl (Environmental Grade) was added to obtain a pH in the range of 3 to 4 to ensure no co-precipitation of barium carbonate. The sample was then heated until the volume was reduced to <25mL to concentrate the precipitate. The solution containing $BaSO_4$ was filtered using pre-weighed 47mm diameter,

0.45μm pore size Nucleopore track-etch filters and dried overnight at room temperature. Filter and precipitate were weighed on an analytical balance (MDL = 0.00001g) after drying. The Nucleopore filter and precipitate were placed in a clean crucible and ashed in a muffle furnace for 60 minutes at 800^0C. The filter was completely burned and $BaSO_4$ was carefully scooped out of the crucible and placed into a small tin capsule for $\delta^{34}S$ analysis. Remaining $BaSO_4$ was kept for replicate analysis.

2.5.2 Sulphur Dioxide Sample Preparation

The method of extracting SO_2 from the filters was very similar to that for aerosol sulphate. The difference between methods was, prior to sonication, 2mL of 0.3M H_2O_2 was added to the beaker and mixed well to promote sulphate formation. The solution was then filtered and 5mL of Environmental Grade 10% $BaCl_2$ was added to the solution. Approximately 2 to 10 ml of 3M HCl was added to the solution dropwise to create an acidic solution. The sample was then reduced by heating until the volume was less then 50mL, and then filtered through a pre-weighed Nucleopore filter. The weight of $BaSO_4$ precipitate was calculated in the same manner as for sulphate aerosol samples. The samples were fused and $BaSO_4$ was packed for isotopic analysis.

2.6 Fuel and Oil Sample Preparation

The sulphur isotopic compositions of the fuel and oil samples were determined on total sulphur extracted from the samples. This was accomplished by complete

combustion at high temperatures in a Parr-Bomb™. Approximately one gram of fuel or oil was placed in a clean combustion cylindrical cup and a nickel alloy fuse wire was attached with the filament just above the sample. Ten mL of deionized water was added, along with 0.09ml – 0.15mL (3 to 5 drops) of 0.5M H_2O_2 to the bottom of the Parr-Bomb™ to ensure the sulphur was in the form of soluble sulphate after combustion. The bomb was filled with 30 atmospheres of oxygen, and its lower portion placed in a water bath to dissipate heat. The electrodes were attached to feed through to the filament which was then ignited. After fifteen minutes the bomb was removed from the water bath and unreacted O_2, CO_2 and other gases were released from the bomb slowly. The inner part of the bomb was rinsed with deionized water, and the washings were collected in a 500mL Pyrex beaker. The solution was then acidified to a pH of 4 (addition of HCl), brought to a rolling boil (to remove all remaining H_2O_2) and 10mL of 0.5M $BaCl_2$ was added, resulting in the production of $BaSO_4$. The solution plus precipitate was reduced to approximately 10mL with further heating and filtering through ashless Millipore 45μm filter paper. Once the filter paper was dry it was ignited in a clean crucible. The $BaSO_4$ remaining was packed for isotopic analysis.

2.7 Isotopic Analysis

Isotopic analysis of the prepared $BaSO_4$ samples was carried out at the Isotope Sciences Laboratory at the University of Calgary. The samples were converted to SO_2 and purified by GC in a Carlo ERBA NA1500 elemental analyzer. The effluent SO_2 entered the source of a VG II PRISM mass spectrometer operating in continuous

flow mode. In this procedure, ion currents corresponding to masses 64 and 66 were integrated throughout the time that the SO_2 passed through the mass spectrometer source. The detector electronics displayed peaks of isotopic ion currents versus time and areas under these peaks were used for calculating the sulphur content of the sample and isotopic abundances. The column used in the elemental analysis was a 6mm x 0.8m long sulphur separation column from Elemental Microanalysis©.

Isotope abundance ratios were calibrated using internal laboratory standards STB and SW. STB is a barite standard used at the University of Calgary, with an isotopic composition of -2.0‰. SW is pure barium sulphate precipitated from seawater with an isotopic composition of +20.8‰. International standards, NBS 127, IAEA S-1 and IAEA S-2 were used at the beginning and end of each run to check for drift during a run and to calibrate the data. The data were corrected using a two point linear regression of the internal standards, STB and SW. Three different masses (0.100, 0.150 and 0.200mg) of STB and SW were run at the beginning and end of each run. After each ten samples one of each different mass (0.10 or 0.15 or 0.20mg) of STB and SW were run to correct for instrumentation drift and assist in the calibration.

Yield is the percentage of signal as determined from the mass 64 peak for the sample, relative to a standard of the same mass of $BaSO_4$. Samples with yields >120% were rejected, as it indicates a memory effect. Conversely samples with small yields (<40%) had small peaks areas. Major peak areas $<4.5 \times 10^{-9}$ amp seconds were

discarded, as the peak area was not large enough to give a representative $\delta^{34}S$ value. The average precision for all of the samples within the run was found to be 0.3±0.4‰ (n=264). Duplicate analysis of the same sample was conducted during isotopic and chemical analysis whenever possible. Duplicate or triplicate analysis was run for approximately 30% of all samples collected. The precision of these sample replicates ranged from 2.3‰ to 0.01‰. Less than 5% of the replicates had a precision worse than 1.0‰ and are indicated throughout this thesis by larger error bars. $\delta^{34}S_{NSS}$ values which had uncertainties greater than 5‰ were removed from the data set. Blank filters were collected to correct for the isotopic and chemical composition of background sulphur in the filters. Aerosol and SO_2 samples were blank corrected (*Appendix II.2*).

Isotopic analysis of the fuel and oil samples was conducted at Memorial University of Newfoundland. The instrument used was a Finnigan MAT 252 isotope ratio mass spectrometer, interfaced with a Carlo ERBA NA1500 elemental analyzer. The column used was a 0.635cm x 1.2m Teflon column. Combustion reactor temperature was set at 1050°C. International standards NBS-123, IAEA-S-1, IAEA-S-2 and internal standard $BaSO_4$#10 were used to calibrate the instrument and correct for drift. The data was corrected using STB and SW standards, as previously described for the VG II PRISM. Vanadium pentaoxide (V_2O_5) was added to $BaSO_4$ packed in tin capsules to aid in thermal decomposition.

2.8 Chemical Analysis

Chemical analysis of water soluble ions from the aerosol filters was completed at Memorial University of Newfoundland, using a Dionex 100 ion chromatograph. Size segregated and total particulate filters were analyzed for sodium (Na^+), ammonium (NH_4^+), potassium (K^+), magnesium (Mg^{2+}), calcium (Ca^{2+}), chloride (Cl^-), nitrate (NO_3^-), sulphate (SO_4^{2-}), phosphate (PO_4^{3-}) and MSA ($CH_3SOH_3^-$). The instrument was calibrated using a linear regression of 4 or 5 (dependent on method) National Institute of Standards and Technology (NIST) standards, prepared to concentrations ranging between 0.01 and 10mg·L^{-1}. External standards, QCP Rain, ESD-Anion and ESD-Cation were used to ensure the instrument was performing correctly. Version 3.2.1 of the AI-450 Chromatograph Automation Software was used for analysis. Samples were blank corrected for field blank corrections after ion chromatography analysis (*Appendix II.3*). Data are presented in ng·m^{-3} according to the procedure outlined in *Appendix II.4*. Samples with concentrations less than 1.5 times of the detection limit were eliminated from the data set. Uncertainties for concentrations is ±10%

2.8.1 Anion Analysis

Analysis of the major anions (Cl^-, SO_4^{2-}, NO_3^- and PO_4^{3-}), used a 1.8mM H_2CO_3 / 1.7mM $NaHCO_3$ eluent. An IonPac® AG4A-SC Guard column (4x50mm) in combination with an IonPac® AS4A-SC analytical column (4x250mm) was used, using an ASRS-Ultra II 4mm self regenerating suppressor (4mm). The flow rate was set at 1.5mLmin^{-1}. Due to the wide ranging concentrations of the anions, specifically

Cl^-, different methods were used. Some samples had such high Cl^- concentrations that the aliquot had to be diluted with deionized water to determine concentrations.

A linear calibration was used in all calibrations. External reference standards were used after calibration to ensure the machine was performing optimally. Standard QCP-RAIN (lot number: W-QCP13035), produced by Inorganic Ventures/Iv Labs, was used when analyzing low (0-3 mgL^{-1}) concentrations. ESD-Anion (a reference standard) produced by Inorganic Ventures/Iv Labs were used when analyzing higher (1-10 mgL^{-1}) concentrations. All of the standards used by Inorganic Ventures/Iv Labs were traceable to NIST standards.

2.8.2 Cation Analysis

Major cations (Na^+, NH_4^+, K^+, $Mg^{2+}$and Ca^{2+}) were also analyzed by ion chromatography. A 20mM H_2SO_4 eluent was used. The flow rate was set at $1mLmin^{-1}$. Due to the wide ranging concentrations of cations, especially Na^+, different methods were utilized to determine concentrations. Again, external reference standards were used to ensure the machine was performing optimally. Standard QCP-RAIN (lot number: W-QCP13035) produced by Inorganic Ventures/Iv Labs, was used when analyzing low (0-3 $mg{\cdot}L^{-1}$) concentrations. The reference standard ESD-ANION-1 made by Inorganic Ventures/Iv Labs was useful when looking at high (1-10 mgL^{-1}) concentrations of cations. All of the standards used by Inorganic Ventures/Iv Labs are traceable to NIST standards. The precisions of the standards determined through analysis are displayed in *Table 2-4*.

Table 2-4 – Precision of anion and cation concentrations ($mg \cdot L^{-1}$) for ion chromatography determined by replicate analysis of standards, and the accepted range for each standard.

Standard Name	**Na^+**	**NH_4^+**	**K^+**	**Mg^{2+}**	**Ca^{2+}**
ESD-Cation-1	2.8±0.3	1.6±0.2	1.6±0.2	1.7±0.1	1.5±0.0
Accepted Range	3.0±0.4	2.7-1.3	1.5±0.2	1.5±0.1	1.5±.3
W-QCP13035	0.35±0.09	0.29±0.02	0.24±0.03	0.14±0.03	N/A
Accepted Range	0.26±0.01	0.27±0.01	0.30±0.4	0.15±0.01	N/A
N	20	20	20	20	20
Standard Name	**Cl^-**	**NO_3^-**	**PO_4^{3-}**	**SO_4^{2-}**	
ESD-Anion-1	2.93±0.07	1.7±0.1	1.68±0.08	1.58±0.05	
Accepted Range	3.0±0.26	1.5±0.5	1.50±0.21	1.5±1.9	
W-QCP13035	0.5±0.2	1.27±0.05	N/A	2.6±0.1	
Accepted Range	0.4±0.1	1.15±0.04	N/A	2.4±0.1	
N	10	10	10	10	

Note: N represents the number of samples used in the calculation.

2.8.3 Methanesulphonic Acid Analysis

Methanesulphonic acid (MSA) was analyzed by ion chromatography and calibrated using a linear calibration of NIST standards, ranging between 0.1 and 1 mgL^{-1}. An internal reference standard with a composition of 0.5 mgL^{-1} of MSA, Cl^-, NO_3^-, PO_4^{3-} and SO_4^{2-} was used to ensure the machine was calibrated correctly. The precision of this standard was found to be 0.52±0.02 mgL^{-1}(n=12). To separate MSA from other anion components, two eluents were used, 1.2mM $NaHCO_3$ to elute the MSA and Cl^-, and 3.6 mM H_2CO_3 / 3.7mM $NaHCO_3$ to elute the other anion components. The instrument used the same set up as was used for the anion analysis. The flow rate was set at $2mL \cdot min^{-1}$.

2.9 Back Trajectory Analysis

Air mass back trajectories were determined using the National Oceanic and Atmospheric Administration (NOAA) Hysplit Model. Hysplit is an acronym for "Hybrid Single-Particle Lagrangian Integrated Trajectory" and it computes the forward trajectory and backward trajectory of a single air mass, or pollutant. Hysplit was created in combination with NOAA and Australia's Bureau of Meteorology. The model is run through the internet through the "Ready" system; with meteorological data stored on the NOAA sever (http://www.arl.noaa.gov/ready/hysplit4.html). The error associated with trajectories is < 20% (Stohl 1998).

Hysplit was used to compute the back trajectories of individual air masses on a 48 hour time scale. The air mass height was being tracked at three different values: 0m,

100m and 500m above sea level to ensure the capture of marine air masses, and any overlying air masses. The meteorological data were gridded to the Mercator polar projection (NOAA 2004). The "FNL" meteorological data set was used. The data set started in 1997 and continues to present (NOAA 2004). The data are six hour archive data that are run through the NCEP model, giving hourly data points for each part of the grid (NOAA 2004).

The plots were classified on a five point classification scheme (*Table 2-5*), and air masses were classified based on where the air mass originated and how the air mass moved vertically. If the air mass was not purely marine (1.0) and not aged continental (2.0), but rather the transition or combination of both, the air mass was signified by a classification of 1.5. Samples taken over a period of two to three days may have been influenced by more than one air mass, resulting in a combination of types. For each sample, a 48 hour back trajectory was completed to determine where the air mass originated. Marine air masses had back trajectories which did not originate over a land mass and were purely marine in origin *(Figure 2-6)*. Strongly continental air masses originated over a populated land mass (*Figure 2-7*). *Figure 2-8* shows an example of an air mass with both marine and continental air masses. All air mass back trajectories are found in *Appendix II.5*. *Tables 2-6* and *2-7* show the air mass classifications for both the day and night samples.

Table 2-5 – Air mass classification scheme.

Air Mass Classification	Classification Number
Purely Marine	1
Aged Continental	2
Continental with Marine Influence	3
Strongly Continental	4
Arctic Air Mass	5

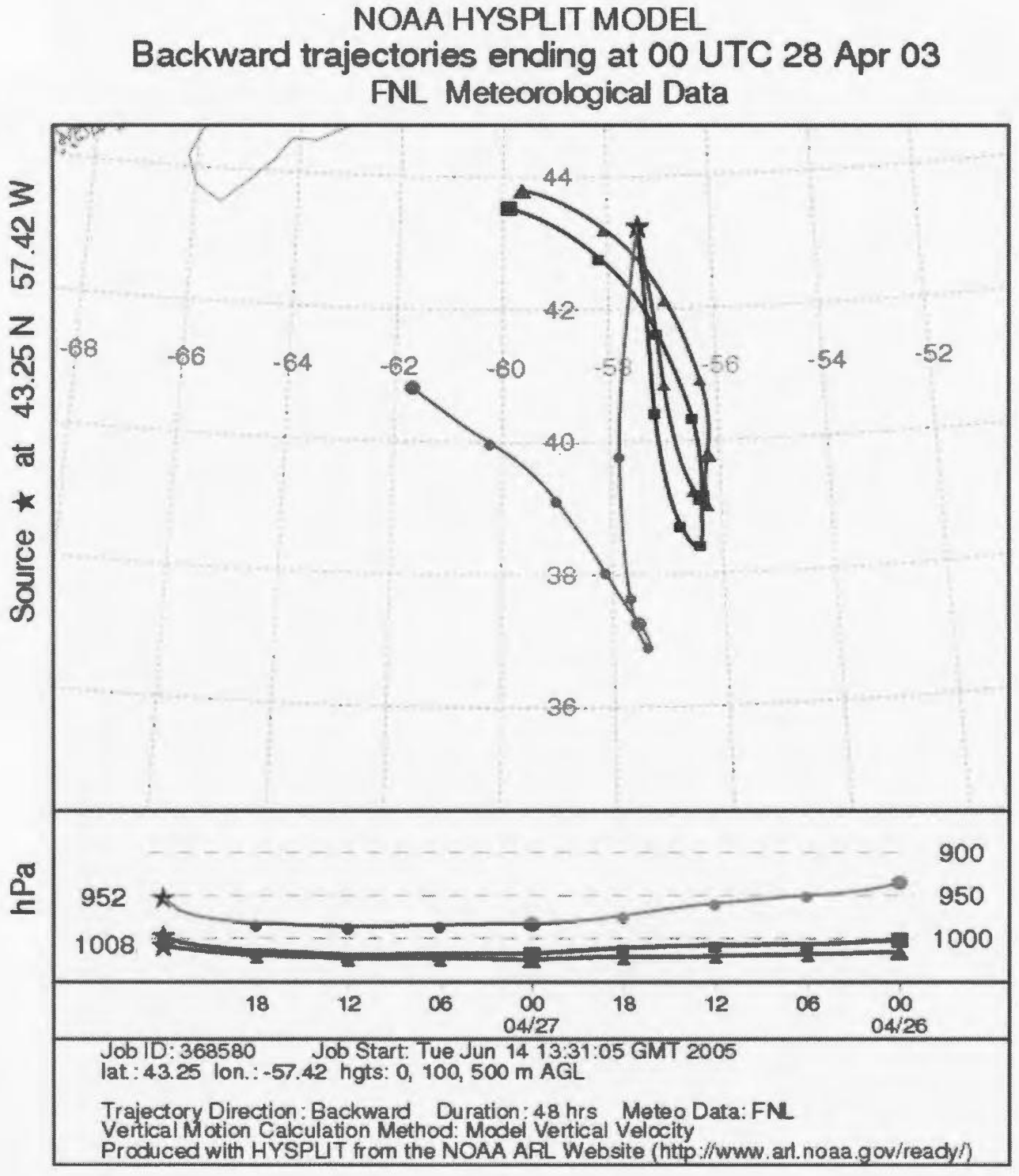

Figure 2-6 – Back trajectory for a purely marine air mass. Circles represent 500m asl, squares 100m asl and triangles 0m asl.

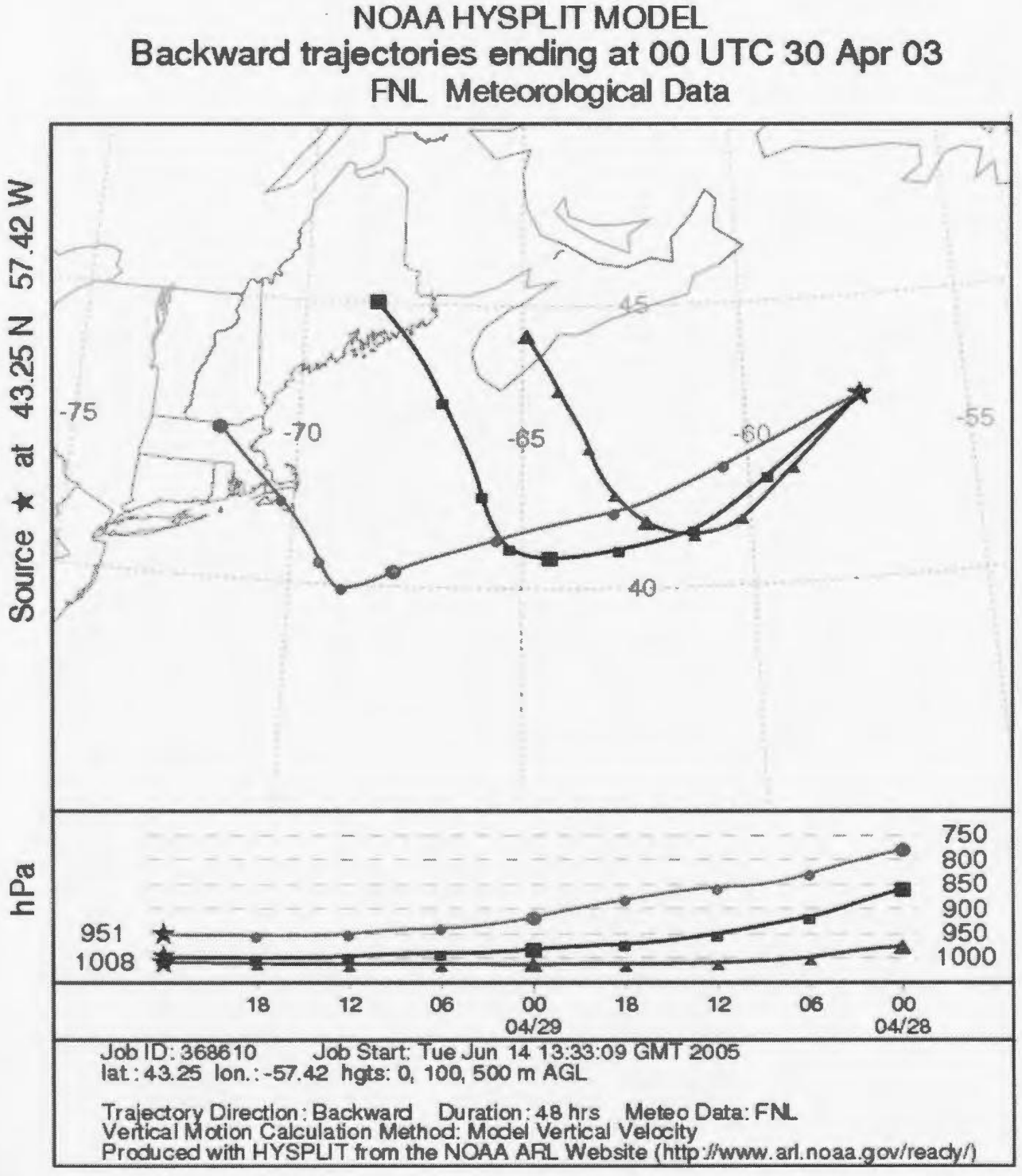

Figure 2-7– Back trajectory for a strongly continental air mass. Circles represent 500m asl, squares 100m asl and triangles 0m asl.

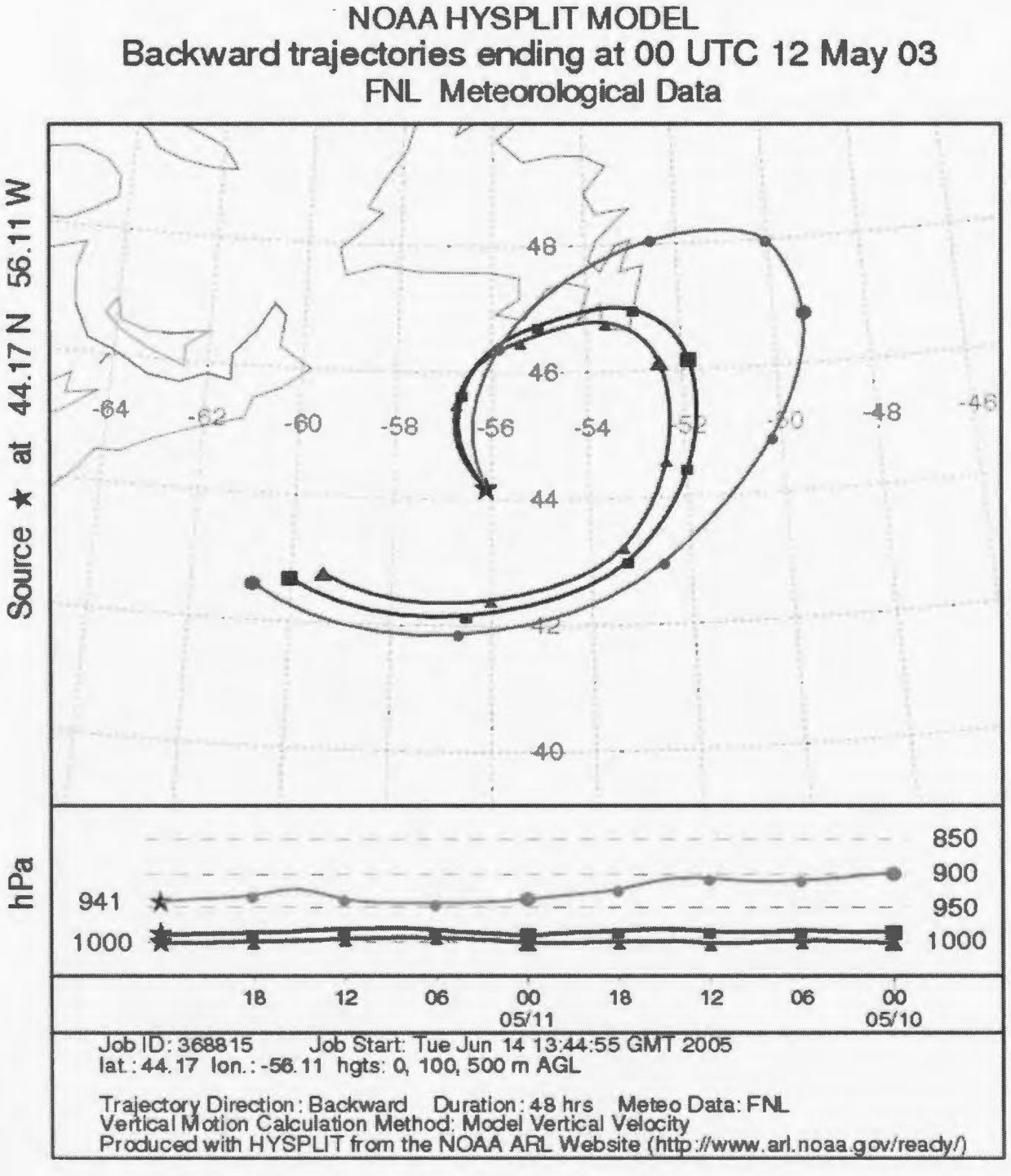

Figure 2-8 – Back trajectory for a continental air mass with marine influence. Circles represent 500m asl, squares 100m asl and triangles 0m asl.

Table 2-6 – Air mass classifications for day samples.

Date	Julian Day	Air Mass Classification	Air Mass Origin
April 25 & 26	115&116	1.5	Marine
April 27 & 28	117&118	1	Marine
April 29 & 30	119&120	4	Western North America
May 1 & 2	121&122	2	Nova Scotia
May 3	123	1	Marine
May 4 & 5	124&125	1	Marine
May 6	126	1	Marine
May 7	127	3.5	Newfoundland
May 8	128	2.5	Newfoundland and shipping lane
May 9	129	5	Baffin Bay
May 10	130	5	Baffin Bay
May 11	131	1	Marine
May 12	132	3	Newfoundland
May 13	133	3	Sable Island
May 14	134	2	Northeastern USA
May 15	135	2	Northeastern USA

Table 2-7 – Air mass classification for night samples.

Date	Julian Day	Air Mass Classification	Air Mass Origin
April 26 & 27	116&117	1.5	Marine
April 28 - 30	118-120	3	Western North America
May 1 & 2	121&122	2	Nova Scotia
4-May	124	1	Marine
5-May	125	1	Marine
6-May	126	1	Marine
7-May	127	3.5	Newfoundland
8-May	128	2.5	Newfoundland and shipping lane
9-May	129	5	Baffin Bay
10-May	130	5	Baffin Bay
11-May	131	1	Marine
12-May	132	3	Newfoundland
13-May	133	3	Sable Island
14-May	134	2	Northeastern USA
15-May	135	2	Northeastern USA

2.10 Statistical Analysis

Statistical analysis was completed on the data set, and the results are presented throughout the thesis. For the Transect Study (JD 122 to 130) analysis was conducted for both aerosol and SO_2 data. The Transect Study (stations T1 to T6 (*Figure 2*-1)) was the primary focus of the thesis to determine if there were differences in oxidation pathways at different temperatures (illustrated by higher latitudes). For the aerosol data, only aerosols <7.2μm were used in the analysis, so that comparison of day and night aerosols could be conducted. The data were normally distributed for $\delta^{34}S$, $\delta^{34}S_{NSS}$, $\delta^{34}S_{SO2}$, PO_4^{3-}, MSA, MSA/NSS-SO_4^{2-} ratios, biogenic SO_2 and anthropogenic SO_2 thus F-tests and t-tests are appropriate.

Chapter Three: Results

3.1 Introduction

This chapter presents the results of the chemical and isotopic analyses for both sulphate aerosols and gaseous SO_2. The complete data set is presented in *Appendix III*. The results are divided into two main sections: the Lagrangian study and the Transect study. The Lagrangian study was closer to land and pollutant sources compared to the Transect study. Differences in DMS oxidation resulting from higher NO_3 concentrations and/or sources of aerosol sulphate due to the proximity of anthropogenic SO_2 emissions were expected to produce contrasting data for the Lagrangian and Transect studies. Photo-oxidation patterns differ diurnally; therefore there is a further division between day and night samples. In instances where the concentration or isotopic composition of a sample was not detected or below the detection limit of the mass spectrometer or the ion chromatograph, the sample is left blank. In instances where the analytical uncertainty is larger than ±0.4‰, error bars are shown. Standard deviations are represented using the notation SD.

3.2 Fuel and Oil Samples

Four fuel samples and two oil samples from the CCGS Hudson were analysed for $\delta^{34}S$. The average for the fuel samples was +4.0 (SD = 0.2‰ (n=7)). For the oil samples, the average was +2.5 (SD = 0.1‰ (n=2)).

3.3 Isotopic and Chemical Characterization; Lagrangian Study

3.3.1 Daytime Samples

Four daytime sample sets comprising 52 total sampling hours spanning 7 days were collected during the daytime Lagrangian study, April 25th to May 2nd (Julian Day 115-122 – hereafter Julian Date (JD) is given in parenthesis after the date). Some samples from the Lagrangian study were collected over a period of two or three days to ensure enough sulphur was present for analysis. Typically a minimum of 8 hours per sample was required to obtain sufficient material for isotope analysis. Interruptions in sampling due to the ship's motion or the direction of the wind relative to the ship's heading, to reduce ship-stack contamination, resulted in several samples with an insufficient number of hours during a single diel cycle. In instances where the sample was collected over a period of daytime diel cycles, but not at night, all the sample days are listed as the sample name. The chemical concentrations of the size segregated sample collected on April 25th & 26th (JD 115&116) had to be discounted as the flow rate of the hi-volume sampler was not constant. The chemical concentrations of the total particulate sample collected on April 29th & 30th (JD 119&120) also had to be discounted as the cover of the filter casing was not removed on the 30th (JD 120) which prevented aerosols from becoming trapped on the filter. The corresponding SO_2 filter was acceptable to report as SO_2 is present in a gaseous form, and the cover would not negatively affect the SO_2 sampling.

3.3.1.1 Sulphur Dioxide

Four SO_2 filters were collected during the daytime Lagrangian study on April 25th & 26th, April 27th & 28th, April 29th & 30th, and May 1st & 2nd (JD: 115&116, 117&118, 119&120, 121&122). The samples from April 27th & 28th (JD 117&118) and April 29th & 30th (JD 119 & 120) were both mistakenly labelled "H21C", resulting in two samples with the same label. For the mislabelled samples the SO_2 concentrations were within one standard deviation from the mean, which allows the interpretation of the data. $\delta^{34}S_{SO2}$ and SO_2 concentrations for the daytime Lagrangian samples are presented in *Table 3-1*. The average SO_2 concentration was 3000, SD = 1300ng·m^{-3} (n=4), with a mean isotopic value of +8.2, SD = 0.8‰ (n=4). Note that SO_2 samples were collected consecutively on a single high volume sampler dedicated to daytime sampling: if insufficient number sampling hours were collected in a single day, the filter was left in place to collect sample on consecutive days. No trends were apparent in either the $\delta^{34}S$ value or the concentration of SO_2.

3.3.1.2 Total Particulate

Figure 3-1 displays $\delta^{34}S$ and $\delta^{34}S_{NSS}$ for the daytime Lagrangian total particulate samples. Error bars have not been plotted on the graph as they are approximately twice the size of the symbols. $\delta^{34}S$ values for samples with uncertainties larger than 0.4‰ are shown with error bars throughout the thesis. Total $\delta^{34}S$ values, incorporating sea salt, anthropogenic and biogenic sulphate ranged between +2.8 and +16.9‰, with a mean of +8.9, (SD = 6.1‰). The range of $\delta^{34}S_{NSS}$values, where the

Table 3-1 – $\delta^{34}S_{SO2}$ (‰) and SO_2 concentrations (ngm^{-3}) for the Lagrangian daytime samples. Isotope values have a measurement error of 0.4‰ and concentration measurements have an error of 10%.

Sample	$\delta^{34}S_{SO2}$	SO_2
April 25 & 26 (JD 115&116)	+7.4	3190
H12C#1	+8.3	1890
H12C#2	+9.2	2120
May 1 & 2 (JD 121&122)	+7.9	4710

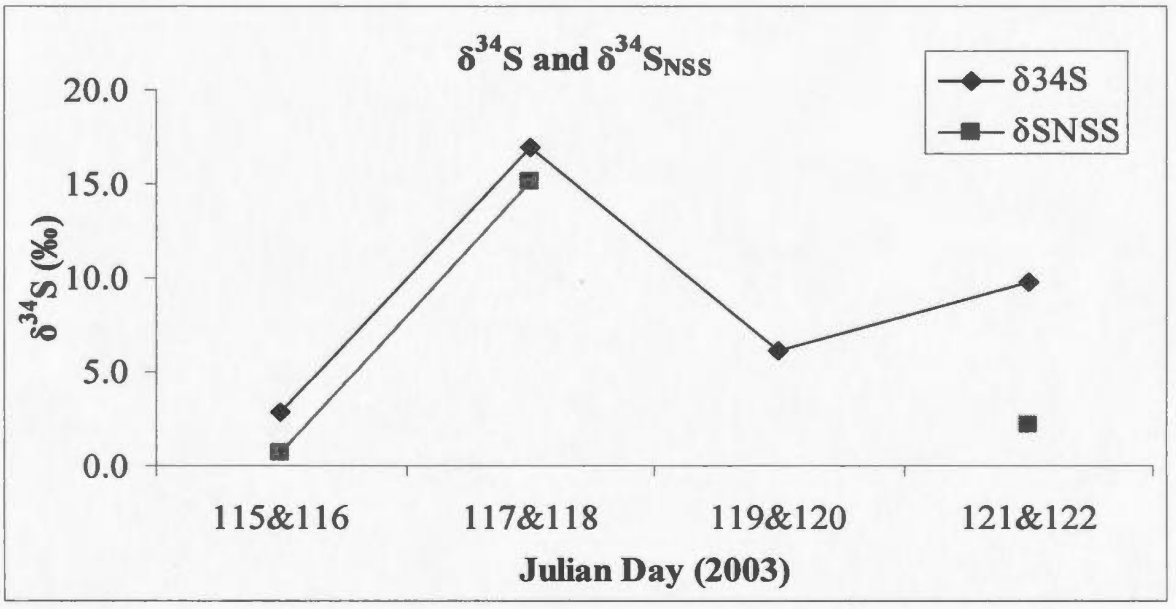

Figure 3-1 – $\delta^{34}S$ and $\delta^{34}S_{NSS}$ for daytime Lagrangian total particulate samples vs. Julian Day. $\delta^{34}S$ values have a measurement error of 0.4‰.

sea salt component has been removed, was +0.7 to +15.1‰, with a mean of +5.1 (SD = 6.7‰). Temporal trends were not apparent in these data.

The chemical concentrations for primary sea salt components, anions and cations for the daytime total particulate samples are presented in *Table 3-2*. The sea salt components (Na^+, Cl^-, Mg^{2+} and $SS\text{-}SO_4^{2-}$) all increased over this period, reaching a maximum on May 1st & 2nd (JD 121&122). The anions, (NO_3^-, SO_4^{2-} and $NSS\text{-}SO_4^{2-}$) followed a common trend as well; lower concentrations over the first two sampling periods were lower than on May 1st & 2nd (JD 121&122). Sulphate concentrations on May 1st & 2nd (JD 121&122) were much higher than for the remaining samples, and this sampling period coincides with the highest concentrations for all constituents, including SO_2 (*Table 3-1*), with the exception of MSA.

3.3.1.3 Size Segregated Samples

Daytime $\delta^{34}S$ and $\delta^{34}S_{NSS}$ values for the Lagrangian size segregated samples are shown in *Figure 3-2*. The range in $\delta^{34}S$ values for the daytime samples was +0.9 to +18.6‰ (mean = +8.0, SD = 5.6‰), while the range for $\delta^{34}S_{NSS}$ values was -4.1 to +14.8‰ (mean = +6.0, SD = 4.9‰). $\delta^{34}S$ values for aerosols 3.0-1.5μm diameters in size progressively increased from the beginning of the Lagrangian study to the end. It is worthwhile noting that the range in $\delta^{34}S$ values for all size fractions (except 0.95-0.49μm) was <3‰ on April 25th & 26th (JD 115&116) and for $\delta^{34}S_{NSS}$ on April 27th & 28th (JD 117&118). Since the sulphur isotope composition can be used to assess

Table 3-2 – Cation and anion concentrations (ngm^{-3}) for the daytime Lagrangian total particulate samples (sample from April 29 & 30 (JD 119& 120) discounted). Concentration measurements have an error of ±10%.

	Julian Day, 2003			
	115&116	**117&118**	**119&120**	**121&122**
Na^+		927		5182
Cl^-	320	1686		8483
Mg^{2+}	35	110		765
SS-SO_4^{2-}	74	232		1607
NO_3^-	229	220		1100
SO_4^{2-}	707	737		3943
NSS-SO_4^{2-}	632	505		2336
PO_4^{2-}				
MSA	19.4	16.1		22.9
Ca^{2+}	139	181		520
K^+	14	49		231
NH_4^+				262

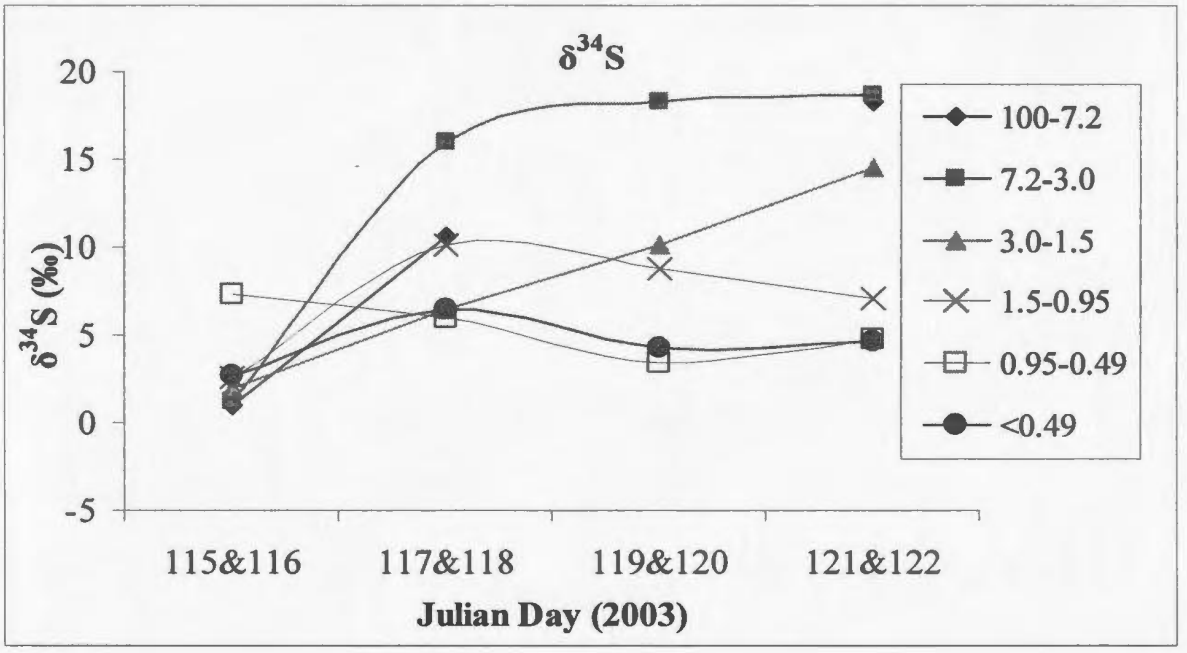

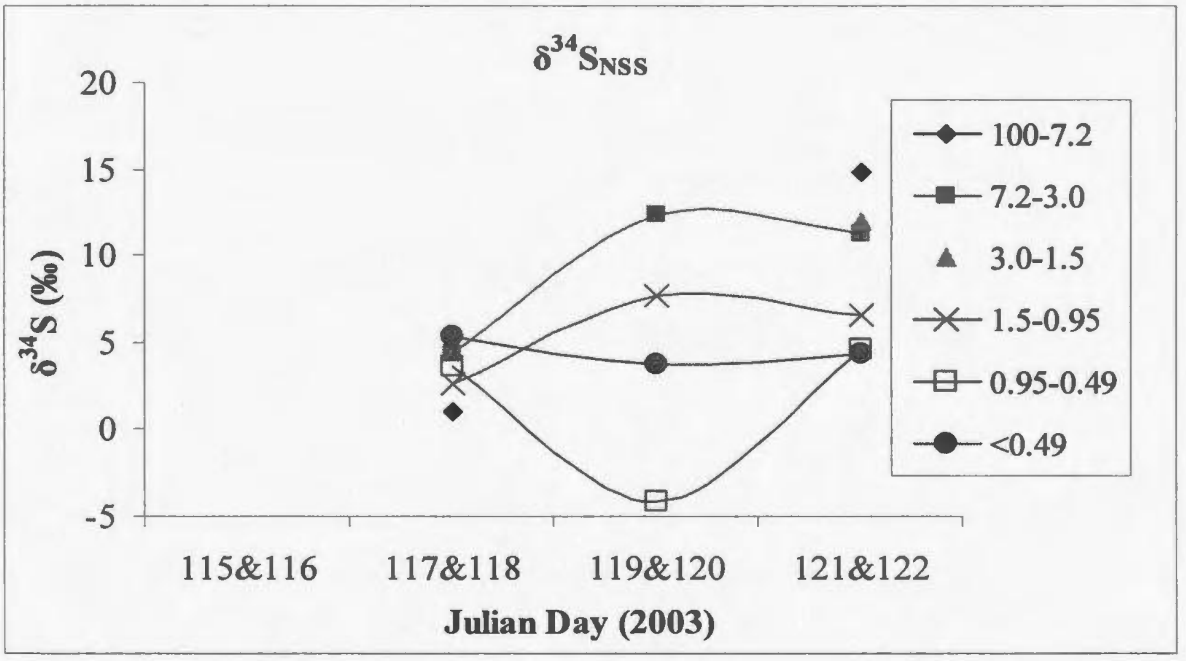

Figure 3-2 – $\delta^{34}S$ (‰) (top) and $\delta^{34}S_{NSS}$ (‰) (bottom) for daytime Lagrangian size segregated samples, where the legend shows aerodynamic diameter of the aerosols (μm). $\delta^{34}S$ values have a measurement error of ±0.4‰.

sulphate sources, it suggests the same source is present in almost all size fractions on these two days.

Figures 3-3a-d presents sea salt component (Na^+, Cl^-, Mg^{2+} and $SS\text{-}SO_4^{2-}$) concentrations for the daytime size segregated Lagrangian samples. Sodium and Cl^- (*Figures 3-3 a&b*) were concentrated in the 100-7.2μm and 7.2-3.0μm size fraction, with concentrations generally decreasing with size. Sea salt sulphate ($SS\text{-}SO_4^{2-}$, *Figure 3-3d*) was also concentrated in the same size fractions as Cl^- and followed a similar trend.

Anion concentrations (NO_3^-, SO_4^{2-}, $NSS\text{-}SO_4^{2-}$ and MSA) are presented in *Figures 3-4 a-d.* Most interesting is that SO_4^{2-}, $NSS\text{-}SO_4^{2-}$ and MSA (*Figures 3-4 b,c&e* respectively) concentrations were significantly greater in the smallest size fraction <0.49μm compared to the other fractions, but not NO_3^- (*Figure 3-4a*).

Cation concentrations (Ca^{2+}, K^+ and NH_4^+) for the size segregated daytime Lagrangian samples are displayed in *Figure 3-5 a-c*. Ammonium was rarely above the detection limit, except in the smallest size fraction on April 29th & 30th (JD 119&120) and May 1st & 2nd (JD 121&122) (*Figure 3-5c*) and the range in K^+ concentrations between the different size fractions was generally small (*Figure 3-5b*).

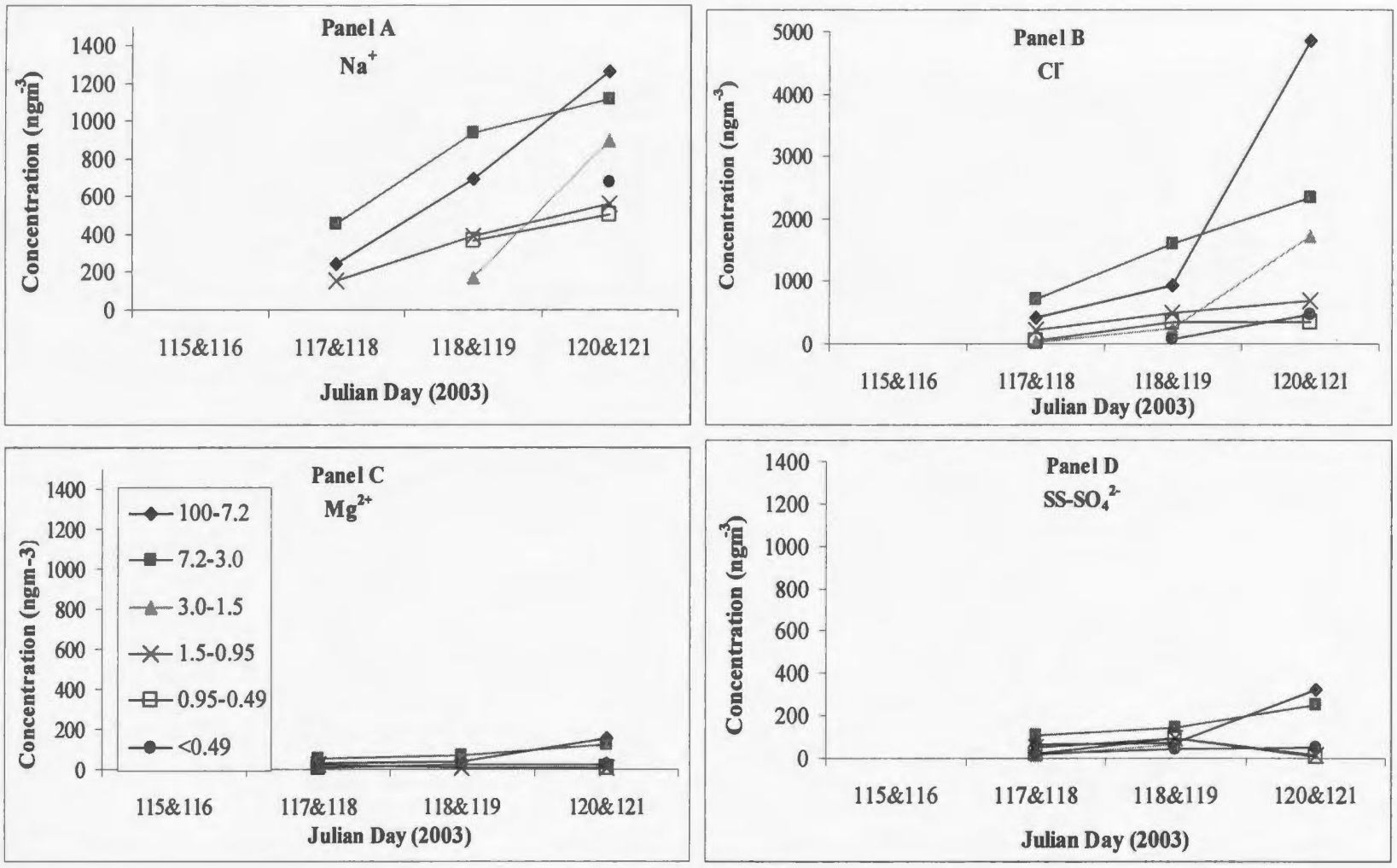

Figure 3-3 – Sea salt component concentrations (ngm^{-3}) for the Lagrangian daytime size segregated samples panels A-C. Concentration measurements have an error of ±10%.

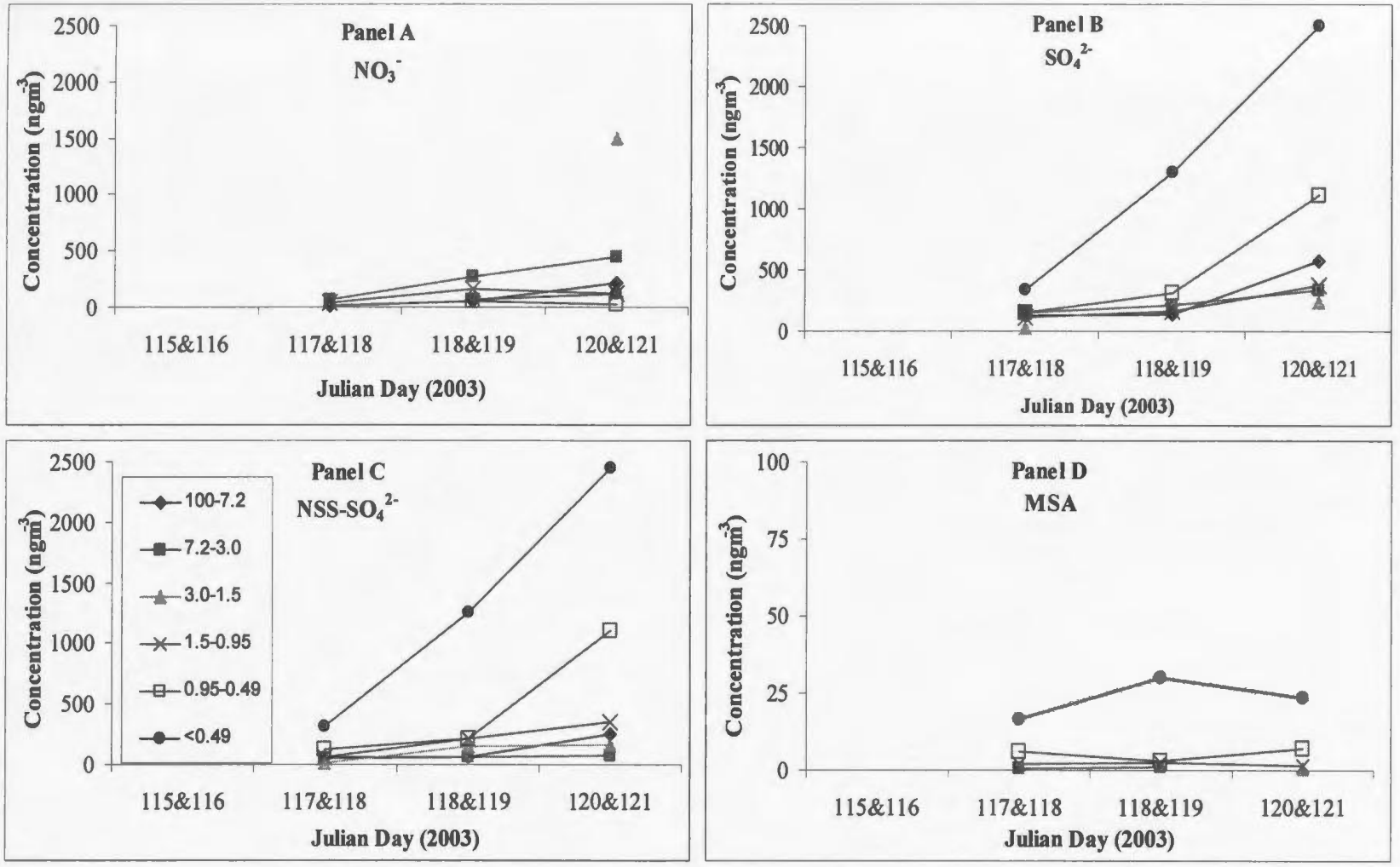

Figure 3-4 – Anion concentrations (ngm^{-3}) for the Lagrangian daytime size segregated samples panels A-C. Concentration measurements have an error of ±10%.

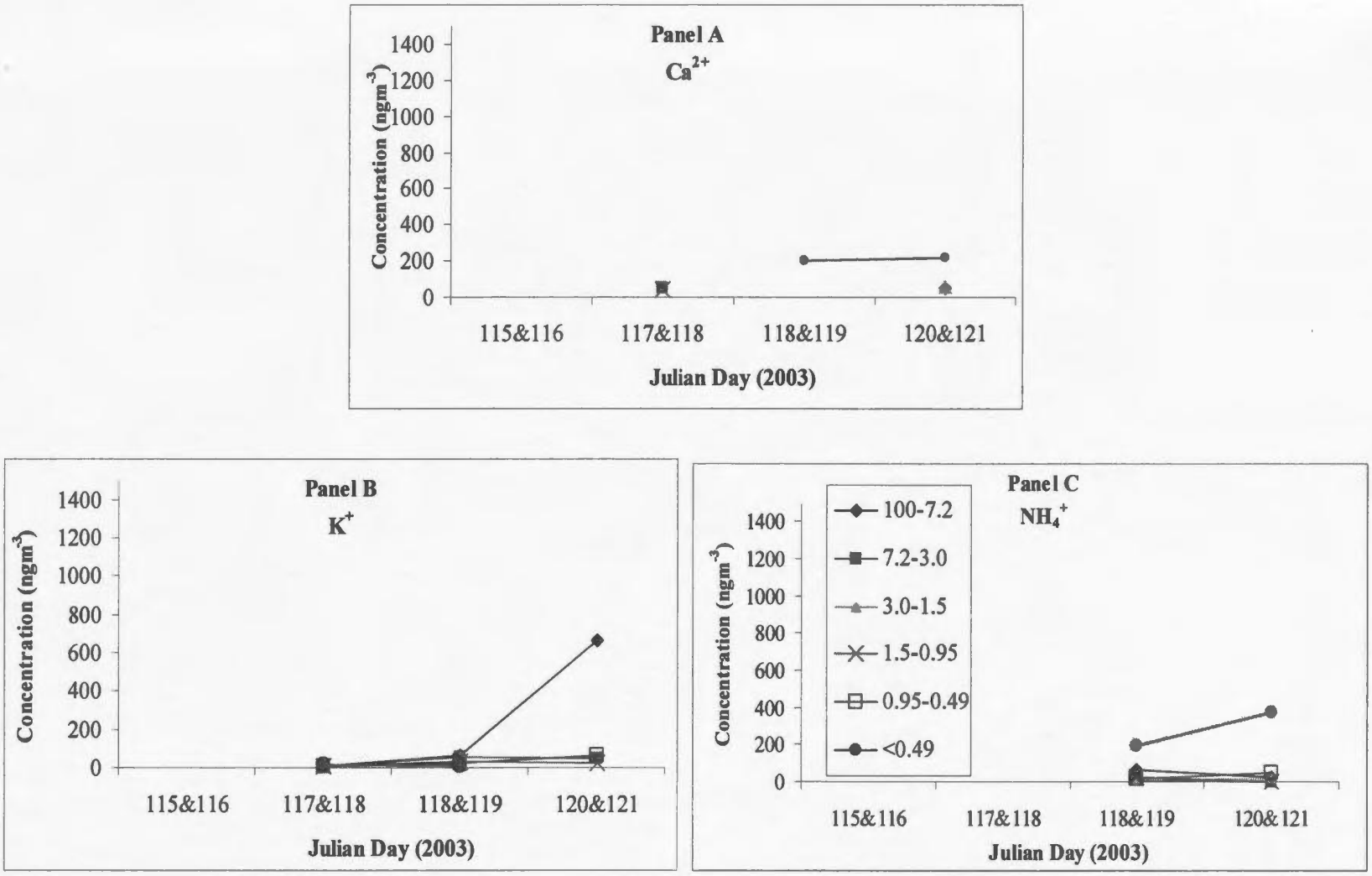

Figure 3-5 – Cation concentrations (ngm^{-3}) for the Lagrangian daytime size segregated samples panels A-C. Concentration measurements have an error of ±10%.

3.3.2 Night-time Samples

Two sample sets were collected over 30 hours, from April 25th to April 30th (JD 115-120) during the night-time Lagrangian Study. The samples were collected on April 26th & 27th (JD 116&117) and April 28th to 30th (JD 118-120).

3.3.2.1 Sulphur Dioxide

Table 3-3 shows $\delta^{34}S_{SO2}$ (‰) and SO_2 concentrations (ngm^{-3}) for the night Lagrangian SO_2 samples. The sulphur isotope composition of the two samples, April 26th & 27th (JD 116&117), and April 28th to 30th (JD 118-120) was relatively uniform, (mean = +13.4, SD = 0.4‰) and the concentrations were similar (mean = 1110, SD =263ngm^{-3}).

3.3.2.2 Total Particulate

$\delta^{34}S$ and $\delta^{34}S_{NSS}$ values for the night total particulate Lagrangian samples are found in *Table 3-4*. The average $\delta^{34}S$ value for total sulphate was lower than that for the SO_2 samples; +5.7 (SD = 2.3‰) versus +13.4 (SD=0.4‰), and the $\delta^{34}S_{NSS}$ value had an average that was even lower, +2.1 (SD = 0.2‰). The concentrations of primary sea salt components, anions and cations for the night-time total particulate samples are presented in *Table 3-5*. The concentrations of the night samples spanned a similar range to those for daytime samples (*Table 3-2*). The sample collected on April 28th – 30th (JD 118-120) had high MSA concentrations which were similar to the largest concentrations found in the smallest size fraction (<0.49μm) of the daytime Lagrangian study which reached a maximum on JD 119&120.

Table 3-3 – $\delta^{34}S_{SO2}$ (‰) and SO_2 concentrations (ngm^{-3}) for the night-time Lagrangian SO_2 samples. $\delta^{34}S$ values have a measurement error of ±0.4‰ and concentration measurements have an error of ±10%.

Date	$\delta^{34}S_{SO2}$	SO_2
April 26 & 27 (JD 116&117)	+13.6	1290
April 28 - 30 (JD 118-120)	+13.1	921

Table 3-4 - $\delta^{34}S$ and $\delta^{34}S_{NSS}$ for the night Lagrangian total particulate samples. $\delta^{34}S$ values have a measurement error of ±0.4‰ and concentration measurements have an error of ±10%.

Date	Size (um)	$\delta^{34}S$	$\delta^{34}S_{NSS}$
April 26 & 27 (JD 116&117)	<10	+4.0	+1.9
April 28 - 30 (JD 118-120)	<10	+7.3	+2.2

Table 3-5 – Concentrations (ngm^{-3}) of anions and cations for the total particulate night-time Lagrangian samples. Concentration measurements have an error of ±10%.

	116&117	118-120
Na^+		1650
Cl^-	294	2430
Mg^{2+}	47.2	280
$SS\text{-}SO_4^{2-}$	99.0	588
NO_3^-	264	493
SO_4^{2-}	908	2160
MSA	22.7	25.6
$NSS\text{-}SO_4^{2-}$	809	1570
PO_4^{3-}		
Ca^{2+}	142	371
K^+	43.7	324
NH_4^+	37.1	82.9

3.3.2.3 Size Segregated

The range in isotope composition for the night-time Lagrangian size-segregated samples was +4.5 to +15.7‰ (mean = +9.0, SD = 3.5‰) for $\delta^{34}S$ and +0.2 to +13.2‰ (mean = +5.4, SD = 3.8‰) for $\delta^{34}S_{NSS}$ (*Table 3-6*) and exhibit a similar range to those for Lagrangian day size-segregated aerosols (*Figure 3.2*) Sea salt, anion and cation concentrations for the two night size segregated samples are displayed in *Tables 3-7, 3-8 & 3-9* respectively. Sodium was not above the detection limit for any of the samples collected on April 26th & 27th (JD 116&117). Chloride concentrations were higher in the April 28thto30th (JD 118-120) sample, and had the highest concentrations in the 7.2-3.0μm size fraction. Sea salt sulphate, NO_3^-, NSS-SO_4^{2-}, MSA and NH_4^+ concentrations were highest in the <0.49μm size fraction.

3.4 Isotopic and Chemical Characterization; Transect Study

Two samples collected during the Transect study on day and the night of May 13th (JD 133) were both incorrectly labelled as daytime samples. The samples were inspected and after comparative analysis of concentrations of Ca^{2+}, NO_3^- and SO_4^{2-} from samples collected prior and directly after the incorrectly labelled samples, the samples were assigned what is believed to be their proper designation. Calcium, NO_3^- and SO_4^{2-} concentrations showed relatively stable patterns that were distinguishable between the day and night. These patterns were used to distinguish which sample was a daytime sample, and which was a night sample. Samples collected on May 13th (JD 133) are flagged as there is a possibility the designation could be incorrect.

Table 3-6 – Night size segregated samples, $\delta^{34}S$ (‰) and $\delta^{34}S_{NSS}$ (‰) for the Lagrangian study. $\delta^{34}S$ values have a measurement error of ±0.4‰.

	April 26 & 27 (JD 116&117)	
Size (um)	**$\delta^{34}S$**	**$\delta^{34}S_{NSS}$**
10-7.2	+10.7	+0.2
7.2-3.0	+9.3	+4.2
3.0-1.5	+9.8	+4.3
1.5-0.95	+6.9	+3.4
0.95-0.49		
<0.49	+4.7	+2.2
	April 28 - 30 (JD 118-120)	
Size (um)	**$\delta^{34}S$**	**$\delta^{34}S_{NSS}$**
10-7.2	+12.0	+7.8
7.2-3.0	+15.7	+13.2
3.0-1.5	+12.4	+10.2
1.5-0.95	+7.2	+6.5
0.95-0.49	+6.4	+4.9
<0.49	+4.5	+3.0

Table 3-7 – Primary sea salt component concentrations (ngm^{-3}) for night Lagrangian size segregated samples. Concentration measurement uncertainties are ±10 %. Empty cells indicate samples were below detection limit.

	April 26 & 27 (JD 116&117)			
Size (um)	**Na^+**	**Cl^-**	**Mg^{2+}**	**SS-SO_4^{2-}**
10-7.2		10.9	23.1	48.6
7.2-3.0		106	25.5	53.5
3.0-1.5			29.6	62.2
1.5-0.95			25.9	54.4
0.95-0.49			5.8	12.2
<0.49			35.3	74.2
	April 28 - 30 (JD 118-120)			
Size (um)	**Na^+**	**Cl^-**	**Mg^{2+}**	**SS-SO_4^{2-}**
10-7.2	267	363	12.4	26.0
7.2-3.0	426	549	21.1	44.4
3.0-1.5	270	304	13.5	28.4
1.5-0.95	295	247	3.5	7.3
0.95-0.49	325	342	11.7	24.6
<0.49	349	52.3	23.4	49.1

Table 3-8 – Anion concentrations (ngm^{-3}) for night Lagrangian size segregated samples. Concentration measurement uncertainties are ±10 %. Empty cells indicate samples were below detection limit.

	April 26 & 27 (JD 116&117)				
Size (um)	**NO_3^-**	**NSS-SO_4^{2-}**	**SO_4^{2-}**	**PO_4^{3-}**	**MSA**
10-7.2	20.0	43.2	91.8		
7.2-3.0	118	120	173		0.87
3.0-1.5	32.8	123	185		0.87
1.5-0.95	35.6	216	270		2.55
0.95-0.49	12.9	17.5	29.8		0.07
<0.49	105	473	547		18.6
	April 28 - 30 (JD 118-120)				
Size (um)	**NO_3^-**	**NSS-SO_4^{2-}**	**SO_4^{2-}**	**PO_4^{3-}**	**MSA**
10-7.2	20.2	52.2	78.2		
7.2-3.0	75.7	90.5	135		1.24
3.0-1.5	58.9	109	137		1.41
1.5-0.95	57.7	159	166		2.41
0.95-0.49	71.8	225	249		3.83
<0.49	74.6	507	556		8.32

Table 3-9 – Cation concentrations (ngm^{-3}) of night Lagrangian size segregated samples. Concentration measurement uncertainties are ±10 %. Empty cells indicate samples were below detection limit.

	April 26 & 27 (JD 116&117)		
Size (um)	**Ca^{2+}**	**K^+**	**NH_4^+**
10-7.2	86.5		4.8
7.2-3.0	88.2		8.7
3.0-1.5	122		3.9
1.5-0.95	109		10.8
0.95-0.49	39.1	6.5	7.9
<0.49	180		16.3
	April 28 - 30 (JD 118-120)		
Size (um)	**Ca^{2+}**	**K^+**	**NH_4^+**
10-7.2		8.1	21.6
7.2-3.0		17.8	15.1
3.0-1.5	31.4	14.2	15.5
1.5-0.95		15.9	19.8
0.95-0.49	27.9	16.7	20.1
<0.49	82.1	4.4	23.7

3.4.1 Daytime Samples

Twelve sample sets were collected during the daytime Transect study, from May 3rd to May 15th (JD 123-135). Ideally a filter set was sampled over 8 hours in one day. However, interruptions during periods when oceanographic sampling was conducted and the high volume samplers were turned off meant that less than 8 hours of sampling time was often achieved in one day. In such instances, the filters were left in place overnight with the high volume samplers turned off and the sampling was resumed for the following one or two days (as is the case with May 4th & 5th, JD 124&125).

3.4.1.1 Sulphur Dioxide

Figure 3-6 displays $\delta^{34}S_{SO2}$ (‰) values and SO_2 concentrations ($ng \cdot m^{-3}$) for the daytime Transect SO_2 samples so that trends, particularly during the north-south transect (JD 126-130), could be evaluated. The range in $\delta^{34}S_{SO2}$ values was +5.8‰ to +16.4‰ (mean = +11.9, SD = 3.0‰), with a range of concentrations from 229 to 1920 $ng \cdot m^{-3}$ (mean = 948, SD = 623ngm^{-3}). Sulphur dioxide concentrations generally declined as the ship moved from south to north along the transect (JD 126 to JD 130, *Figure 3-6*) and approached values similar to those measured by Pszenny *et al.* (1990) (30-301ngm^{-3}) reported for a cruise of the North Atlantic during the summer of 1989. The isotope compositions of the samples showed little variation and remained relatively steady after a peak on May 6th (JD 126). It is worth noting that the highest SO_2 concentration (1920ngm^{-3}) occurred one day after the $\delta^{34}S_{SO2}$ peak and the

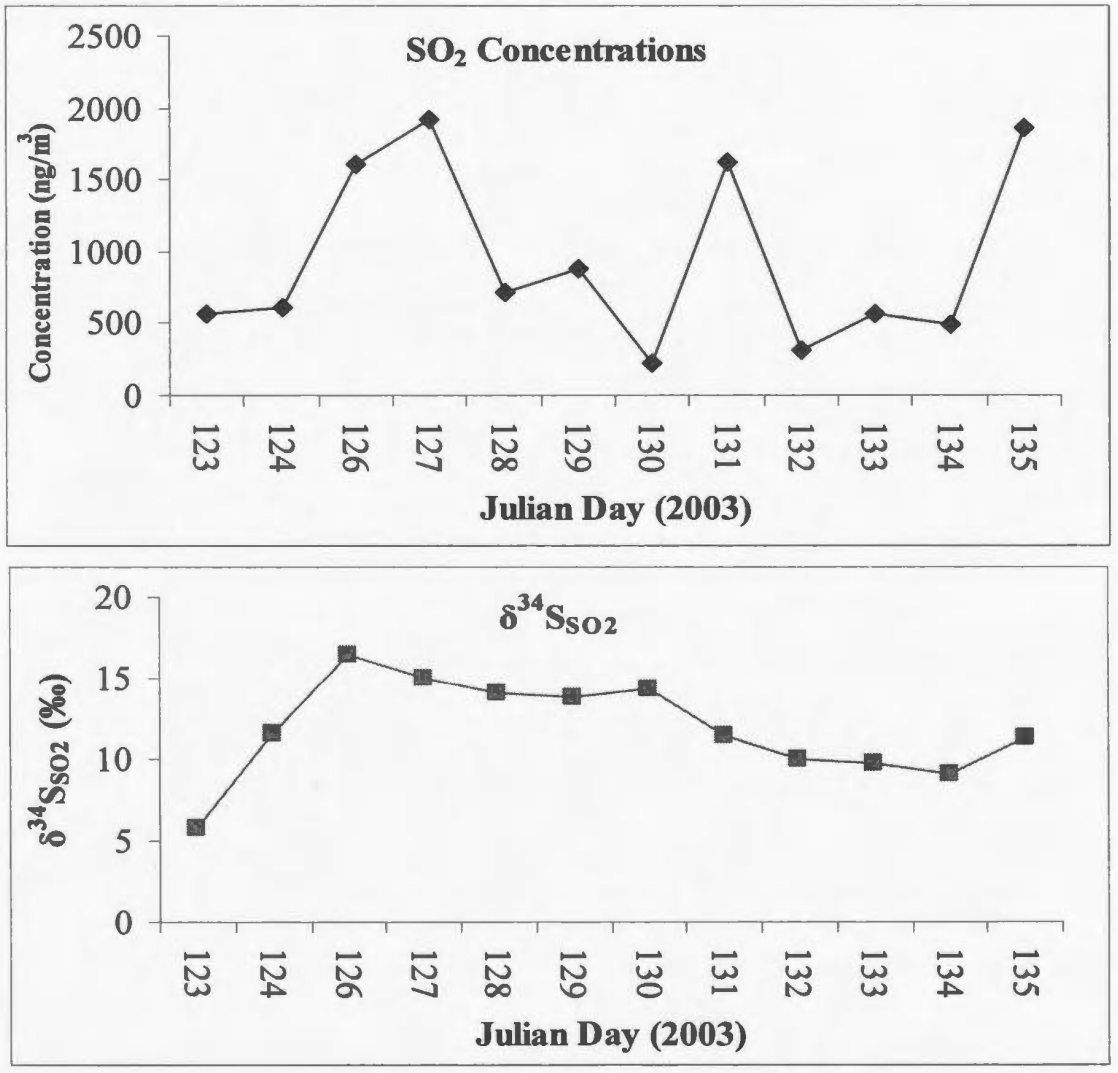

Figure 3-6 – SO_2 concentrations (ngm^{-3}, top panel) and $\delta^{34}S_{SO2}$ (‰, bottom panel) for the daytime transect SO_2 samples. $\delta^{34}S$ values have a measurement error of ±0.4‰ and concentration measurements have an error of ±10%.

lowest $\delta^{34}S_{SO2}$ value was found upon leaving the SOLAS Mooring site near Sable Island and transiting to the Southerly stations (JD 123, T-T2 (*Figure 2-1*)).

3.4.1.2 Total Particulate

The range of $\delta^{34}S$ and $\delta^{34}S_{NSS}$ values for the daytime total particulate samples can be seen in *Figure 3-7*. There was a progressive decrease in both $\delta^{34}S$ and $\delta^{34}S_{NSS}$ from May 6th (JD 126) until May 11th (JD 131) as the ship transited from south to north along 45°W from T3 to T6, (JD 126-129) and back to T5 again (JD 130) (*Figure 2-1).* The most negative $\delta^{34}S_{NSS}$ values were observed as the ship transited southward from station T6 to T5, and from station T5 to L1 (JD 130, JD131). These dates coincide with the closest approach of the ship to Newfoundland (*Figure 2-1*). Note that there is no corresponding decrease in $\delta^{34}S_{SO2}$ to match the decrease in the $\delta^{34}S$ and $\delta^{34}S_{NSS}$ values (*Figure 3-6*).

Figure 3-8 shows the concentrations of the primary sea salt components (Na^+, Cl-, Mg^{2+} and SS-SO_4^{2-}). Sea salt components all follow the same general trend, with a decrease from the start of the Transect (May 3rd) (JD 123), resulting in low concentrations on May 9th (JD 129) at the most northerly station T6 (*Figure 2-1*). Sodium and Cl^- had the highest concentrations of all the sea salt components, while

Figure 3-9 presents the remaining anion concentrations (NO_3^-, SO_4^{2-}, NSS-SO_4^{2-}, PO_4^{3-} and MSA) for the daytime total particulate samples. Nitrate and NSS-SO_4^{2-} follow a very similar trend from May 3rd to 7th (JD 123-127) as the ship transited

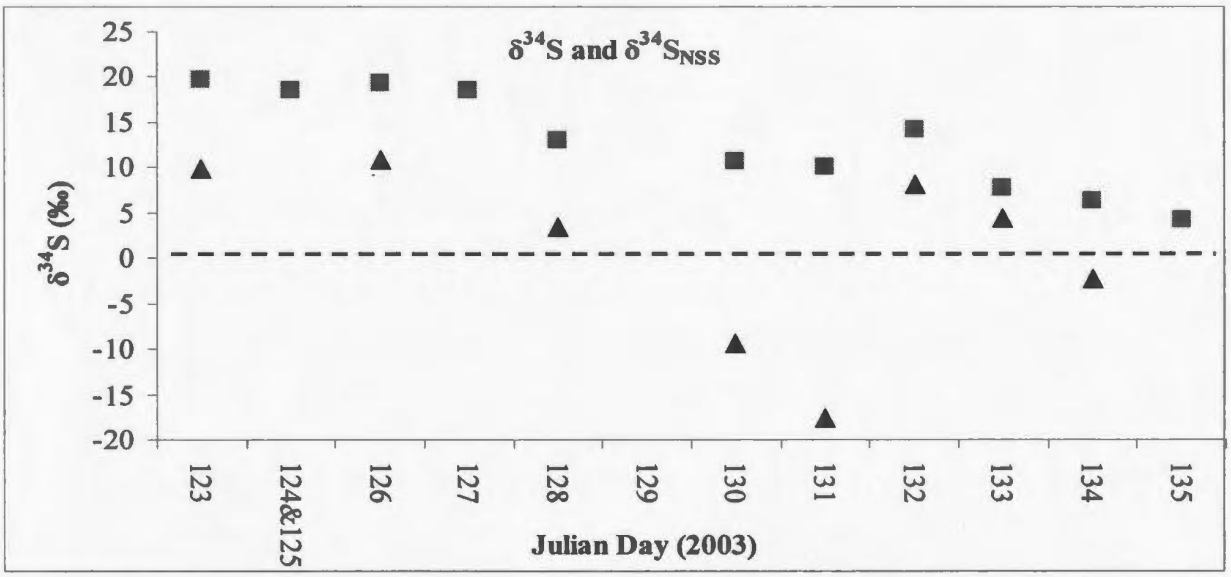

Figure 3-7 – $\delta^{34}S$ (‰, squares) and $\delta^{34}S_{NSS}$ (‰, triangles) for the daytime total particulate Transect samples. Isotope values have a measurement error of 0.±4‰.

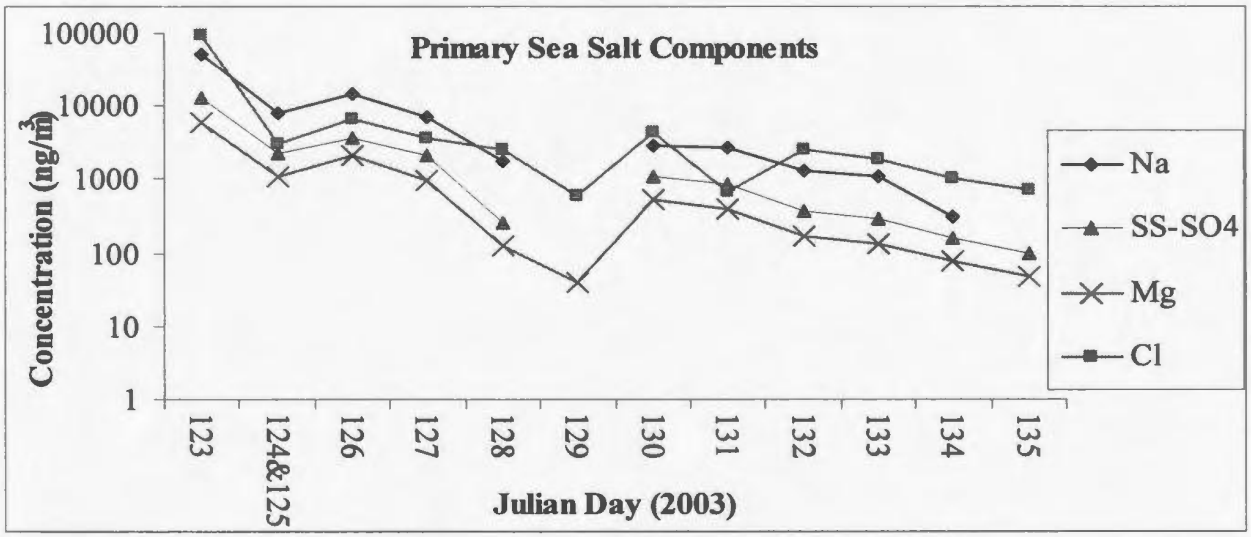

Figure 3-8 – Concentrations (ngm^{-3}) of the primary sea salt components for the daytime total particulate Transect samples (note: logarithmic scale). Measurement uncertainties are ±10%.

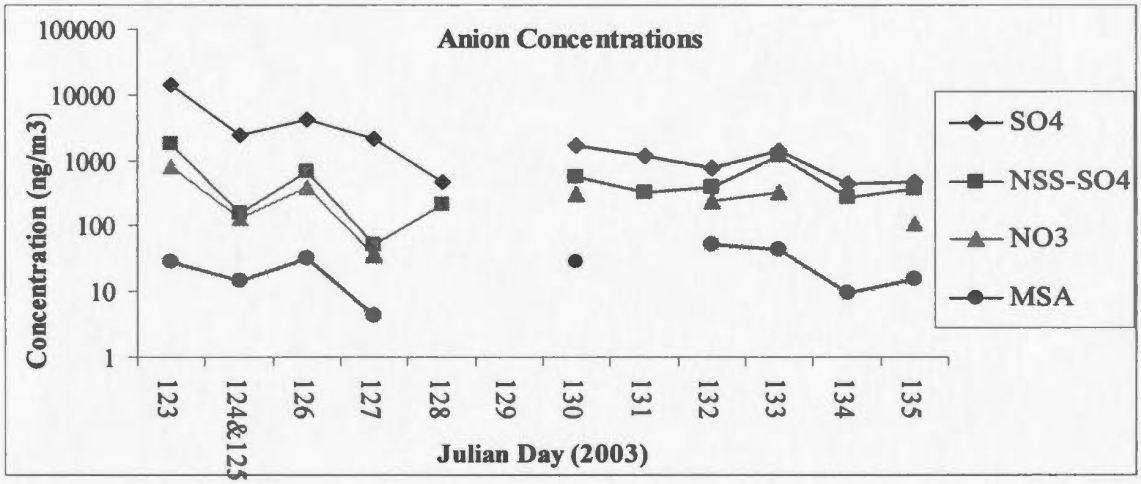

Figure 3-9 – Anion concentrations (ngm^{-3}) for the daytime total particulate Transect samples (note: logarithmic scale). Concentration measurements have an error of ±10%.

Mg^{2+} had the lowest concentrations. Contour plots of primary sea salt concentrations vs. latitude and longitude are shown in *Appendix III.2*.

from T1 in the Gulf Stream to T4 in the Subtropical Gyre (*Figure 2-2*). Sulphate experienced a maximum concentration on May 3rd (JD 123) (14400ngm^{-3}), near station T1, the same day as a maximum in NSS-SO_4^{2-}concentration was observed (1150ngm^{-3}). These maximum concentrations occurred one day after high (1620ngm^{-3}) SO_2 concentrations were observed (*Figure 3-6*). Methanesulphonic acid concentrations peaked (51.3ngm^{-3}) on May 12th (JD 132) as the ship crossed the Labrador Current (pink region in *Figure 2-2*). Concentrations for the anions were all below the detection limit on May 9th (JD 129) when the ship reached the most Northerly station, T6 (*Figure 2-1*). Contour plots of anion concentrations vs. latitude and longitude are presented in *Appendix III.2*.

Cations (Ca^{2+}, K^+ and NH_4^{2+}) concentrations for the daytime total particulate samples are displayed in *Figure 3-10*. Calcium and K^+ follow a similar trend for all samples with exceptions on May 7th (JD 127) and 11th (JD 131), when K^+ had higher concentrations than Ca^{2+}. Due to the low concentrations of NH_4^+, there were few data, with most concentrations falling below 250ngm^{-3}. None of the cations had concentrations above detection limit on May 14th and 15th (JD 134&135). Contour plots of cation concentrations vs. latitude and longitude are found in *Appendix III.2*.

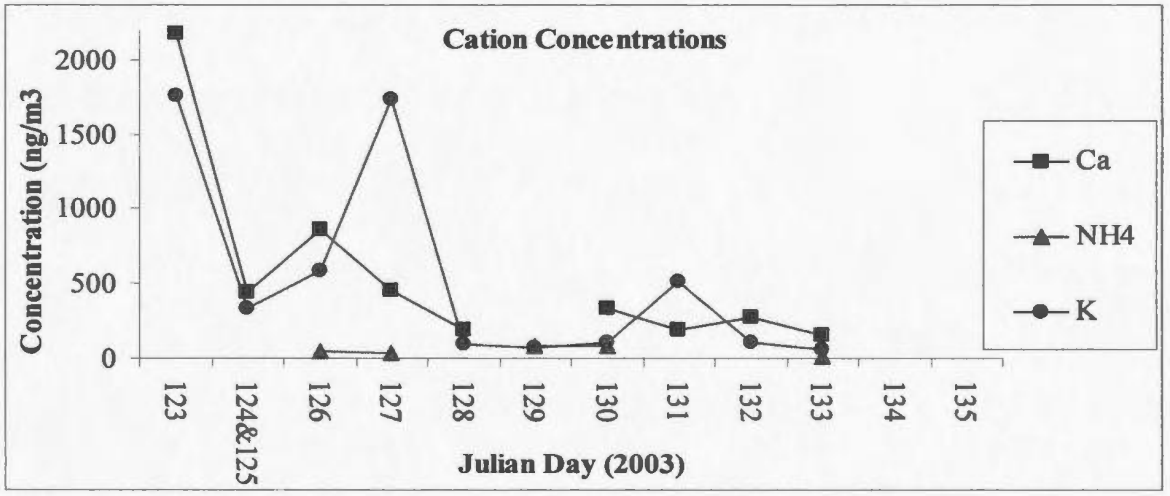

Figure 3-10 – Cation concentrations (ngm^{-3}) for the daytime total particulate Transect samples. Measurement uncertainties are ±10%.

3.4.1.3 Size Segregated

$\delta^{34}S$ and $\delta^{34}S_{NSS}$ values for the size segregated daytime samples are displayed in *Tables 3-10 & 3-11*. The $\delta^{34}S$ values for the two largest size fractions (100-7.2μm and 7.2-3.0μm) follow a similar trend, and generally had higher $\delta^{34}S$ values than the smaller size fractions. Negative $\delta^{34}S_{NSS}$ values were found on May 6th, 7th, 10th, 11th, 12th and 14th (JD 126, 127, 130, 131, 132, and 134). It is worthwhile noting that the ship was headed toward Newfoundland on JD 130 and 131 and that the lowest δ^{34}Snss values for total particulate sulphate were also found on May 11th (JD 131) as the ship passed Newfoundland. Aside from three negative δ^{34}Snss values in the course aerosol fraction on JD 129, 131 and 133, lighter isotopic values in the Aitken range were observed when the ship was closer to Newfoundland and/or station T4 (*Figure 2-1*).

Figures 3-11a-d displays the concentrations of the primary sea salt components, (Na^+, Cl^-, Mg^{2+} and SS-SO_4^{2-}). A trend similar to what was observed for $\delta^{34}S$ values, where sea salt components decreased as the ship moved away from the Lagrangian site and the shore at the beginning of the transect (May 3rd) (JD 123), and levelled off after May 7th (JD 127) at the start of the north-south transect (*Figure 2-1*), were observed for the primary sea salt components. It is very interesting to note that Na^+ (*Figure 3-11a*) as well as Mg^{2+} (*Figure 3-11b*) and therefore SS-SO_4^{2-} (*Figure 3-11c*) were dominantly found in the largest size fraction (100-7.2 υm) from JD 123 (T1) until Julian day 127 (T4) but a switch occurred after that point. After station T4, Na^+

Table 3-10 – $\delta^{34}S$ (‰) for daytime size segregated Transect samples. Uncertainties greater than ±0.4‰ are shown in parentheses.

	Julian Day					
Size	**123**	**124&125**	**126**	**127**	**128**	**129**
100-7.2	20.5	17.2	19.5	18.2		15.8 (5.0)
7.2-3.0	20.7	16.4	18.4	15.6		22.0
3.0-1.5	19.3		15.2	7.7 (2.0)		
1.5-0.95	13.9	6.8 (2.0)	12.8	5.5		11.6 (5.0)
0.95-0.49	14.7		9.4	3.9	20.3	
<0.49	8.7		4.3	3.2	8.1	5.4
	Julian Day					
Size	**130**	**131**	**132**	**133**	**134**	**135**
100-7.2	10.0		11.1	12.6 (5.0)	10.5	13.4
7.2-3.0	14.8		14.3 (5.0)		17.6 (5.0)	11.9
3.0-1.5				8.9 (5.0)	14.2	10.9
1.5-0.95	8.4		11.5 (5.0)	7.4 (5.0)	7.5 (5.0)	9.8
0.95-0.49				4.3 (5.0)	5.6	5.5
<0.49	4.6	5.1	10.9	3.6	5.2	4.8

Table 3-11 – $\delta^{34}S_{NSS}$ (‰) for the daytime size segregated Transect samples. $\delta^{34}S$ values have a measurement error of ±0.4‰.

	Julian Day					
Size	**123**	**124&125**	**126**	**127**	**128**	**129**
100-7.2	7.8		5.0			-5.8
7.2-3.0		13.7	5.4	6.0		22.7
3.0-1.5	17.5		12.0			
1.5-0.95	12.2		11.0	-9.4		
0.95-0.49				-19.1		
<0.49	7.1		-0.3	1.6	4.3	3.2
	Julian Day					
Size	**130**	**131**	**132**	**133**	**134**	**135**
100-7.2		-22.1		-5.5	2.9	
7.2-3.0	-3.4				3.5	
3.0-1.5					6.5	3.9
1.5-0.95						3.9
0.95-0.49					4.3	3.3
<0.49	3.1	-8.0	7.2	1.2	3.7	3.9

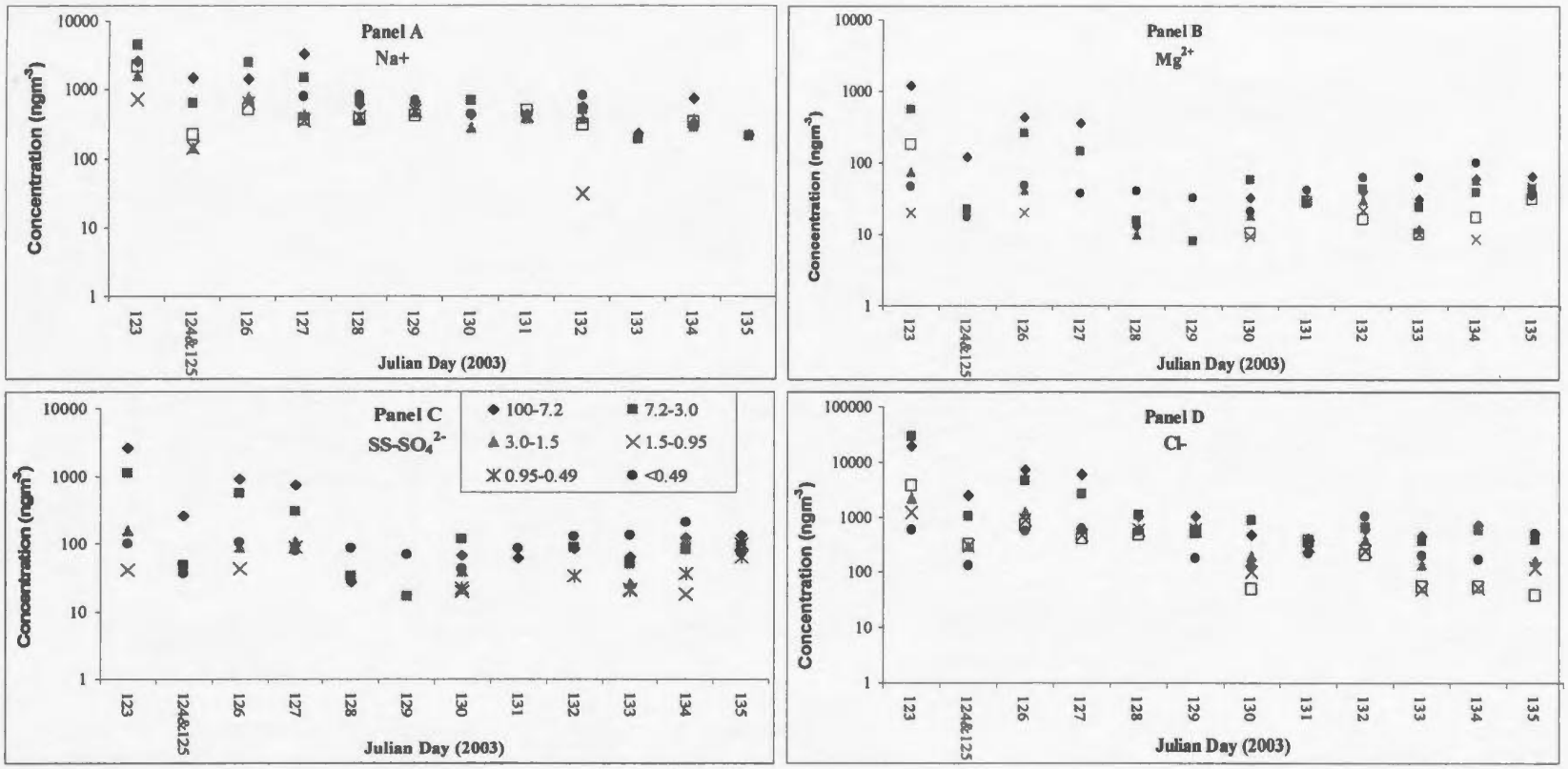

Figure 3-11 – Primary sea salt components for the daytime size segregated Transect samples, labelled panels A-D. (Note: logarithmic scale). Legend indicates aerodynamic size (μm). Concentration measurements have an error of ±10%.

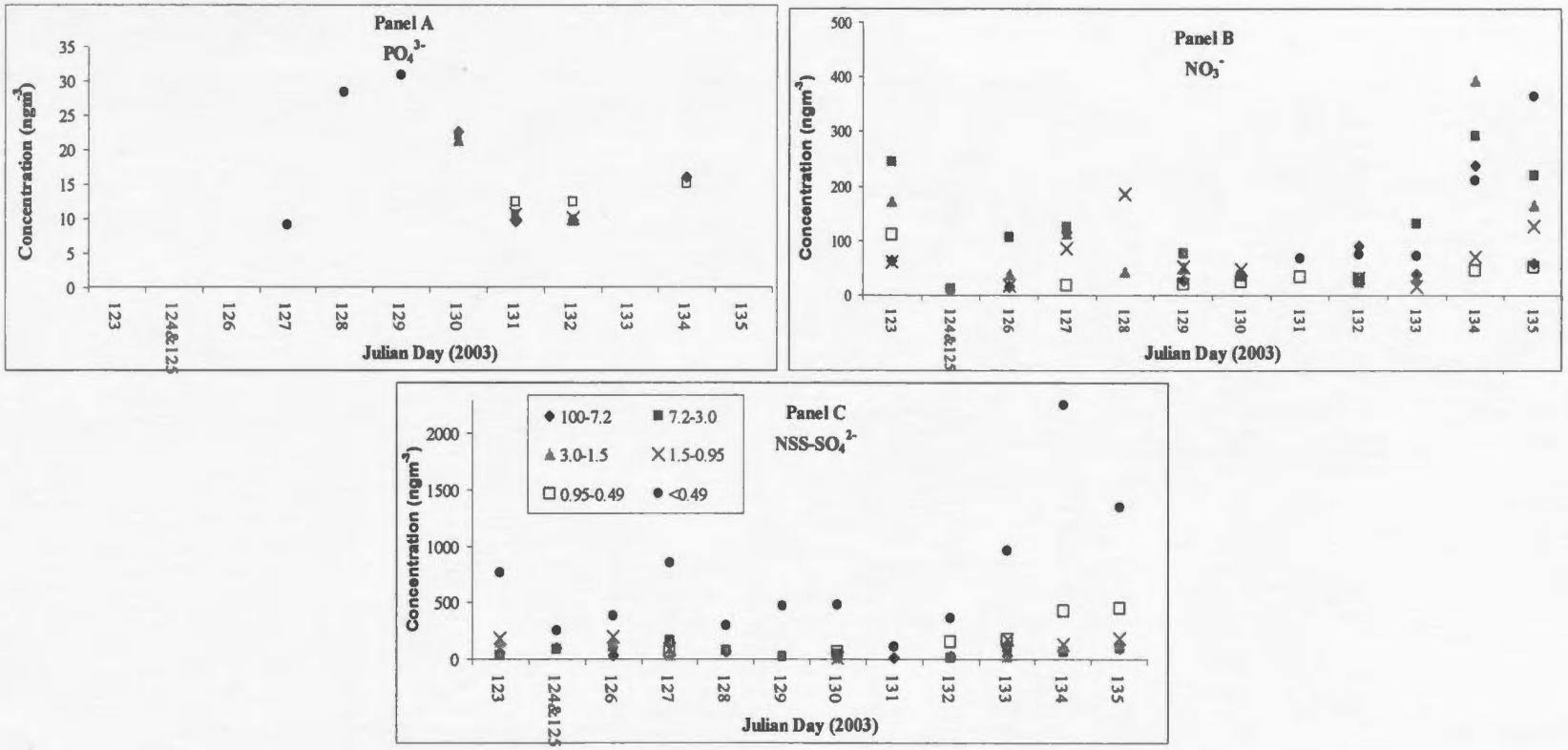

Figure 3-12- Anion concentrations (ngm^{-3}) for the daytime size segregated Transect samples labelled panels A-C. Legend indicates aerodynamic size (μm). Concentration measurements have an error of ±10%.

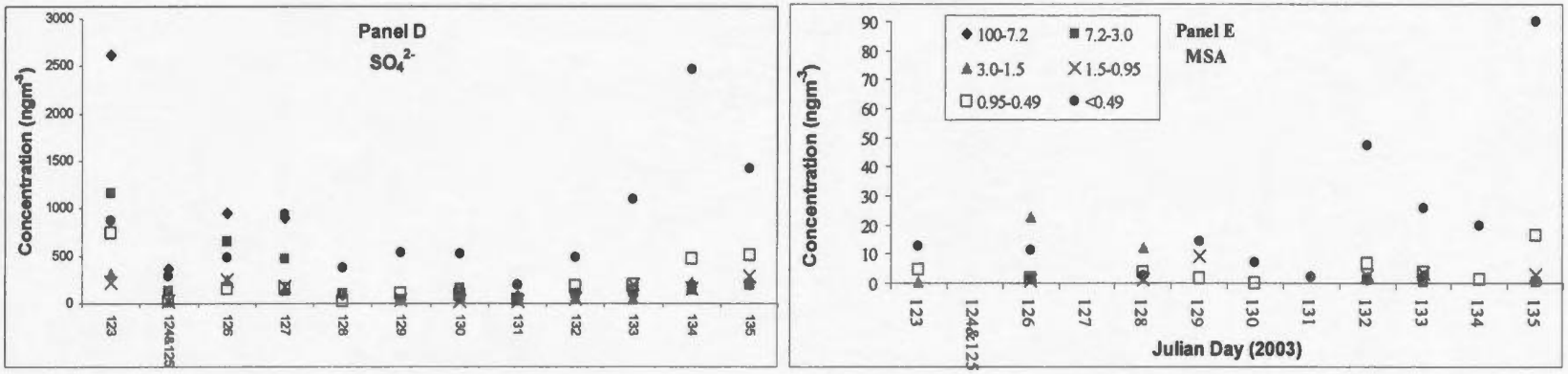

Figure 3-12- Anion concentrations (ngm^{-3}) for the daytime size segregated Transect samples labelled panels D-E.

concentrations were highest in the smallest aerodynamic aerosol size fraction (JD 128 to 134, except 130). The remainder of the anions (NO_3^-, SO_4^{2-}, NSS-SO_4^{2-}, PO_4^{3-} and MSA) are presented in *Figures 3-12a-e*. Nitrate concentrations peaked in four of the six size fractions on May 14th and 15th (JD 134 & 135) (*Figure 3-12a)*. Higher NSS-SO_4^{2-} concentrations were found in the <0.49μm size fraction than other size fractions, with a maximum occurring on May 14th (JD 134) (*Figure 3-12c).* The 100-7.2μm size fraction had the largest SO_4^{2-} concentrations on May 3rd to 6th, (JD 123-126). The smallest size fraction (<0.49μm) had higher concentrations from May 7th (JD 127) until the end of the cruise (*Figure 3-12c*). This is very interesting and closely follows the shift in dominance of sea salt components from the largest to smallest size fractions on May 6th (JD 126). Phosphate was only detected in the <0.49 μm size fraction, from May 4th & 5th (JD 124&125) until May 9th (JD 129) (*Figure 3-12d)*. After the maximum concentration (30.9ng·m^{-3}) was reached on May 9th (JD 129) at the most northerly station, T6; PO_4 was detected in the larger size fractions as well. High MSA concentrations were found in the <0.49μm size fraction, except on May 6th and May 7th, (JD 126, 127) when the highest concentration was observed in the 3.0-1.5μm size fraction (*Figure 3-12e*). Concentrations of MSA were within the range (1.3 to 53ngm^{-3}) as reported by Patris *et al.* (2000), though the mean was lower than Wadleigh (2004) reported for size segregated North Atlantic aerosols.

Size segregated cation concentrations (Ca^{2+}, K^+ and NH_4^+) are presented in *Figures 3-13a-c*. Higher concentrations for Ca^{2+}, with the exception of May 3rd (JD 123) were

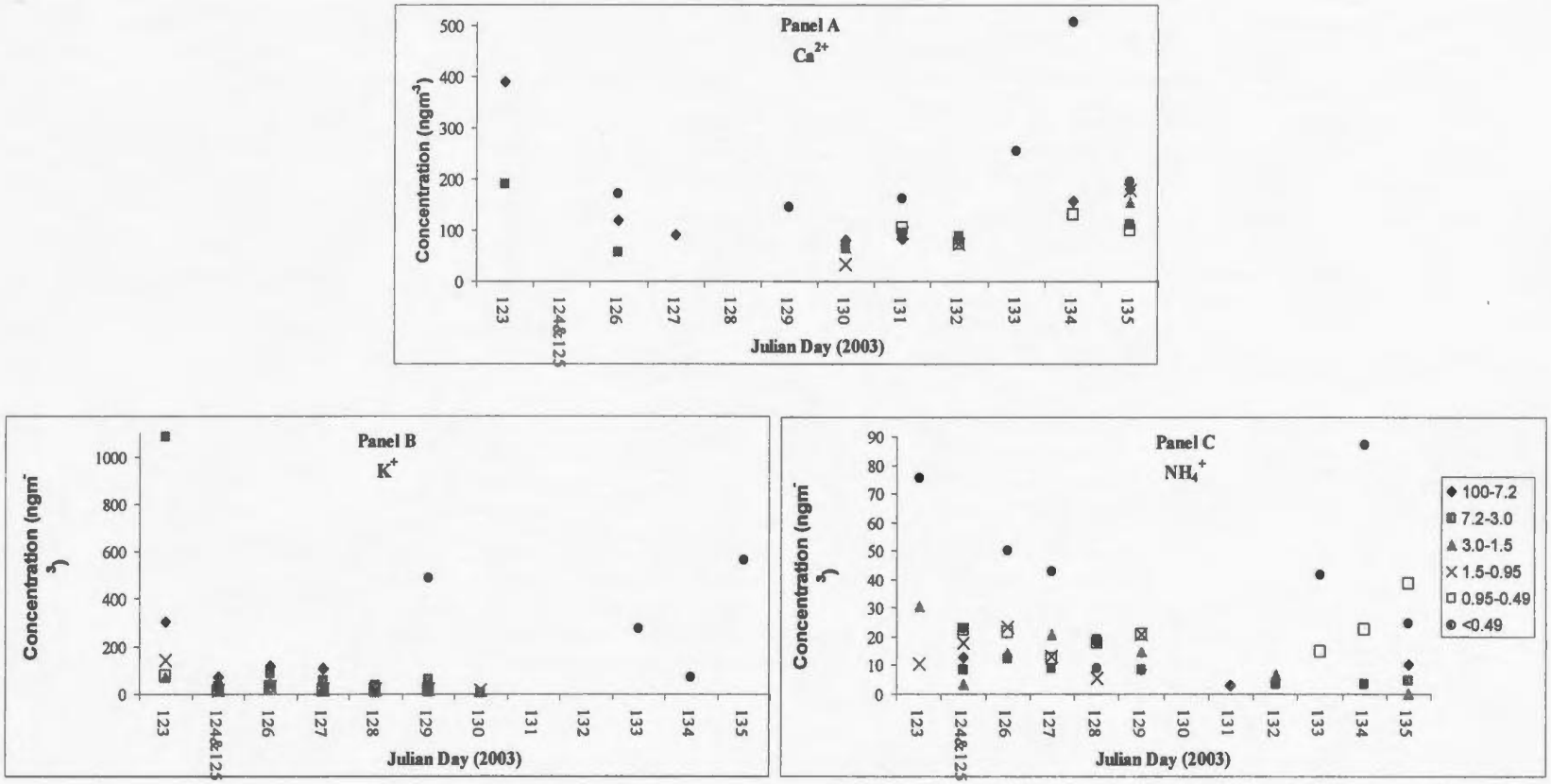

Figure 3-13 – Cation concentrations (ngm^{-3}) for the daytime size segregated Transect samples labelled panels A-C. Legend indicates aerodynamic size (μm). Concentration measurements have an error of ±10%.

found in the <0.49μm size fraction (*Figure 3-13a*). Calcium concentrations in this study were higher than those previously reported by Barrie and Barrie (1990) for total particulate aerosol samples from Alert, Canada. Higher NH_4^+ concentrations were found in the smallest size fraction (as was also determined by Gravenhorst (1977) in North Atlantic aerosol samples) with maximum concentrations on May 3rd and 14th (JD 123&134) *Figure 3-13c*). Ammonium concentrations reported here were lower than those reported by Pszenny *et al.* (1990) during a summer North Atlantic cruise.

3.4.2 Night Samples

Fifteen night sample sets were collected from May 1st to May 15th (JD 121–135). There was no total particulate sample collected on May 6th (JD 126) as the sampler did not restart after a rainstorm (May 5th, JD 125). A daytime high-volume sampler replaced the PM_{10} night sampler from May 7th (JD 127) until the end of the cruise (May 15th) (JD 135) so that all total particulate samples collected after May 6th (JD 126) accumulated aerosols <100μm, as opposed to <10μm for the earlier samples. For samples collected prior to May 5th, a comparision of trends can be completed on the day/night data set.

3.4.2.1 Sulphur Dioxide

Figure 3-14 shows both $\delta^{34}S_{SO2}$ (‰) and SO_2 concentrations (ngm^{-3}) for the night Transect samples. $\delta^{34}S_{SO2}$ ranged from +20.3‰ to +7.5‰, with an average of +13.9 (SD = 3.3‰). SO_2 concentrations ranged from 10500 to 61.9ngm^{-3}, with an average

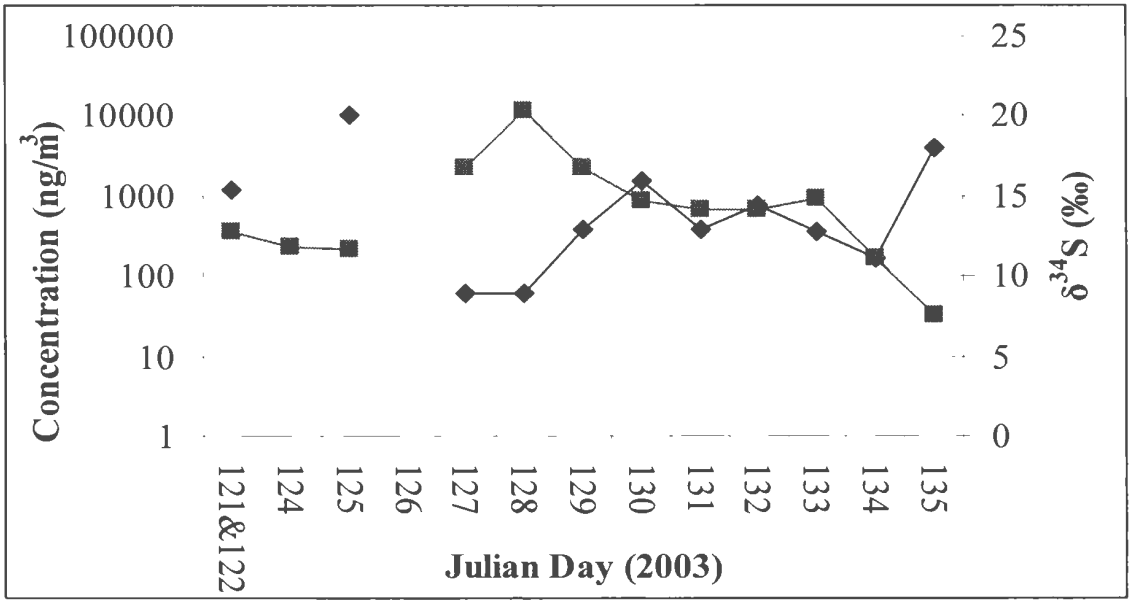

Figure 3-14 – SO_2 concentrations (ngm^{-3}, diamonds) and $\delta^{34}S_{SO2}$ (‰, squares) for the night Transect samples (note: logarithmic scale). Isotope values have a measurement error of ±0.4‰ and concentration measurements have an error of ±10%.

of 1770 (SD = 3100 ngm^{-3}). The May 8th (JD 128) sample had one of the lowest SO_2 concentrations (62.1ngm^{-3}) and the highest $\delta^{34}S$ value ($\delta^{34}S_{SO2}$ = +20.3‰) for the night transect samples. The $\delta^{34}S$ values increased to a maximum on May 8th (JD 127) and then declined until the end of the cruise.

3.4.2.2 Total Particulate

$\delta^{34}S$ and $\delta^{34}S_{NSS}$ values for the night Transect total particulate samples are shown in *Figure 3-15*. $\delta^{34}S$ and $\delta^{34}S_{NSS}$ values follow a similar trend and a shift to lighter isotope values is seen after the PM_{10} sampling head was replaced with the PM_{10} on May 7th (JD 127). However, it is worth noting that a shift to lower $\delta^{34}S$ values was also observed for SO_2 a day later (*Figure 3-14*). $\delta^{34}S$ values ranged from +6.0‰ to+20.8 while $\delta^{34}S_{NSS}$ values ranged from -10.6‰ to +16.7‰. There was a consistent difference of approximately -10‰ between $\delta^{34}S$ and $\delta^{34}S_{NSS}$ values from May 7th to10th (JD 127-130) as the ship moved to the most northerly location 54°N but this did not persist. A much larger difference between $\delta^{34}S$ and $\delta^{34}S_{NSS}$ values was observed on May 13th (JD 133) when $\delta^{34}S$nss values reached (-10‰) when the ship first returned to L1, and much smaller differences were observed on May 14th&15th (JD 134&135) when the ship left L1 and headed toward Halifax.

The concentrations of primary sea salt components (Na^+, Cl^-, Mg^{2+} and SS-SO_4^{2-}) are displayed in *Figure 3-16*. The sea salt components all followed a similar trend with higher concentrations at the start of the cruise, reaching a minimum on May 7th (JD 127) when a larger aerosol size fraction was collected after a very intense rainstorm

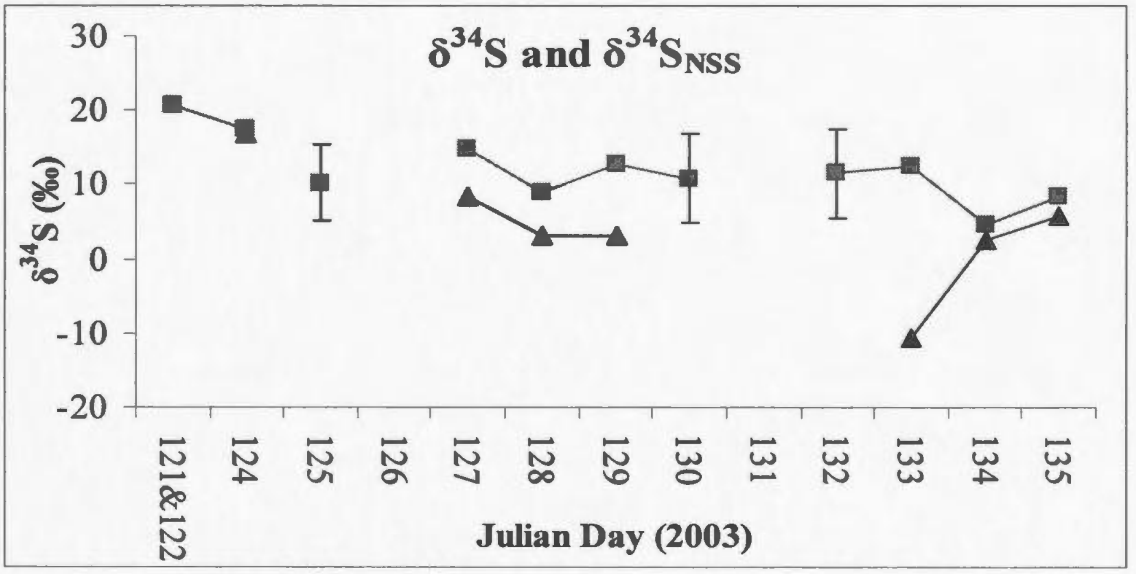

Figure 3-15 – $\delta^{34}S$ (‰, squares) and $\delta^{34}S_{NSS}$ (‰, triangles) for the night total particulate Transect samples. Error bars indicate analytical uncertainty in analysis (‰), where error bars are not present, the analytical uncertainty is ±0.4‰. PM^{10} sampler used from JD 121 to 125.

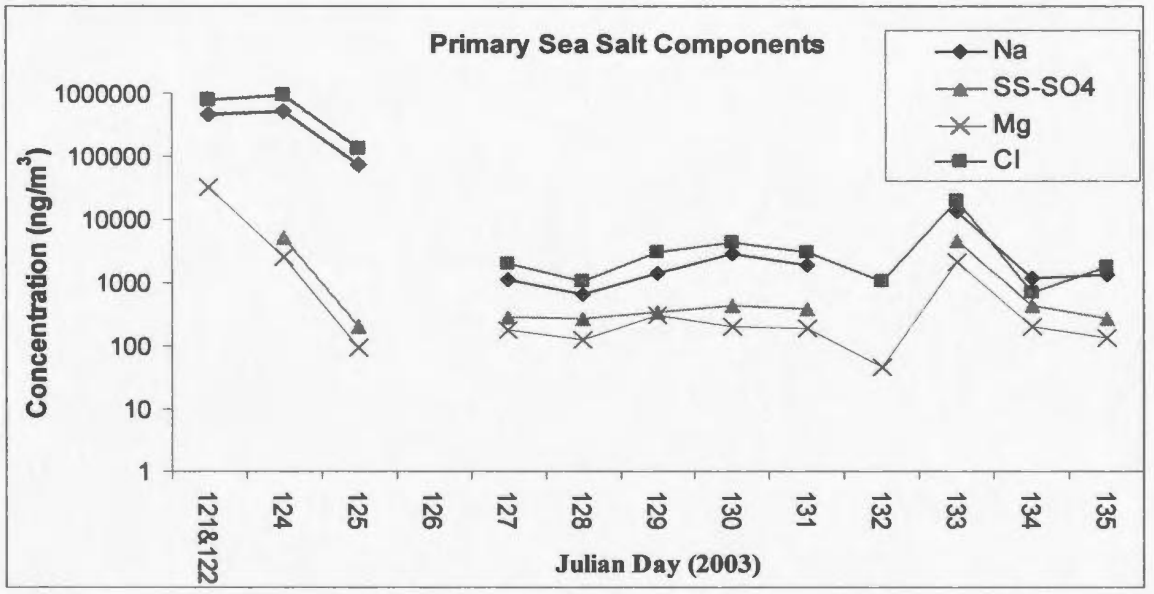

Figure 3-16 – Concentrations (ngm^{-3}) of the primary sea salt components for the night total particulate Transect samples (note: logarithmic scale). Concentration measurements have an error of ±10%; $SS\text{-}SO_4^{2-}$ has a propagated error of 15%. PM^{10} sampler used from JD 121 to 125.

on May 5th (JD 125). There was a pronounced decrease in sea salt components on May 12th (JD 132) and a maximum on the 13th (JD 133).

Figure 3-17 displays anion concentrations (NO_3^-, SO_4^{2-}, NSS-SO_4^{2-}, PO_4^{3-} and MSA) for total particulate samples at night from the transect study, while the remaining cation concentrations (Ca^{2+}, K^+ and NH_4^+) are found in *Figure 3-18*. There was a similar trend, for all the anions and cations, with a large peak on May 4th and 5th, (JD 124&125) and a large decrease on May 7th (JD 127) after the rainstorm on May 5th. Sulphate had the highest concentrations of all the anions, and its trend was closely mimicked by NSS-SO_4^{2-}, and NO_3^- to a lesser degree.

3.4.2.3 Size Segregated

$\delta^{34}S$ values for the night transect size segregated samples are presented in *Table 3-12,* and the lowest values were generally found in the <0.49μm size fraction. Samples taken on May 4th (JD 124) and most size fractions on May 6th (JD 126) had little variation (<5‰) in isotopic compositions between size fractions. There was a decrease in $\delta^{34}S$ values in nearly all size fractions on May 14th and 15th (JD 134&135) upon return to the SOLAS Mooring site, L1.

$\delta^{34}S_{NSS}$ values for the night size segregated samples are shown in *Table 3-13*. $\delta^{34}S_{NSS}$ had higher isotopic compositions in the 7.2-3.0μm and 3.0-1.5μm size fractions. The smaller aerosols (0.95-0.49μm and <0.49μm) had lower isotopic compositions and on JD 128,129 at stations T5 and T6 and again on day 132, when the ship was closest to

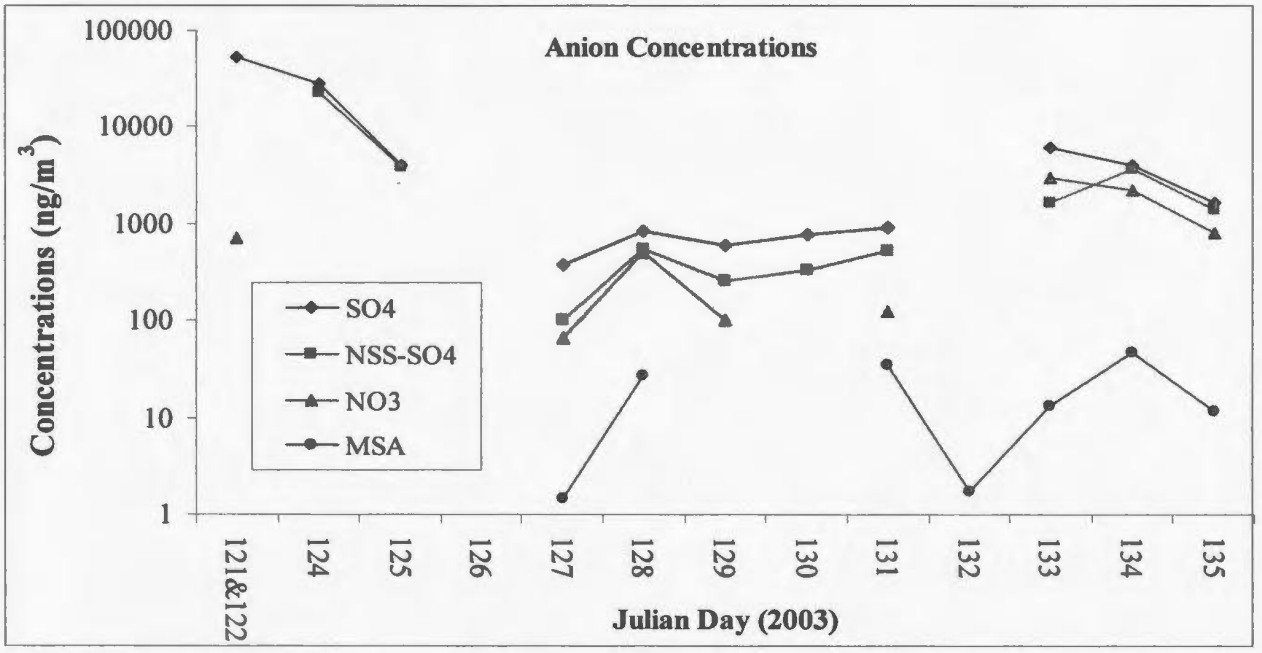

Figure 3-17 – Anion concentrations (ngm^{-3}) for the night total particulate Transect samples (note: logarithmic scale). Concentration measurements have an error of ±10%. PM^{10} sampler used from JD 121 to 125.

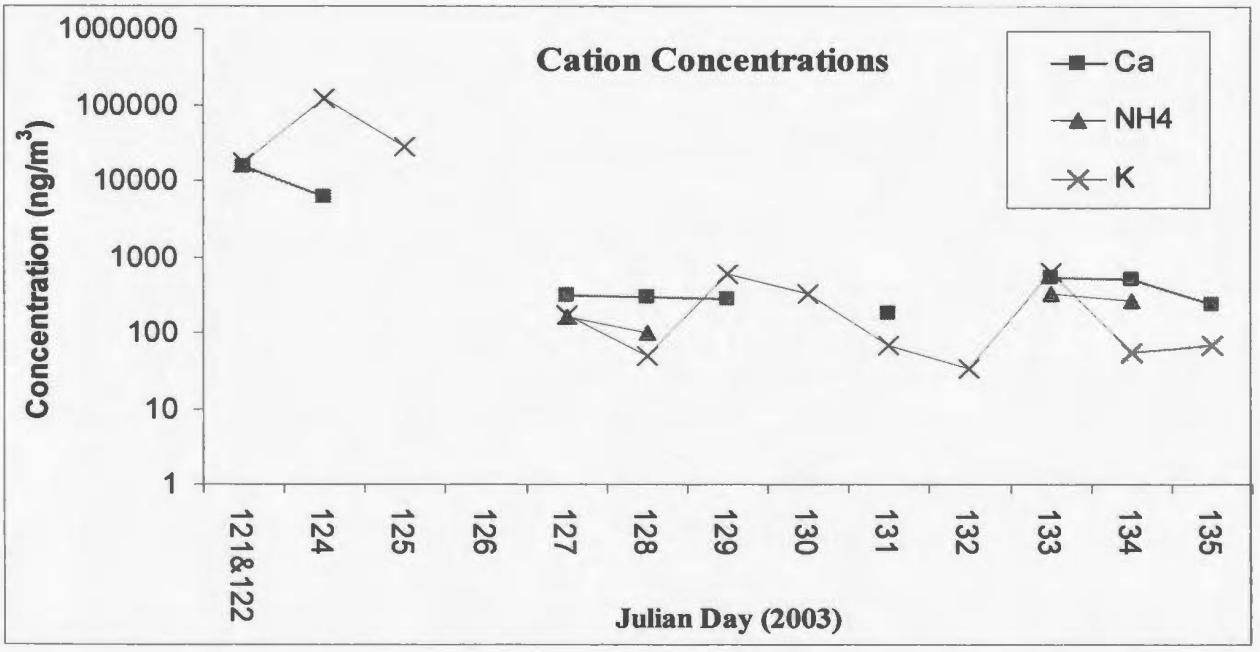

Figure 3-18 – Cation concentrations (ngm^{-3}) for the night total particulate Transect samples. (note: logarithmic scale). Concentration measurements have an error of ±10%. PM^{10} sampler used from JD 121 to 125.

Table 3-12 – $\delta^{34}S$ (‰) for the night size segregated Transect samples. Uncertainties greater than ±0.4‰ are shown in parentheses.

	Julian Day						
Size	**121&122**	**124**	**125**	**126**	**127**	**128**	**129**
10-7.2	15.3		19.7	20.6	21.2		
7.2-3.0	15.8	21.5	19.8	21.7	21.1	19.8	23.1
3.0-1.5	11.8	19.6	17.1	20.0	19.0 (2.0)	13.5	
1.5-0.95	6.2	20.8	15.9	13.4	14.4	17.5 (5.0)	13.7
0.95-0.49	5.0	20.6	17.0		13.1 (2.0)	8.4	7.3
<0.49	4.8	19.8	6.9	21.1	8.5	7.1	5.6
Size	**130**	**131**	**132**	**133**	**134**	**135**	
10-7.2	16.5	18.5	21.5 (2.0)	18.5	12.1	11.9	
7.2-3.0	18.9	23.2	21.1	16.5	3.8	11.7	
3.0-1.5	13.5	19.8	14.9	10.4	12.7	6.9	
1.5-0.95	11.0	13.6	8.3	8.1	6.0	7.8	
0.95-0.49	7.4		8.6	4.9	5.8	10.5	
<0.49	5.6		4.5	4.6	3.8		

Table 3-13 – $\delta^{34}S_{NSS}$ (‰) for the night size segregated Transect samples. Isotope values have a measurement error of ±0.4‰.

	Julian Day						
Size	**121&122**	**124**	**125**	**126**	**127**	**128**	**129**
10-7.2	11.4		17.7	20.3	21.3		
7.2-3.0	11.8	22.2	14.8	22.4	21.2	19.5	25.2
3.0-1.5	9.8	17.5	15.0	19.6		9.0	
1.5-0.95	5.5	20.6			9.4		11.0
0.95-0.49	4.8	17.9				-4.2	-13.4
<0.49	4.2		2.6		7.5	4.6	
Size	**130**	**131**	**132**	**133**	**134**	**135**	
10-7.2	12.2				2.1		
7.2-3.0	10.0			8.0	-7.7	4.1	
3.0-1.5	1.7	15.5		8.2	0.5	-3.6	
1.5-0.95	8.1	10.6	1.0	5.9	4.8	3.0	
0.95-0.49	5.9		6.6	4.5	4.0	7.6	
<0.49			-1.8	3.5	2.4		

Newfoundland, and negative δ^{34}Snss values were observed in the Aitken nuclei range. There was generally a decreasing trend from the beginning to the end of the Transect for all size fractions. The largest spread of values was found on May 9th (JD 129) with a range of $\delta^{34}S_{NSS}$ of ~40‰.

Figure 3-19 displays the concentrations of the primary sea salt components for the night-time size segregated samples. Sodium concentrations (*Figure 3-19a)* were relatively constant, and the variance between the different size fractions for most samples was not large. Chloride, Mg^{2+} and SS-SO_4^{2-} (*Figures 3-19b-d*) followed the same trend as Na^{+}. It is interesting to see that the dates for reversal in Mg from the larger size fractions (in this case 7.2-3.0μm) from JD 123-127 to the smaller size fractions (JD 128-135) coincides with the results for daytime samples (Figure 3-11). The maximum concentration for all salt salt components was on May 4th (JD 124).

Anion concentrations (NO_3^-, SO_4^{2-}, NSS-SO_4^{2-}, PO_4^{3-} and MSA) are displayed in *Figures 3-20a-e*. Nitrate concentrations in the smaller size fractions (<1.5μm) reached a maximum on May 10th (JD 130) at the northernmost station, T6, and afterward declined to values that were ~3 times those from aerosols collected during the transit north (*Figure 3-20a*). Non sea salt sulphate displayed high concentrations at the start of the cruise and then decreased to a minimum value of 55ngm^{-3} on May 10th (JD 130) (*Figure 3-20c*). Higher NSS-SO_4^{2-} concentrations were seen again on May 13th (JD 133) and 15th (JD 135), upon return to the SOLAS Mooring site L1 (*Figure 2-1*). Concentrations of NSS-SO_4^{2-} were highest in the smallest size fraction

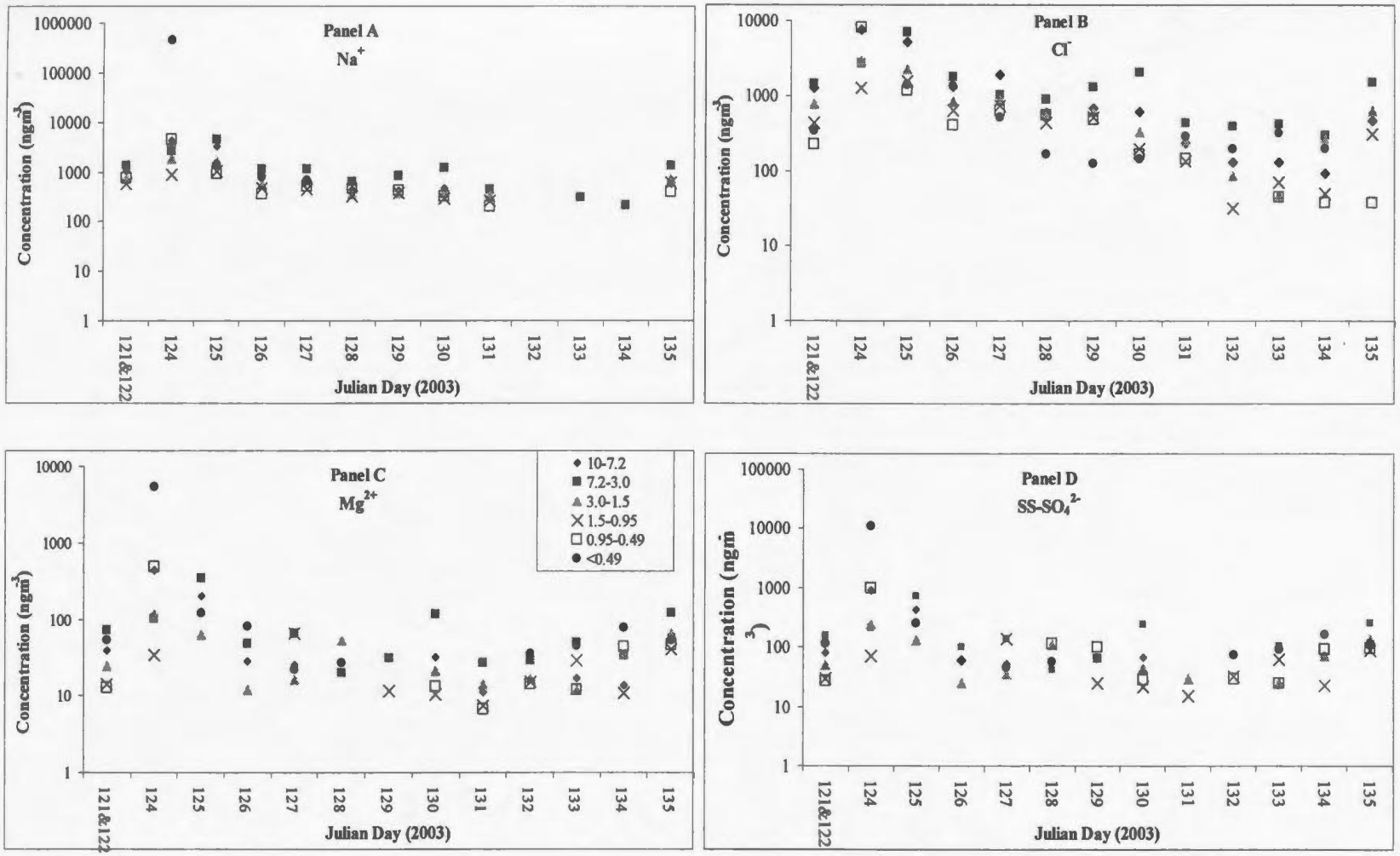

Figure 3-19 – Primary sea salt component concentrations (ngm^{-3}) for the night size segregated Transect samples, labelled panels A-D (note: logarithmic scale). Concentration measurements have an error of ±10%.

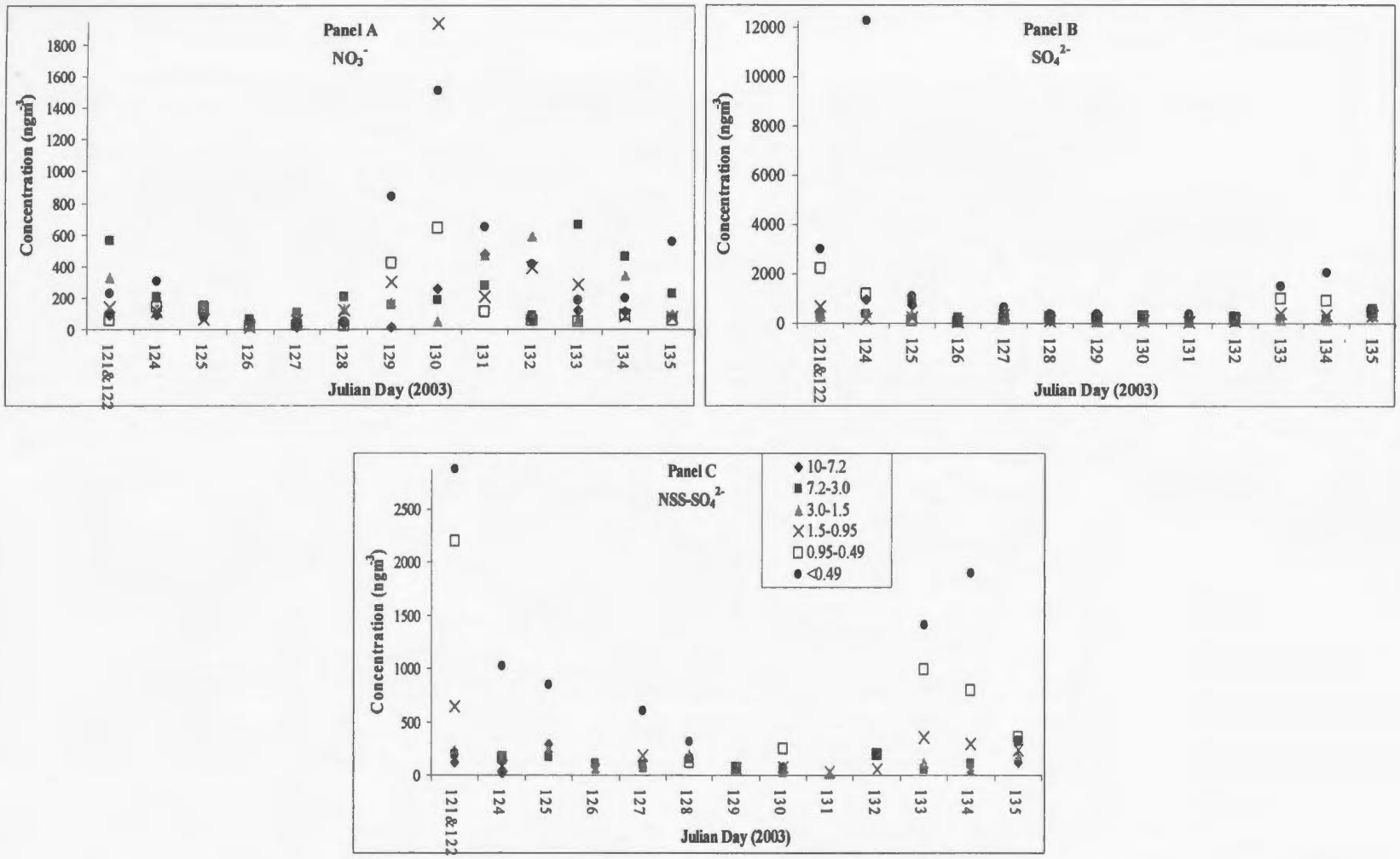

Figure 3-20 – Anion concentrations (ngm^{-3}) for the night size segregated Transect samples, labelled panels A-C. Concentration measurements have an error of ±10%.

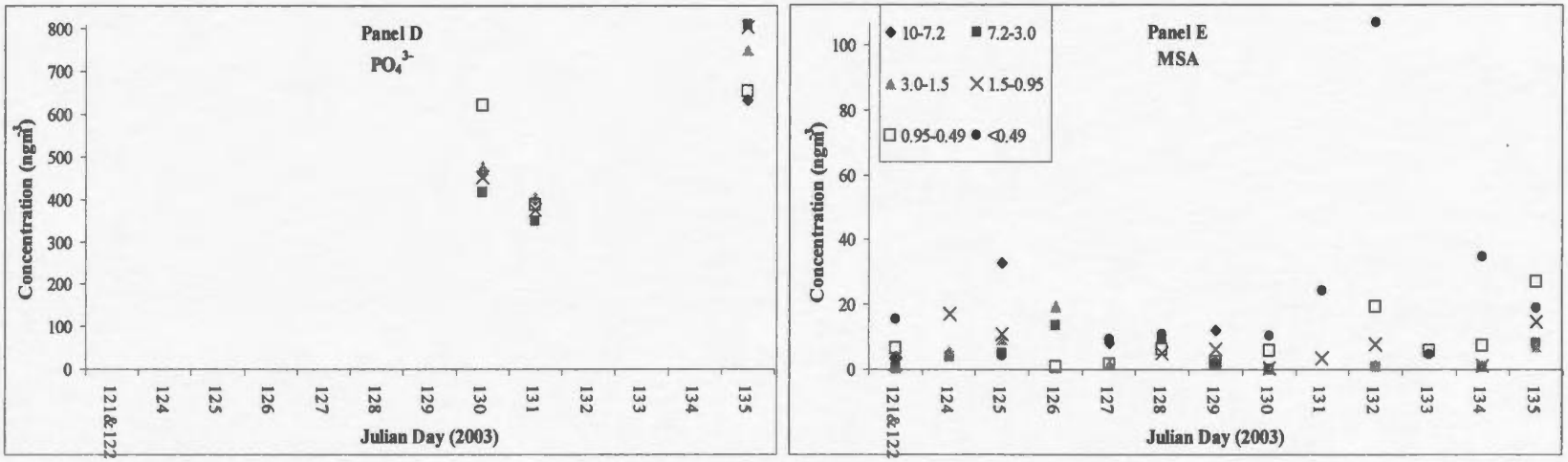

Figure 3-20 – Anion concentrations (ngm^{-3}) for the night size segregated Transect samples, labelled panels D-E. Concentration measurements have an error of ±10%.

(<0.49μm). Methanesulphonic acid had the highest concentration (107ngm^{-3}) for the entire cruise for both day and night samples on May 12th (JD 132) (*Figure 3-20e*) but did not follow the trend for NO_3^- (*Figure 3-20a*). Methanesulphonic acid concentrations were highest in the smallest aerosols (<0.49μm).

Cation concentrations (Ca^{2+}, K^+ and NH_4^{2+}) for the night size segregated Transect samples are presented in *Figure 3-21a-c*. The maximum concentration for Ca^+ and K^+, was found on May 4th (JD 124) in the <0.49μm size fraction (*Figures 3-21a&b*). Nearly all concentrations were below 200ngm^{-3}, for NH_4^+ and K^+ and all but one Ca^+ concentration was below 500ngm^{-3}. Concentrations of K^+ and NH_4^+ were largest in the smallest aerosols (<0.49μm) (*Figure 3-21b&c*).

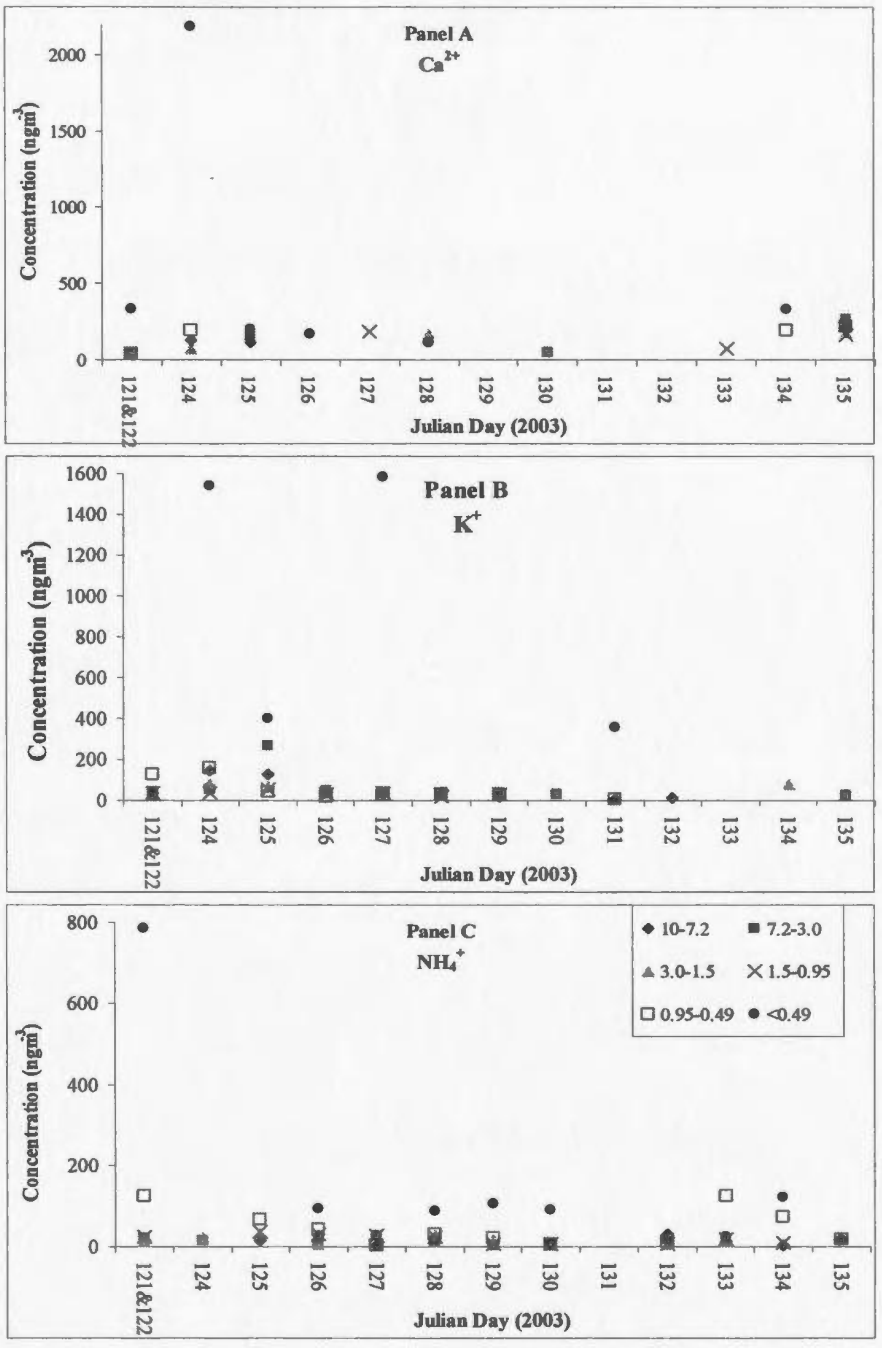

Figure 3-21 – Cation concentrations (ngm^{-3}) for the night size segregated samples, labelled panels A-C. Concentration measurements have an error of ±10%.

Chapter Four: Discussion of Results

4.1 Introduction

This chapter is a discussion of the results presented in Chapter 3, broken into two main parts; the Lagrangian study and the Transect study. The focus is on source apportionment of atmospheric sources of SO_2 and SO_4^{2-} affecting the North West Atlantic during the spring SABINA study and their relationship to DMS oxidation products.

4.2 Lagrangian Study

The Lagrangian study was of great importance to the oceanographers who participated in the spring SABINA cruise as it provided insight regarding how phytoplankton and bacterial communities responded during a rapid decline in biomass. While the oceanographers followed the water mass, the atmospheric scientists sampled the overlying air mass, which changed from day to day. The location of the Lagrangian study was not ideal for background air mass characterisation as it was ~160km away from the Sable Island gas platforms, and continental Canada and the United States. The proximity to continental sources increased the possibility of point source anthropogenic emissions affecting the samples.

The Sable Island gas platforms flare "sweet" gas, which is a natural gas containing <5% H_2S (Hale, personal communication). A review of the literature indicates the isotope composition of sulphate from oxidation of a sweet gas flare could be

isotopically light. Maximov *et al.* (1975) reported values as low as -16‰ for H_2S in gases associated with Jurassic deposits. A search of the National Pollutant Release Inventory (NPRI) indicates that the Nova Scotia offshore gas platforms located on Sable Island do not emit enough SO_2 to be included on the inventory. The inventory does not report SO_2 emissions lower than 20 tonnes (NPRI, 2003). There is an Imperial Oil refinery located in Dartmouth, Nova Scotia which emitted 5976 tonnes of SO_2 in 2003 and over 620 tonnes of particulate matter (NPRI, 2003). Due to the proximity of Dartmouth to the SOLAS Mooring station (~500km), the refinery could be a point source of SO_2, or SO_4^{2-} particulate matter resulting from SO_2 oxidation. Background sulphur emissions from North America were also believed to be present at the Lagrangian study.

4.2.1 Day/Night Differences

4.2.1.1 $\delta^{34}S_{SO2}$, $\delta^{34}S_{NSS}$ and $\delta^{34}S$

Night $\delta^{34}S_{SO2}$ (mean = +13.1, SD = 0.3‰ (n=2)) values were higher ($F_{(1,5)}$=75.8, p=0.001) than those for the day (mean = +8.2, SD = 0.8‰ (n=4)), and were coincident with lower SO_2 concentrations, though diurnal differences in concentration were not statistically significant. The F-test used in this analysis and all further analyses is based on three assumptions; 1) that the data is normally distributed, 2) that the samples are independent and 3) the variance is homogenous. Statistical significance for all F-tests is set at 5%.

Using the two source model described in *Appendix V*, with biogenic and anthropogenic end-members of $\delta^{34}S$ = +18‰ and +3‰ respectively, the fraction of biogenic and anthropogenic sulphur as SO_2 was calculated. *Figure 4-1* displays biogenic, anthropogenic and total SO_2 concentrations for the Lagrangian suite of samples. Biogenic SO_2 concentrations for both the day and night samples were similar ($F_{(1,5)}$=0.64, p=0.469) (mean = 925±329ngm^{-3}). The smallest concentrations were associated with larger propagated errors. It is beneficial to also examine the fractional or percent contribution of biogenic to total SO_2. The percent contribution of biogenic SO_2 (biogenic SO_2/total SO_2) in the day samples averaged 34.6, (SD = 5.2%), while the night samples averaged (69.1, SD = 2.2%). This is very important: despite the fact that anthropogenic SO_2 concentrations varied, the biogenic concentrations were essentially stable. Anthropogenic emissions were high, and this is keeping with the expected greater influence of anthropogenic emissions over the North Atlantic from the continental United States and Canada in daytime as turbulent mixing and advection occur.

A common method of apportioning sources of SO_4^{2-} is made with the assistance of $\delta^{34}S$ vs. percent sea salt sulphate plots (*Figure 4-2*). Three end-members were used, sea salt (δ = +21‰, 100% sea salt sulphate), biogenic sulphur (δ = +18‰, 0% sea salt sulphate), and anthropogenic sulphur (δ = +3‰, 0% sea salt sulphate). Wadleigh (2004) used an anthropogenic end-member of +3‰ for the NODEM studies and as the collection sites were similar, and the value is based on integrated measurements from a large number of sites over several decades throughout the American

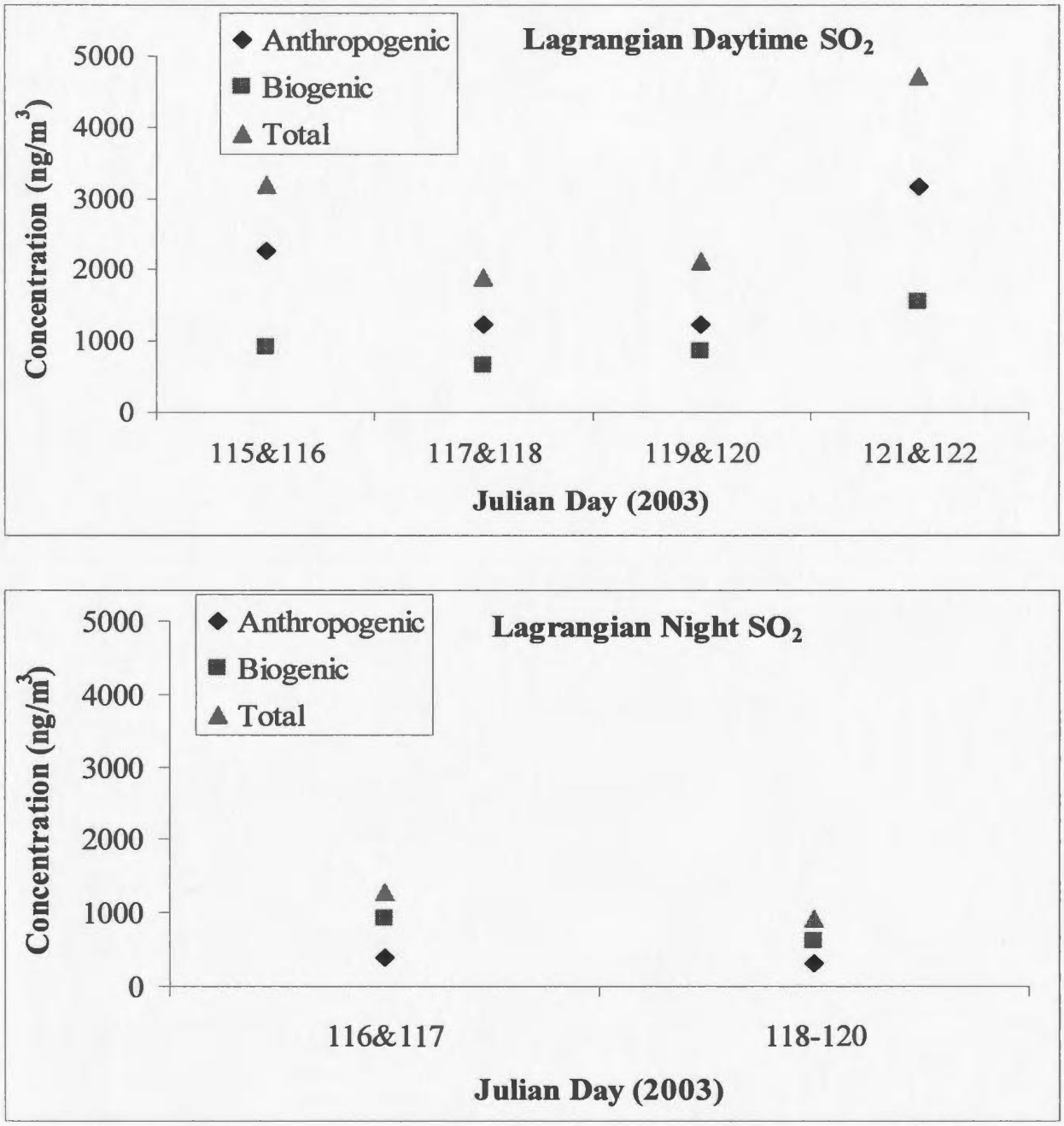

Figure 4-1 – Lagrangian day (top) and night (bottom) SO_2 concentrations (ngm^{-3}), classified as: anthropogenic SO_2, biogenic SO_2 and the sum of both (total SO_2). Propagated uncertainty for biogenic SO_2 was ~17% and 28% for anthropogenic SO_2.

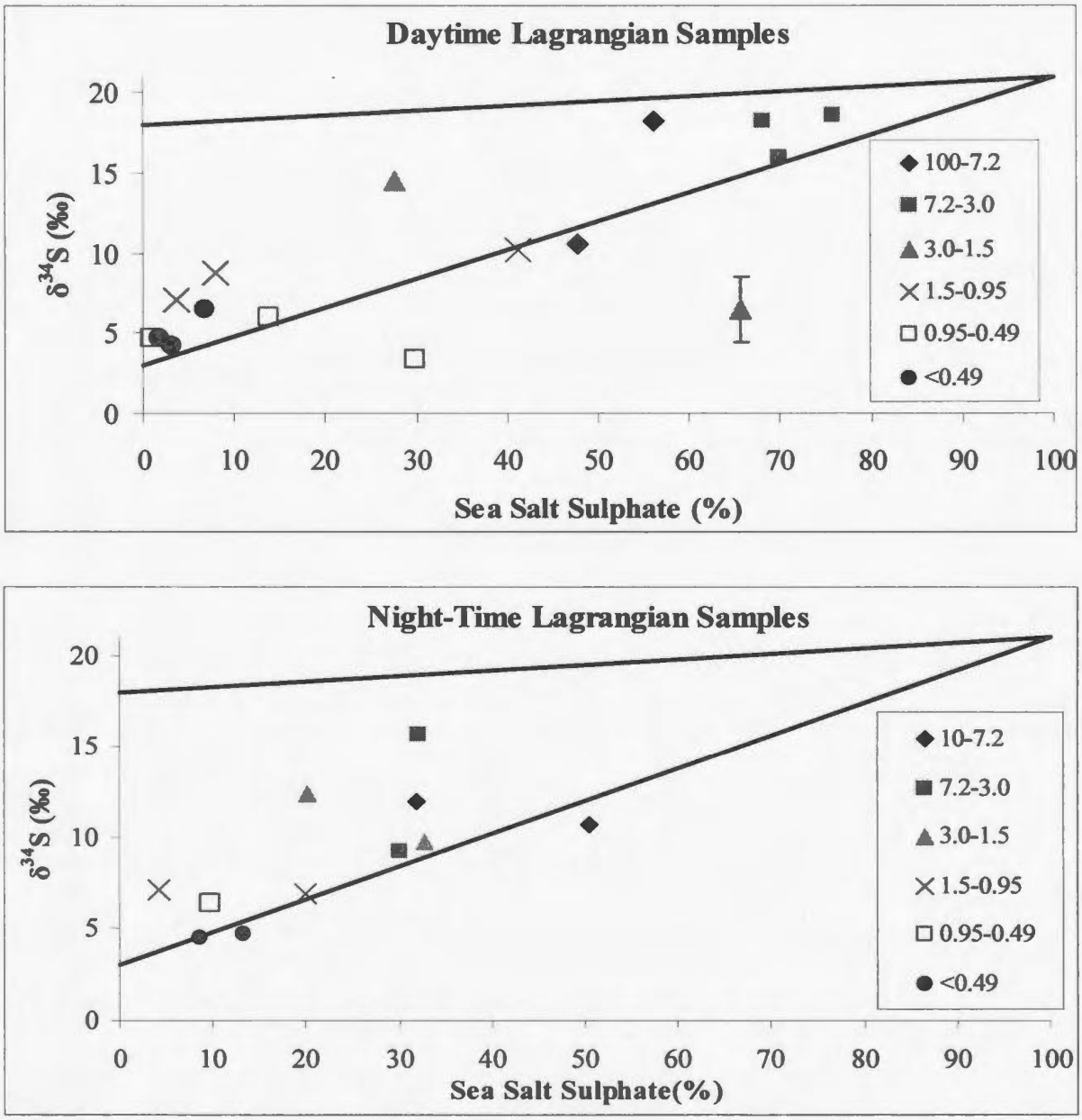

Figure 4-2 – $\delta^{34}S$ (‰) vs. sea salt sulphate (%) for the size segregated day (top) and night (bottom) Lagrangian samples. Error bars illustrate analytical uncertainty. Samples with no error bars have an analytical uncertainty <0.4‰.

Northeast, it is believed that this was an appropriate end-member. Percent sea salt was calculated using Mg^{2+} as the conservative sea salt tracer (Chapter 1, equation 4). Patris *et al.* (2000) and Turkeian *et al.* (2001) have previously used Mg^{2+} as a sea salt tracer with positive outcomes. The difference in sea salt concentrations when using Mg^{2+} or Na^{+} as a conservative sea salt tracer was minimal (mean = 4.3, SD 28.1%). The triangle in *Figure 4-2* presents a mixing area between the three end-members; anthropogenic, biogenic and sea spray sulphate. Except for two points, the daytime samples conform to the proposed three way mixing plot bounded by the triangular region (*Figure 4-2*) as do the night samples.

Mass balance calculations, with $\delta^{34}S_{anthropogenic}$ as the unknown variable, show that for all the day samples within the mixing area the lower end-member would have to be -25‰. A possible reason why the points fall below the mixing area is there was another source of sulphur/sulphate which was isotopically depleted in ^{34}S with an isotopic composition lower than +3‰. Intermittent influence of this source of sulphur on aerosol sulphate altered the isotopic composition of the sulphur in the samples.

A possible source of isotopically light sulphate is H_2S. Charlson *et al.* (1987) reported that the amount of H_2S emitted to the atmosphere is not significant. Andreae (1990) reported a global annual flux of H_2S into the atmosphere of 3.6-10.8TgS·year^{-1}, with 5.9TgS·year^{-1} coming from soil and coastal wetlands. Soil fluxes account for 0.39TgS·year^{-1} H_2S, while wetlands flux $3.8*10^{-3}$ TgS·year^{-1} H_2S into the Northern

Hemisphere (Bates et al 1992). In comparison the DMS flux is 8-50TgSyear^{-1} (Andreae 1990; Bates *et al.* 1992). It is unlikely that there were large H_2S emissions in open ocean areas as it is known that the largest source of H_2S is in coastal tidal flats, and emission over the open ocean is minimal. Thus it is unlikely that the source of isotopically depleted sulphur was from H_2S.

If the source of the negative sulphate resulted from SO_2 oxidation, one would expect that the SO_2 samples would also have had very light isotope compositions. This was not the case, and indicates that if the source was originally as SO_2, there must have been rapid oxidation to SO_4^{2-} via excess oxidants (such as with metal catalysts, O_2, O_3 and NO_3) in the atmosphere. A detailed discussion of possible sources of ^{34}S depleted sulphur in both the Lagrangian and Transect studies is presented in section 4.3.2.1 and 4.3.2.2.

Generally the daytime $\delta^{34}S$ values for samples with >50% sea salt were higher in the larger size fractions, as expected. Samples <1.5μm had <50% sea salt and $\delta^{34}S$ values <+10‰ indicating a greater proportion of anthropogenic sulphate than sea salt sulphate. Night-time samples <1.5μm also generally had isotope compositions indicating a significant proportion of anthropogenic sulphate was present.

All of the night samples had sea salt contributions <50% and suggests that either sea salt particles were less prevalent in night than day time aerosols, or that the PM_{10} head on the night-time samplers reduced the number of large sea salt particles

(<10μm) present in the aerosols sampled. Sampling mode for the day and night samples was the same with the exception of the PM_{10} heads equipped on the night-time samplers. The samplers were otherwise identical in operation, filtration media, and particle retention. The daytime samples had a wider and higher range of sea salt contributions. Sea salt is constantly present in the marine atmosphere and higher wind speeds would result in greater amounts of sea spray being distributed into the atmosphere. During the Lagrangian study the daytime average wind speed was not higher than the night wind speeds (one tailed t-test, 2 degrees of freedom, p=0.31), thus this could not have been the cause of the greater sea salt contributions found in the daytime samples. The Transect samples also showed higher percent sea salt in the day samples, so it is possible that the PM_{10} head on the night samplers removed sea salt particles larger than 10μm, and that a large portion of sea salt particles are larger than 10μm.

$\delta^{34}S_{NSS}$ data for the Lagrangian study are presented in *Figure 4-3a&b* (day and night respectively). The $\delta^{34}S$ value from the April 27th & 28th (JD 117&118) total particulate sample indicated there was a large proportion of biogenic (or sea salt) sulphate present (+15.1‰); while the size segregated samples contained more anthropogenic sulphate (+9.3, SD = 3.8‰) (*Figures 3-1&3-2* respectively) and the opposite was true for samples from JD 21&122.) The $\delta^{34}S_{NSS}$ data for April 27th & 28th (JD 117&118) also indicated that the total particulate sample was biogenic in origin, while the size segregated samples were dominated by anthropogenic sulphate (*Figure 4-3,* top panel). It is unusual that the isotope data for both total particulate

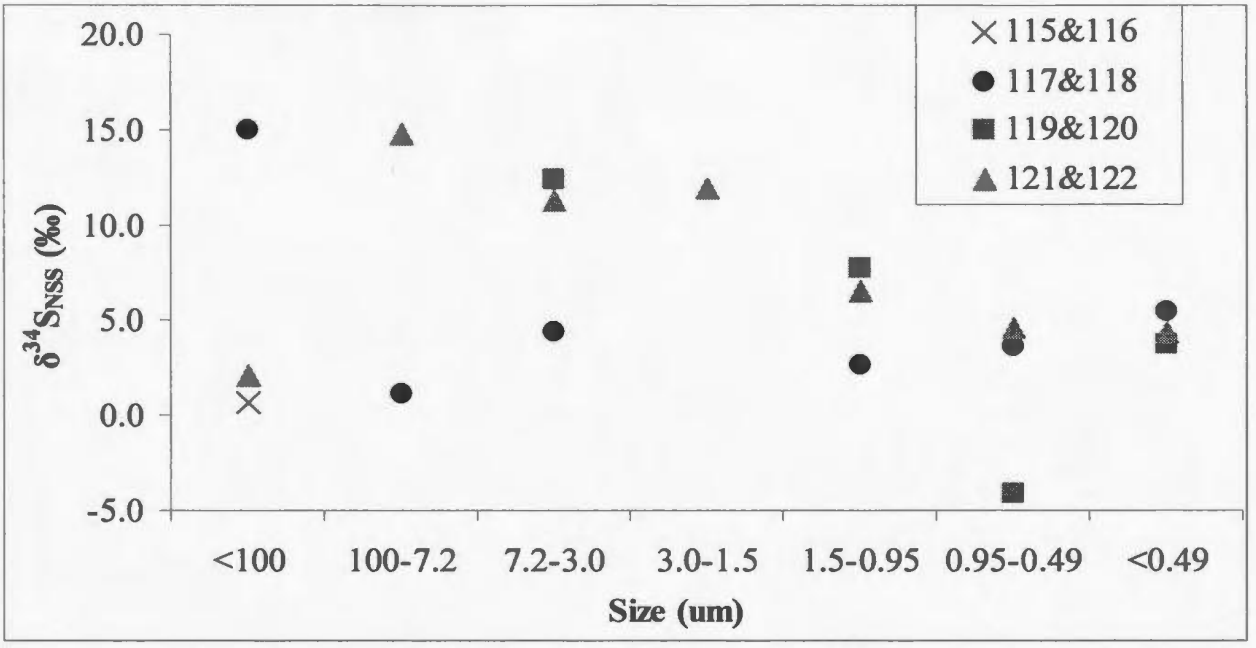

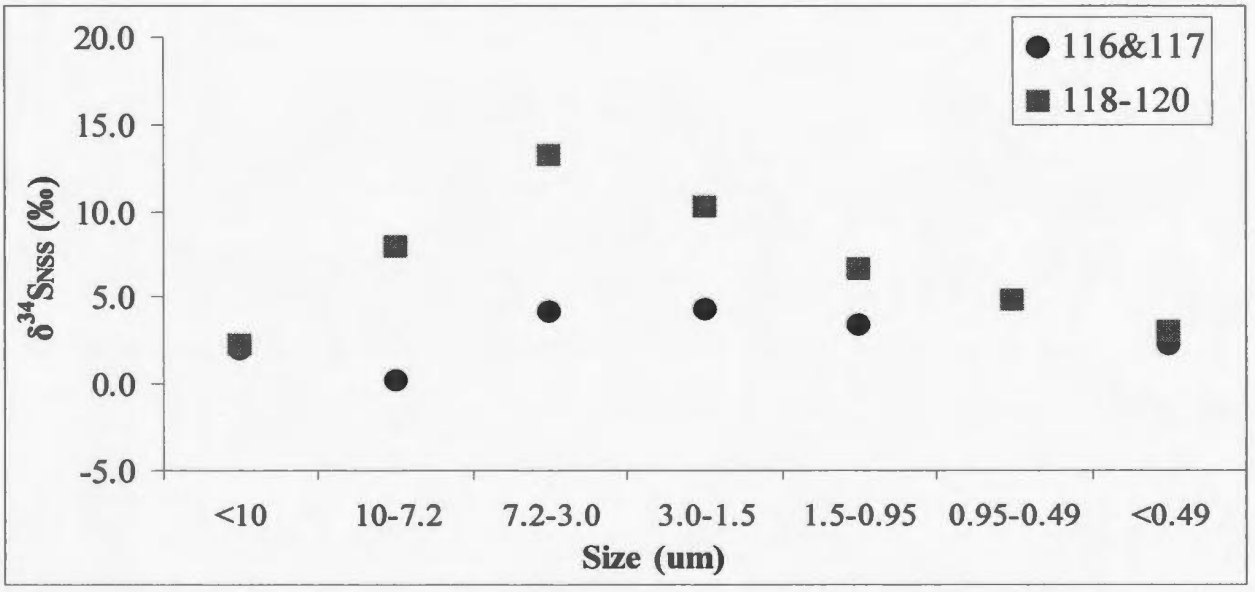

Figure 4-3 – $\delta^{34}S_{NSS}$ (‰) from the day (top, panel a) and night (bottom, panel b) Lagrangian samples. The total particulate samples for the day are indicated by the size <100μm and <10μm for the night on the left hand side of the figures. Isotope values have a measurement error of ±0.4‰.

samples do not match that for the size segregated samples for these sampling periods (*Figure 4-3a*) The author cannot propose an explanation for this discrepancy between the total particulate and size segregated samples at this time though it seems likely that the two total particulate samples may have been mixed up. These samples are removed from subsequent analysis.

An interesting feature of the $\delta^{34}S_{NSS}$ Lagrangian data was the presence of slightly positive and very negative values. These values were unusual as the anthropogenic end-member for North American sulphur emissions ranged between +2‰ and +6‰ in other studies (e.g. Norman *et al.* 1999, Turkeian *et al.* 2001, Wadleigh 2004,). For negative $\delta^{34}S_{NSS}$ values to be present there must have been a source of isotopically depleted ^{34}S in the atmosphere or an isotope fractionation. Seventeen negative $\delta^{34}S_{NSS}$ values were found during the Transect study, and a more detailed look at the possible source of these negative values is discussed in sections 4.3.2.1 and 4.3.2.2.

The night-time samples had low $\delta^{34}S_{NSS}$ values, but they were generally >+2‰ (*Figure 4-3*). Two interesting points were noted in this data set; 1. The size segregated sample collected on April 26th & 27th (JD 116&117) had low $\delta^{34}S_{NSS}$ compositions, with most below +4‰. The corresponding SO_2 filter had a relatively high $\delta^{34}S_{SO2}$ value (+12.9‰), indicating that while the particulate filter was dominated by anthropogenic sulphate; the SO_2 in the atmosphere was biogenic, and 2. The size segregated sample collected on April 28th to 30th (JD 118-120) had a wider range of isotopic compositions, with the highest $\delta^{34}S_{NSS}$ (+13.2‰) in the 7.2-3.0μm

size fraction, which indicated biogenic sulphate contributions possibly from the oxidation of DMS or biogenic SO_2 on pre-existing aerosols.

High $\delta^{34}S_{NSS}$ values found in aerosols 7.2-3.0μm and 3.0-1.5μm in both the day and night samples indicated aged biogenic aerosols were present or that oxidation of biogenic sulphur on the surface of pre-existing aerosols occurred. The isotopic composition for the night-time samples had $\delta^{34}S_{NSS}$ values in the <0.49μm aerosols that were similar to those for the total particulate samples, as was expected given the dominance of SO_4^{2-} in the smallest size fraction.

4.2.1.2 Anions and Cations

Size segregated MSA concentrations for the Lagrangian Study were comparable and did not differ between the day and night ($F_{(1,25)}$=0.296, p=0.591). These results were not expected as we specifically collected diurnal samples to determine if oxidation patterns for DMS were distinct between the day and night as NO_3^- concentrations varied. The lack of diurnal differences is likely the result of the constant continental influence on the oxidation of DMS in association with O_3 and NO_3^- in aged polluted air masses at the Lagrangian site. The proximity to the North American continent during the Lagrangian resulted in high anthropogenic SO_2 concentrations and the isotope data indicated that smaller size segregated samples were generally dominated by anthropogenic sulphate. Methanesulphonic acid concentrations did not increase as the bloom declined, but rather NO_3^- concentrations increased near the end of the Lagrangian study possibly indicating oxidation of NO_x from anthropogenic emissions as the study progressed. The phytoplankton bloom did not affect the atmospheric

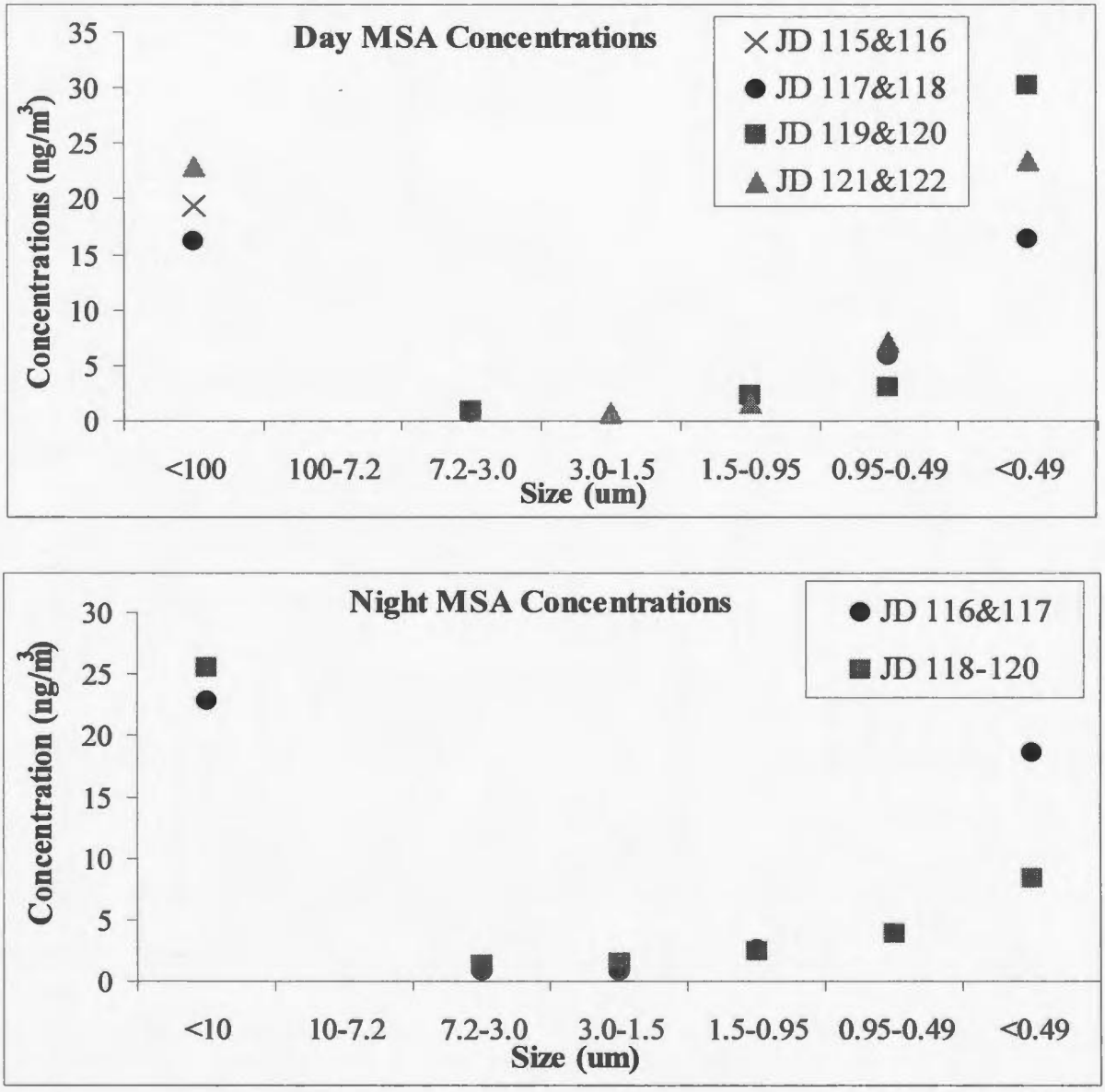

Figure 4-4 – Daytime (top, panel a) and night (bottom, panel b) MSA concentrations (ngm^{-3}) in total particulate (denoted by <100μm for the day and <10μm for the night) and size segregated Lagrangian samples. Concentration measurements have an uncertainty of 10%.

components studied in the overlying atmosphere during the Lagrangian study, and anthropogenic emissions from the North American continent likely dominated the samples.

4.2.1.3 MSA/NSS-SO_4^{2-} Ratios

MSA/NSS-SO_4^{2-} (%) ratios are presented in *Table 4-1*, arranged by size fraction. The average of all size fractions for both the day (2.9, SD = 2.1% (n=15)) and night Lagrangian samples (2.3, SD = 1.3% (n=11)) was similar to the average North Atlantic ratio (2.8%) reported by Savoie *et al.* (1989) with higher MSA/NSS-SO_4^{2-} ratios in the smallest size fractions consistent with the results by Turkein *et al.* (2001).

4.2.2 Summary of Lagrangian Study

As previously stated the location of the Lagrangian site was not preferable for atmospheric studies due to its location. At the Lagrangian site, samples were subjected to increased anthropogenic contamination from Sable Island, Come by Chance Refinery, the continent as well as the numerous ships in the area. $\delta^{34}S_{SO2}$ values were significantly higher in the night-time than in the daytime samples ($F_{(1,5)}$=75.85, p=0.001), indicating an increase in the proportion of biogenic sulphur at night, though there was no diurnal difference in biogenic SO_2 concentrations ($F_{(1,5)}$=0.640, p=0.469). However, the percent contribution of biogenic SO_2 was higher in the night than the day samples ($F_{(1,5)}$ =74.81, p=0.001). These results were coincident with high NO_3 concentrations found throughout the Lagrangian study and potentially suggest DMS oxidation by NO_3 forming SO_2 rather than MSA at night.

Table 4-1 – MSA/NSS-SO_4^{2-} (%) ratios for the Lagrangian total particulate (denoted by <100 μm for the day and <10μm for the night) and size segregated samples (size = μm). BD indicates MSA/NSS-SO_4^{2-} ratios could not be calculated as MSA or NSS-SO_4^{2-} was below detection. Measurement uncertainty is ±30%.

Day Samples	**<100**	**- -**	**7.2-3.0**	**3.0-1.5**	**1.5-0.95**	**0.95-0.49**	**<0.49**
JD 115&116	4.3	- -	BD	BD	BD	BD	BD
JD 117&118	4.5	- -	2.2	BD	4.2	6.7	7.3
JD 119&120	BD	- -	1.9	BD	2.2	1.9	3.4
JD 121&122	1.4	- -	BD	0.6	0.6	0.9	1.3
Night Samples	**- -**	**<10**	**7.2-3.0**	**3.0-1.5**	**1.5-0.95**	**0.95-0.49**	**<0.49**
JD 116&117	- -	4.0	1.0	1.0	1.6	BD	5.4
JD 118-120	- -	2.3	1.9	1.8	2.1	2.4	2.3

MSA concentrations were stable for day and night samples ($F_{(1,25)}$=0.296, p=0.591). The absence of diurnal differences in MSA is postulated to result from the constant influence of aged continental pollutants such as O_3 and NO_x at the Lagrangian site. The phytoplankton bloom was important to all SOLAS scientists studying the ocean biota for atmospheric researchers it did not appear to affect the overlying atmosphere.

Larger aerosol size fractions were generally dominated by sea salt sulphate, and the smaller size fractions dominated by anthropogenic sulphate from the nearby sources during the Lagrangian study. One negative $\delta^{34}S_{NSS}$ value (-4.1‰) was observed on April 29th and 30th (JD 119&120) during the Lagrangian study. This value is similar to the average isotopic composition of Middle Eastern Oil (Come by Chance Refinery), and also possibly the flaring of H_2S (Sable Island) and as these sources are relatively close, this value may be attributed to either of these sources.

4.3 Transect Study

The primary purpose of the Transect study was to sample air masses of different temperatures. This was important because oxidation patterns for DMS are expected to differ with temperature (e.g. Bates *et al.* 1992; Wadleigh 2004). The Transect differed from the Lagrangian study in that most samples were collected on one day, and more importantly, the Transect was believed to be under less continental influence than the Lagrangian study. Samples were collected while transiting to oceanographic stations and while on station (*Figure 2-1*). As samples were collected

in transit, day samples were not concurrent with night samples, though in most cases the samples were collected while overlying the same water mass.

4.3.1 Interpretation of Concentration & Isotopic Trends

4.3.1.1 Sulphur Dioxide

Day and night total SO_2 concentrations from the Transect study were relatively constant averaging ~900ngm^{-3}. However, there was one exception, a night sample that had a large concentration (10500ngm^{-3}) on May 5th (JD 125; coincident with very low SO_4^{2-} concentrations), when an intense rain shower occurred. The shower was so intense that one of the high-volume samplers did not restart. It is very likely that the total particulate matter was washed onto the underlying SO_2 filter. When the May 5th (JD 125) sample is removed, the average SO_2 concentration for night samples was ~900ngm^{-3}, which was similar to the daytime average ($F_{(1,21)}$=0.805, p=0.380). For this reason, the May 5th (JD 125) sample is not included in data analysis.

The uniformity of the SO_2 concentrations throughout the study was worthy of note and were much higher than previously reported for the North Atlantic. This illustrates that the North Atlantic is continually being influenced by continental emissions and these emissions have increased (or biogenic SO_2 emissions have increased) compared to summertime measurements in previous studies. Pszenny *et al.* (1990) and Berresheim (1987) reported SO_2 concentrations ranging between 32 to 310ngm^{-3} (summer 1989) and 5.4 to 22.4ngm^{-3} (Southern Hemisphere fall 1986) respectively. The increase in SO_2 concentrations is an important finding and it will

be interesting to compare the spring data with the summer and fall SABINA data once these analyses are available. It is important to note that SO_2 measurements reported here were obtained using high-volume sampling whereas other studies have used spectroscopy and fluorescence techniques and that the differences in concentration, may, in part, be due to differing measurement techniques.

Despite temporal and spatial differences in sampling during the Transect, it is common to examine the data sets as distinct day and night-time sample sets when dealing with atmospheric samples which are expected to represent scales of several thousand kilometres. The night-time samples had an average $\delta^{34}S_{SO2}$ (+13.9‰, SD = 3.3) value whereas the daytime samples had an average $\delta^{34}S_{SO2}$ of (+11.9‰, SD = 3.0), but this difference was not statistically different ($F_{(1,23)}$=2.74, p=0.130).

The anthropogenic, biogenic and total SO_2 concentrations (ngm^{-3}) calculated using a mass balance approach, are presented in *Figure 4-5*. For simplicity error bars are not shown on each plot. Propagated uncertainties were calculated for both the daytime and night-time samples and found to be approximately 27% for anthropogenic and 17% for biogenic SO_2 concentrations. The $\delta^{34}S$ value for a night-time SO_2 sample (May 8th, JD 128) had an isotopic composition which was greater (+20.3‰) than the assigned $\delta^{34}S$ value for biogenic sulphur derived from DMS oxidation (~18‰) used in the apportionment calculation. If we consider the uncertainty in the measurements, +20.3±0.4‰, and +18±3‰ it is likely that the isotope composition for this sample can be attributed to biogenic SO_2. Therefore, its concentration is assigned to be equal to the total SO_2 concentration. There was an increase in biogenic SO_2 at the northerly

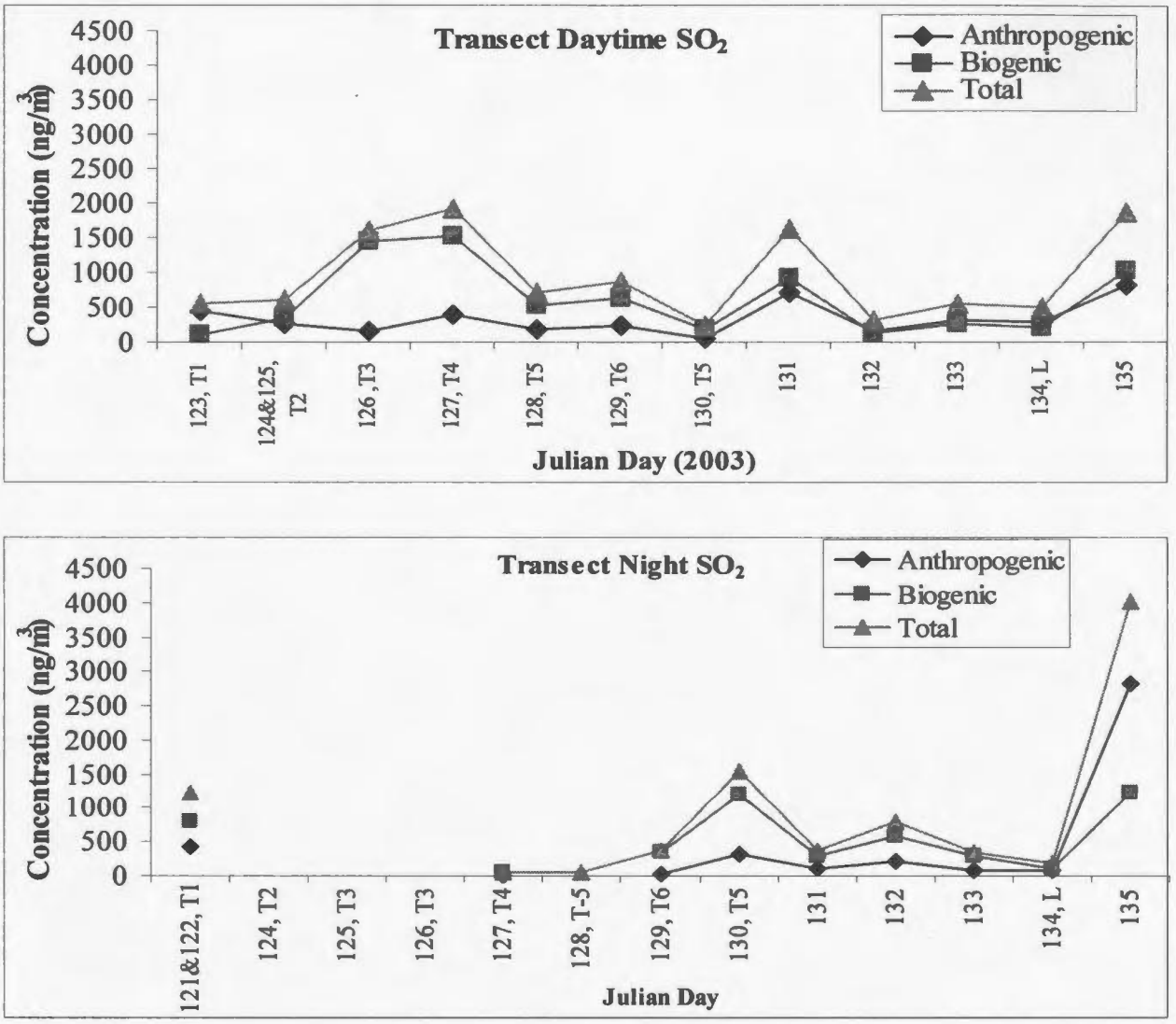

Figure 4-5 – Transect day (top) and night (bottom) anthropogenic, biogenic and total SO_2 concentrations (ngm^{-3}). The x-axis indicates the Julian Day on which the sample was collected, and also the station for the Transect study. Samples collected while transiting back to the Lagrangian station are listed as having no station. Propagated uncertainty is ±17% for biogenic SO_2 and ±28% for anthropogenic SO_2.

stations, reaching a peak concentration on May 10th (JD 130) the second highest night-time SO_2 concentration. Biogenic were greater than anthropogenic SO_2 concentrations in nearly all daytime samples (one tailed t-test, 2 degrees of freedom, p=0.041). Increased anthropogenic SO_2 was observed on May 3rd (JD 123), as the ship was leaving the Lagrangian site, May 11th as the ship was transiting near Newfoundland, and May 15th when the ship returned to Halifax. As an example of the information contained in this data, the results from May 3rd will be considered.

The air mass on May 3rd (JD 123) was classified as purely marine (1.0), and the isotopic $\delta^{34}S$ values for the corresponding total particulate sample ($\delta^{34}S$ = +19.6‰ and $\delta^{34}S_{NSS}$ = +10.0‰) were generally indicative of biogenic activity or DMS oxidation. The $\delta^{34}S_{SO2}$ value was +5.8‰ indicating that while large amounts of biogenic sulphate was present in the atmosphere, the proportion of anthropogenic SO_2 was also high (81.5%), which represents background contamination of the North Atlantic by continental air masses. Sulphur dioxide concentrations were below average on this date (563ngm^{-3}), and such periods of low SO_2 concentrations are typically used in other studies to be representative of clean marine air masses (Savoie *et al.* 1989). The average $\delta^{34}S$ value of the Hudson's fuel was +4.0 (SD = 0.2‰), which was very similar to the $\delta^{34}S_{SO2}$ composition on May 3rd (JD 123) so it is possible that some contamination from the ship's emissions influenced the sample, but the lack of higher SO_2 concentrations suggest that the sample was influenced by background continental SO_2 .

There was little difference in the trends for biogenic and total SO_2, illustrating the dominance of biogenic SO_2 in the data set. The May 15th (JD 135) night sample had a high anthropogenic SO_2 concentration which corresponded with the lowest $\delta^{34}S_{SO2}$ value (+7.6‰) for the night samples. Comparison with air mass trajectories showed the air mass originated from the North Eastern United States, explaining the anthropogenic isotopic composition. The remainder of the night samples had high biogenic concentrations.

Biogenic SO_2 is omnipresent in the remote marine atmosphere over the NW Atlantic. The maximum concentrations for the daytime samples occurred on JD 126 & 127 (1440 ngm^{-3} and 1540ngm^{-3} respectively). The night samples have no values from JD 124-126 because of an intense rain-shower that rendered one of the air samplers unusable. The night samples had the highest biogenic concentrations on May 10th (JD 130, 1540ngm^{-3}) while transiting through the Labrador Current and again while transiting towards Halifax (JD 135, 1220ngm^{-3}). This indicates that location was of great importance. Increased biogenic SO_2 concentrations were observed while transiting through cold waters associated with the Labrador Current. These waters were biologically productive with high ocean DMS concentrations (personal communication M. Savard) that coincided with high atmospheric DMS concentrations (Wadleigh, personal communication).

There was no statistical significance between $\delta^{34}S_{SO2}$ values ($F_{(3,23)}$=2.474, p=0.130) and SO_2 concentrations ($F_{(3,23)}$=0.48, p=0.84) and air mass classification. This

signified that the air mass origin was not a significant factor controlling SO_2 concentrations.

4.3.1.2 Sea Salt Components

Sea salt components for the day and night Transect samples had wide ranging concentrations (*Figures 3-8, 3-11, 3-16 & 3-19*). Both the day and night samples indicated higher concentrations at the start of the Transect with concentrations leveling off as the ship reached more northerly stations. Cl^- was showed significantly higher concentrations at the start of the Transect ($F_{(7,64)}$=2.407, p=0.031). This was coincident with average wind speeds that were higher at the beginning of the daytime Transect Study (JD 123-127) (one tailed t-test, 2 degrees of freedom, p=0.0467). The daytime average wind speed from May 3rd to 7th (JD 123-127) was 49 (SD = 21km/hr), and for the night samples the average was 21 (SD = 3.8 km/hr). From May 7th to 10th (JD 127-130) the average wind speed for the day samples was 38 (SD = 14km/hr) and the night average was 27 (SD = 9km/hr). Higher wind speeds as a result of synoptic scale events that are evident over large spatial scales would result in a disturbed sea state, with more sea salt being lifted into the atmosphere. This would lead to deposition of more sea salt constituents due to their short atmospheric residence time. The elevated sea salt component concentrations at the start of the Transect can therefore be explained by this mechanism.

4.3.1.3 Cations

The day and night cations had low concentrations, with most below 500ngm^{-3}. Berresheim *et al.* (1991) reported that NH_4^+ concentrations were higher in continental air masses, and larger NH_4^+ concentrations were generally found in fine aerosol particles. This was also true for the spring SABINA data. Ammonium concentrations were largest in the smallest aerosols (<0.49μm), though there was no correlation between NH_4^+ concentrations and air mass back trajectory (Pearson Correlation, r = -0.0421).

The trend found for cation concentrations was comparable to what was found to sea salt components, with higher concentrations at the beginning of the Transect study. Magnesium and Ca^{2+} exhibited similar trends and were directly correlated (Pearson Correlation, r=0.956, *Table 4-2*). The correlation between Ca^{2+} and other sea salt components indicted that Ca^{2+} was derived in association with marine aerosols rather than continental dust, as Mg^{2+} and Na^+ are both known to be conservative sea salt tracers. Calcium has been often used as tracer for continental sources (e.g. Barrie & Barrie 1990), but that is not appropriate for this study. It is interesting to note that the ratio of Ca^{2+}/Mg^{2+} in average seawater is 0.32, and in this study, in fine aerosols (<0.95μm) the average Ca^{2+}/Mg^{2+} ratio was 4.4 (SD = 2.4), closer to ratios for seawater that were present in the benthic foraminiferal calcite (Lear et al, 2000). The very good correspondence between typical SS parameters such as Cl^-, Na^+ and Mg^{2+} with Ca^{2+} (*Table 4-2*), suggests calcium enrichment in the fine aerosols was not the result of dust transport.

Table 4-2 – Pearson correlation (r) of components compared to Ca^{2+}.

Data Set	Pearson Correlation
SS-SO_4^{2-}	0.658
Na^+	0.777
Mg^{2+}	0.956
Cl^-	0.874
SO_4^{2-}	0.980

4.3.1.4 Anions

Phosphate is not often discussed in previous aerosol studies, though in this study there was an interesting trend to discuss. Phosphate was only detected in the <0.49μm size fraction for the daytime size segregated samples from May 4th to 9th (JD 124-129) and after the maximum concentration was reached on May 9th (30.9ngm^{-3}, JD 129). PO_4^{3-} was detected in the larger size fractions (*Figure 3-12a*). Phosphate concentrations also differed diurnally ($F_{(1,8)}$=142.12, $p<0.001$). Phosphate was detected in three air masses in the night samples associated with purely marine (1.0), aged continental (2.0) and arctic (5.0) air mass back trajectories (*Figure 4-6*). Phosphate was detected in the nearly all air masses in the daytime Transect samples, but higher than average concentrations were found in the aged continental and arctic air masses. Higher concentrations were also observed when the ship entered northerly waters. The increases in PO_4^{3-} concentrations could potentially be related to colder water masses and colder atmospheric temperatures, leading to a shift in the production and/or removal of PO_4^{3-} (in sea salt aerosols). Phosphate concentrations began to increase only after reaching the colder water masses during the Transect study. There are few known sources of atmospheric PO_4^{3-}, and no known marine sources. Surface ocean PO_4^{3-} concentrations were not higher than expected for that time period (Pommier, personal communication). This is an intriguing finding but one that is not easily understood.

Nitrate is used as an indicator of aged anthropogenic pollutants as there are no known sources of significant aerosol NO_3^- in the remote marine atmosphere (Patris *et al.*

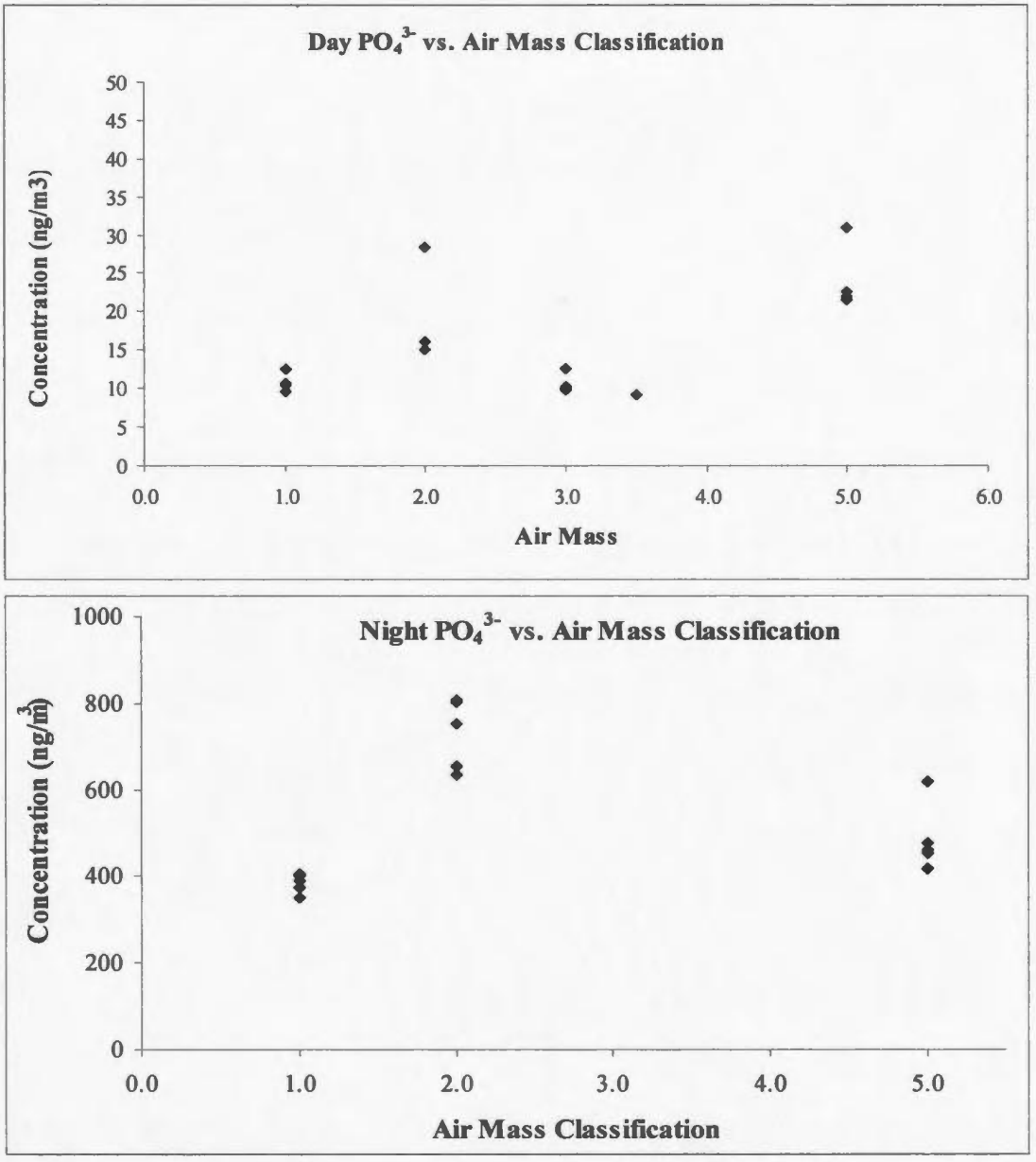

Figure 4-6 – Phosphate concentrations vs. air mass classification for both day (top) and night (bottom) samples. Uncertainty in concentration measurements is ±10%. (Note: Air mass classification: 1 purely marine, 2 aged continental, 3 continental with marine influence, 4 strongly continental and 5 arctic air mass.)

2000). Higher than average concentrations of NO_3^- were not found in specific air mass classifications (Pearson Correlation, r=0.198). This was not surprising as aerosol NO_3^- is not only directly transported in continental air masses, but forms from oxidation of NO_x during long range transport. Nitrate is a known oxidant of DMS resulting in the production of biogenic SO_2. A possible scenario is as follows: as more NO_3^- became available at night as NO_2 photolysis reactions ceased, NO_3^- could have replaced OH photo-oxidation of DMS, producing more biogenic SO_2. Some biogenic SO_2 produced would be further oxidized into SO_4^{2-} aerosols. This explains the isotopic compositions for SO_2 and SO_4^{2-} indicating biogenic sulphate at night. NSS-SO_4^{2-} was the one of the more abundant anions, and had the highest concentrations in the smallest size fraction ($F_{(4,53)}$=4.76, p=0.003)). Concentrations of NSS-SO_4^{2-} were comparable in both the day and night samples ($F_{(1,53)}$=1.61, p=0.21), with maximum concentrations at the end of the cruise, upon return to the SOLAS Mooring site, and minimums when sampling Northerly stations (JD 128 & 129), indicating the anthropogenic influence near the Lagrangian study location.

MSA concentrations, an oxidation product of DMS, were highest in the smallest aerosols and in the total particulate samples ($F_{(1,6)}$=0.32, p=0.864) which, due to the very short lifetime of this fine aerosol, suggests the majority of MSA was formed during or shortly prior to sampling. The highest concentration, 107ngm^{-3}, was found in a night-time sample (<0.49μm) on May 12th (JD 132) while transiting to the SOLAS Mooring station and crossing the Labrador Current. A DMS maximum occurred the same day (Wadleigh *et al.* 2004), which strongly suggests that

atmospheric DMS was quickly oxidized to MSA on aerosols. The range in air temperature during sampling was from 2.5 to 21.9^{0}C. MSA concentrations collected from JD 122-135 were statistically significant for the atmospheric temperature during sampling (one tailed t-test, 2 degrees of freedom, $p<0.001$), although a single temperature dependence was not observed for all size fractions. Generally higher concentrations of MSA were found in the smaller size fractions at colder temperatures, whereas the opposite was found in the larger size fractions. This is an extremely interesting result, which will require further interpretation when this data is compiled with the DMS data in future papers. Potentially the data could indicate that DMS oxidation to MSA results in new aerosol formation at colder temperatures, whereas it adds mass to pre-existing aerosols at warmer temperatures.

There were no correlations between MSA and anthropogenic, biogenic or total SO_4^{2-} for either day or night-time transect samples. There were no correlations between anthropogenic or biogenic SO_4^{2-} and aerosol NO_3^- in the day and night samples, and no relationship was observed for total, biogenic, or anthropogenic SO_4^{2-} fractions with temperature (Pearson Correlation, r=-0.064). This strongly suggests that formation of biogenic SO_4^{2-} was not temperature dependent. Most importantly, and contrary to the assumptions found in the literature (e.g. Berresheim 1987; Calhoun 1990; Bates *et al.* 1992; Savoie *et al.* 1989; Saltzman *et al.* 1983) there was no relationship between MSA and NSS-SO_4^{2-} for daytime (Pearson Correlation, r=0.4185), or night-time samples (Pearson Correlation, r=0.2381).

4.3.2 Sulphate Sources

Whereas chemical data can assist in apportioning sources of sulphate, it is not conclusive. Source apportionment with sulphur isotopes to obtain biogenic sulphate concentrations, along with MSA concentrations allows in-depth source discrimination. The following sections describe detailed source apportionment scenarios for the Transect study.

4.3.2.1 $\delta^{34}S$ Values

$\delta^{34}S$ can be used to apportion sources of sulphur when the end-member sources are known. The triangular mixing area presented in this section helps apportion sources of sulphate to the remote marine atmosphere. *Figure 4-7* shows the three way mixing plot between sea spray sulphate, anthropogenic sulphate and biogenic sulphate for the day and night total particulate Transect samples. Mixing of sea salt sulphate and anthropogenic sulphate with a $\delta^{34}S$ value of +3‰ would be expected to fall along the lower line of the triangle shown in *Figure 4-7*. Mixing of sea salt sulphate and biogenic sulphate with a $\delta^{34}S$ value of +18‰ would be expected to fall along the upper line shown in *Figure 4-7*. Mixing between biogenic sulphate and anthropogenic sulphate lies along the y-axis and forms the third line of the triangle. Thus, the triangle indicates a mixing area between the three end-members. Six points fall below the mixing area for the daytime samples, when a value of +3‰ is assumed for the anthropogenic sulphate end-member.

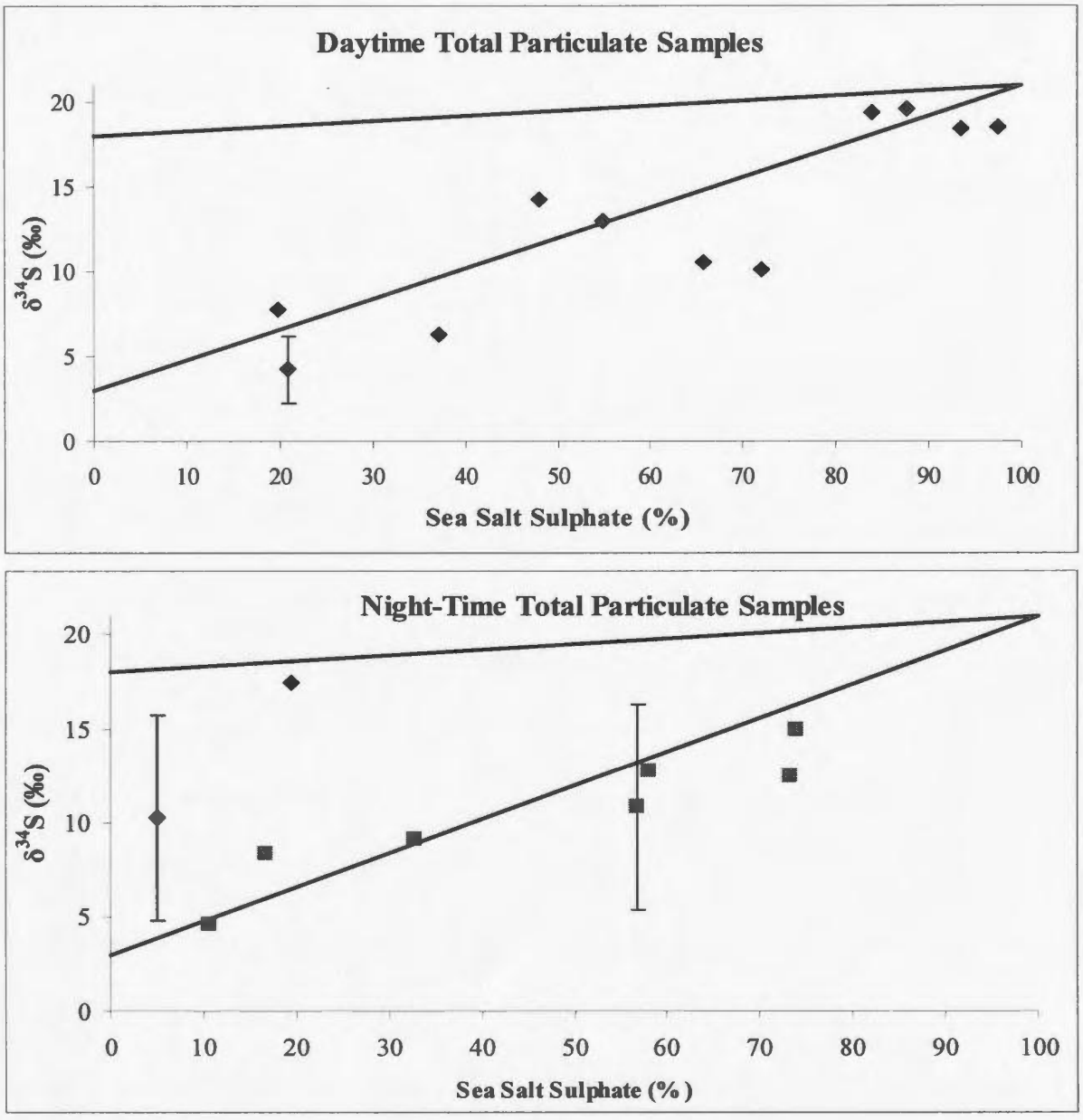

Figure 4-7 – Three way mixing plot for the day (top) and night (bottom) total particulate samples. The night samples which were collected using a PM_{10} head are denoted by diamonds. Error bars illustrate analytical uncertainty, and where error bars are absent, the uncertainty is ±0.4‰. Percentage sea salt sulphate has a ±10% uncertainty.

Higher $\delta^{34}S$ values were associated with higher percent sea salt and this is congruent with what was expected since sea salt has a $\delta^{34}S$ value of +21‰. The daytime total particulate Transect samples generally trended along the line between anthropogenic and sea salt sulphate (lower line in *Figure 4-7*), indicating that biogenic sulphate was not of great importance to many of these samples. The night samples had a similar isotopic average (+12.9, SD = 4.9‰) as the daytime samples; though the average sea salt contribution was lower (39, SD = 26%). Due to the sampling problems described in Section 2.3 the night samplers for total aerosols were equipped with a PM_{10} head for two samples (diamonds; *Figure 4-8*), otherwise aerosols in the size range <100 microns were collected. The samples which were collected using the PM_{10} head had less sea salt contributions but there were not enough points to determine if this was significant. Only samples of the same aerodynamic size were compared. As previously discussed Section 4.2.1 it is believed that a large proportion sea salt particles were found in the size fraction >10μm, which resulted in the PM_{10} head collecting less sea salt particles. Higher biogenic concentrations of SO_4^{2-} in the night samples (Section 4.3.2.4) indicate that either there was more biogenic sulphate produced during the night in association with nitrate oxidation of biogenic SO_2, or that more DMS oxidized directly to sulphate on pre-existing aerosol particles.

Both the day and night size segregated Transect samples did not conform to the triangular mixing plot when an lower end-member of +3‰ was assumed. Using the data as a guide, the values on *Figure 4-8* suggest a better fit would be obtained if an end member with a $\delta^{34}S$ value of -25‰ rather than +3‰ was used.

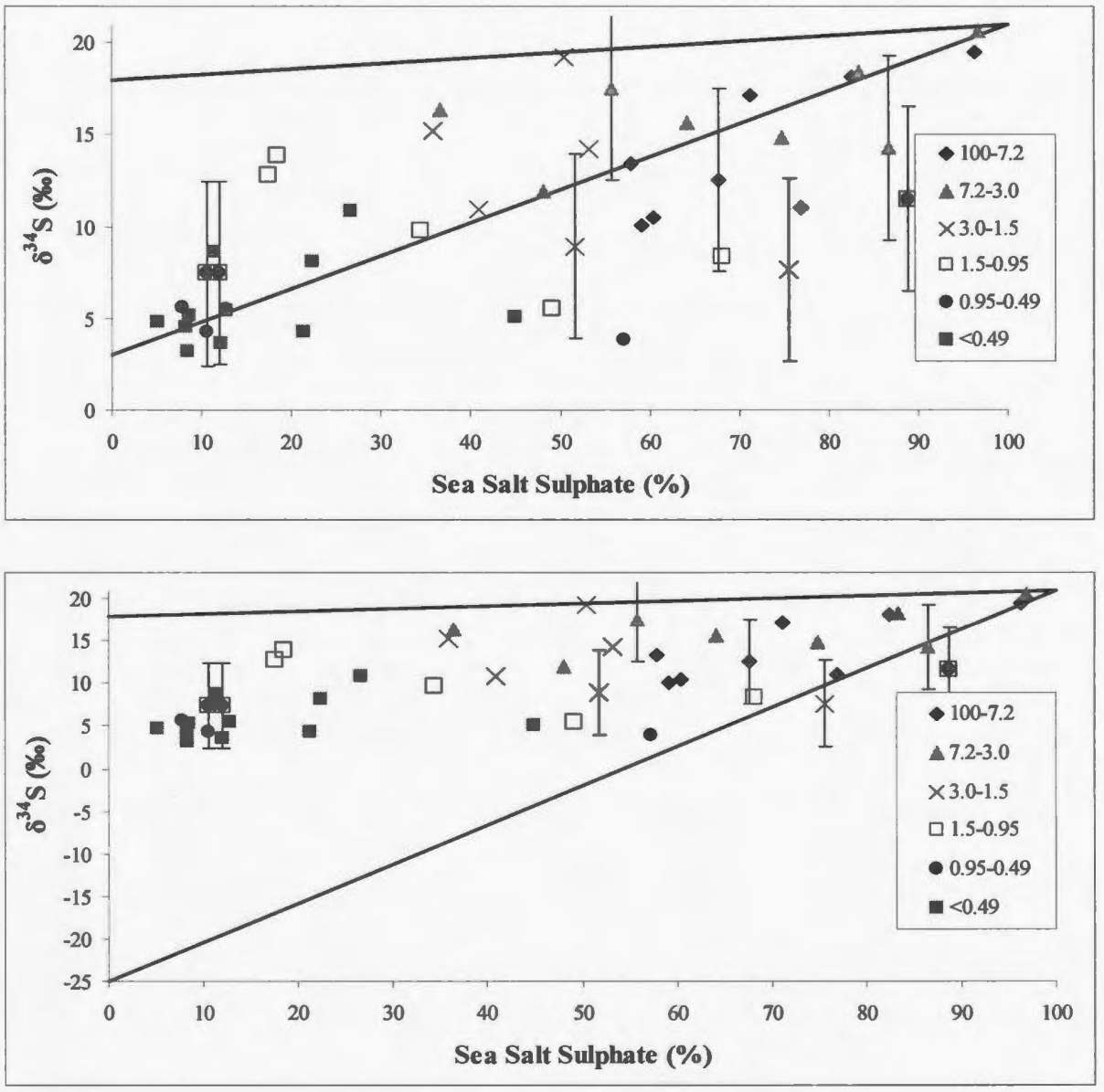

Figure 4-8 – Daytime size segregated $\delta^{34}S$ (‰) vs. sea salt (%) using +3‰ as the anthropogenic end member (top) and -25‰ as the other end-member (bottom). Error bars illustrate analytical uncertainty, and where error bars are absent $\delta^{34}S$ uncertainty is <0.4‰. Sea salt sulphate uncertainty is ±10%.

Triangular plots using both -25‰ and +3‰ as the lower end-member for the daytime size segregated samples are shown on *Figure 4-8*. To conclusively state that the source was anthropogenic, all possible negative sources of $\delta^{34}S$ must be excluded. As previously discussed in section 4.2.2.1, a possible source of an isotopically depleted SO_4^{2-} is H_2S. Hydrogen sulphide is often only detected in coastal and tidal flats. As no sampling occurred near shallow marine flats, and isotopically light SO_4^{2-} and SO_2 were observed in previous studies of the North Atlantic, this suggests a marine H_2S source can be discounted.

Figure 4-8 illustrates how the -25‰ end-member constrains the samples with compositions <+10‰, and high percent sea salt (>50%). In other studies, aerosols with a high percent sea salt sulphate have high isotopic compositions similar to sea salt sulphate (+21‰). This is not the case in the Transect data, where samples with isotopic compositions as low as +5% were observed to have a sea salt contribution of 75%. This was unlike previous data presented from the North West Atlantic (Patris *et al.* 2000; Wadleigh 2004). Mixing between an isotopically depleted source of SO_4^{2-}, or isotopically depleted SO_4^{2-} condensing on sea salt particles is possibly the reason these samples do not conform to the mixing model. Note that the -25‰ end-member was not necessary for explaining the values of $\delta^{34}S_{SO2}$, and it is curious that there should be such a large discrepancy between the $\delta^{34}S_{SO2}$ and $\delta^{34}S_{NSS}$ values.

The $\delta^{34}S$ values for daytime Transect samples ranged between +20‰ and 0‰. The average percent sea salt was 45 (SD = 27%), with the largest size fraction (100-

7.2μm) having the largest sea salt contributions (71, SD = 19.4%) and higher $\delta^{34}S$ values (+14.9, SD = 3.9‰). The 1.5-0.95μm size fraction had a relatively constant $\delta^{34}S$ value of +9.5 (SD = 2.8‰), but sea salt sulphate content ranged from ~15% to 90% in this fraction, indicating that the aerosols were composed of both sea salt sulphate and biogenic sulphate. This is similar to data reported by Wadleigh (2004), who found high sea salt contributions in aerosols >0.95μm. The smallest size fraction, <0.49μm had an average percent sea salt of 16 (SD = 11%), with an average isotopic composition of +5.8 (SD=2.4‰), indicating dominance by anthropogenic sulphate. The source of the anthropogenic sulphate is long range transport or; less likely as SO_2 concentrations did not vary significantly, from the Hudson's and other nearby ship stack emissions.

The triangular mixing plot for the night size segregated samples is presented in *Figure 4-9* using two end-members, -10‰ and +3‰. Again, the data were used to define the best value for $\delta^{34}S$ to represent the anthropogenic end member. In contrast to the daytime samples which suggested a much more negative $\delta^{34}S$ end member (-25‰), the night-time $\delta^{34}S$ value suggested was less extreme (-10‰). The SO_2 data illustrated that the night samples had greater biogenic contributions than the day samples and a similar result is suggested by the less negative $\delta^{34}S$ end-member shown in *Figure 4-9*. The mixing plot had a lot of scatter, with a wide range of $\delta^{34}S$ values and percent sea salt sulphate. The smallest size fraction (<0.49μm) had the least sea salt contribution (23, SD = 27%) (except the sample collected on May 6th (JD 126) after the rainstorm on May 5th, which had a sea salt contribution of 91.8%, likely due

to the stormy conditions the day prior). The larger aerosols were primarily composed of sea salt particles, while the smallest size fraction was dominated by anthropogenic and biogenic sulphate.

Data from the night-time size segregated samples indicate that sea salt is present in all size fractions, and the average amount of sea salt in the smallest size fraction is unusual and relatively large compared to values in the literature. Patris *et al.* (2000) and Murphy *et al.* (1998) reported aerosols <0.95μm with considerable sea salt concentrations (up to 65% and 20ngm^{-3} respectively). Conversely Wadleigh (2004) reported only aerosols <0.95μm having an average sea salt contribution of 15%. It is curious that despite the similarity in sampling protocol and site with the NODEM studies reported by Wadleigh (2004), there should be such a large difference between the North Atlantic data sets. It will be interesting to observe whether the NODEM data are in better agreement with the summer and fall SABINA data.

4.3.1.2 $\delta^{34}S_{NSS}$ Values

$\delta^{34}S_{NSS}$ values refer to the non sea salt component of $\delta^{34}S$ values, while $\delta^{34}S$ values are the total isotopic value of all components of sulphur in the sample. Generally the $\delta^{34}S$ values found for the Transect were similar to those presented by previous authors (e.g. Gravenhorst 1977; McArdle and Liss 1995; Turkeian *et al.* 2001, Wadleigh 2004). The $\delta^{34}S_{NSS}$ values presented here are very unusual and unlike previous studies. What makes the entire data set (Lagrangian and Transect) unusual is the presence of negative $\delta^{34}S_{NSS}$ values. These results are not likely an artifact as

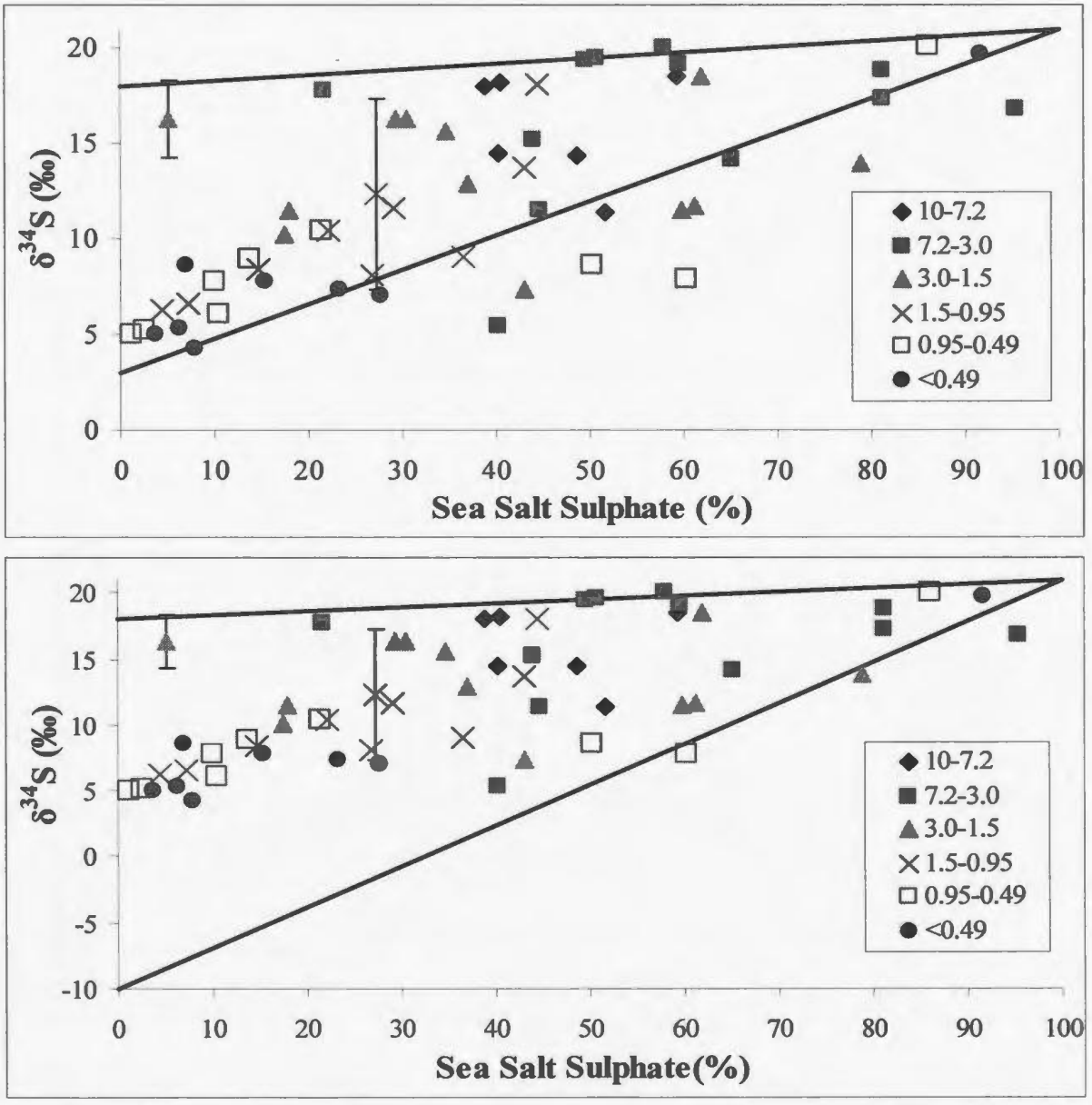

Figure 4-9 – Night size segregated $\delta^{34}S$ (‰) vs. sea salt (%) using +3‰ (top) and -10‰ (bottom) as the end members. Error bars illustrate analytical uncertainty, and where no error bars are present $\delta^{34}S$ uncertainty is <0.4‰. Sea salt sulphate uncertainty is ±10%.

negative $\delta^{34}S_{NSS}$ values were present in all sample sizes. The size and manufacturer of the large quartz filters used for the total, and <0.49 micron size fractions, differed from those for the slotted filters. If an artifact were present it would likely be confined to a particular filter type and this was not observed. It is also worthwhile noting that considerable precautions in sample preparation and analyses were taken throughout this study and filter blanks were subtracted. Due to the very unusual nature of the $\delta^{34}S_{NSS}$ values presented here, the presence of an artifact was thoroughly examined and discarded as a potential source of the extremely negative $\delta^{34}S_{NSS}$ values.

There are few references to negative $\delta^{34}S_{NSS}$ values in recent studies. Gravenhorst (1977) reported a $\delta^{34}S_{NSS}$ value of -12‰ from a maritime aerosol sample influenced by continental sources, though the data point was excluded from the discussion. Norman (1991) reported a $\delta^{34}S_{NSS}$ value of -7.8‰ from a rainwater sample collected near a biologically productive marsh at Bermuda. The lower $\delta^{34}S$ value was attributed to the oxidation of H_2S emissions from the marsh. Motoyama *et al.* (2000) reported $\delta^{34}S_{NSS}$ values from precipitation and aerosol samples collected at two sites, Yamagata and Sakata, Japan. Negative $\delta^{34}S_{NSS}$ values (-1‰) were reported for precipitation samples in 1991, 1993 and 1999 at Sakata. At Yamagata there was a range of negative $\delta^{34}S_{NSS}$ values (0 to -5‰). The aerosol samples had a minimum $\delta^{34}S_{NSS}$ value of -3‰ at Yamagata, and the negative values were attributed to the combustion of ^{34}S depleted oil and coal.

For the purpose of simplicity the negative $\delta^{34}S_{NSS}$ values found in both the Lagrangian and Transect studies are presented together in *Table 4-3*. There were no correlations between negative $\delta^{34}S_{NSS}$ values and air mass, wind speed, diurnal sampling, date, aerodynamic aerosol size, percent sea salt sulphate, oceanic and atmospheric temperatures, MSA/NSS-SO_4^{2-} ratios or any chemical component. There was a wide range of concentrations for all the chemical constituents in the negative $\delta^{34}S_{NSS}$ samples.

After it was determined that the negative values did not correspond to any measurable component or situation, the possibility of an unknown fractionation was considered. If a fractionation associated with the oxidation from SO_2 to SO_4^{2-} occurred there should be indications of the direction of the fractionation in *Figure 4-10*, a plot of $\delta^{34}S_{NSS}$ vs. SO_2 concentration. The SO_2 concentration used in *Figure 4-10* was the corresponding SO_2 filter, thus if there were two or three size segregated samples from the same sampling day they would have the same SO_2 concentration. It was assumed that if there was a single first order kinetic isotope fractionation during the transformation from SO_2 to SO_4^{2-} the plots in *Figure 4-10* would indicate the direction of the fractionation. Kinetic fractionation results when the heavier or lighter isotope is favored in the formation of the product. In this case SO_2 is the reactant and NSS-SO_4^{2-} is the product. If NSS-SO_4^{2-} aerosols were formed from SO_2, then as the SO_2 concentration decreased, heavier or lighter S would be preferentially removed, leaving the remaining SO_2 isotopically altered and a corresponding change in isotope composition would be apparent in the NSS-SO_4^{2-} $\delta^{34}S$ values.

Table 4-3 – Samples with negative $\delta^{34}S_{NSS}$ values and corresponding meteorological and sample information.

	Julian Day	Size (μm)	$\delta^{34}S$	%SS	$\delta^{34}S_{NSS}$	MSA/ NSS	Temp (°C)	Wind Speed (km/hr)	Air Mass	Weather Conditions
Day	***119&120***	***0.95-0.49***	***3.4***	***30.0***	***-4.1***	1.9	***7.0***	***38.5***	***4.0***	***Fog+ clear***
Day	126	<0.49	4.3	21.3	-0.3	4.3	16.7	30.7	1.0	Rain showers
Day	***127***	***1.5-0.95***	***5.5***	***49.1***	***-9.4***		***14.0***	***50.9***	***3.5***	***Stormy***
Day	***127***	***0.95-0.49***	***3.9***	***57.2***	***-19.1***		***14.0***	***50.9***	***3.5***	***Stormy***
Day	130	<100	10.6	65.7	-9.3	7.0	4.4	23.2	5.0	Overcast
Day	130	100-7.2	10.0	59.1	-5.8		4.4	23.2	5.0	Overcast
Day	130	7.2-3.0	14.8	74.8	-3.4		4.4	23.2	5.0	Overcast
Day	131	<100	10.1	72.0	-17.7		9.3	52.0	1.0	Drizzle & fog
Day	131	<0.49	5.1	45.0	-8.0	2.9	9.3	52.0	1.0	Drizzle & fog
Day	132	100-7.2	11.1	76.9	-22.1	6.5	7.6	29.3	3.0	Drizzle & fog
Day	134	<100	6.3	37.1	-2.3	5.0	9.0	15.2	2.0	Rain showers
Day	134	100-7.2	10.5	60.4	-5.5		9.0	15.2	2.0	Rain showers
Night	128	0.95-0.49	8.4	50.2	-4.2	7.6	6.6	20.0	1.0	Clear
Night	129	0.95-0.49	7.3	60.3	-13.4	4.8	4.3	21.9	2.5	Clear
Night	132	<0.49	4.5	27.8	-1.8	77.2	4.7	25.6	3.0	Clear
Night	133	<100	12.6	73.4	-10.6	1.2	7.9	28.5	3.0	Fog
Night	134	7.2-3.0	3.8	40.3	-7.7	0.8	5.7	20.9	2.0	Fog, clearing
Night	135	3.0-1.5	6.9	42.9	-3.6	5.4	4.0	29.8	2.0	Fog

Note: Samples in italics indicate that $\delta^{34}S$ was determined using Na^+ as the conservative sea salt tracer as opposed to Mg^{2+}.

As the concentration of SO_2 decreased the resulting $\delta^{34}S_{NSS}$ value would become either depleted or enriched with respect to ^{34}S if kinetic fractionation exists. The daytime plot (*Figure 4-10*) does not reveal any patterns, though speculatively the night-time plot might be interpreted to show a logarithmic relationship between $\delta^{34}S_{NSS}$ values and SO_2, with smaller concentrations of SO_2 resulting in lighter $\delta^{34}S$ values for sulphate that was formed. The relationship is driven by a pair of points with high SO_2 concentrations and obviously requires more data to reveal whether these results are robust. If true, however, this relationship may suggest an oxidation mechanism attended by a kinetic isotope fractionation consistent with favoring the heavy isotope in the product. Saltzman *et al.* (1983) suggested such results might be attributed to heterogeneous SO_2 oxidation. The relationship between SO_2 concentration and $\delta\,^{34}S_{NSS}$ values in the night-time samples is more apparent than for the daytime samples and the very negative $\delta^{34}S_{NSS}$ values imply that the sulphate formed is an instantaneous rather than a cumulative product. Presumably this would occur more often when night time conditions were foggy, and many negative values were found on foggy days (*Table 4-3*). Also, homogeneous oxidation would likely be higher in the day when photolytic reactions producing OH and O_3 are important, than at night. Thus, if night-time oxidation of SO_2 was primarily heterogeneous, this could explain why there is an apparent day/night difference. Clearly there are not enough data points to conclusively state whether the negative $\delta^{34}S_{NSS}$ values can be attributed to kinetic fractionation. Also, as the heavy isotope is preferentially oxidized, remaining SO_2 should become isotopically lighter. Lighter SO_2 isotope compositions

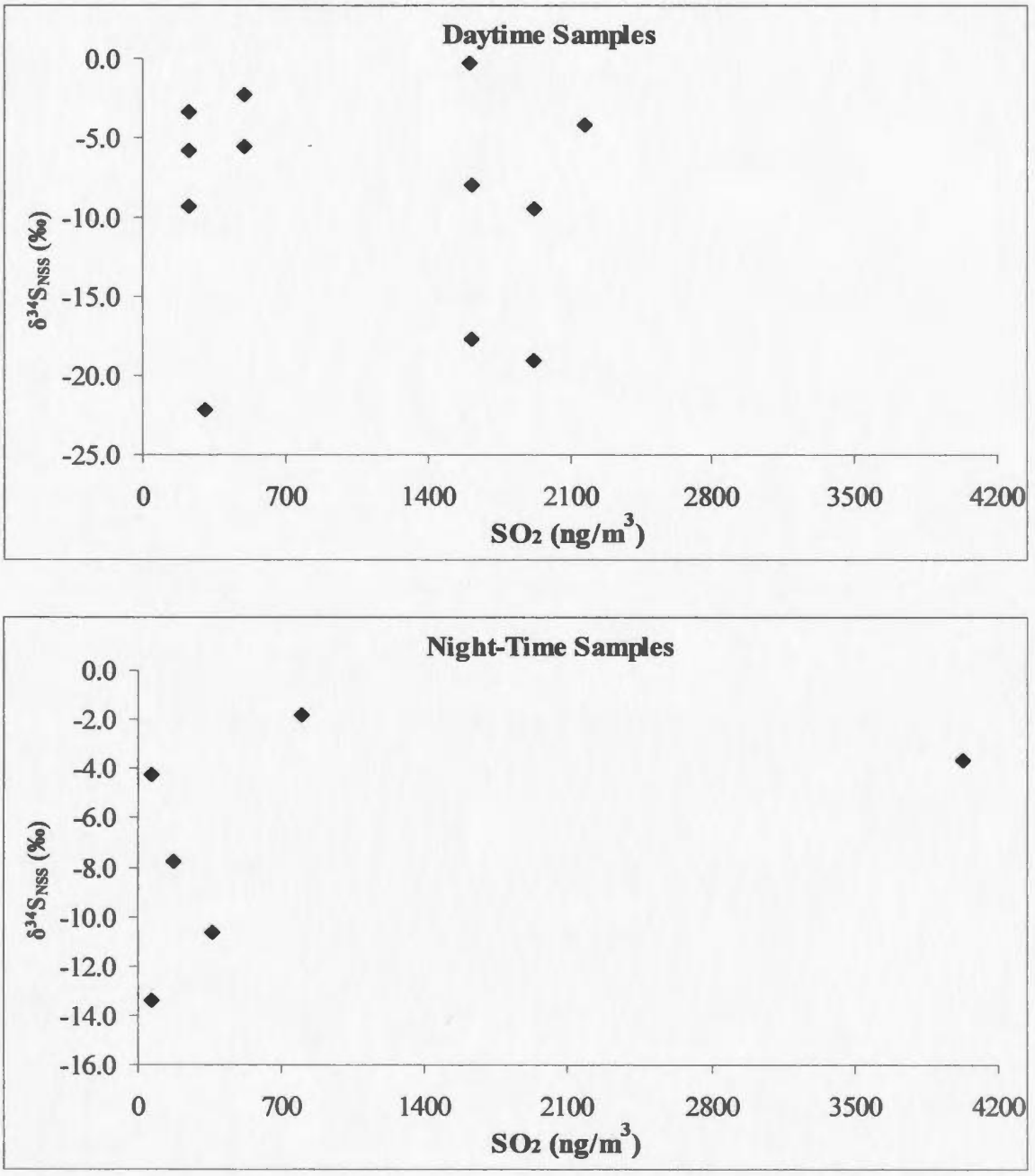

Figure 4-10 – $\delta^{34}S_{NSS}$ (‰) vs. SO_2 (ngm^{-3}) for both day (top) and night (bottom) samples with negative $\delta^{34}S_{NSS}$. Uncertainties in $\delta^{34}S$ values are ±0.4‰, and ±10% for concentrations.

were not associated with lower isotope compositions, which is further indication that kinetic fractionation is likely not occurring. However it is interesting that more positive $\delta^{34}S$ values for SO_2 occurred at night compared to the day and this opposed the proposed fractionation if heterogenous oxidation were more important at night. These results are intriguing and it will be interesting to see whether similar results will be found for the summer and fall cruise samples.

Another possible fractionation which could cause negative $\delta^{34}S_{NSS}$ values are the numerous oxidation pathways for DMS fractionation during DMSO and/or MSA production, and potentially direct oxidation of DMS to SO_4^{2-} on pre-existing particles. If this direct oxidation had a large fractionation (20 to 40‰) the resulting SO_4^{2-} particles could have negative $\delta^{34}S_{NSS}$ values. The analysis of such an oxidation mechanism has been studied by Sanusi *et al.* (2006), and little to no isotope fractionation was observed for total particulate aerosols in samples from the Pacific. However, that study did not consist of day and night samples.

The last possible explanation for negative $\delta^{34}S_{NSS}$ values was the existence of a negative source of sulphate. There were no low or negative $\delta^{34}S_{SO2}$ values, which signify that the source would either have to be so remote that all SO_2 from that source was previously be oxidized to SO_4^{2-}, or there was a SO_4^{2-} source and little to no SO_2 Another possibility is that an SO_2 source was emitted in the presence of metal catalysts and other oxidants and rapidly oxidized to SO_4^{2-}. One potential source of isotopically depleted $^{34}SO_4^{2-}$ and SO_2 during the study was emissions from the

refinery in Come by Chance, Newfoundland which refines crude oil into petroleum products. The North Atlantic Petroleum Refinery is owned by Vitol Refining S.A. Inc, and refined in excess of 105,000 barrels of oil per day (Slade, personal communication). Since 1995 the refinery has refined oil from the Middle East and during the spring of 2003, the refinery used fuel from Trinidad (Slade, personal communication). The refinery emissions in 2003 were: 14,136 tonnes of SO_2, 2.2 tonnes of COS and 4.6 tonnes of H_2S (NPRI, 2003). The isotope composition of the refinery emissions are not expected to differ from the crude oil itself (Jamieson and Wadleigh 1999; Wadleigh and Blake 1999). In the refining process part of the material being refined is combusted. It is also unknown how much of the SO_2 emitted is derived from Middle Eastern oils.

Thode and Monster (1970) presented sulphur isotopic data for crude oil samples from the Middle East. It was determined that Iraqi oil had $\delta^{34}S$ values raging from +6.5 to -5.5‰. The oxidation of a depleted source such as Middle Eastern oil may be the source of depleted SO_4^{2-} which could explain some of the negative $\delta^{34}S_{NSS}$ values, though the $\delta^{34}S$ values from Middle Eastern oil are not as low as the results found in this study. Flaring from the Sable Island gas field is also a possible source of isotopically light sulphate. Maximov et al. (1975) showed that gases in the Amu-Dariya syncline (Jurassic) deposits with less than 1% H_2S had $\delta^{34}S$ values as low as –16 ‰. The isotopic composition of Trinidad oil is unknown and future research into this would be beneficial to the further knowledge of the possible point sources of sulphur pollution to Newfoundland and the North Atlantic.

The $\delta^{34}S$ values vs. % sea salt sulphate plots (*Figures 4-8* and *4-9*) did not fit the model as presented by previous authors (Jamieson and Wadleigh, 1999; Wadleigh 2004) for similar studies of North Atlantic aerosols in summer and fall. This was due to the presence of isotopically light SO_4^{2-} and samples with high sea salt sulphate contributions and low $\delta^{34}S$ values. If the refinery was a point source it would be expected that the $\delta^{34}S_{NSS}$ negative values would correspond to a location or air mass, but that was not the case. There were numerous air masses which originated or traveled over the area near the refinery, in particular on May 7th, 8th and 12th (JD 127, 128&132) (see *Appendix II.5*). These days exhibit negative $\delta^{34}S_{NSS}$ values in all size fractions which suggest that the refinery emitted depleted SO_4^{2-}, or SO_2 which was quickly oxidized into SO_4^{2-} particles rather than an effect due to kinetic fractionation. The presence of nearby ships is also an important factor as the origin of the fuel they are using is often unknown. Calpado *et al.* (1999) reported that the SO_2 emitted from ship emissions was significant enough to affect the global sulphur cycle and have climatic implications. According to the model ship's emissions could account for 10-30% of NSS-SO_4^{2-} over oceans in the Northern Hemisphere, and up to 90% of global emissions over the North Atlantic in January (Calpado *et al.* 1999). While travelling from the most northerly station to the SOLAS Mooring site, the CCGS Hudson passed through common shipping lanes (JD131-133), and the aerosols collected may have been affected by direct SO_2 emissions (though this does not seem to be an important source of SO_2) and SO_4^{2-} particles. Ship's emissions may be a source of very fine aerosols (<0.49μm) which form quickly and accumulate with other particles

to become larger aerosols. Very small aerosols (<0.95μm) have a short atmospheric lifetime, whereas fine aerosols (between 0.95 and 2.5μm) can persist in the atmosphere for weeks (Prospero *et al.* 1983), allowing them to be transported long distances. Based on the size fractions where the most negative $\delta^{34}S_{NSS}$ values were observed, ship stack emissions were not a dominant source of this negative aerosol SO_4^{2-}.

4.3.2.2 MSA/NSS-SO_4^{2-} Ratios

The average MSA/NSS-SO_4^{2-} (%) ratios for the day and night Transect samples are presented in *Table 4-4*. The average for the night (8.2, SD = 13.3%) and daytime (5.6, SD = 5.6%) samples were similar ($F_{(1,32)}$=0.808, p=0.356). The ratios for the night samples were variable, whereas the daytime samples had relatively low and constant ratios. MSA/NSS-SO_4^{2-} ratios were statistically significant for the latitude where the sample was collected ($F_{(12,32)}$=3.024, p=0.014) which is similar to findings in the literature of higher ratios observed at higher latitudes (e.g. Calhoun 1990, Bates *et al.* 1990). Turkeian *et al.* (2001) and Wadleigh (2004) both found higher ratios at higher latitudes. Interestingly, the highest MSA/NSS-SO_4^{2-} ratio did not correspond to the highest latitude, but was from a northerly station while transiting through the Labrador Sea upon return to the SOLAS Mooring station on May 12th (JD 132).

Previous authors (Berresheim 1987; Calhoun 1990; Wadleigh 2004) have reported correlations of MSA/NSS-SO_4^{2-} ratios with temperature, but that was not found in this study (Pearson Correlation, r=0.0441), though the highest ratio (78%) was found

Table 4-4 – Mean MSA/NSS-SO_4^{2-} (%) ratios and standard deviations (SD) for day and night samples, arranged by size fraction. Measurement uncertainty is ±30%.

Day									
Size (um)	**<100**	**- -**	**100-7.2**	**- -**	**7.2-3.0**	**3.0-1.5**	**1.5-0.95**	**0.95-0.49**	**<0.49**
Mean	8.4	- -	9.3	- -	3.7	1.8	3	5	5
SD	5.1	- -	4	- -	6.1	11.5	1.1	2.6	5.4
N	9	- -	2	- -	4	3	3	6	10
Night									
Size (um)	- -	**<10**	- -	**10-7.2**	**7.2-3.0**	**3.0-1.5**	**1.5-0.95**	**0.95-0.49**	**<0.49**
SD	- -	3.7	- -	11.5	10.1	10.7	10.6	5.4	13.8
Std Dev	- -	3.4	- -	6.3	13.6	17.1	9.9	5.1	28.1
N	- -	6	- -	3	8	6	8	8	7

while sampling at one of the lowest air temperatures (4.7°C), which was similar to the data presented by Calhoun (1990) and Berresheim (1987). While transiting through the Labrador Current, high MSA concentrations (*Appendix III, Figure III-7&III-8*) were found in nearly all samples, coincident with high atmospheric (Norman, personal communication) and surface water DMS concentrations (Michaud, personal communication) indicating that the Labrador Sea was biologically productive. Wadleigh (2004) also found very high MSA/NSS-SO_4^{2-} ratios while sampling the Labrador Sea in the fall of 1999 (though at a higher latitude), and higher ratios were also identified with air masses associated with this biologically productive region. MSA/NSS- SO_4^{2-} was not correlated with any of the chemical components measured in this study, air mass origin, or air temperature though there was a slight relationship between MSA/NSS-)$_4^{2-}$ ratios for the daytime samples (Pearson Correlation, r=0.4), with less of a relationship at night. (Pearson Correlation, r=0.2).

MSA/NSS-SO_4^{2-} ratios should be used with caution as extreme concentrations of MSA or NSS-SO_4^{2-} bias the ratio. Isotopic data and the calculation of biogenic SO_4^{2-} concentrations are better indicators of biogenic contributions. MSA/NSS-SO_4^{2-} ratios may be a reasonable indicator at regional scales, whereas $\delta^{34}S$ and biogenic SO_4^{2-} concentrations are more appropriate for looking at biogenic SO_4^{2-} in finer geographical detail and/or during process studies where the mechanisms and details of DMS oxidation are examined.

4.3.1.3 Biogenic and Anthropogenic Sulphate Concentrations

The fraction of biogenic SO_4^{2-} was calculated using three end-members; similar to the mixing plots previously presented (*Appendix I.2*). The biogenic end member was set at ~+18‰, and sea salt sulphate was constant at +21‰. The lower end-member was difficult to assign because of the presence of negative $\delta^{34}S_{NSS}$ values. The data from this study suggest a $\delta^{34}S$ end-member ranging from -10 to -25‰. This is lighter than reported values for a potential atmospheric anthropogenic sulphur end-member. The lightest possible $\delta^{34}S$ value reported in the literature is for H_2S associated with sweet gas, -16‰ (Maximov *et al.* 1995). Based on the relative volumes of sulphur emitted to the atmosphere by these two sources (see section 4.2.1.1) this is less likely than oil from the Come By Chance refinery which is expected to have a $\delta^{34}S$ value of ~-5‰ if oil from the Middle East were processed (Thode and Monster 1970). Therefore, the proportion of biogenic sulphate was tested using two values for the other end-member in the mixing model, +3‰, and -5‰. When the average isotopic composition of Iraqi oil was used (-5‰) the average biogenic fraction was 0.43 (SD = 0.29), and when the average value of North American continental/anthropogenic emissions (+3‰) was used the average was0.30 (SD = 0.26). This appears to be different, but when average biogenic concentrations of SO_4^{2-} (*Appendix IV*) were determined, the concentrations were similar (306, SD = 2020ngm^{-3} and 422, SD = 1430ngm^{-3}) for +3‰ and -5‰ respectively. Average anthropogenic SO_4^{2-} concentrations were similar with the two different end-members 346 (SD = 895ngm^{-3}) for -5‰ and 382 (SD = 577ngm^{-3}) for +3‰. The lower end-member previously defined by other authors (+3‰) is believed to be the most appropriate end-member for the larger North

Atlantic region, as that has been determined to be the dominant source of anthropogenic SO_4^{2-} to the remote marine North Atlantic in at least three other studies (Wadleigh 2004; Calhoun 1990; Norman *et al.* 1999). The negative $\delta^{34}S_{NSS}$ values confound the issue in this study but the negative values are possibly from an isotopically depleted oil source at the Come by Chance refinery, and/or gas flaring near the Sable Island gas fields based on the arguments presented in the previous section and the fact that the lighter $\delta^{34}S$ values were observed in newly formed aerosols (Aitken range) in the proximity of Newfoundland, and in larger aerosols, consistent with flaring, near Sable Island. It is possible that events where negative $\delta^{34}S$ values were observed in the aerosols resulted from pollutant plumes from the Come by Chance refinery and/or Sable Island Gas flaring and did not significantly alter the isotope composition of background sulphate over the larger North Atlantic. $\delta^{34}S$ values greater than +3‰ were assumed to result from long range transport from continental sources other than the refinery and Sable Island flaring and not oxidation occurring by kinetic fractionation resulting in negative $\delta^{34}S_{NSS}$. $\delta^{34}S$ values less than +3‰ could not be apportioned as they are attributed to isotopically depleted ^{34}S that is not well constrained.

Table 4-5 – 4-15 show the concentrations of anthropogenic (anth), biogenic (bio) and sea salt sulphate (ss) for the day and night samples for the Transect study using +3‰ as the endmember. The Lagrangian data are presented in *Tables 4-13* and *4-14*. *Table 4-15* shows the data from the total particulate samples when different aerodynamic sizes of the aerosols were collected. The concentrations show varying

Table 4-5 - Day and night SO_4^{2-} concentrations for the total particulate samples <100μm for the Transect study (ss = sea salt, bio = biogenic and anth = anthropogenic). Uncertainties larger than 10ngm^{-3} are shown in parentheses.

	Julian Day	Size	SS	Bio	Anth
Day	123	<100	12600	830	960
Day	124&125	<100	2280		
Day	126	<100	3640	360 (280)	330 (250)
Day	127	<100	2080		
Day	128	<100	260	4.5	206 (32)
Day	128	<100			
Day	130	<100	1090		
Day	132	<100	830		
Day	132	<100	360	130 (160)	260 (300)
Day	133	<100	290	110 (41)	1040
Day	134	<100	160		
Day	135	<100	99		
Night	126				
Night	127	<100	280	36	63
Night	128	<100	270	4.7 (1)	560 (80)
Night	129	<100	350		
Night	130	<100	430		
Night	131	<100	390		
Night	132	<100			
Night	133	<100	4510		
Night	134	<100	440		
Night	135	<100	280	240 (160)	1140 (780)

Table 4-6 - Day SO_4^{2-} concentrations for the total particulate samples 100-7.2μm for the Transect study (ss = sea salt, bio = biogenic and anth = anthropogenic). Uncertainties larger than 10ngm^{-3} are shown in parentheses.

	Julian Day	**Size**	**SS**	**Bio**	**Anth**
Day	123	100-7.2	2570		
Day	124&125	100-7.2	260	33 (25)	71 (50)
Day	126	100-7.2	920		
Day	127	100-7.2	740	21	140
Day	128	100-7.2	27		
Day	128	100-7.2			
Day	130	100-7.2	68		
Day	132	100-7.2	60		
Day	132	100-7.2	84		
Day	133	100-7.2	65		
Day	134	100-7.2	120		
Day	135	100-7.2	130		

Table 4-7 - Night SO_4^{2-} concentrations for the total particulate samples 10-7.2μm for the Transect study (ss = sea salt, bio = biogenic and anth = anthropogenic). Uncertainties larger than 10ngm^{-3} are shown in parentheses.

	Julian Day	**Size**	**SS**	**Bio**	**Anth**
Night	121&122	10-7.2	82	68 (170)	53 (130)
Night	124	10-7.2	920		
Night	125	10-7.2	420	290 (1000)	4.8 (17)
Night	126	10-7.2	59	110	
Night	127	10-7.2	53	95	
Night	128	10-7.2			
Night	129	10-7.2			
Night	130	10-7.2	68	44 (100)	18 (67)
Night	131	10-7.2			
Night	132	10-7.2			
Night	133	10-7.2			
Night	134	10-7.2			
Night	135	10-7.2	130		

Table 4-8 – Day and night SO_4^{2-} concentrations for the total particulate samples 7.2-3.0μm for the Transect study (ss = sea salt, bio = biogenic and anth = anthropogenic). Uncertainties larger than 10ngm^{-3} are shown in parentheses.

	Julian Day	**Size**	**SS**	**Bio**	**Anth**
Day	123	7.2-3.0	1130	21	17
Day	124&125	7.2-3.0	48	60 (200)	24 (80)
Day	126	7.2-3.0	550	17	93
Day	127	7.2-3.0	300	34 (18)	134 (70)
Day	128	7.2-3.0	33		
Day	128	7.2-3.0	17	28	
Day	130	7.2-3.0	120		
Day	132	7.2-3.0			
Day	132	7.2-3.0	90		
Day	133	7.2-3.0	50		
Day	134	7.2-3.0	80	43 (110)	20
Day	135	7.2-3.0	92	3.4	96 (17)
Night	121&122	7.2-3.0	150	120	81
Night	124	7.2-3.0	210	200	
Night	125	7.2-3.0	720	130	
Night	126	7.2-3.0	100	140	
Night	127	7.2-3.0	140	110	
Night	128	7.2-3.0	42	170	
Night	129	7.2-3.0	65	94	
Night	130	7.2-3.0	240	26 (20)	30 (23)
Night	131	7.2-3.0			
Night	132	7.2-3.0			
Night	133	7.2-3.0	110	19	38
Night	134	7.2-3.0	72		
Night	135	7.2-3.0	260	24 (6)	290 (83)

Table 4-9 – Day and night SO_4^{2-} concentrations for the total particulate samples 3.0-1.5μm for the Transect study (ss = sea salt, bio = biogenic and anth = anthropogenic). Uncertainties larger than 10ngm^{-3} are shown in parentheses.

	Julian Day	Size	SS	Bio	Anth
Day	123	3.0-1.5	159	150 (620)	5.5 (23)
Day	124&125	3.0-1.5			
Day	126	3.0-1.5	88.2	94 (260)	64 (170)
Day	127	3.0-1.5	107		
Day	128	3.0-1.5			
Day	128	3.0-1.5			
Day	130	3.0-1.5	39		
Day	132	3.0-1.5			
Day	132	3.0-1.5			
Day	133	3.0-1.5	26		
Day	134	3.0-1.5	120	45 (19)	79 (62)
Day	135	3.0-1.5	95	8.3	129
Night	121&122	3.0-1.5	51	110 (230)	129 (280)
Night	124	3.0-1.5	250	150 (480)	5.5
Night	125	3.0-1.5	130	200	48.8
Night	126	3.0-1.5	25	66	
Night	127	3.0-1.5	35	80	
Night	128	3.0-1.5	110	76	113
Night	129	3.0-1.5			
Night	130	3.0-1.5	44		
Night	131	3.0-1.5	30	6.6 (10)	1.3
Night	132	3.0-1.5			
Night	133	3.0-1.5	26	41 (63)	78 (120)
Night	134	3.0-1.5	72		
Night	135	3.0-1.5	140		

Table 4-10 – Day and night SO_4^{2-} concentrations for the total particulate samples 1.5-0.95μm for the Transect study (ss = sea salt, bio = biogenic and anth = anthropogenic). Uncertainties larger than 10ngm^{-3} are shown in parentheses.

	Julian Day	Size	SS	Bio	Anth
Day	123	1.5-0.95	41.4	110 (370)	70 (230)
Day	124&125	1.5-0.95			
Day	126	1.5-0.95	42.7	108 (300)	93 (250)
Day	127	1.5-0.95	87.5		
Day	128	1.5-0.95			
Day	128	1.5-0.95			
Day	130	1.5-0.95	19.5		
Day	132	1.5-0.95			
Day	132	1.5-0.95			
Day	133	1.5-0.95	21.2	34 (25)	146 (110)
Day	134	1.5-0.95	18.3	23 (16)	110 (77)
Day	135	1.5-0.95	99.0	10.8	178
Night	121&122	1.5-0.95	29.7	110 (70)	539 (350)
Night	124	1.5-0.95	71.3	105 (1300)	
Night	125	1.5-0.95			
Night	126	1.5-0.95			
Night	127	1.5-0.95	138	77 (130)	105
Night	128	1.5-0.95			
Night	129	1.5-0.95	24.3	35 (85)	30 (77)
Night	130	1.5-0.95	21.6	26.1	50.5
Night	131	1.5-0.95	15.4	19 (45)	19 (43)
Night	132	1.5-0.95	31.5		
Night	133	1.5-0.95	61.1	69 (53)	290 (220)
Night	134	1.5-0.95	22.5	35 (16)	254 (120)
Night	135	1.5-0.95	86.6	0.2	238 (30)

Table 4-11 – Day and night SO_4^{2-} concentrations for the total particulate samples 0.95-0.49μm for the Transect study (ss = sea salt, bio = biogenic and anth = anthropogenic). Uncertainties larger than 10ngm^{-3} are shown in parentheses.

	Julian Day	Size	SS	Bio	Anth
Day	123	0.95-0.49			
Day	124&125	0.95-0.49			
Day	126	0.95-0.49			
Day	127	0.95-0.49	90		
Day	128	0.95-0.49			
Day	128	0.95-0.49			
Day	130	0.95-0.49	22		
Day	132	0.95-0.49			
Day	132	0.95-0.49	33.8		
Day	133	0.95-0.49	20.7		
Day	134	0.95-0.49	36.6	36 (11)	395 (130)
Day	135	0.95-0.49	64.9	8.3	437
Night	121&122	0.95-0.49	26.8	260 (110)	1930
Night	124	0.95-0.49	1010	164 (210)	0.7
Night	125	0.95-0.49			
Night	126	0.95-0.49			
Night	127	0.95-0.49			
Night	128	0.95-0.49	115		
Night	129	0.95-0.49	103		
Night	130	0.95-0.49	28	48 (38)	201 (156)
Night	131	0.95-0.49			
Night	132	0.95-0.49	30	45	140
Night	133	0.95-0.49	25	97	890
Night	134	0.95-0.49	92	53 (14)	740 (200)
Night	135	0.95-0.49	97	110	245

Table 4-12 – Day and night SO_4^{2-} concentrations for the total particulate samples <0.49μm for the Transect study (ss = sea salt, bio = biogenic and anth = anthropogenic). Uncertainties larger than 10ngm^{-3} are shown in parentheses.

	Julian Day	Size	SS	Bio	Anth
Day	126	<0.49	102.5		
Day	127	<0.49	78.8		
Day	128	<0.49	84.3	26.0	266.1
Day	128	<0.49	68.3	5.4	463.3
Day	130	<0.49	43.0	2.6	474.1
Day	132	<0.49	86.3		
Day	132	<0.49	130	110 (114)	257
Day	133	<0.49	133		
Day	134	<0.49	210	107 (21)	2150
Day	135	<0.49	72.6	82 (19)	1260 (320)
Night	121&122	<0.49	113	230 (70)	2700 (830)
Night	124	<0.49	11200	286	740 (110)
Night	125	<0.49	257		
Night	126	<0.49			
Night	127	<0.49	45.7	180 (67)	421
Night	128	<0.49	56.6	33 (240)	277
Night	129	<0.49			
Night	130	<0.49			
Night	131	<0.49			
Night	132	<0.49	75.4		
Night	133	<0.49	93.3	51.1	1360
Night	134	<0.49	164		
Night	135	<0.49	112		

Table 4-13– Daytime SO_4^{2-} concentrations for size segregated samples collected during the Lagrangian Study (ss = sea salt, bio = biogenic and anth = anthropogenic). Uncertainties larger than 10ngm^{-3} are shown in parentheses.

Julian Day	Size	SS	Bio	Anth
115&116	<100	74		
117&118	<100	230	400 (720)	99 (110)
119&120	<100			
121&122	<100	1600		
115&116	100-7.2			
117&118	100-7.2	61		
119&120	100-7.2	74		
121&122	100-7.2	320	200 (240)	54 (64)
115&116	7.2-3.0			
117&118	7.2-3.0	110	4.3	42
119&120	7.2-3.0	150	40 (30)	27 (24)
121&122	7.2-3.0	250	42 (21)	36 (28)
115&116	3.0-1.5			
117&118	3.0-1.5	12		
119&120	3.0-1.5			
121&122	3.0-1.5	65	100 (135)	68 (86)
115&116	1.5-0.95			
117&118	1.5-0.95	47		
119&120	1.5-0.95	13	47 (35)	100 (100)
121&122	1.5-0.95	14	84 (46)	270 (250)
115&116	0.95-0.49			
117&118	0.95-0.49	20	5.2	
119&120	0.95-0.49	92		
121&122	0.95-0.49	10	120 (15)	
115&116	<0.49			
117&118	<0.49	23	50 (15)	260 (190)
119&120	<0.49	41	58	1200
121&122	<0.49	48	220 (130)	2200 (1300)

Table 4-14 – Night SO_4^{2-} concentrations for size segregated samples collected during the Lagrangian Study (ss = sea salt, bio = biogenic and anth = anthropogenic). Uncertainties larger than 10ngm^{-3} are shown in parentheses.

Julian Day	Size	SS	Bio	Anth
116&117	<10	99.0		
118-120	<10	588		
116&117	10-7.2	48.6		
118-120	10-7.2	26.0	18 (11)	38 (32)
116&117	7.2-3.0	53.5	10	
118-120	7.2-3.0	44.4	64 (93)	30 (35)
116&117	3.0-1.5	62.2	11	125 (60)
118-120	3.0-1.5	28.4	54 (60)	59 (69)
116&117	1.5-0.95	54.4	5.8	210
118-120	1.5-0.95	7.3	38 (21)	120 (100)
116&117	0.95-0.49	12.2		
118-120	0.95-0.49	24.6	28	200 (120)
116&117	<0.49	74.2		
118-120	<0.49	49.1		

Table 4-15 – Daytime and night-time SO_4^{2-} concentrations for total particulate samples for the Transect Study were samples could not be compared due to differences in aerodynamic size (ss = sea salt, bio = biogenic and anth = anthropogenic). Uncertainties larger than 10ngm^{-3} are shown in parentheses.

	Julian Day	**Size**	**SS**	**Bio**	**Anth**
Day	123	<100	13000	830	960
Day	123&125	<100	2300		
Day	126	<100	3600	360	330
Night	121&122	<10			
Night	124	<10			
Night	125	<10	200	1720 (3900)	2100

trends in the total particulate aerosols (*Table 4-5)*, with higher sea salt concentrations in the day samples, except on day 133, and concentrations of biogenic SO_4^{2-} which, on average, were twice as large in the night samples. Sea salt SO_4^{2-} dominated the total particulate, (100-7.2μm) (*Table 4-6*) and (10-7.2μm) (*Table 4-7)* size fractions in the size segregated samples. Note that the results for these two size fractions are shown for completeness, but no comparison is possible as the size differed. The concentrations of sea salt, dominate biogenic and anthropogenic SO_4^{2-} in the 7.2-3.0μm size fraction (*Table 4-8*) for both the day and night samples. Sea salt and biogenic sulphate were more prevalent in the 3.0-1.5μm aerosols (*Table 4-9*).

Anthropogenic SO_4^{2-} dominated the smaller (0.95-0.49 and 0.49μm) size fractions (*Tables 4-10 & 4-11*) and based on the very short lifetime (a few minutes) of particles in this size fraction, was likely mainly from the Hudson's emissions and other ships (the lack of increase in SO_2 concentrations suggest this is possible but not conclusive –continental SO_2 from the buffer layer and may have oxidized as it entered the marine boundary layer). Fuel from the Hudson was analyzed and found to be 4.0±0.2‰, which was similar to average North American emissions, making it difficult to determine whether the aerosols were from the Hudson or ambient North American emissions. The highest concentration (1720ngm^{-3}) of biogenic SO_4^{2-} was found in a daytime total particulate aerosol sample on May 5th (JD 125) (*Table 4-7*). The biogenic SO_2 concentration for that same sample was very low (104ngm^{-3}), indicating that high biogenic SO_4^{2-} concentrations were not coincident with high biogenic SO_2 concentrations. The largest concentration (2700ngm^{3}) of anthropogenic SO_4^{2-} was

found on May 1st (JD 121) in the smallest size fraction of a night sample (*Table 4-11*) and was higher than average NSS-SO_4^{2-} concentrations in other studies (e.g. Savoie *et al.* 1989; Berresheim *et al.* 1991; Pszenny *et al.* 1990). There were no previous studies where anthropogenic SO_4^{2-} concentrations could be compared.

The highest concentrations of biogenic SO_4^{2-} were not related to high MSA/NSS-SO_4^{2-} ratios. The highest MSA/NSS-SO_4^{2-} ratios corresponded with instances where biogenic SO_4^{2-} could not be calculated because of missing data, or negative values were present for the biogenic fraction. This was an interesting finding, and could potentially indicate that the negative $\delta^{34}S_{NSS}$ values were the result of a fractionation when MSA was produced. *Figure 4-11* shows $\delta^{34}S_{NSS}$ vs. MSA concentrations, and as can be seen from both plots there is no evidence of that in the data.

4.3.3 Summary of Transect Study

The Transect data are extensive with many surprises. Sulphur dioxide concentrations from the Transect Study were much higher than previously reported for the North Atlantic. There was a lack of significance between day and night $\delta^{34}S_{SO2}$ values ($F_{(1,23)}$=2.474, p=0.130). Biogenic SO_2 concentrations were greater than anthropogenic during the Transect Study (JD 122-130) for the day samples (one tailed t-test, 2 degrees of freedom, p=0.041). There was no statistical difference between the biogenic and anthropogenic SO_2 concentrations for the night samples due to the high variance of the data set. However, an increase in biogenic SO_2 was observed at the northerly stations.

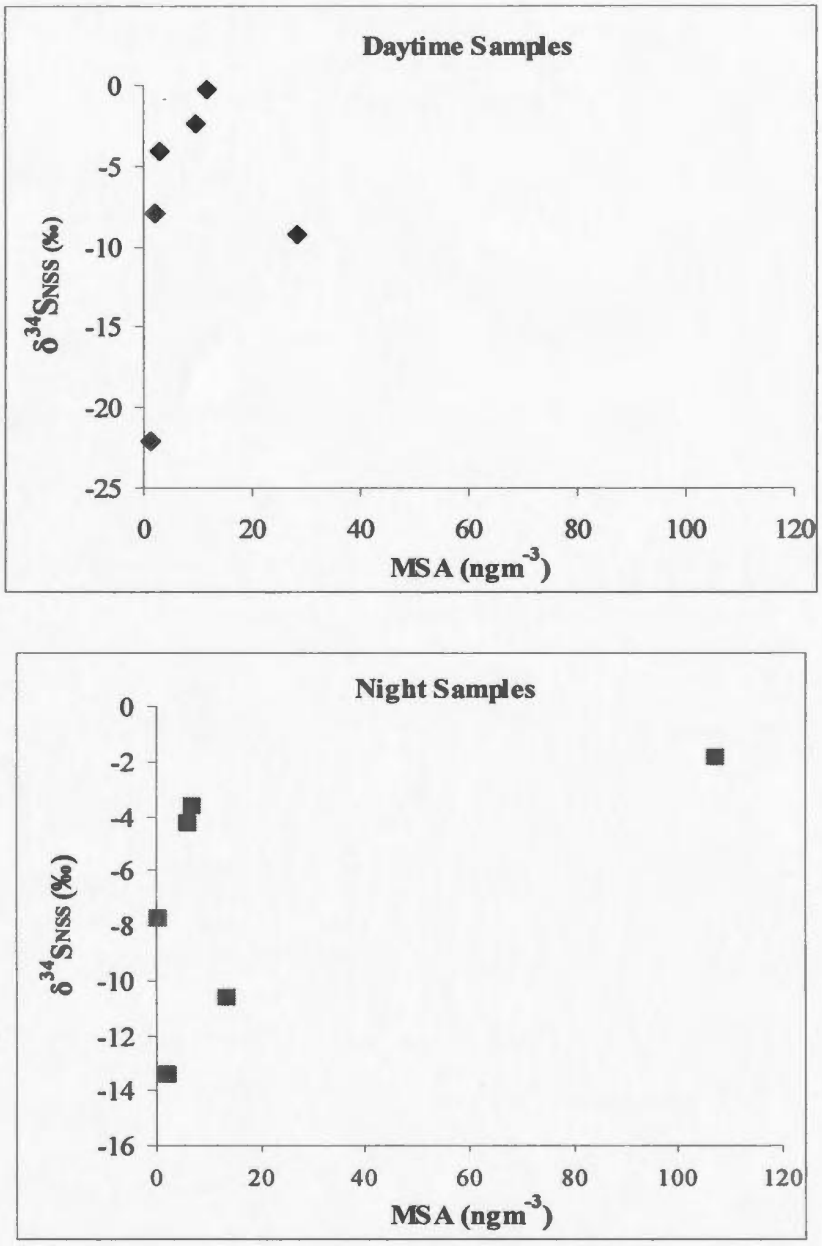

Figure 4-11- $\delta^{34}S_{NSS}$ (‰) vs. MSA concentrations (ngm^{-3}) for daytime (top) and night-time (bottom) samples with negative $\delta^{34}S_{NSS}$ values. $\delta^{34}S$ values have an uncertainty of ±0.4‰; MSA concentrations have an uncertainty of ±10%.

Interestingly there was a correlation between Ca^{2+} and aerosol sea salt components indicating that Ca^{2+} was sea salt derived. In previous studies Ca^{2+} was used as a continental tracer, but was not apparent for this study. Phosphate trends were also interesting as concentrations differed diurnally ($F_{(1,8)}$=142.17, $p<0.001$), and higher concentrations were found when the ship entered northerly waters, indicating a potential link between cold water/air masses and a production/removal of PO_4^{3-} in aerosols. The $\delta^{34}S_{NSS}$ data set is extremely unusual in this study as negative $\delta^{34}S_{NSS}$ values were observed. The negative values ranged from -0.3 to -22.1‰, with values in all size fractions, varying air masses, wind speeds, atmospheric and oceanic temperatures and weather systems. The data are not correlated to any external parameter and is not an artifact of sampling. Fractionation mechanisms were discussed, but deemed unlikely. Neither the day nor night Transect samples conformed to the mixing end-members used in previous aerosol studies. This has been attributed to a source of isotopically depleted ^{34}S. Potential sources identified include the Come by Chance Newfoundland refinery emissions and flaring from the Sable Island gas fields

Chapter Five: Conclusions and Future Work

5.1 Spring SABINA Data Set Conclusions

The objective of this thesis was to investigate DMS oxidation products, sulphate and MSA in aerosols, and sulphur dioxide over the NW Atlantic during a 26 day cruise in the spring of 2003 in support of a larger study to examine DMS oxidation. Aerosols and SO_2 were collected during both a Lagrangian study and a Transect study ranging from 36^0N to 55^0N. The spring SABINA data presented here are part of a larger seasonal study, yet to be reported, with cruises in the summer and fall of 2003. The three cruises will allow the examination of the seasonality effects of DMS oxidation over the NW Atlantic, but these results can not presented in a single thesis due to the complexity and size of the data set.

Estimates for the average biogenic and anthropogenic sulphur dioxide concentration over the North Atlantic are presented here for the first time. Biogenic SO_2 concentrations were relatively constant over the Lagrangian (925, SD 330ngm^{-3}) and Transect (604, SD 530ngm^{-3}) studies. Anthropogenic SO_2 concentrations were highly variable for the Lagrangian and Transect studies (1430, SD 1110ngm^{-3} and 390, SD 600ngm^{-3} respectively).

Previous studies have completed measurements similar to those for total and size segregated aerosol sulphate, but the results obtained from the spring SABINA cruise were different. This study represents the first set of integrated measurements conducted on a diurnal basis where biogenic SO_2, size-segregated aerosol sulphate

and MSA were measured simultaneously. Although the largest size fractions could not be directly compared due to size differences, all size fractions <7.2μm and total particulate samples collected after May 5th can be directly compared. A surprising result was the lack of correspondence between biogenic SO_2 and biogenic SO_4^{2-} and MSA concentrations. A confounding factor affecting the author's ability to resolve the issue was the presence of isotopically light sulphate during the cruise The presence of negative $\delta^{34}S_{NSS}$ values has rarely been reported by previous authors (e.g. Norman 1991; Motoyama 2000) and only once in the North Atlantic (Gravenhorst 1977). Negative $\delta^{34}S_{NSS}$ values may be linked to the combustion of Middle Eastern Oil by a Newfoundland-based refinery and/or gas flaring near Sable Island, though further work should be completed near the refinery when it is processing oil originating from similar fields to conclusively determine if the source of the isotopically depleted SO_4^{2-} was the refinery. Such a study is not easily conducted and would require analysis of atmospheric samples from nearby the refinery at a time when Middle Eastern oil was processed. Although this information is desirable, such information requirements were unforeseen in the design of the experiment, and it is beyond the scope of the thesis to verify whether this in fact was the source of the isotopically lighter sulphate.

Possible fractionation mechanisms of SO_2 to sulphate were discussed in attempt to explain the negative $\delta^{34}S_{NSS}$ values. Kinetic fractionation was deemed unlikely. However, isotope fractionation during DMS oxidation remains a possible source of

isotope fractionation, but the focus of this thesis was sulphur dioxide, sulphate and MSA and the discussion of this fractionation was beyond the scope of the thesis.

MSA/NSS-SO_4^{2-} ratios were used to examine whether the relative contribution of biogenic SO_4^{2-} was comparable to that determined using isotope apportionment techniques. In this study the MSA/NSS-SO_4^{2-} ratios indicated biogenic contributions in the <0.49μm size fraction while the data for $\delta^{34}S_{NSS}$ and $\delta^{34}S$ indicated a large contribution from anthropogenic SO_4^{2-}. In fact the smaller size fractions generally appear to be dominated by anthropogenic SO_4^{2-} throughout the majority of the study and their prevalence in the very fine fraction suggests the particles result from oxidation of SO_2 from ships stack emissions and/or anthropogenic pollution from the continent. MSA/NSS-SO_4^{2-} ratios were helpful in determining the fractional biogenic contributions to SO_4^{2-}, but the isotopic values and the concentrations of biogenic and anthropogenic SO_4^{2-} were more appropriate. MSA/NSS-SO_4^{2-} values were not coincident with increased biogenic sulphate as indicated by isotope apportionment calculations. This potentially reflects temporal variations in factors affecting oxidation pathways to MSA and biogenic sulphate and suggests that isotope calculations along with MSA concentrations alone are more useful than MSA/NSS-SO_4^{2-} in studies where information on DMS oxidation products and their resulting size distributions is required.

Concentrations of SO_2 in the spring SABINA data set were higher than previously reported in the literature (32-301ngm^{-3}) (Berresheim 1987, Pszenny *et al.* 1990).

Different methods for measuring SO_2 have been used in other studies and this may have resulted in higher concentrations for this study. The shipboard measurement used on the SABINA cruise was the same technique used on SERIES (2002, Pacific). Sulphur dioxide concentration data from SERIES high volume sampler measurements (Burridge 2004) compared well with average SO_2 fluorescence measurements (Leaitch, personal communication; Phinney *et al.* 2005 which suggests these two methods can be compared. However, other methods may not be comparable.

Aerosol NO_3^- concentrations were an order of magnitude larger than those reported by Wadleigh (2004) from the same location five years prior. In Canada NO_x emissions in 2000 were over 2.5 million tonnes, an increase from estimates of 2.3 million tones in 1992, while US emissions were in excess of 20 million tones in 2001 (EPA 2004, Environment Canada 2004). Increased NO_3 concentrations allow for increased oxidation of biogenic and anthropogenic SO_2. Larger concentrations of NO_3 and SO_2 over the North Atlantic indicate that anthropogenic emissions are omnipresent in the remote marine atmosphere, and they appear to be increasing and further reaching.

Indications that higher SO_2 concentrations could result in increased aerosol numbers, and potentially increased cloud cover, were supported in the spring SABINA observations. Anthropogenic SO_2 concentrations were higher (620, SD = 840ngm^{-3}) than anthropogenic SO_4^{2-} concentrations (380, SD = 580ngm^{-3}), but both were quite variable. The anthropogenic concentrations were a combination of local ship stack

emissions, Newfoundland refinery emissions and long range transport of pollutants advected from North America. Biogenic SO_2 concentrations were relatively constant (mean = 660, SD = 460ngm^{-3}) throughout the day and night during the Lagrangian and Transect studies. Contrastingly, biogenic SO_4^{2-} concentrations were highly variable (mean = 310, SD = 2000ngm^{-3}) with higher concentrations generally found in the total particulate samples and smallest size fraction. The highest average (110, SD = 92ngm^{-3}) biogenic SO_4^{2-} concentrations were found in the smallest aerodynamic size fraction, but the standard deviation is large and the concentrations were not consistent throughout the study, which suggests that a modeling approach to oxidation of DMS would be useful, before conclusive remarks can be made regarding the radiative effects of biogenic SO_4^{2-}. The presence of high biogenic sulphate concentrations in the <0.49μm size fraction does indicate that some biogenic SO_2 is oxidized to fine aerosol sulphate and this study provides a range in concentrations for modelers to use. Fine aerosols (<1μm) are important climatically as they scatter incoming solar radiation more efficiently than larger aerosols and can act as cloud condensation nuclei (Shaw 1983). However, it is difficult to state unequivocally that the finer aerosols are largely composed of biogenic SO_4^{2-} due to the apparent presence of isotopically depleted SO_4^{2-} which weakens the ability to attribute sources definitively. There is also considerable variance in the data set which precludes a decisive conclusion.

5.2 Future Work Recommendations

Sulphate aerosol and gaseous SO_2 can provide insight about the CLAW hypothesis and also the remote marine atmosphere. While source apportionment using stable sulphur isotopes and chemical data has been helpful in determining the sources of sulphate and SO_2, further work still needs to be done. Analysing the soluble ions from the aerosol samples by inductively coupled plasma mass spectrometry (ICP-MS) to measure the concentrations of trace metals and other metals would be of interest. With ICP-MS it would be possible to look for correlations between trace metals and DMS oxidation.

Organic aerosols may be important in determining the source of the aerosols over the NW Atlantic. Determining the organic component of the aerosols could potentially help decipher some of the unusual values observed in the spring SABINA data set. High concentrations of aerosol PO_4^{3-} were found in the SABINA data set, but there is little understanding of PO_4^{3-} sources to the remote marine atmosphere. The high concentrations appear to be linked to cold air temperatures and cold water masses. Calcium was found to be correlated with sea salt, not continental dust as expected. It would be useful to determine if both Ca^{+} and PO_4^{3-} were related to the biological activity in the surface ocean by comparing the ratios of these ions to that in calcareous organic matter in aerosols such as those studied by Lohman and Leck (2005).

MSA concentrations were relatively constant (mean = 10.7, SD = 15.8ngm^{-3}) for the size segregated day and night samples. An important finding is that aerosols with higher concentrations of anthropogenic SO_4^{2-} tended to have higher MSA concentrations. Further research should be concentrated on the mechanisms which promote MSA formation and whether MSA formation is linked to pre-existing aerosols containing anthropogenic sulphate or whether the presence of gaseous anthropogenic pollutants initiates MSA formation.

Extensive field campaigns with aerosol and SO_2 isotope measurements are integral to the synthesis of aerosol formation and source apportionment. There is a distinct lack of SO_2 isotope measurements, which are important for modelers attempting to determine the oxidation pathways of DMS and which of these pathways dominate the NW Atlantic.

References

Andreae, M.O. and Barnard, W.R. (1984): **The Marine Chemistry of Dimethylsulphide.** Marine Chemisty, Vol. 14: 267-279.

Andreae, M.O., Charlson, R.J., Bruynseels, F., Storms, H., Greiken, R.V., Maenhaut, W. (1986): **Internal Mixture of Sea Salt, Silicates, and Excess Sulphate in Marine Aerosols.** Science Vol 232: 1620-1623.

Andreae, M. O. (1990): **Ocean-atmosphere interactions in the global biogeochemical sulphur cycle.** Marine Chemistry, 30: 1- 29.

Andreae, M.O., and Jaeschke, W.A. (1992): **Exchange of Sulphur Between Biosphere and Atmosphere Over Temperate and Tropical Regions.** In Sulphur Cycling on the Continents, Wetlands, Terresterial Ecosystems, and Associated Water Bodies. Scope 48, Howarth, R.W, Stewart, J.W.B, and Ivanov, M.V. (Eds). John Wiley and Sons.

Andreae, M.O. and Crutzen, P.J. (1997): **Atmospheric Aerosols: Biogeochemical Sources and Role in Atmospheric Chemistry.** Science 276: 1052-1057

Aneja, V.P. and Cooper, W.J. (1989): **Biogenic Sulphur Emissions, a Review.** In Biogenic Sulphur in the Environment, Chapter 1, ACS Symposium Series 393 Saltzman, E.S and Cooper, W.J. (Eds.).

Barnard, W.R., Andreae, M.O., Watkins, W.E., Bingemer, H. and Georgh, H.W. (1982): **The Flux of Dimethylsulphide From the Oceans to the Atmosphere.** Journal of Geophysical Research Vol. 87, No. C11: 8787-8793.

Barrie, L.A. and Hoff, R.M. (1984): **The Oxidation Rate and Residence Time of Sulphur Dioxide in the Arctic Atmosphere.** Atmospheric Environment, Vol. 18, No. 12: 2711-2722.

Barrie, L.A. and Barrie, M.J. (1990): **Chemical Components of Lower Tropospheric Aerosols in the High Arctic: Six Years of Observations.** Journal of Atmospheric Chemistry, Vol. 11: 211-226.

Barrie, L., Ahier, B., Bottenheim, J., Niki, H. and Nriagu, J. (1992): **Atmospheric Methane and Sulphur Compounds at a Remote Central Canadian Location.** Atmospheric Environment, Vol. 26A, No. 5: 907-925.

Bates, T., Calhoun, J. and Quinn, P. (1992): **Variations in the Methanesulphonate to Sulphate Molar Ratio Ratio in Submicrometre Marine Aerosol Particles Over the South Pacific Ocean.** Journal of Geophysical Research Vol. 97: 9859-9865.

Bate, T.S., Lamb, B.K., Guenther, A., Dignon, J. and Stoiber, R.E. (1992): **Sulfur Emissions to the Atmosphere from Natural Sources.** Journal of Atmospheric Chemistry, Vol. 14: 315-337.

Berresheim, H. (1987): **Biogenic Sulphur Emissions from the Subantarctic and Antarctic Oceans.** Journal of Geophysical Research, Vol. 92, No. D11: 13245-13262.

Berresheim, H., Andreae, M.O., Ayers, A.P., Gillett, R.W., Merrill, J.T., Davis, V.J. and Chameides, W.L. (1990): **Airborne Measurements of Dimethylsulphide, Sulphur Dioxide, and Aerosol Ions over the Southern Ocean South of Australia.** Journal of Atmospheric Chemistry Vol. 10: 341-370.

Berresheim, H., Andreae, M.O., Iverson, R.L. & Li, S.M. (1991): **Seasonal variations of dimethylsulphide emissions and atmospheric sulphur and nitrogen species over the western north Atlantic Ocean.** Tellus 43B: 353-372.

Bonsang, B., Nguyen, B.C. & Lambert, G. (1980): **Sulfate Enrichment in Marine Aerosols Owing to Biogenic Gaseous Sulphur Compounds.** Journal of Geophysical Research Vol. 85 No. C12: 7410-7416.

Boyd, P., Watson, A.J., Law, C.S., Abraham, E.R., Trull, T., Murdoch, B., Bakker, D.C.E., Bowie, A.R., Buessler, K.O., Change, H., Charette, M., Croot, P., Downing, K., Frew, R., Gall, M., Hadfield, M., Hall, J., Harvey, M., Jameson, G., Laroche, J., Liddicoat, M., Ling, R., Maldonado, McKay, M., Nodder, S., M.T., Pickmere, S., Pridmore, R., Rintoul, S., Safi, K., Sutton, P., Strzepek, R., Tanneberger, K., Turner, S., Waite, A., Zeldis, J., (2000): **A Mesoscale Phytoplankton Bloom in the Polar Southern Ocean Simulated by Iron Fertilization.** Nature, Vol. 407 No. 6805: 695-702

Boyd, P., Law, C.S., Wong, C.S., Nojiri, Y.;, Tsuda. A., Levasseur M., Takeda, S., Rivkin, R., Harrison, P.J., Strzepek, R., Abraham, E., Arychuk, M., Barwell-Clarke, J., Crawford, J., Crawford. D., Hale, M., Harada, K., Johnson, K., Kiyosawa, H., Kudo, I., Marchetti, A., Miller, W., Needoba, J., Nishioka, J., Ogawa, H., Page, J., Robert, M., Saito, H., Sastri, A., Sherry, N., Soutar, T., Sutherland, N., Taira, Y., Whitney, F., Won, S.K.E, Yoshimura, T. (2004): **The Decline and Fate of an Iron-Induced Subarctic Phytoplankton Bloom.** Nature Vol. 428: 549-553

Brimblecombe, P., Hammer, C., Rodhe, H., Ryaboshapko, A. and Boutron, C.F. (1989): **Human Influence on the Sulphur Cycle.** In Evolution of the Global Biogeochemical Sulphur Cycle, Brimblecombe, P. and Yu Lein, A. (Eds.), Scope 39. John Wiley and Sons Ltd.

Burridge, C. (2004): **Determining Source of Sulphur Gases and Sulphate Aerosols during SERIES.** Poster Presentation, C-SOLAS AGM, May, 2004.

C-SOLAS Website (2005) http://csolas.dal.ca

Calhoun, J.A. & Bates, T.S. (1989): **Sulfur Isotope Ratios. Tracers of Non-Sea Salt Sulfate in the Remote Atmosphere.** ACS Symposium Series 393, Biogenic Sulfur in the Environment. American Chemical Society, Washington, D.C. Editors: Saltzman, E.S. & Cooper, W.J.

Calhoun, J.A. (1990): **Chemical and Isotopic Methods for Understanding the Natural Marine Sulfur Cycle.** Doctor of Philosphy Dissertation, University of Washington.

Calhoun, J.A., Bates, T.S., Charlson, R.J. (1991): **Sulphur Isotope Measurements of Submicrometer Sulphate Aerosol Particles Over The Pacific Ocean.** Geophysical Research Letters Vol 18, No. 10:1877-1880.

Capaldo, K, Corbett, J.J., Kasibhalta, P., Fischbeck, P., Pandis, S.N.: (1999): **Effects of Ship Emissions on Sulphur Cycling and Radiative Climate Forcing Over The Ocean.** Nature V. 400.

Caron, F., Tessier, A., Kramer, J.R., Schwartz, H.P. and Rees, C.E. (1986): **Sulfur and Oxygen Isotopes of Sulfate in Precipitation and Lakewater, Quebec, Canada.** Applied Geochemistry, Vol. 1: 601-606.

Challenger, F. and Simpson, M.I. (1948): **Studies on Biological Methylation. Part XIII, A Precusor of the Dimethyl Sulphide evolved by Polysiphonia fastigiata. Dimethyl-2-carboxyethylsulphonium Hydroxide and its Salts.** The Journal of Chemical Society (London), Part II: 1591-1597.

Challenger, F. (1951): **Biological Methylation.** Advanced Ezymology 12: 429-491.

Chambers, L.A. and Trudinger, P.A. (1979): **Microbiological Fractionation of Stable Sulfur Isotopes.** Geomicrobiology Journal, Vol. 1, No. 3: 249-293.

Charlson, R.J., Lovelock, J.E., Andreae, M.O. Warren, S.G. (1987): **Oceanic Phytoplankton, Atmospheric Sulphur, Cloud Albedo and Climate.** Nature V. 326.

Chin, M. and Jacob, D.J. (1996): **Anthropogenic and Natural Contributions to Tropospheric Sulfate: A Global Model Analysis.** Journal of Geophysical Research, Vol. 101, No. D13: 18691-18699.

Cutter G.A. and Krahforst, C.F. (1988): **Sulphide in Surface Waters of the Western Atlantic Ocean**. Geophysical Research Letters, Vol. 15, No. 12: 1393-1396.

De Bruyn, W.J., Shorter, J.A., Davidovits, P., Worsnop, D.R., Zahniser, M.S. and Kolb, C.E. (1994): **Uptake of gas phase sulphur species methanesulfonic acid, dimethylsulfoxide, and dimethyl sulfone by aqueous surfaces.** Journal of Geophysical Research Vol. 99, No. D8: 16927-16932.

De Bruyn, W.J., Harvery, M., Cainey. J.M. and Saltzman, E. (2002): **DMS and SO_2 at Baring Head, New Zealand: Implications for the Yield of SO_2 from DMS.** Journal of Atmospheric Chemistry 41: 189-209.

Devred, E. and Roy, S. (2005): **C-SOLAS SABINA Stations**. C-SOLAS Newsletter, Issue 4: 6-7.

Environment Canada (1994): **The Eastern Canada Acid Rain Control Program.** http://www.ec.gc.ca/acidrain/acidrn/acidrn_e.htm

Environment Canada (2004): **2000 Criteria Air Contaminant Emissions for Canada**. Criteria Air Contaminant Report. Updated December, 2004. http://www.ec.gc.ca/pdb/ape/ape_tables/canada2000_e.cfm

Environmental Protection Agency (2004): **National Emission Trends.** http://www.epa.gov/ttn/chief/trends/index.html

Fitzgerald, J.W. (1991): **Marine Aerosols: A Review.** Atmospheric Environment, Vol. 25A, No.3/4: 533-545.

Forrest, J. and Newman, L. (1977): **Oxidation of Sulphur Dioxide in the Sudbury Smelter Plume.** Atmospheric Environment, Vol. 11: 517-520.

Galloway, J.N. and Whelpdale, D.M. (1980): **An Atmospheric Sulfur Budget for Eastern North America.** Atmospheric Environment, Vol. 14: 409-417.

Galloway, J.N. and Whelpdale, D.M. (1980): **An Atmospheric Sulfur Budget for Eastern North America.** Atmospheric Environment, Vol. 14: 409-417.

Galloway, J.N. and Whelpdale, D.M. (1987): **WATOX-86 Overview and Western North Atlantic Ocean S and N Atmospheric Budgets.** Global Biogeochemical Cycles, Vol. 1, No. 4: 261-281.

Gibson, R.G., Douz, L.I. and Greeley, D.F. (2004): **Shelf Petroleum System of the Columbus Basin, Offshore Trinidad, West Indies.** Marine and Petroleum Geology 21: 97-108.

Gravenhorst, G. (1977): **Maritime Sulfate Over the North Atlantic.** Atmospheric Environment, Vol. 12: 707-713.

Hale, Bob, Personal Communication, 2005, Nova Scotia Offshore Petroleum Board.

Hobbs, P.V. (1993): **Aerosol-Cloud Interactions.** In Aerosol-Cloud-Climate Interactions, Volume 54 in the International Geophysics Series, Hobbs, P.V. (Ed). Academic Press, Inc. Boston.

Houghton, J.T., Meria Filho, L.G., Callander, B.A., Harris, N., Kattenberg, A. and Maskell, K. (1995): **Climate Change 1995, The Science of Climate Change**. Published for Intergovernmental Panel on Climate Change, Cambridge University Press, Lakeman, J.A. (Production, Ed.)

Jamieson, R.E. and Wadleigh, M.A. (1999): **Tracing Sources of Precipitation Sulphate in Eastern Canada using Stable Isotopes and Trace Metals.** Journal of Geophysical Research, Vol. 105, No. D16: 20549-20556.

Jannasch, H.W. (1983): **Interactions Between the Carbon and Sulphur Cycles in the Marine Environment.** In SCOPE 21: The Major Biogeochemical Cycles and their Interactions. John Wiley & Sons.

Junge, C.E. (1960): **Sulphur in the Atmosphere.** Journal of Geophysical Research, Vol. 63, No. 1: 227-237.

Kahn, R. (2003): **MISR Research Goals and Objectives, MISR's study on Atmospheric Aerosols.** http://www-misr.jpl.nasa.gov

Kaplan, I.R. and Rittenberg, S.C. (1964): **Microbiological Fractionation of Sulphur Isotopes.** Journal of General Microbiology Vol. 34: 195-212

Katoshevski, D., Nenes, A., Seinfeld, J.H. (1999): **A Study of Processes that Govern the Maintenance of Aerosols in the Marine Boundary Layer.** Journal of Aerosol Science, Vol. 33 No.4: 503-532.

Kaufman, Y., Tanré, D., Boucher, O. (2002): **A satellite view of aerosols in the climate system.** Nature 419: 215-223

Keene, W.C., Pszenny, A.P., Galloway, J.N. and Hawley, M.E. (1986): **Sea-salt corrections and interpretation of constituent ratios in marine precipitation.** Journal of Geophysical Research, Volume 91, Issue D6: 6647-6658.

Keller, M.D., Bellows, W.K. and Guillard, R.R.L. (1989): **Dimethylsulphide Production in Marine Phytoplankton.** In Biogenic Sulphur in the Environment, Chapter 11, ACS Symposium Series 393 Saltzman, E.S and Cooper, W.J. (Eds.).

Khalil, M.A.K. and Rasmussen, R.A. (1984): **Global Sources, Lifetimes and Mass Balances of Carbonyl Sulfide (OCS) and Carbon Disulfide (CS2) in the Earth's Atmosphere**. Atmospheric Environment, Vol. 18, No. 9: 1805-1813.

Krouse, H.R. and McCready, R.G.L. (1979): **Biochemical Cycling of Sulphur.** In Biogeochemical Cycling of Mineral-Forming Elements. Studies in Environmental Science, 3: 410-430, Trudinger, P.A. and Swaine, D.J. (Eds), Elsevier Scientific Publishing Company.

Krouse, H.R., Grinenko, L.N., Grinenko, V.A., Newman, L, Forest J, Nakai, N, Tsuji, Y, Yatsumimi, T., Takeuchi, U., Robinson, B.W., Stewart, M.K., Gunatilaka, A., Chambers, L.A., Smith, J.W., Plumb, L.A., Buzek, F., Cerny, J., Sramek, J., Menon, A.G., Iyer, G.V.A, Venkatasubramanian, V.S., Egboka, B.E.C., Irogbenachi, M.M., Eligwe, C.A. (1991): **Case Studies and Potential Applications.** Chapter 8, Scope 43, Stable Isotopes: Natural and Anthropogenic Sulphur in the Environment, John Wiley and Sons.

Landry, M.R., Constantinou, J., Latasa, M., Brown, S.L., Bidigare, R.R., Ondrusek, M.E. (2000): **Biological Response to Iron Fertilization in the Eastern Equatorial Pacific (IronExII). Dynamics of Phytoplankton Growth and Microzooplankton Grazing.** Marine Ecology Progress Series, Vol 201: 57-72

Lear, C.H., Elderfield, H., and Wilson, P.A. (2000): **Cenozoic Deep-Sea Tempeatures and Global Ice Volumes from Mg/Ca in Benthic Foraminiferal Calcite.** Science, Vol. 287: 269-272.

Leaitch, R., personal communication, June 2005, Meterological Service of Canada.

Lohman, U. and Leck, C. (2005): **Importance of Submicron Surface-Active Organic Aerosols for Pristine Arctic Clouds.** Tellus, Vol. 57B: 261-268.

Longhurst, A.R. (1998): **Ecological Geography of the Sea.** Academic Press, London.

Lovelock, J.E. and Margulis, L. (1974): **Atmospheric homeostasis by and for the biosphere: the gaia hypothesis.** Tellus, Vol. 26, No. 1-2 :2-9.

Malin, G., and Kirst, G.O. (1997): **Algal Production of Dimethyl Sulfide and its Atmospheric Role.** Minireview in Journal of Phycology Vol. 33: 889-896.

Maximov, S.P., Pankina, R.G., Smakhtina, A.M. (1975): **Genesis of H_2S in Gases of Amu-Daria Syneclise (by Isotopic Composition of Sulphur) (In Russian).** Proc. VINGNI Vol. 174: 122-135.

McArdle, N.C. and Liss, P.S. (1995): **Isotopes and Atmospheric Sulphur.** Atmospheric Environment Vol. 29, No. 18: 2553-2556.

McGovern, F.M., Raes, F., Dingenen, R.V. and Maring, H. (1999): **Anthropogenic Influences on the Chemical and Physical Properties of Aerosols in the Atlantic Subtropical Region during July 1994 and July 1995.** Journal of Geophysical Research, Vol. 104, No. D12: 14309-14319.

Mészãros, E. (1978): **Concentration of Sulfur Compounds in Remote Continental and Oceanic Areas.** Atmospheric Environment, Vol. 12: 699-705.

Mihalopoulos, N., Nguyen, B.C, Putaud, J.P. and Belviso, S. (1992): **The Oceanic Source of Carbonyl Sulphide (COS).** Atmospheric Environment, Vol. 26A, No. 8: 1383-1394.

Möller, D. (1980): **Kinetic Model of Atmospheric SO_2 Oxidation Based on Published Data.** Atmospheric Environment Vol. 14: 1067-1076.

Möller, D. (1984): **Estimation of the Global and Man-Made Sulphur Emission.** Atmospheric Environment Vol. 18, No. 1: 19-27.

Motoyama, R., Yanagisawa, F., Kotani, T., Kawabata, A. and Ueda, A. (2000): **Sulfur Isotope Ratio of Non Sea Salt Sulphate in Aerosol and Wet Deposition in Yamagata, Japan.** Journal of Japanese Society of Snow and Ice, Vol. 62, No. 3: 215-224.

Murphy, D.M., Anderson, J.R., Quinn, P.K., McInnes, L.M., Brechtell, F.J., Kreidenweis, S.M., Middlebrook, A.M., Pósfai, M., Thomson, D.S., Busek, P.R. (1998): **Influence of sea salt on aerosol radiative properties in the Southern Ocean marine boundary layer.** Nature Vol. 392: 62-65.

National Ocean and Atmospheric Administration (2004): **Ready Hysplit Back Trajectory Model.** http://www.arl.noaa.gov/ready/hysplit4.html

National Pollution Release Inventory (2003): **2003 Annual Report.** http://www.ec.gc.ca/pdb/npri/npri_home_e.cfm

National Research Council of Canada (NRCC) (1982): **National Research Council of Canada, NRCC Associate Committee on Scientific Criteria for Environmental Quality. Effects of Aerosols on Atmospheric Processes.**

Natural Resources Canada (1996): **Motor Gasoline Pricing Dynamics**.

Newman, L., Krouse, H.R., Grinenko, V.A. (1991): **Sulphur Isotope Variations in the Atmosphere.** Chapter 3, Scope 43, Stable Isotopes: Natural and Anthropogenic Sulphur in the Environment, John Wiley and Sons.

Nguyen, B.C., Gaudry, A., Bernard, B. & Lambert, G. (1978): **Reevaluation of the Role of Dimethyl Dulphide in the Sulphur Budget.** Nature, 275: 637-639.

Nordlund, G. (1983): **Seasonal Averages of Net Decay Rate of SO_2 Over Northern Europe.** Atmospheric Environment Vol. 17, No. 6: 1199-1201.

Norman, A.L. (1991): **Stable Isotope Studies of Atmospheric Sulphur: Comparison of Calgary, Canada and Bermuda.** Masters Thesis, Department of Physics and Astronomy, University of Calgary

Norman, A.L., Barrie, L.A., Toom-Sauntry, D., Sirois, A., Krouse, H.R., Li, S.M. and Sharma, S. (1999): **Sources of Aerosol Sulphate at Alert: Apportionment using Stable Isotopes.** Journal of Geophysical Research Vol. 104, No. D9: 11619-11631.

Nriagu, J.O., Holdway, D.A. and Coker, R.D. (1987): **Biogenic Sulphur and the Acidity of Rainfall in Remote Areas of Canada.** Science Vol. 237: 1189-1192.

Nrigau, J.O., Coker, R.D. and Barrie, L.A. (1991): **Origin of Sulphur in Canadian Arctic Haze from Isotope Measurements.** Nature, Vol. 349: 142-145.

O'Dowd, C.O., Jimenez, J.L., Flagan, R.C., Seinfeld, J.H., Hämerl, K., Pirjola, L., Kulmala, M., Jennings, S.G., Hoffmann, T. (2002): **Marine aerosol formation from biogenic iodine emissions.** Nature 417: 632-636.

Patris, N., Mihalopoulos, N., Baboukas, E.D., Jouzel, J. (2000): **Isotopic composition of sulphur in size-resolved marine aerosols above the Atlantic Ocean.** Journal of Geophysical Research, Vol. 105, No. D11: 14,449-14,457.

Petelski, T. (2003): **Marine Aerosol Fluxes Over Open Sea Calculated from Vertical Concentration Gradients.** Journal of Aerosol Science 34: 359-371.

Phinney, L., Lohmann, U., Leaitch, R., Marshall, J. (2005): **Characterizing the Atmospheric Aerosol during SERIES. Chemical Diurnal Cycle and Optical Properties.** C-SOLAS Newsletter Issue 4: 12-14.

Pommier, J., personal communication, 2005.

Prospero, J.M., Charlson, R.J., Mohnen, V., Jaenicke, R., Delany, A.C., Moyers, KJ., Zoller, W., Rahn, K., (1983): **The Atmospheric Aerosol System: An Overview.** Reviews of Geophysics and Space Physics Vol. 21: no: 7:1607-1629.

Pszenny, A.A.P., Harvey, G.R., Brown, C.J., Lang, R.F., Kenne, W.C., Galloway, J.N. and Merrill, J.T. (1990): **Measurements of Dimethylsulphide Oxidation Products in the Summertime North Atlantic Marine Boundary Layer**. Global Geochemical Cycles, Vol. 4, No. 4: 367-379.

Rasmussen, R.A. (1974): **Emission of Biogenic Hydrogen Sulphide**. Tellus Vol 26, No. 1-2: 254-261.

Rees, C.E. (1978): **Sulphur Isotope Measurements Using SO_2 and SF_6.** Geochemica, Cosmochima Acta Vol. 42: 383-389.

Russell, L.M., Pandis, S.N. & Seinfeld, J.H.: (1994) **Aerosol production and growth in the marine boundary layer**. Journal of Geophysical Research Vol. 99, No D10: 20989-21003.

Saltzman, E.S., Brass, G.W. and Price, D.A. (1983): **The Mechanism of Sulphate Aerosol Formation: Chemial and Sulphur Isotopic Evedience**. Geophysical Research Letters, Vol. 10, No. 7: 513-516.

Sanusi, A., Norman, A.L., Wadleigh, M.A., Tang, W., Burridge, C. (2006): **A Technique to Determine the Isotope Composition of MSA.** For submission to Analytical Chemistry.

Savard, M, personal communication, 2006.

Savoie, D.L. and Prospero, J.M. (1989): **Effect of Continental Sources on Nitrate Concentrations Over the Pacific Ocean.** Nature Vol. 339: 687-689.

Savoie, D.L., Prospero, J.M. and Saltzman, E.S. (1989): **Non-Sea-Salt Sulphate and Nitrate in Trade Wind Aerosols at Barbados: Evidence for Long Range Transport.** Journal of Geophysical Research Vol. 94, No. D4: 5069-5080.

Schlesinger, W.H. (1997): **Biogeochemistry: an analysis of global change.** Academic Press, San Diego, California. 2nd Edition, pp 337-347

Schlesinger, W.H. and Peterjohn, W.T. (1988): **Ion and Sulfate-Isotope Ratios in Arid Soils Subject to Wind Erosion in the Southwestern USA.** Soil Science Society of America Journal Vol. 52: 48-54.

Sharma, S., Lavoué, D., Cachier, H., Barrie, L.A. and Gong, S.L. (2004): **Long-Term Trends of the Black Carbon Concentrations in the Canadian Arctic.** Journal of Geophysical Research, Vol. 109, D15203.

Shaw, G.E. (1983): **Bio-Controlled Thermostasis Involving the Sulfur Cycle**. Climatic Change 5, pages 297-303. D. Reidel Publishing Company.

Shinn, J.H. and Lynn, S. (1979): **Do Man-Made Sources Affect the Sulphur Cycle of Northeastern States?** Environmental Science and Technology Vol 13, No. 9: 1062-1067.

Slade, G. Personal Communication, 2005. Communication Director, North Atlantic Refinery.

Stohl, Andreas (1998): **Computation, Accuracy and Applications of Trajectories – A Review and Bibliography.** Atmospheric Environment Vol. 32, No. 6: 947-966.

Thode, H.G., Monster (1970): **Sulfur Isotope Abundances and Genetic Relations of Oil Accumulations in Middle East Basin.** American Association of Petroleum Geologists Bulletin, Vol. 54: 627-637.

Tisch Enviromental (2000): **Series 230 High Volume Cascade Impactors.** Instruction Manual Provided with High Volume Air Sampler Purchased from Tisch Environmental.

Turkeian, V.C., Macko, S.A., Keene, W.C. (2001): **Application of stable sulphur isotopes to differentiate sources of size-resolved particulate sulphate in polluted marine air at Bermuda during Spring.** Geophysical Research Letters, Vol. 28 No. 8: 1491-1494

Urey, H.C. (1947): **The Thermodynamic Properties of Isotopic Substances**. Journal of Chemical Society London, Part I: 562-581.

Vairavamurthy, A., Andreae, M.O. and Iverson, R.L. (1985): **Biosynthesis of Dimethylsulfide and Dimethylpropiothetin by *Hymenomonas carterae* in Relation to Sulfur Source and Salinity Variations.** Limnology and Oceanography, Vol. 30, No.1: 59-70.

Visconti, G. (2001): **Fundamentals of Physics and Chemistry of the Atmosphere**. Springer Press, New York.

Wadleigh, M.A., Schwarcz, H.P. and Kramer, J.R. (1996): **Isotopic Evedience for the Origin of Sulphate in Coastal Rain.** Tellus Vol. 48B: 44-59.

Wadleigh, M.A. and Blake, D.M. (1999): **Tracing Sources of Atmospheric Sulphur Using Epiphytic Lichens.** Environmental Pollution, Vol. 106, No. 3: 165-271.

Wadleigh, M.A. (2004): **Sulphur Isotope Composition of Aerosols over the Western North Atlantic**. Canadian Journal of Fishery and Aquatic Sciences Vol. 61: 817-825.

Wadleigh, M.A., Norman, A.L., Eaton, S.J. (2004): **Seasonal Trends in Atmospheric DMS: the C-SOLAS Atlantic Cruises**. Oral Presentation C-SOLAS AGM, May, 2004.

Whatman® Online Catalogue (2005)
www.whatman.com/products/pageID=7.25.6.16

Wojcik, G.S. & Chang, J.S. (1997): **A Re-Evaluation of Sulfur Budgets, Lifetimes, and Scavenging Ratios for Eastern North America**. Journal of Atmospheric Chemistry 26: 109-145.

Yoon, Y.J., Brimblecombe, P. (2001): **Modelling the contribution of sea salt and dimethyl sulphide derived aerosol to marine CCN.** Atmospheric Chemistry and Physics Discussions Vol. 1: 93-123

Appendix I

Appendix I.1

Calculation of δ_{NSS}:

$$\delta_{NSS} = (\delta_{Total} * f_{Total} - \delta_{SS} * f_{SS}) / f_{NSS}$$

Appendix I.2

Calculation of $f_{biogenic}$

$$\delta_{TOTAL} f_{TOTAL} = \delta_{SEASPRAY} f_{SEASPRAY} + \delta_{BIOGENIC} f_{BIOGENIC} + \delta_{ANTHROPOGENIC} f_{ANTHROPOGENIC}$$

Where $f_T = f_{SS} + f_B + f_A$

$\delta_T f_T = \delta_{SS} f_{SS} + \delta_B f_B + \delta_A (f_T - f_{SS} - f_B)$

$\delta_T f_T = \delta_{SS} f_{SS} + \delta_B f_B + \delta_A f_T - \delta_A f_{SS} - \delta_A f_B$

$\delta_T f_T - \delta_{SS} f_{SS} - \delta_A f_T + \delta_A f_{SS} = \delta_A f_B - \delta_B f_B$

$f_B (\delta_B - \delta_A) = \delta_T f_T - \delta_{SS} f_{SS} - \delta_A f_T + \delta_A f_{SS}$

$$f_B = \frac{\delta_T f_T - \delta_{SS} f_{SS} - \delta_A f_T + \delta_A f_{SS}}{(\delta_B - \delta_A)}$$

Note: In the calculation of the $f_{biogenic}$, +3.0 was used for $\delta_{anthropogenic}$, and $\delta_{biogenic}$ = +18‰, which is the average of the range of values for biogenic sulphur (+21‰ to +15‰).

$$\delta_{TOTAL} f_{TOTAL} = \delta_{SEASPRAY} f_{SEASPRAY} + \delta_{BIOGENIC} f_{BIOGENIC} + \delta_{ANTHROPOGENIC} f_{ANTHROPOGENIC}$$

$$\delta_{TOTAL} f_{TOTAL} - \delta_{SEASPRAY} f_{SEASPRAY} - \delta_{BIOGENIC} f_{BIOGENIC} = \delta_{ANTHROPOGENIC} f_{ANTHROPOGENIC}$$

$$f_{ANTHROPOGENIC} = \frac{\delta_{TOTAL} f_{TOTAL} - \delta_{SEASPRAY} f_{SEASPRAY} - \delta_{BIOGENIC} f_{BIOGENIC}}{\delta_{ANTHROPOGENIC}}$$

Appendix II

Appendix II.1

Table II-1 – Cruise time line.

Date	Note	Latitude	Longitude
23-Apr-03	Boat is loaded and set sail at 1:00pm (Halifax Regional Time)		
25-Apr-03	Lagrangian study begins at station L1	43°24'N	57°43'W
1-May-03	Transit to station T1		
3-May-03	Arrive at T1, depart for T2 in the afternoon	39°00'N	57°30'W
4-May-03	Arrive at T2	36°83'N	57°40'W
5-May-03	Transit to T3		
6-May-03	Transit to T3		
7-May-03	Arrive at T3, transit to T4 in the afternoon	42°33'N	45°00'W
8-May-03	Arrive at T4, transit to T5 in the afternoon	46°50'N	45°00'W
9-May-03	Arrive at T5, depart for T6 in the afternoon	50°67'N	45°00'W
10-May-03	Arrive at T6, depart for return to T5 in the afternoon	54°83'N	45°00'W
11-May-03	Arrive at T5, transit to L1	50°67'N	45°00'W
12-May-03	Transit to LI		
13-May-03	Arrive at L1	43°24'N	57°43'W
14-May-03	Depart for Halifax		
15-May-03	Arrive in Halifax		

Appendix II.2

Blank Correction for $\delta^{34}S$:

$$\delta^{34}S_{Corrected} = (\delta^{34}S_{Total} * \{\text{Total } SO_4 \text{ concentration (ppm)}\} - \delta^{34}S_{Blank} * \{SO_4 \text{ blank concentration (ppm)}\}) / \{\text{Blank corrected } SO_4 \text{ concentration (ppm)}\}$$

SO_2 concentration:

$$SO_2 \text{ Concentration} = \{\text{Blank Corrected } BaSO_4 \text{ (g)}/1000\} * \{64.06 \text{ (g) } SO_2 / 1 \text{ mol } SO_2\} / \{1 \text{ mol } BaSO_4 / 233.4 \text{ } BaSO_4\text{(g)}\} * \{1 \text{ mol S}/ 1 \text{ mol } BaSO_4\} * \{1 \text{ mol } SO_2 / 1 \text{ mol S}\} * 1000$$

Appendix II.3

Blank Correction of Ion Chromatograph Concentrations:

Example: Total Particulate Filter H-1-1-D

Average Cl Concentration of Lab Blanks = 0.243 ppm
Average Cl Concentration of Field Blanks = 0.375 ppm
Total Average of Blanks = 0.309 ppm

Blank Corrected Concentration = Original Concentration – Average of Blanks

Appendix II.4

Volume of air sampled = Flow rate (m^3/min) * Total Time (minutes)

Concentration in ngm-3 = (Concentration (ppm)) * Volume of water (sonication (mL))) / (Volume of air sampled) * 1000

Appendix II.5

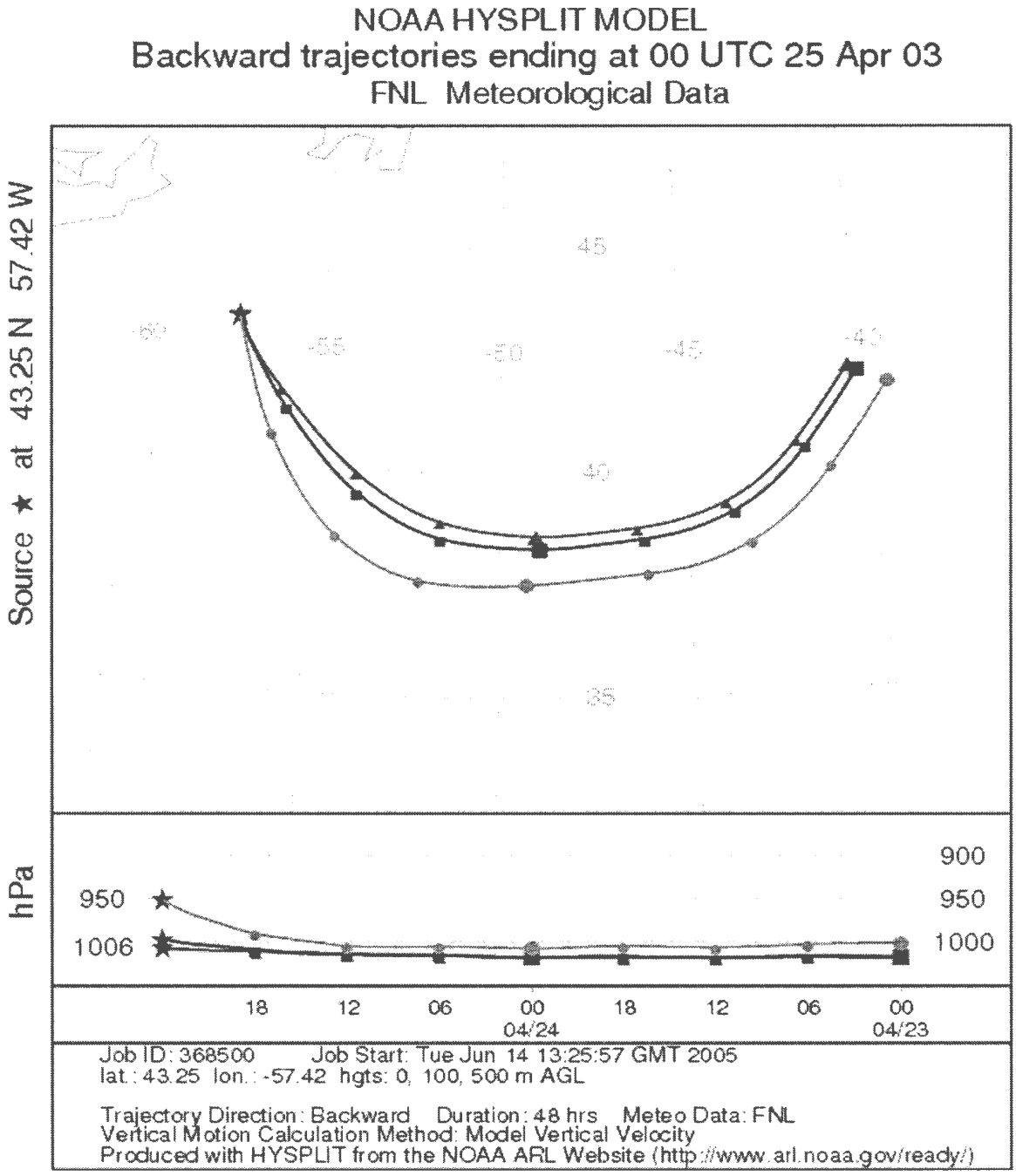

Figure II-1 – Air mass back trajectory for 0m, 100m and 500m above sea level for April 25, 2003. Circles represent 500m asl, squares 100m asl and triangles 0m asl.

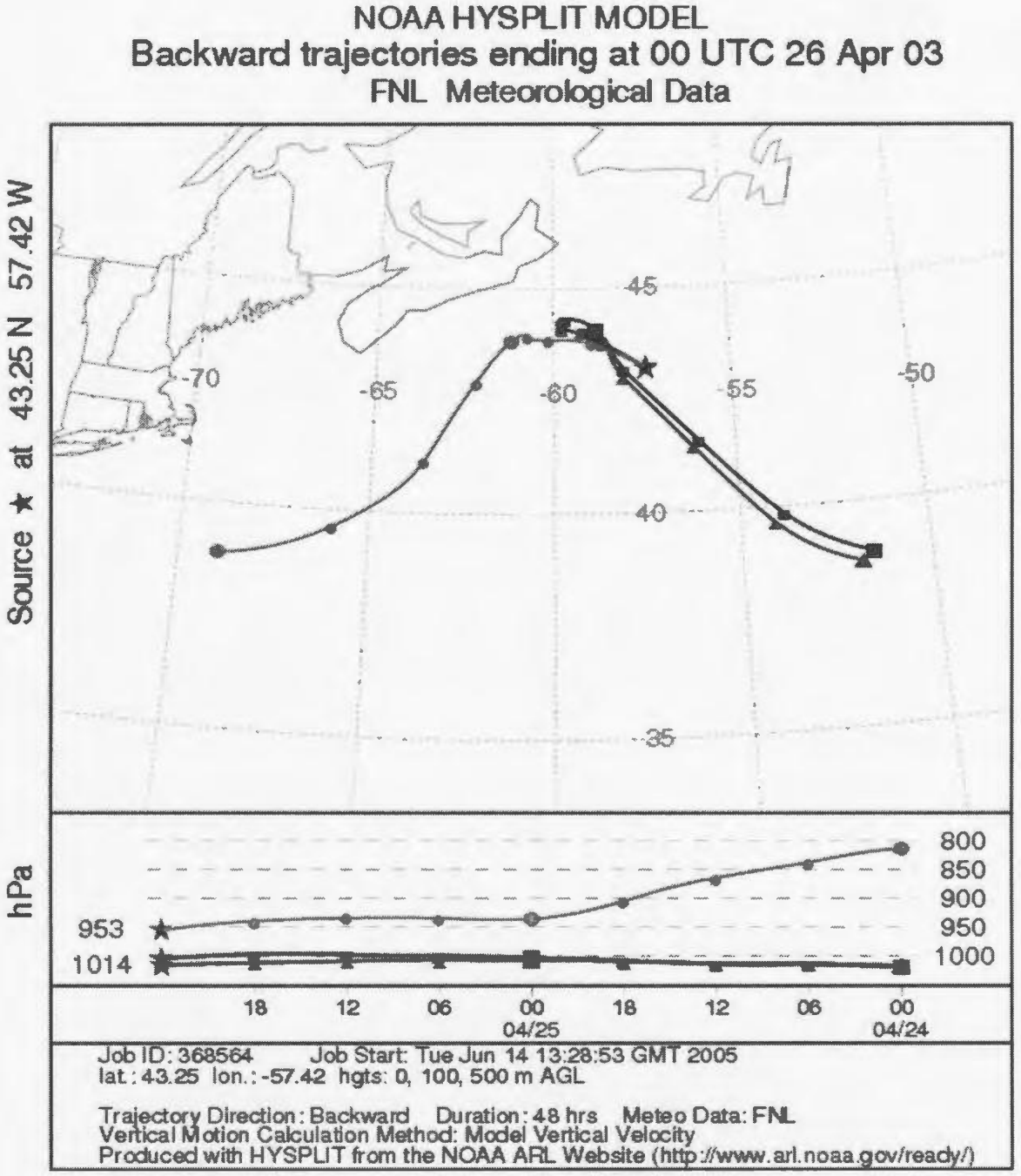

Figure II-2 – Air mass back trajectory for 0m, 100m and 500m above sea level for April 26, 2003. Circles represent 500m asl, squares 100m asl and triangles 0m asl.

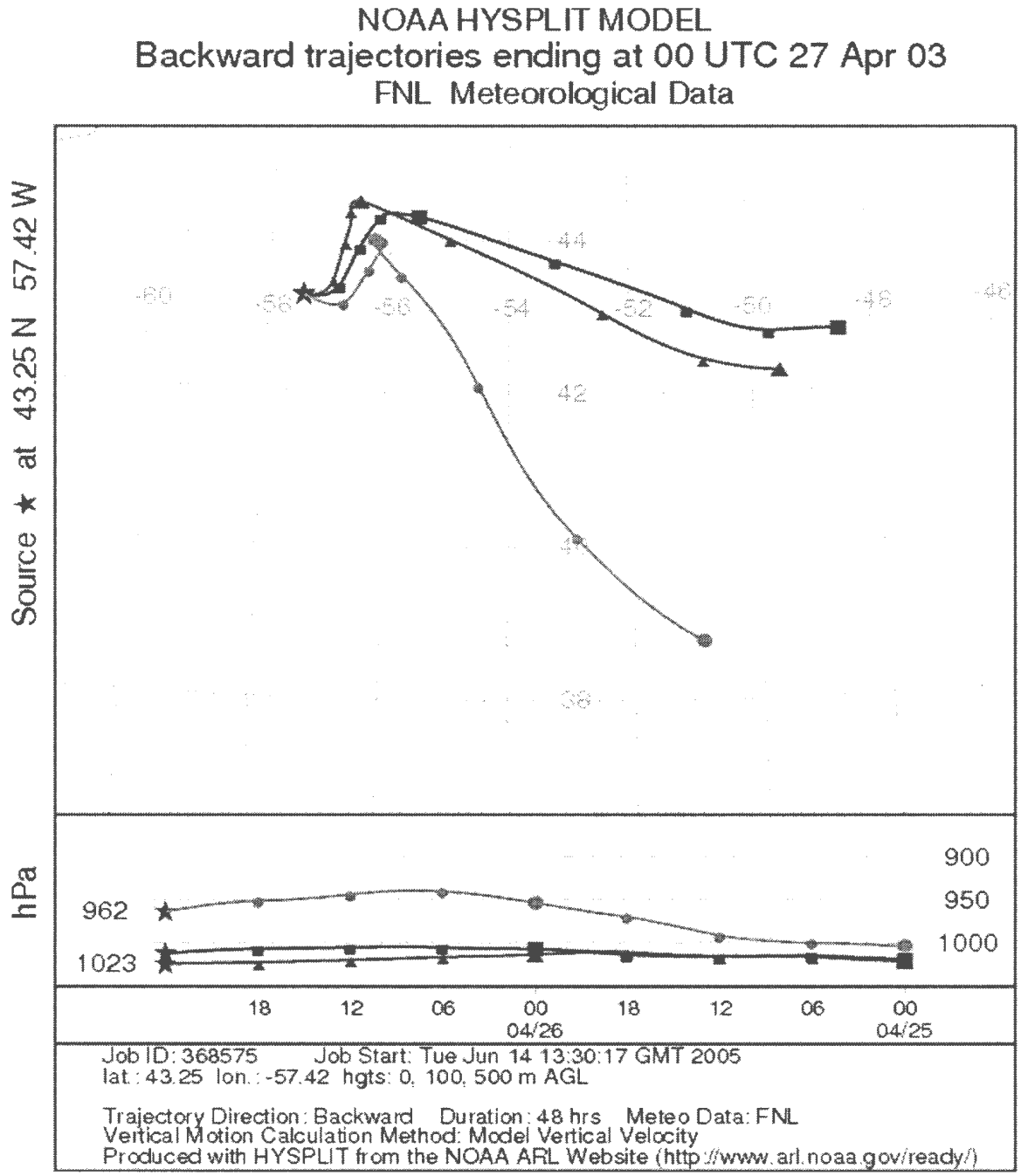

Figure II-3 – Air mass back trajectory for 0m, 100m and 500m above sea level for April 27, 2003. Circles represent 500m asl, squares 100m asl and triangles 0m asl.

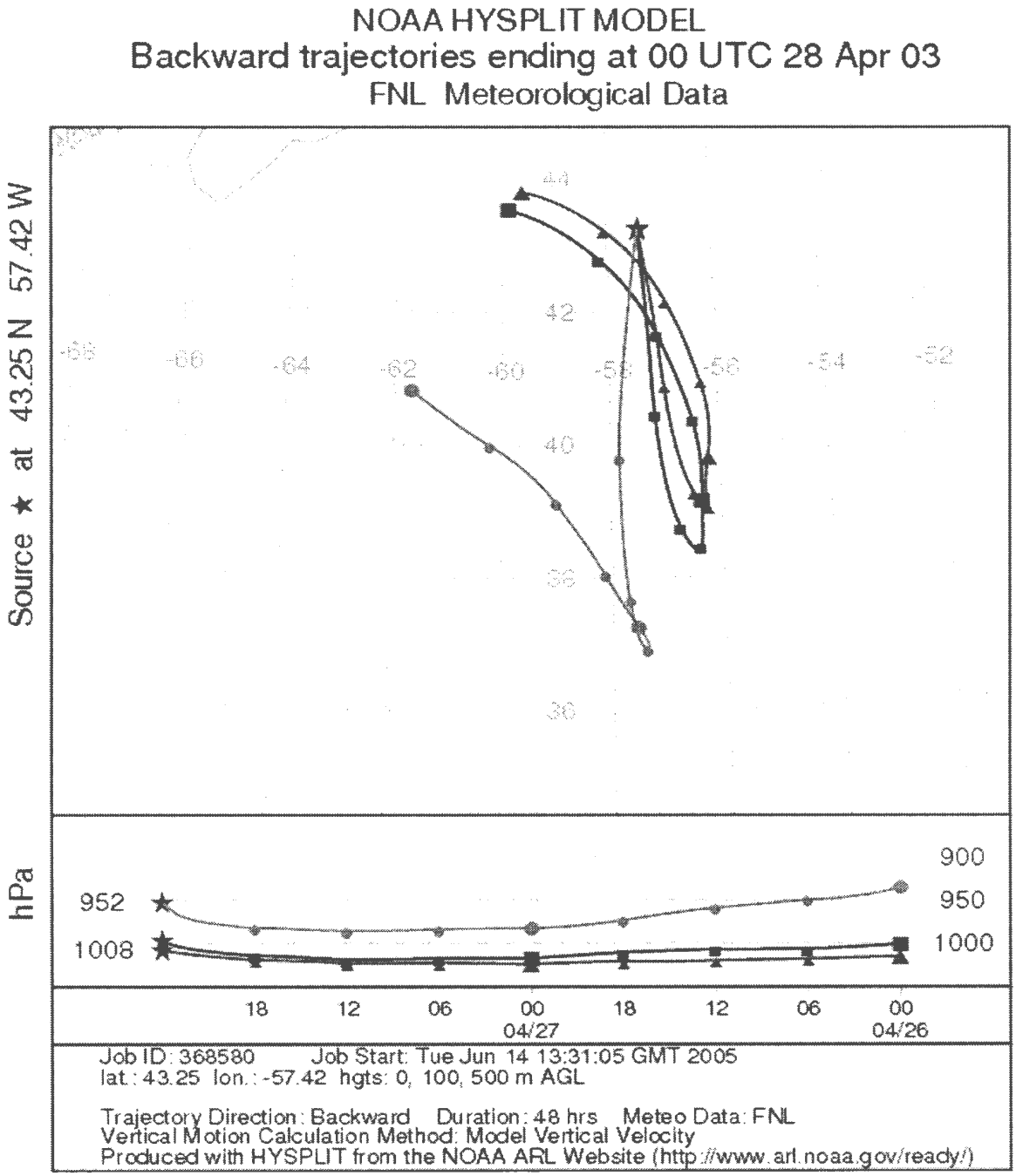

Figure II-4 – Air mass back trajectory for 0m, 100m and 500m above sea level for April 28, 2003. Circles represent 500m asl, squares 100m asl and triangles 0m asl.

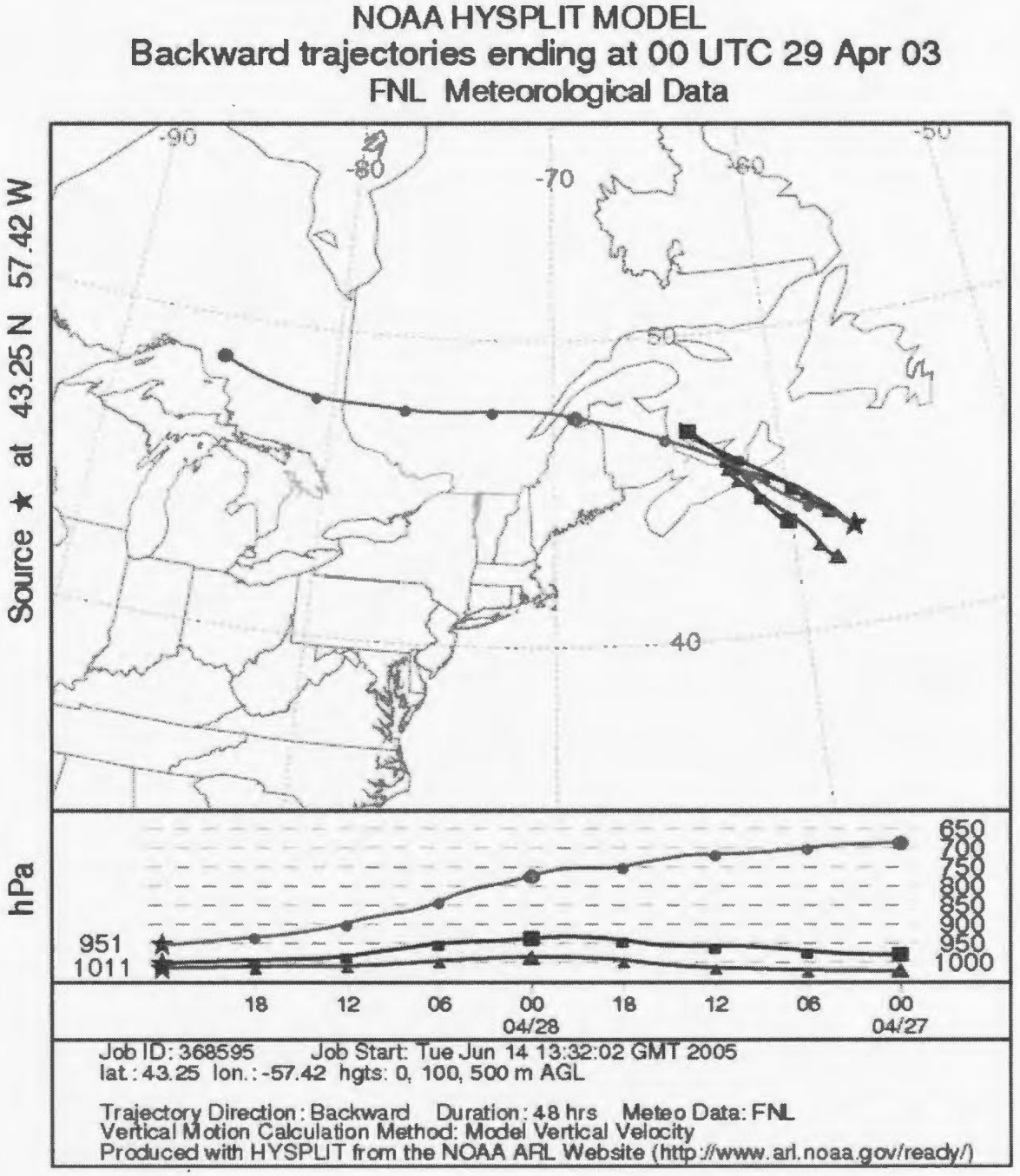

Figure II-5 – Air mass back trajectory for 0m, 100m and 500m above sea level for April 29, 2003. Circles represent 500m asl, squares 100m asl and triangles 0m asl.

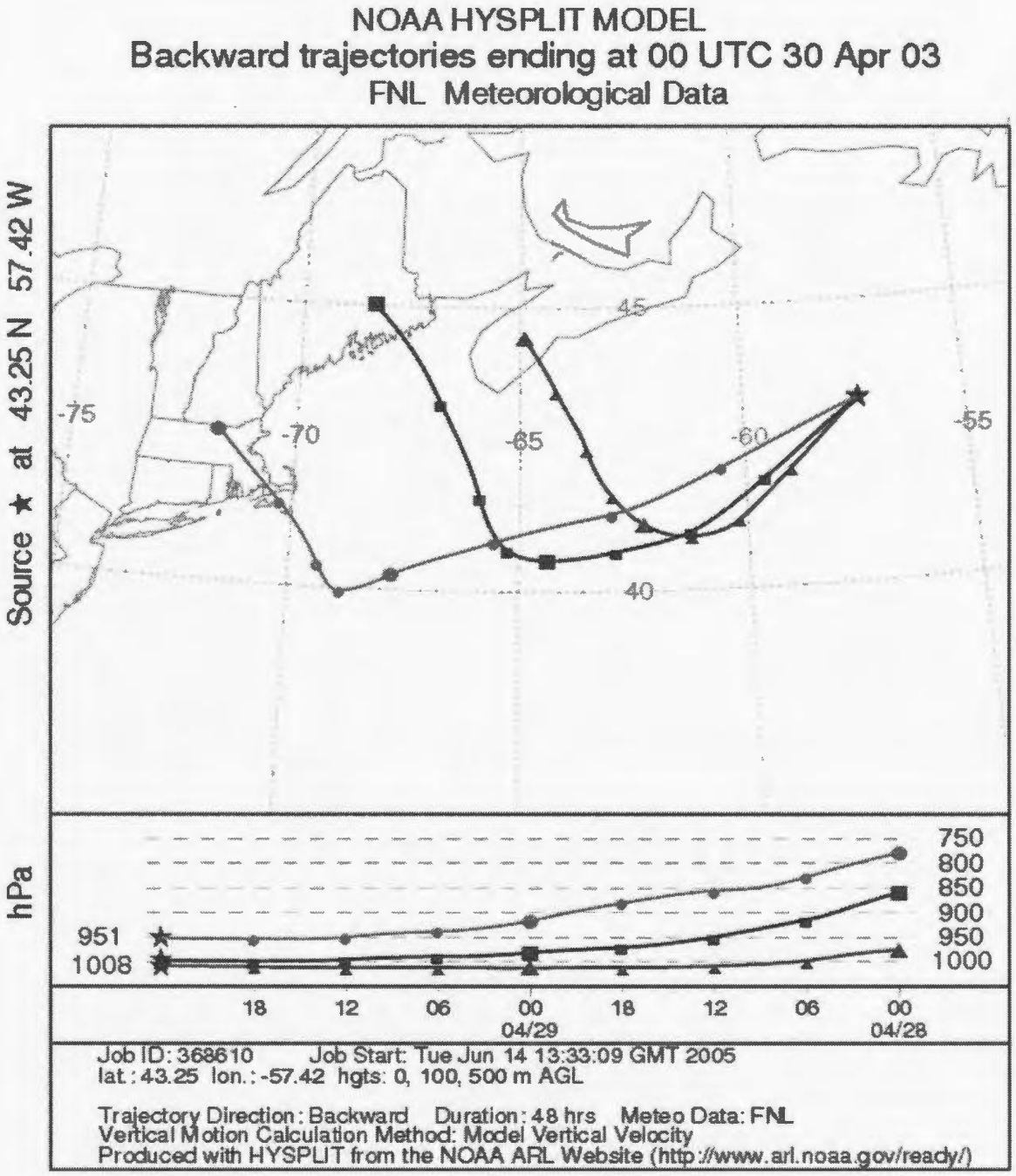

Figure II-6 – Air mass back trajectory for 0m, 100m and 500m above sea level for April 30, 2003. Circles represent 500m asl, squares 100m asl and triangles 0m asl.

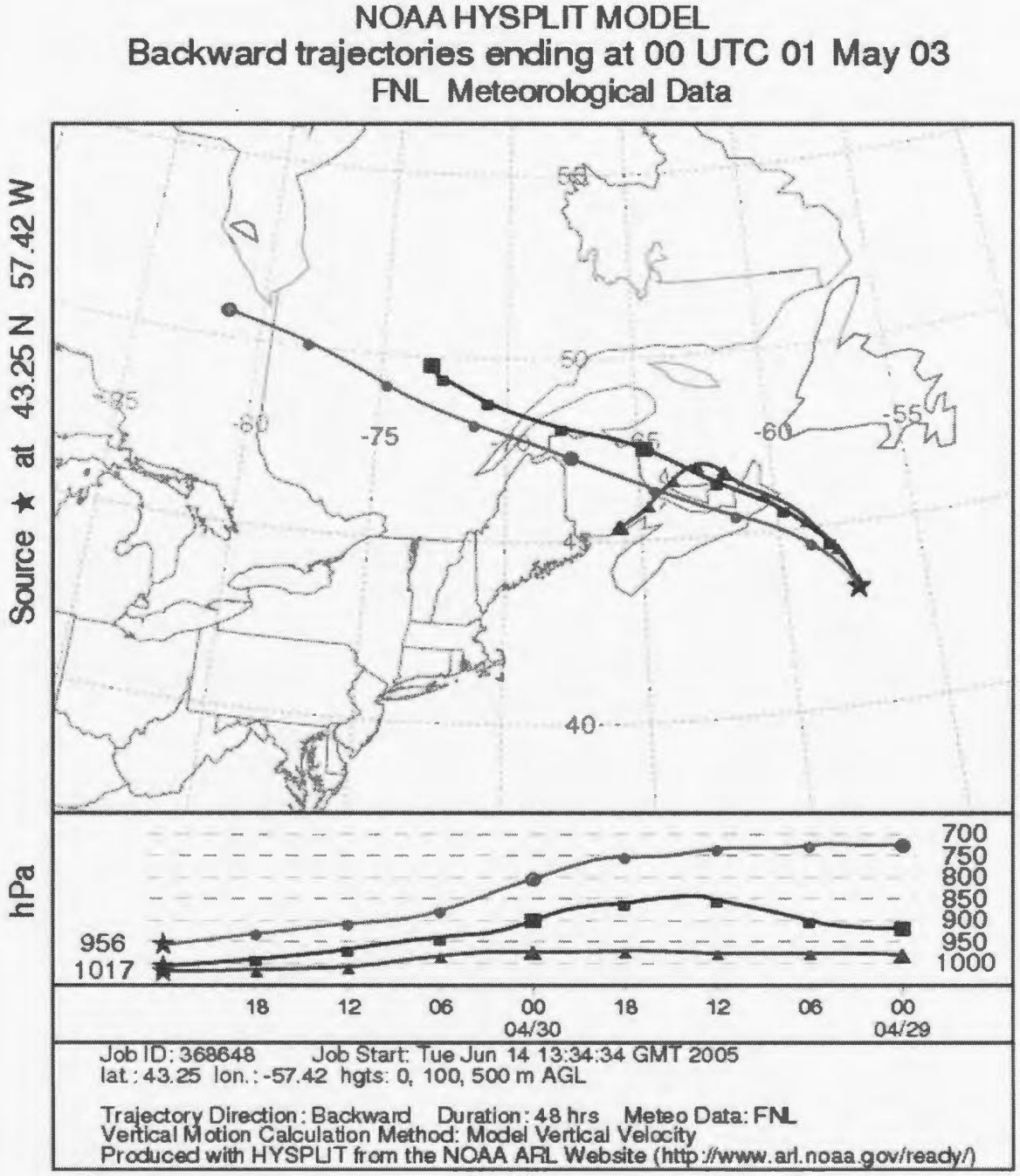

Figure II-7 – Air mass back trajectory for 0m, 100m and 500m above sea level for May 1, 2003. Circles represent 500m asl, squares 100m asl and triangles 0m asl.

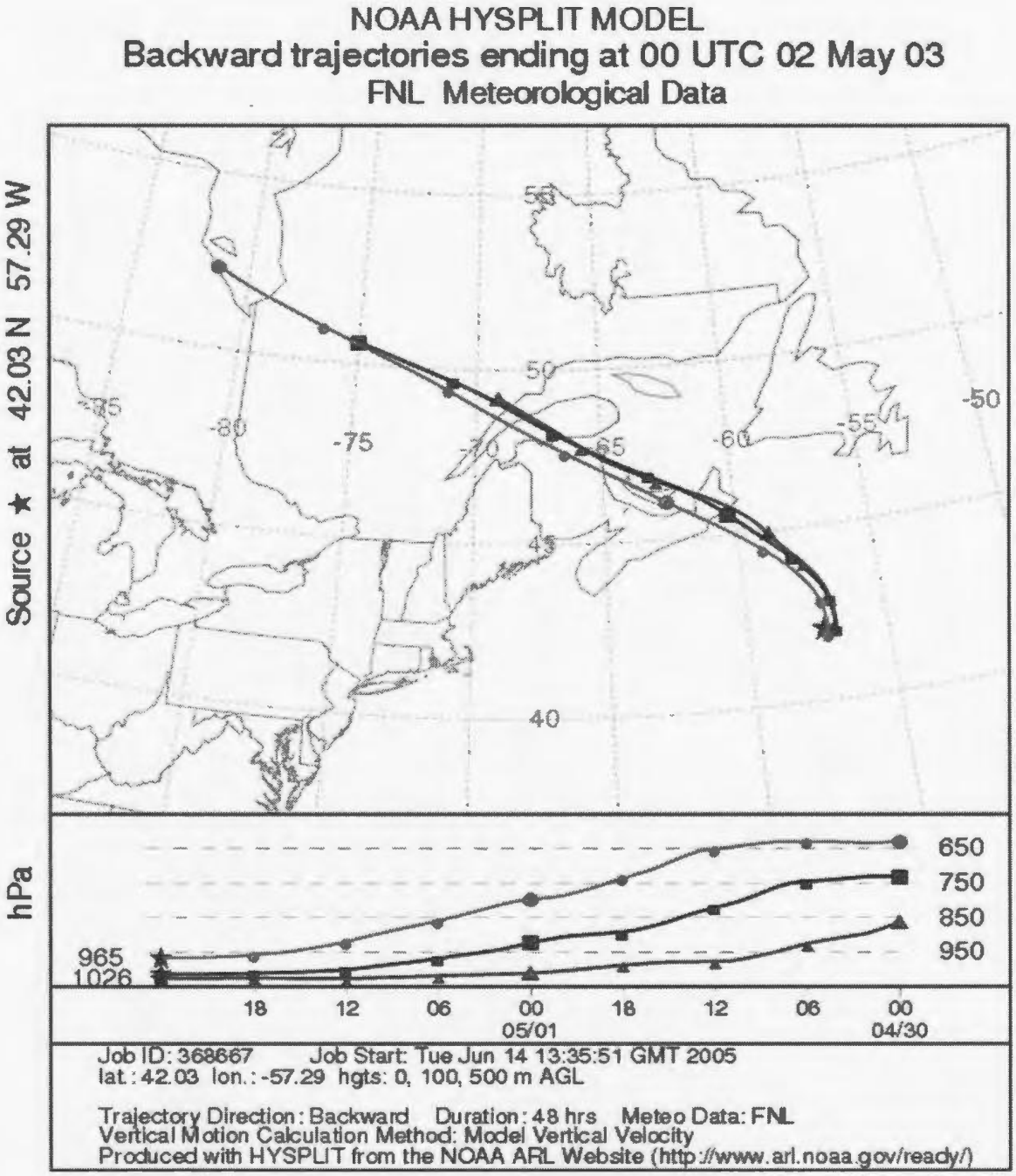

Figure II-8 – Air mass back trajectory for 0m, 100m and 500m above sea level for May 2, 2003. Circles represent 500m asl, squares 100m asl and triangles 0m asl.

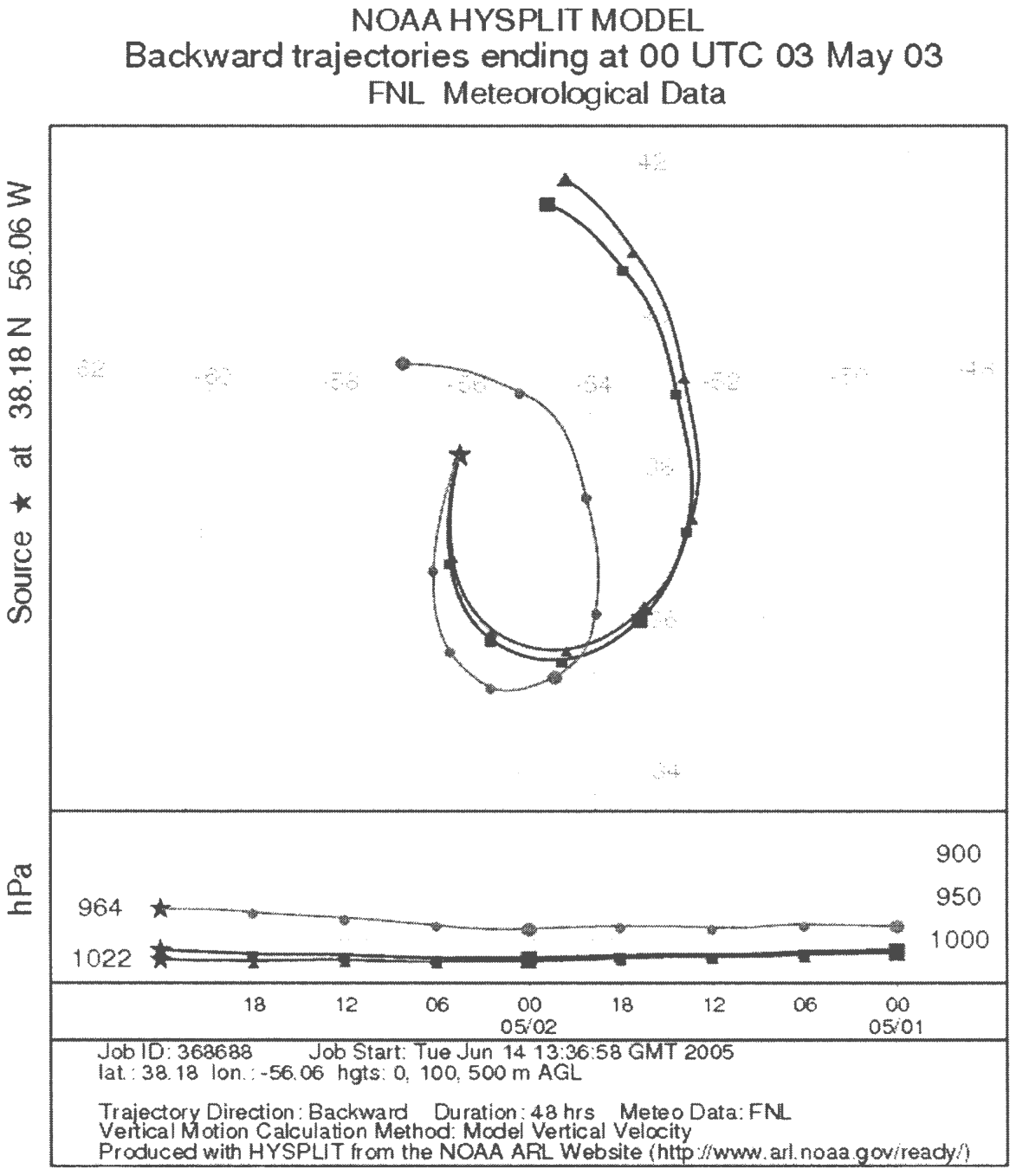

Figure II-9 – Air mass back trajectory for 0m, 100m and 500m above sea level for May 3, 2003. Circles represent 500m asl, squares 100m asl and triangles 0m asl.

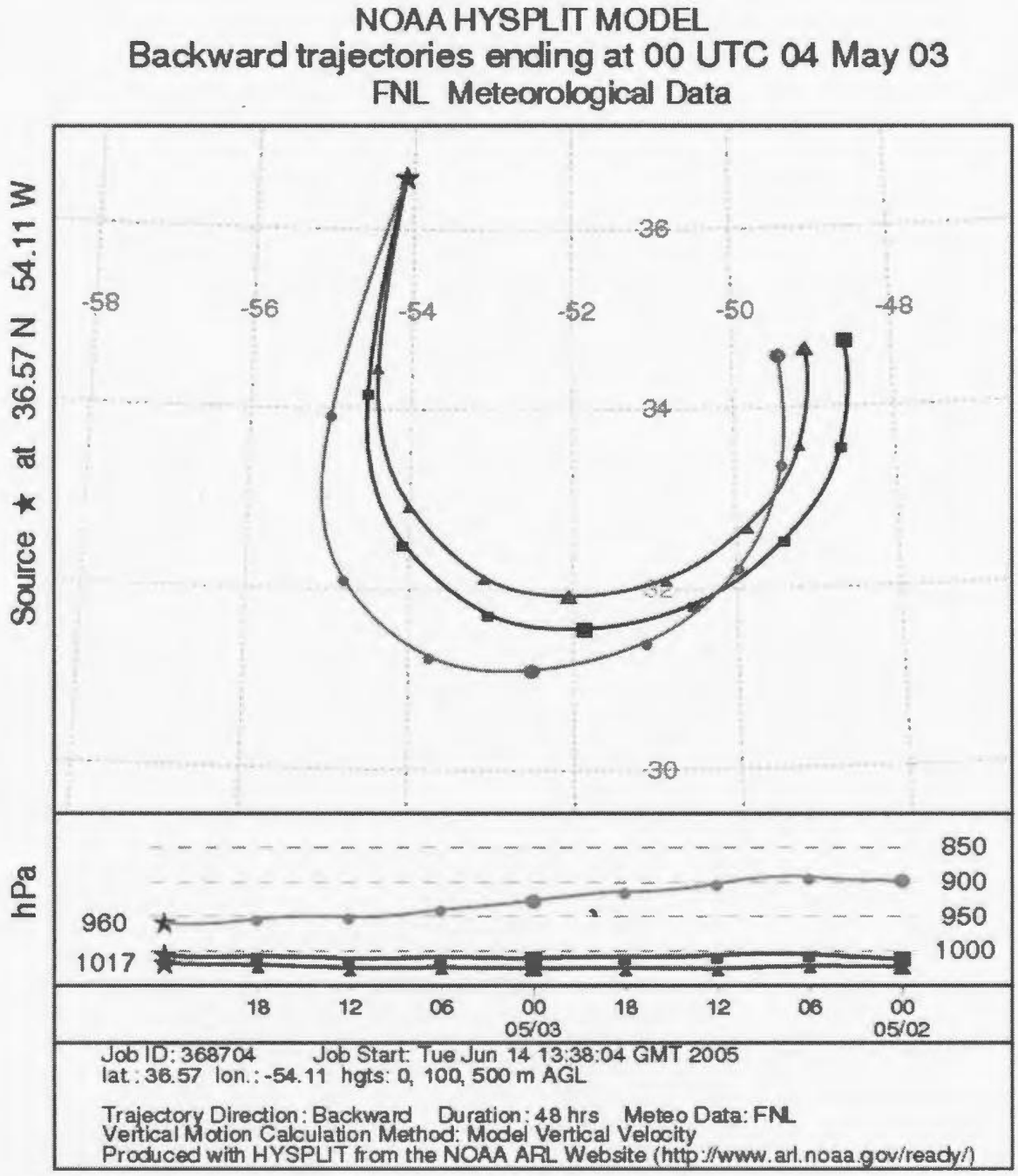

Figure II-10 – Air mass back trajectory for 0m, 100m and 500m above sea level for May 4, 2003. Circles represent 500m asl, squares 100m asl and triangles 0m asl.

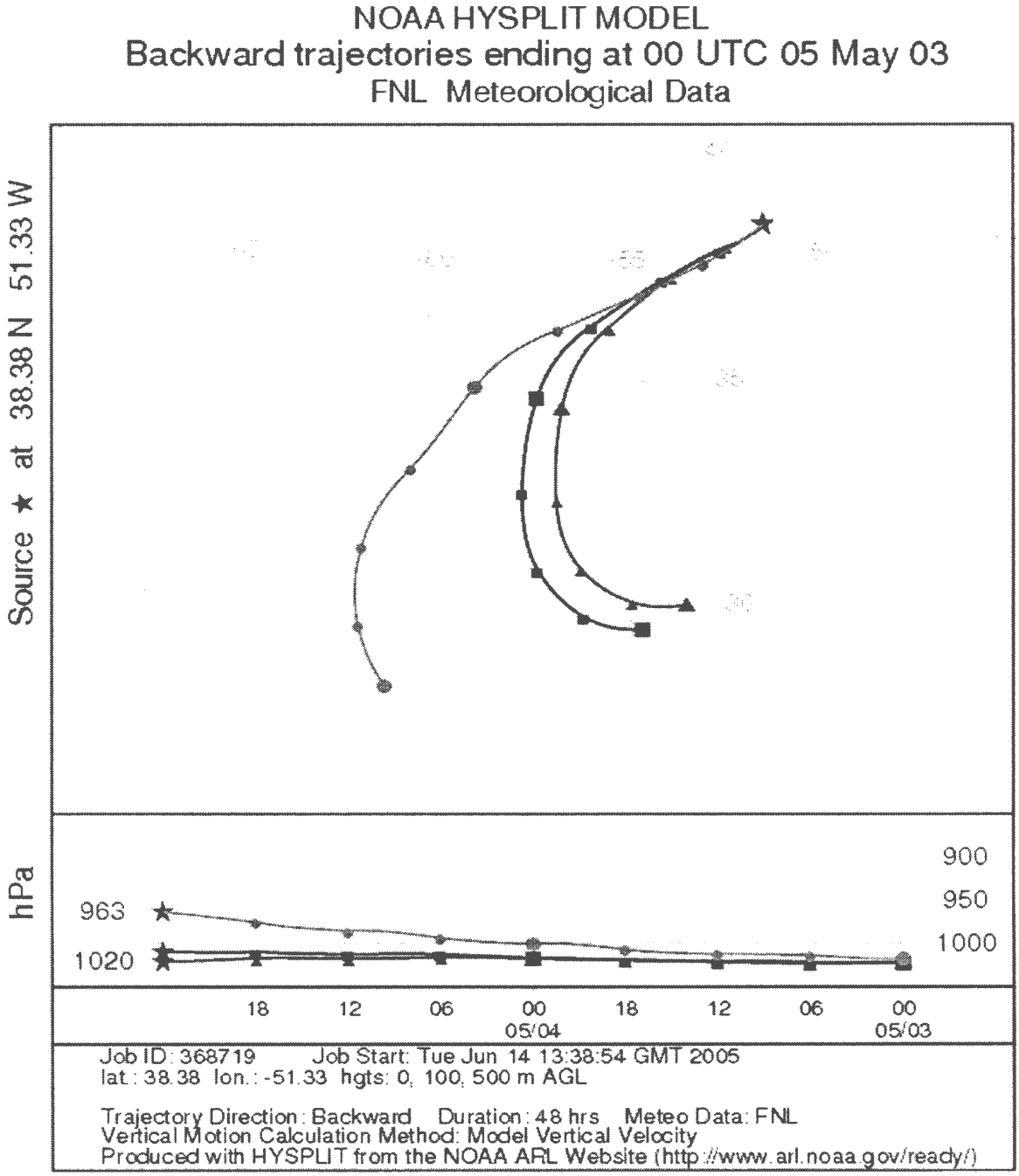

Figure II-10 – Air mass back trajectory for 0m, 100m and 500m above sea level for May 5, 2003. Circles represent 500m asl, squares 100m asl and triangles 0m asl.

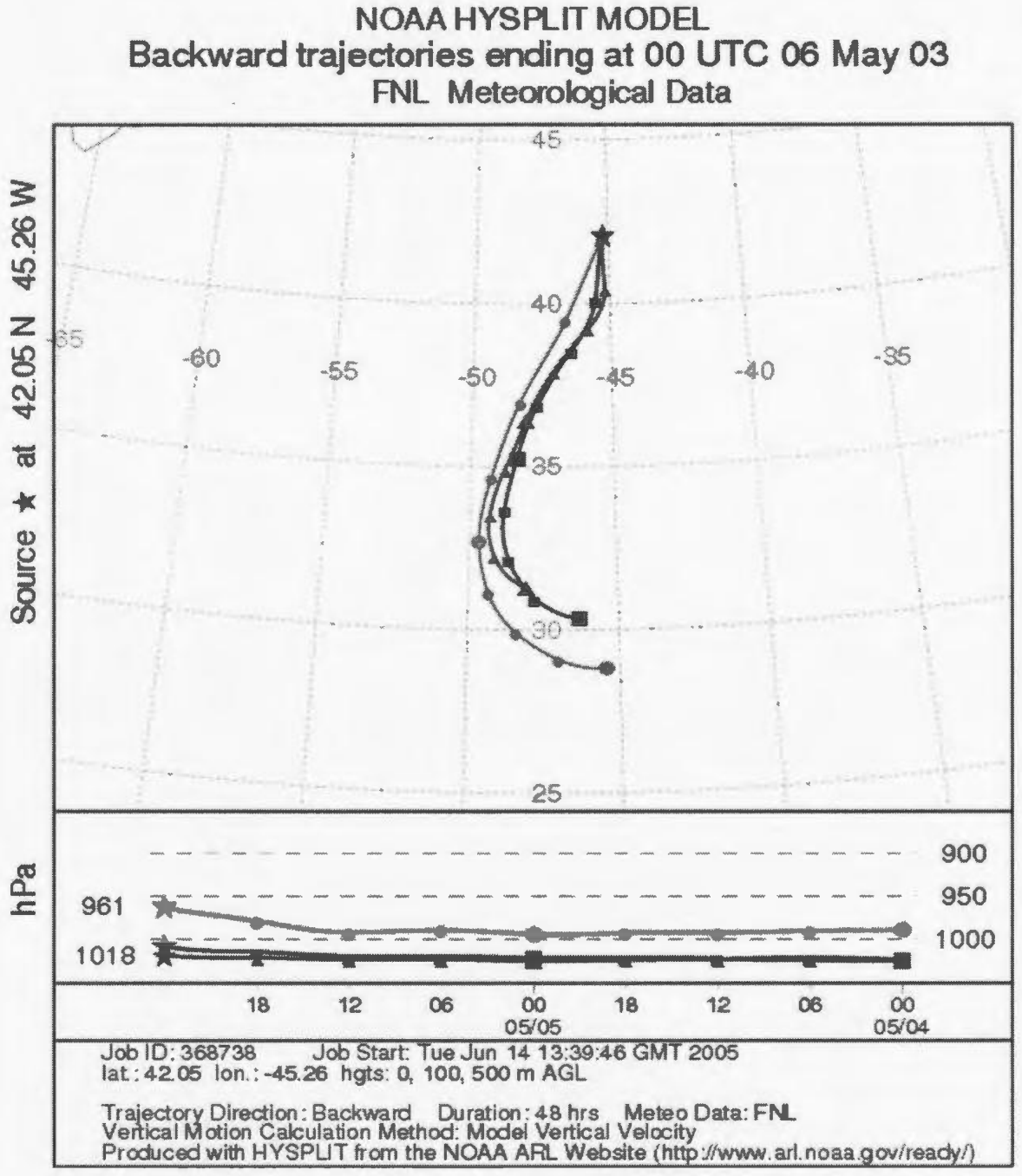

Figure II-11 – Air mass back trajectory for 0m, 100m and 500m above sea level for May 6, 2003. Circles represent 500m asl, squares 100m asl and triangles 0m asl.

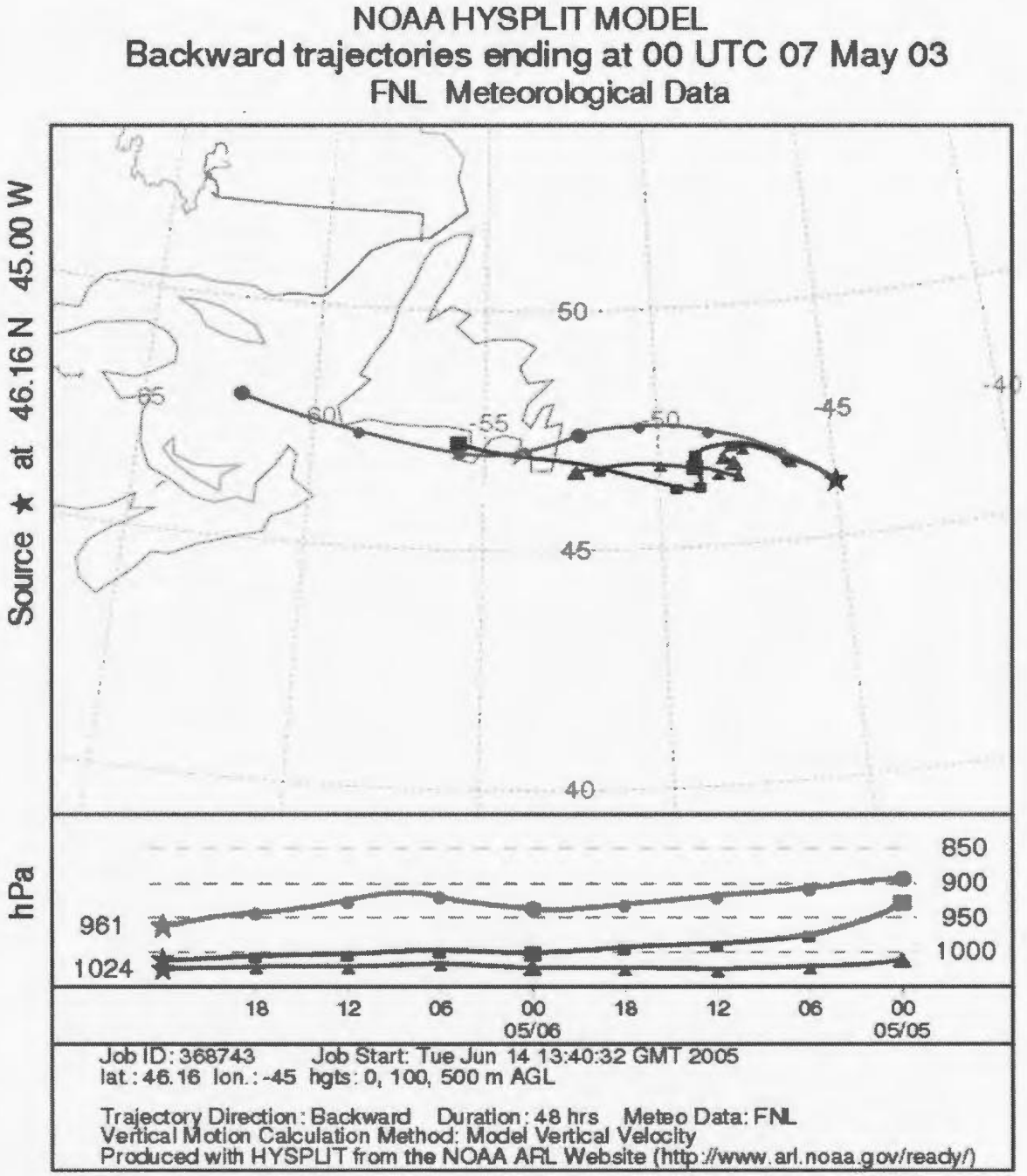

Figure II-12 – Air mass back trajectory for 0m, 100m and 500m above sea level for May 7, 2003. Circles represent 500m asl, squares 100m asl and triangles 0m asl.

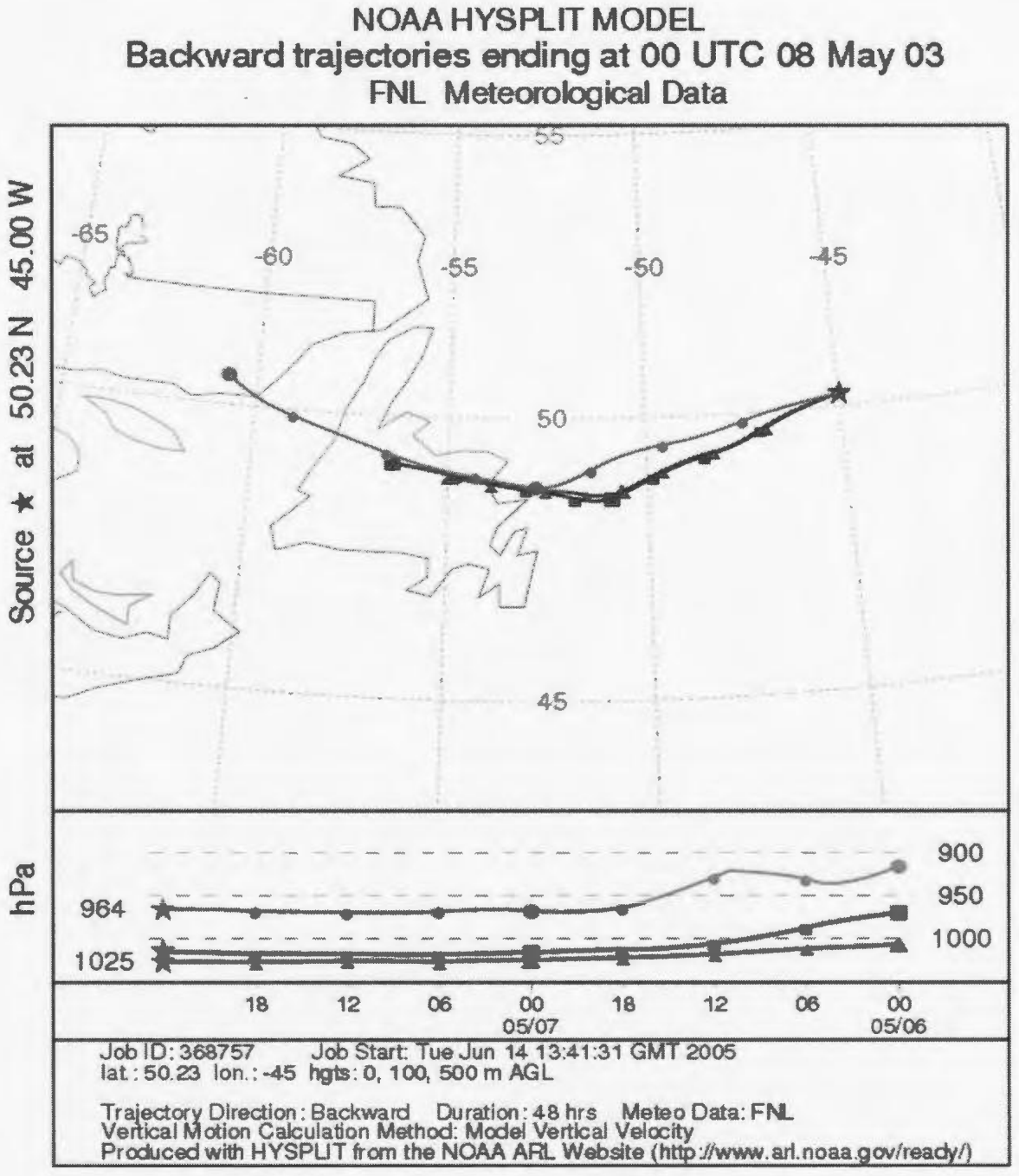

Figure II-13 – Air mass back trajectory for 0m, 100m and 500m above sea level for May 8, 2003. Circles represent 500m asl, squares 100m asl and triangles 0m asl.

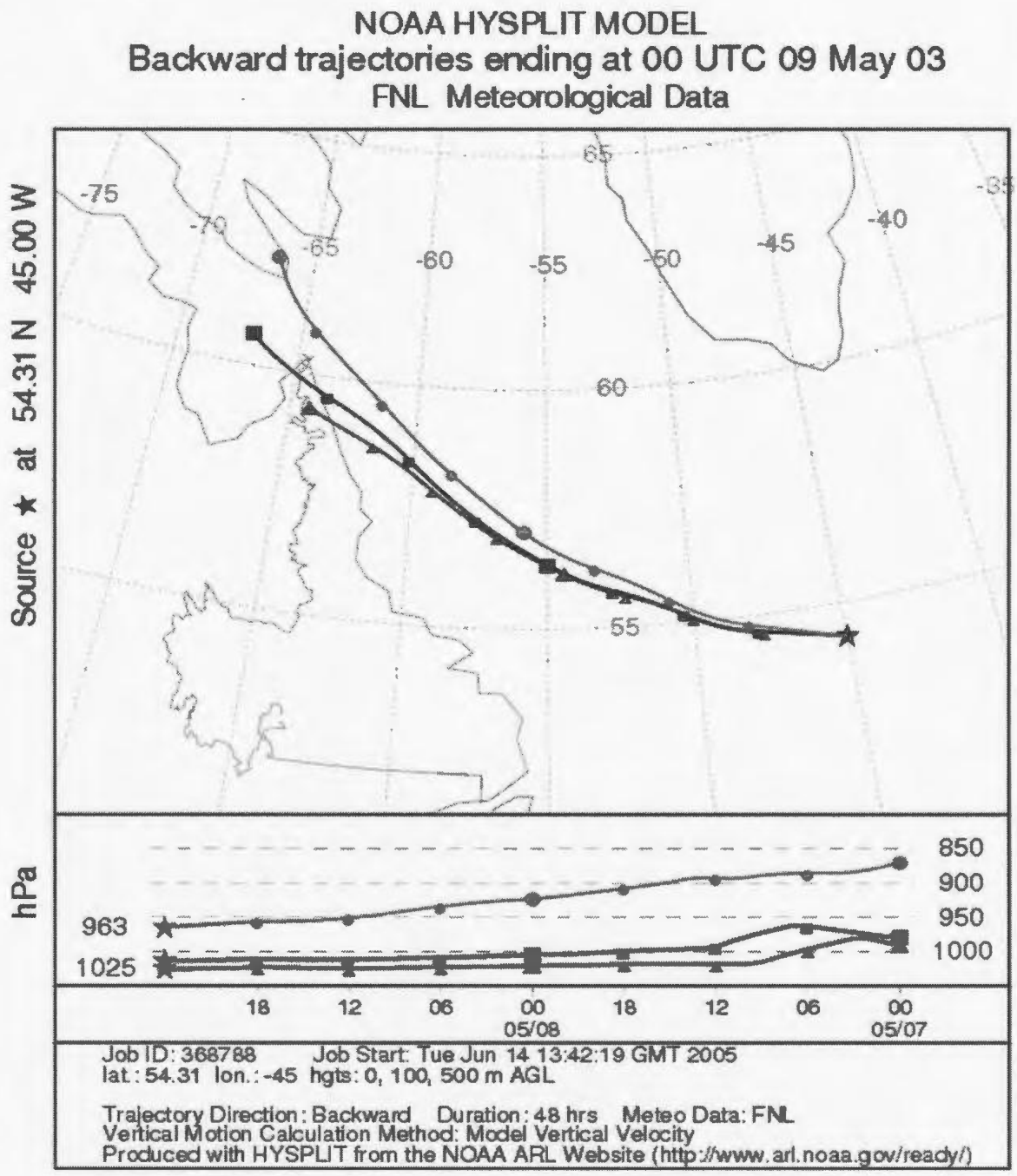

Figure II-14 – Air mass back trajectory for 0m, 100m and 500m above sea level for May 9, 2003. Circles represent 500m asl, squares 100m asl and triangles 0m asl.

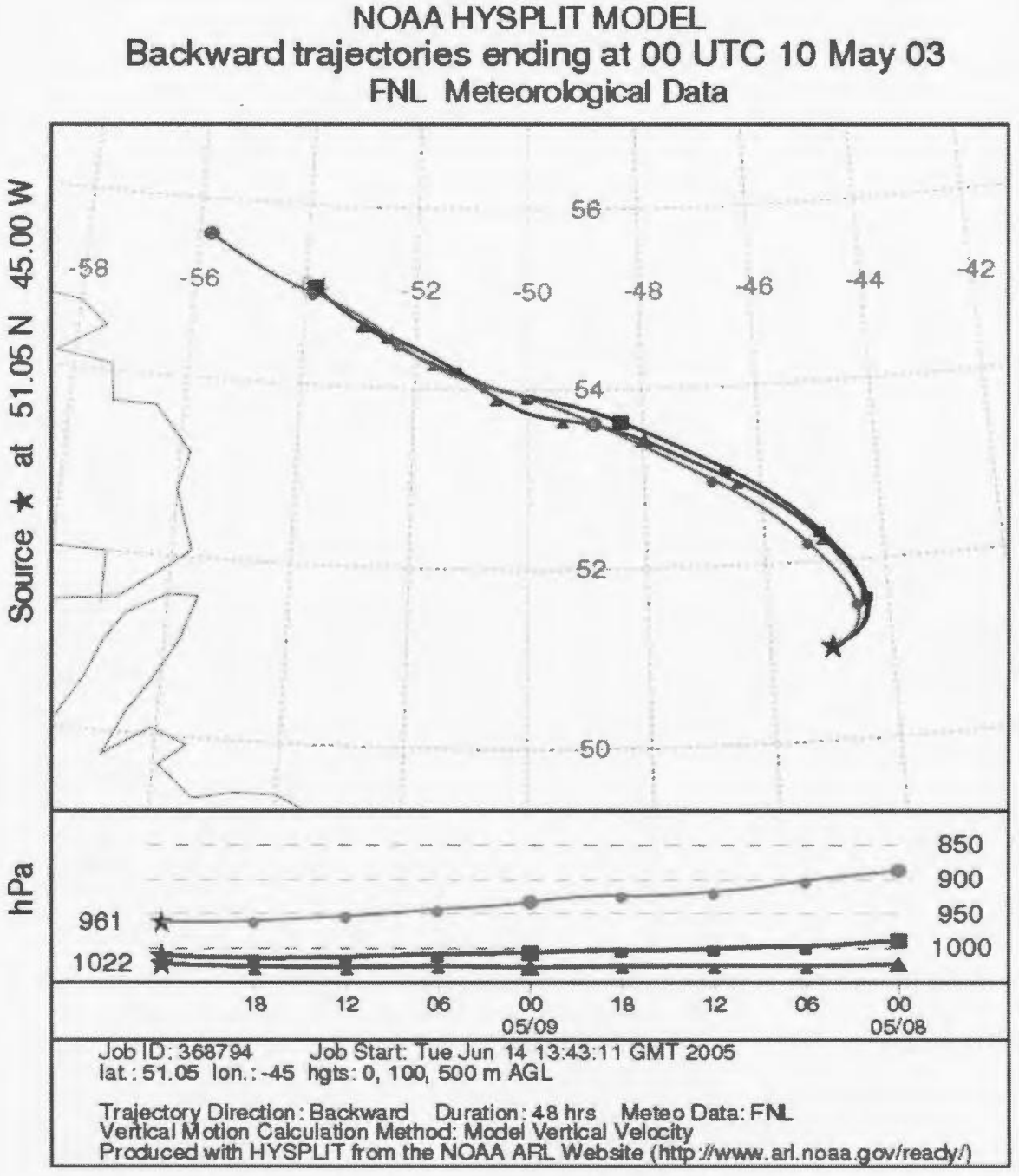

Figure II-15 – Air mass back trajectory for 0m, 100m and 500m above sea level for May 10, 2003. Circles represent 500m asl, squares 100m asl and triangles 0m asl.

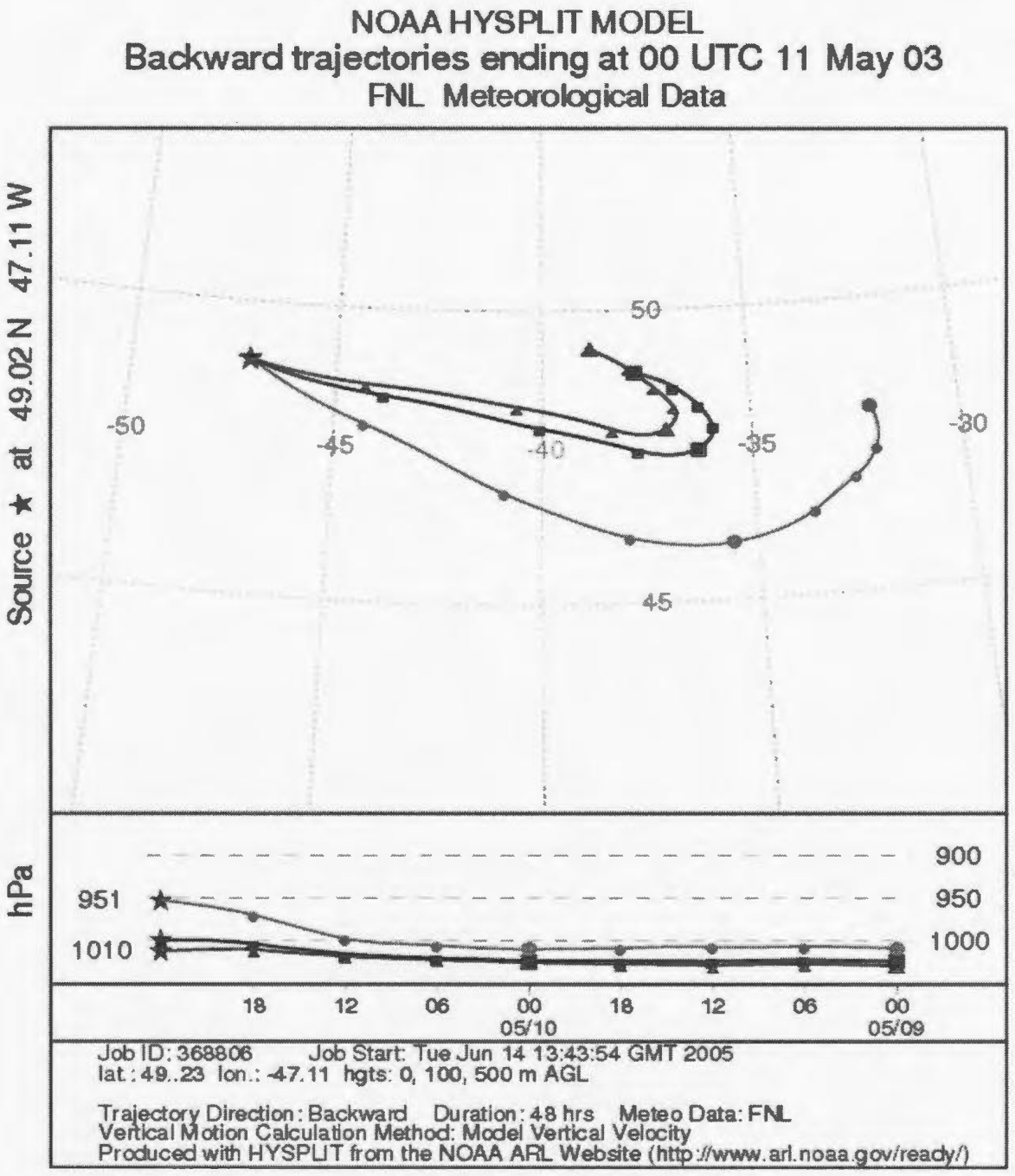

Figure II-16 – Air mass back trajectory for 0m, 100m and 500m above sea level for May 11, 2003. Circles represent 500m asl, squares 100m asl and triangles 0m asl.

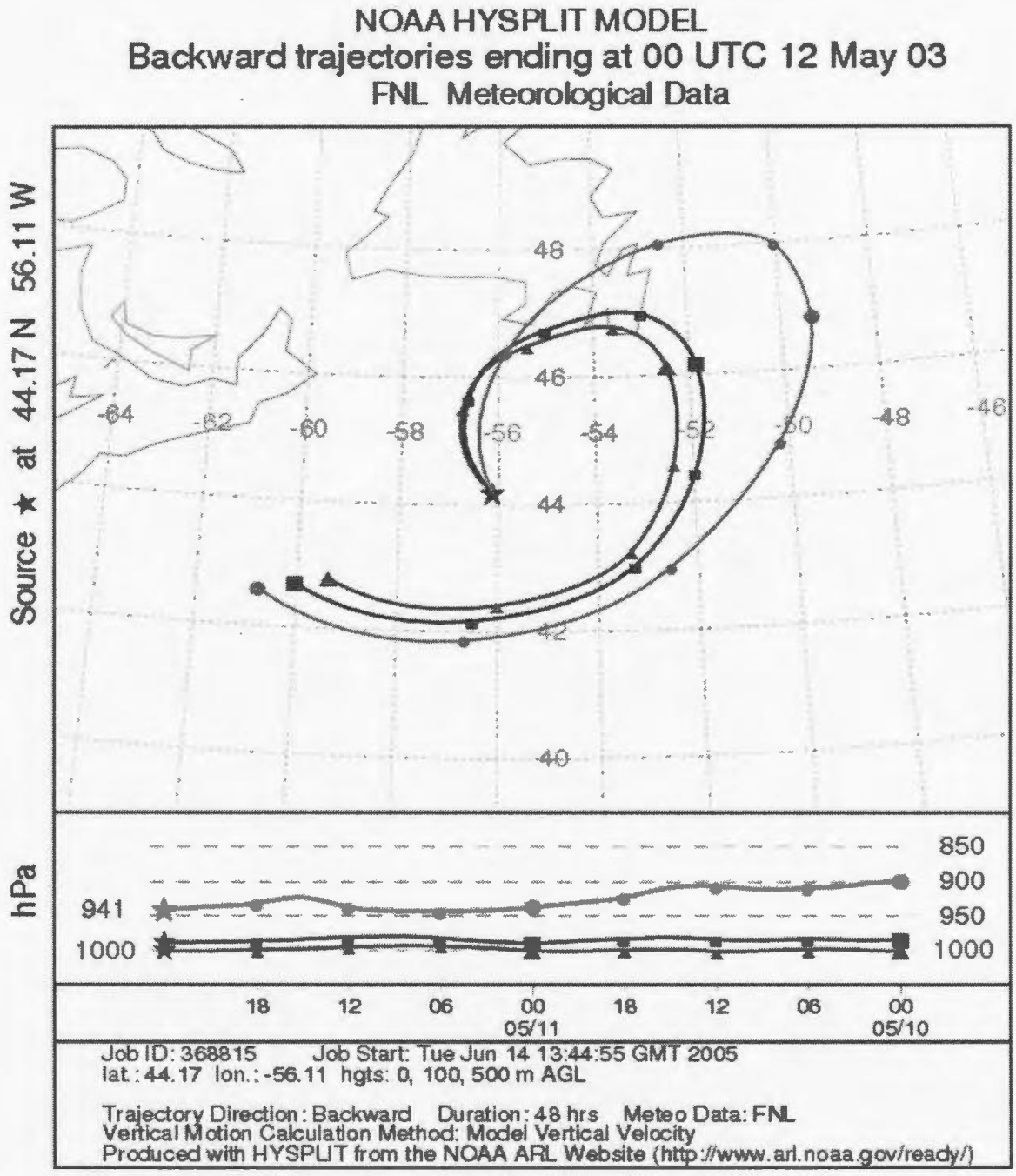

Figure II-17 – Air mass back trajectory for 0m, 100m and 500m above sea level for May 12, 2003. Circles represent 500m asl, squares 100m asl and triangles 0m asl.

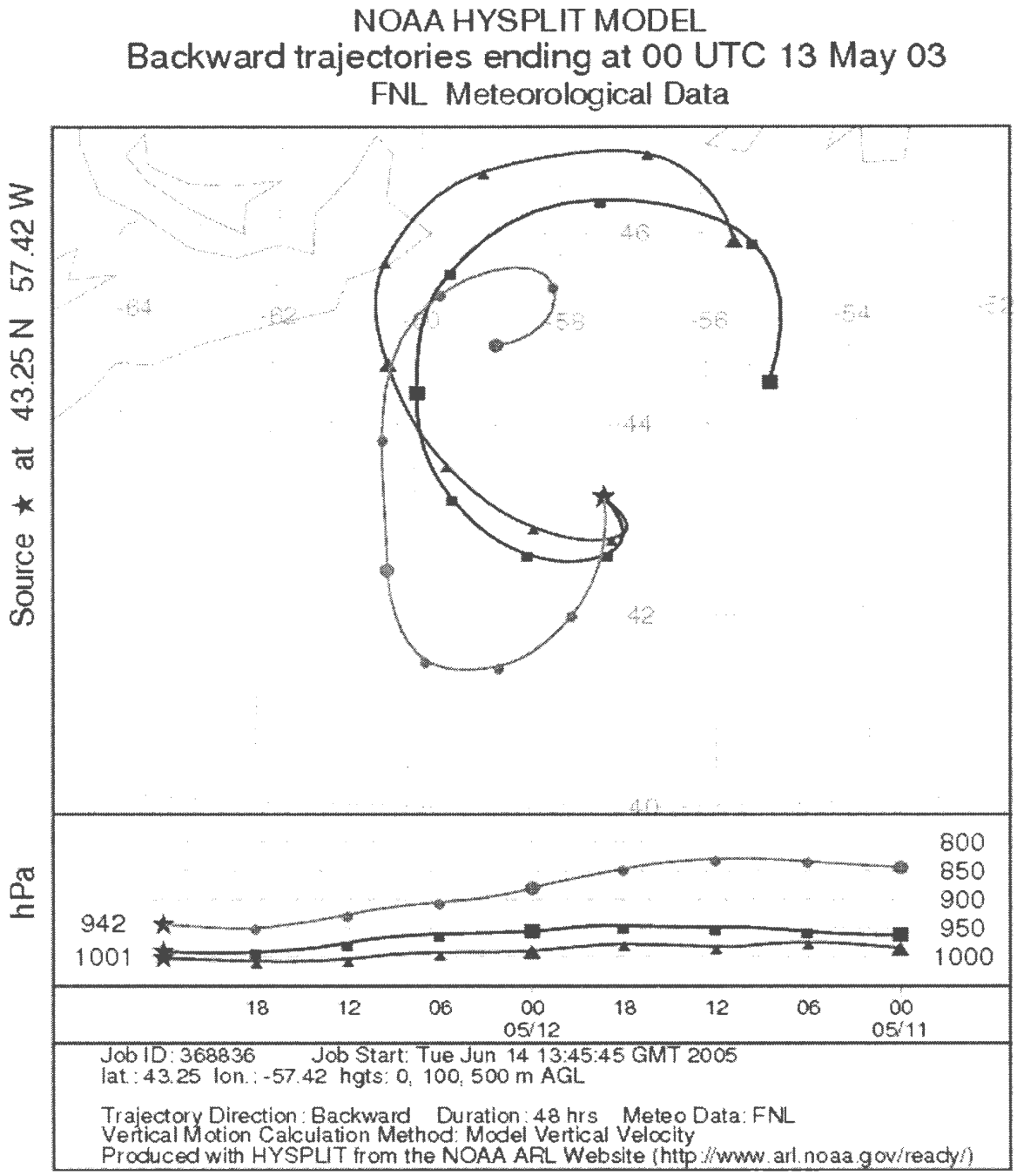

Figure II-18 – Air mass back trajectory for 0m, 100m and 500m above sea level for May 13, 2003. Circles represent 500m asl, squares 100m asl and triangles 0m asl.

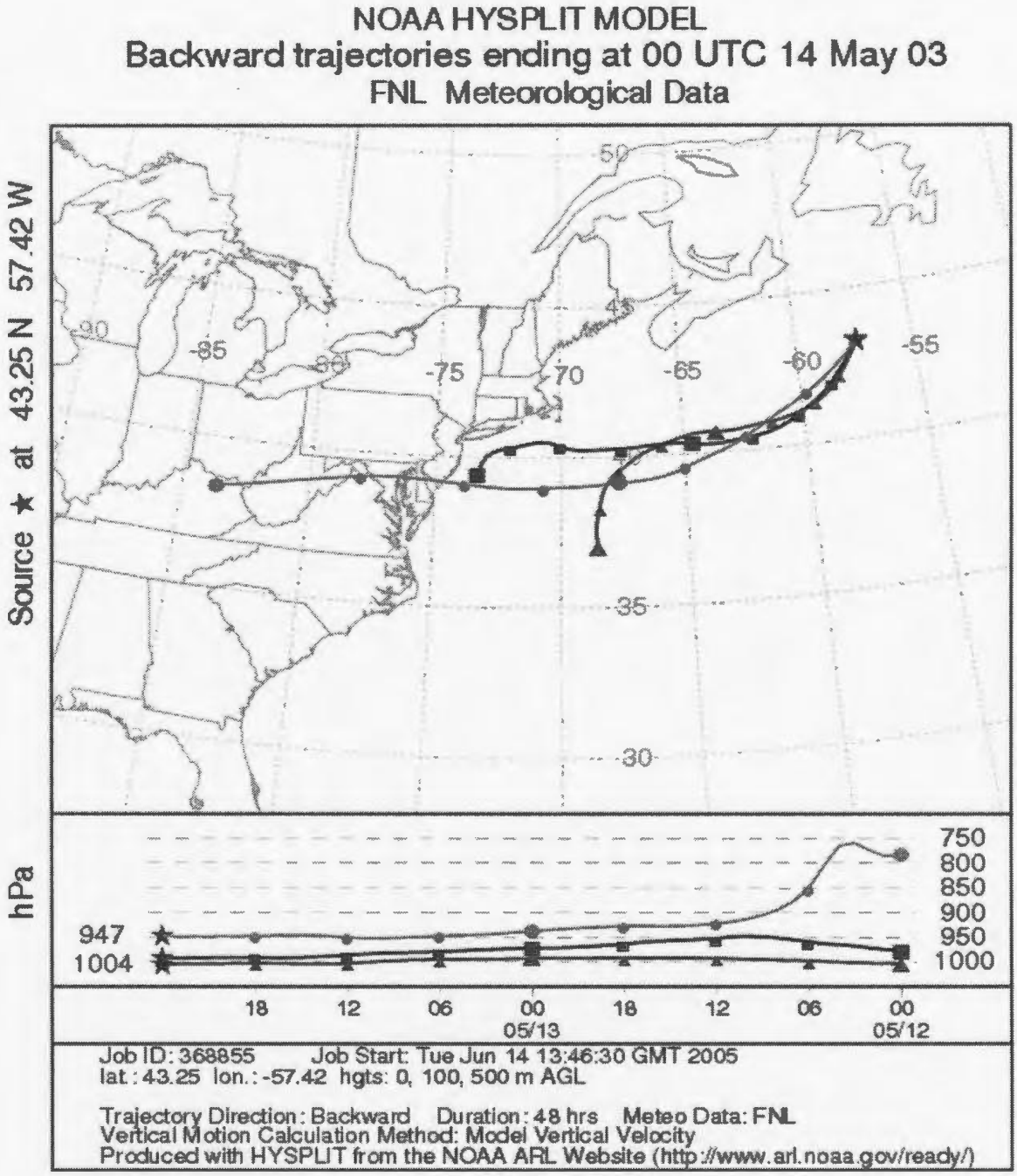

Figure II-19 – Air mass back trajectory for 0m, 100m and 500m above sea level for May 14, 2003. Circles represent 500m asl, squares 100m asl and triangles 0m asl.

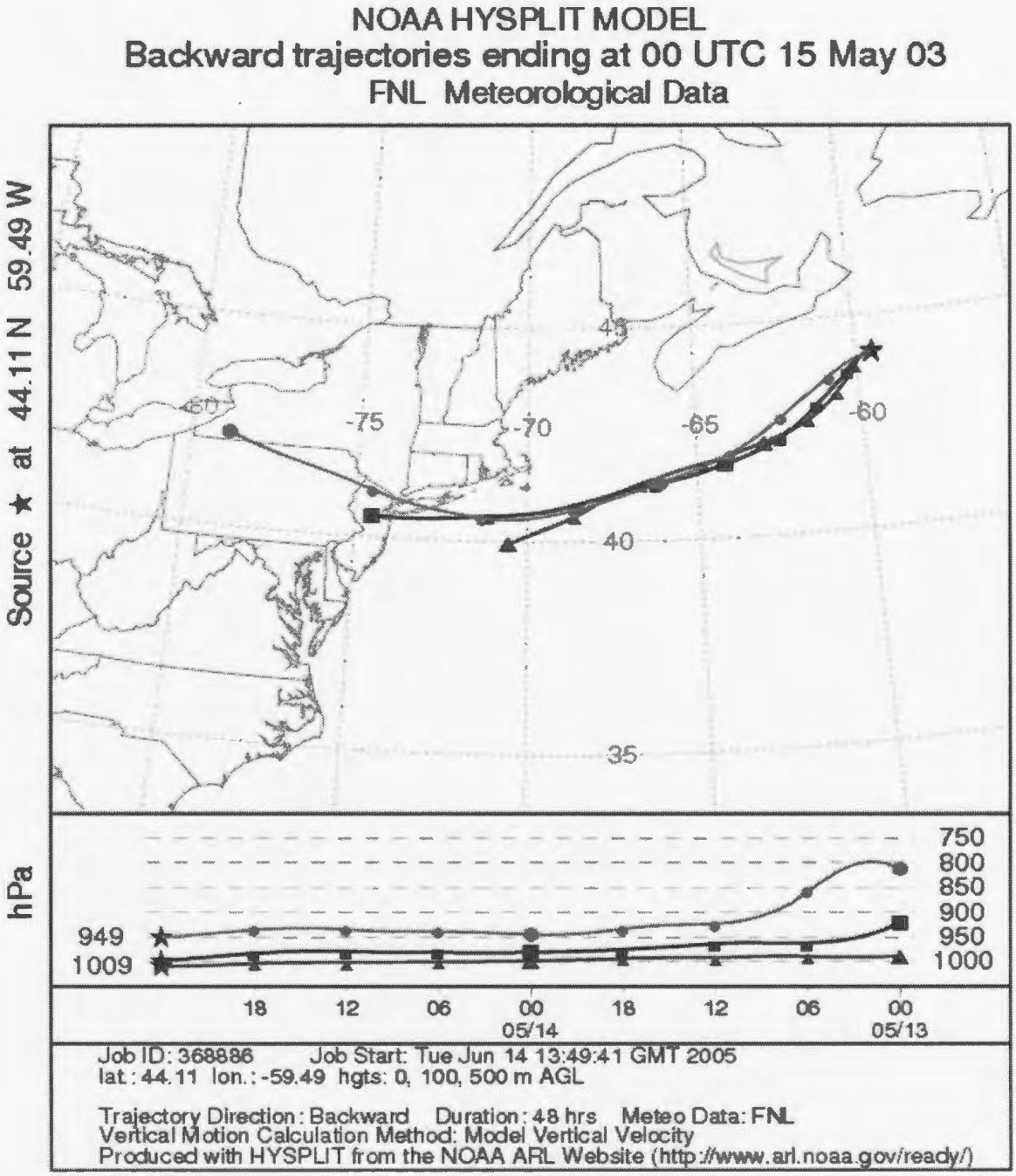

Figure II-20 – Air mass back trajectory for 0m, 100m and 500m above sea level for May 15, 2003. Circles represent 500m asl, squares 100m asl and triangles 0m asl.

Appendix III

Table III-1 – $\delta^{34}S$ (‰) and $\delta^{34}S_{NSS}$ (‰) for total particulate (<10μm) and 100-7.2μm daytime aerosols.

Date	Julian Day (2003)	Size (μm)	$\delta^{34}S$	$\delta^{34}S_{NSS}$
April 25 & 26	115 & 116	<100	+2.8	+0.7
April 27 & 28	117 & 118	<100	+16.9	+15.1
April 29 & 30	119 & 120	<100	+6.1	
May 1 & 2	121 & 122	<100	+9.8	+2.1
3-May	123	<100	+19.6	+10.0
May 4 & 5	124 & 125	<100	+18.4	
6-May	126	<100	+19.4	+10.8
7-May	127	<100	+18.6	
8-May	128	<100	+13.0	+3.3
9-May	129	<100	ND	
10-May	130	<100	+10.6	-9.3
11-May	131	<100	+10.1	-17.7
12-May	132	<100	+14.3	+8.0
13-May	133	<100	+7.8	+4.5
14-May	134	<100	+6.3	-2.3
15-May	135	<100	+4.2	
April 25 & 26	115 & 116	100-7.2	+0.9	
April 27 & 28	117 & 118	100-7.2	+10.6	+1.0
April 29 & 30	119 & 120	100-7.2		
May 1 & 2	121 & 122	100-7.2	+18.3	+14.8
3-May	123	100-7.2	+20.5	
May 4 & 5	124 & 125	100-7.2	+17.2	+7.8
6-May	126	100-7.2	+19.5	
7-May	127	100-7.2	+18.2	+5.0
8-May	128	100-7.2		
9-May	129	100-7.2	+15.8	
10-May	130	100-7.2	+10.0	-5.8
11-May	131	100-7.2		
12-May	132	100-7.2	+11.1	-22.1
13-May	133	100-7.2	+12.6	
14-May	134	100-7.2	+10.5	-5.5
15-May	135	100-7.2	+13.4	+2.9

Note: ND indicates there was no sample.

Table III-2 - $\delta^{34}S$ (‰) and $\delta^{34}S_{NSS}$ (‰) for 7.2-3.0μm and 3.0-1.5μm daytime aerosols.

Date	Julian Day (2003)	Size (μm)	$\delta^{34}S$	$\delta^{34}S_{NSS}$
April 25 & 26	115 & 116	7.2-3.0	+1.2	D
April 27 & 28	117 & 118	7.2-3.0	+16.0	+4.4
April 29 & 30	119 & 120	7.2-3.0	+18.2	+12.4
May 1 & 2	121 & 122	7.2-3.0	+18.6	+11.3
3-May	123	7.2-3.0	+20.7	
May 4 & 5	124 & 125	7.2-3.0	+16.4	+13.7
6-May	126	7.2-3.0	+18.4	+5.4
7-May	127	7.2-3.0	+15.6	+6.0
8-May	128	7.2-3.0		
9-May	129	7.2-3.0	+22.0	+22.7
10-May	130	7.2-3.0	+14.8	-3.4
11-May	131	7.2-3.0		
12-May	132	7.2-3.0	+14.3	
13-May	133	7.2-3.0		
14-May	134	7.2-3.0	+17.6	
15-May	135	7.2-3.0	+11.9	+3.5
April 25 & 26	115 & 116	3.0-1.5	+2.0	D
April 27 & 28	117 & 118	3.0-1.5	+6.5	
April 29 & 30	119 & 120	3.0-1.5	+10.2	
May 1 & 2	121 & 122	3.0-1.5	+14.5	+12.0
3-May	123	3.0-1.5	+19.3	+17.5
May 4 & 5	124 & 125	3.0-1.5		
6-May	126	3.0-1.5	+15.2	+12.0
7-May	127	3.0-1.5	+7.7	
8-May	128	3.0-1.5		
9-May	129	3.0-1.5		
10-May	130	3.0-1.5		
11-May	131	3.0-1.5		
12-May	132	3.0-1.5		
13-May	133	3.0-1.5	+8.9	
14-May	134	3.0-1.5	+14.2	+6.5
15-May	135	3.0-1.5	+10.9	+3.9

Note: D indicates the sample was discarded.

Table III-3 - δ34S (‰) and δ34SNSS (‰) for 1.5-0.95μm and 0.95-0.49μm daytime aerosols.

Date	Julian Day (2003)	Size (μm)	$\delta^{34}S$	$\delta^{34}S_{NSS}$
April 25 & 26	115 & 116	1.5-0.95	+2.6	D
April 27 & 28	117 & 118	1.5-0.95	+10.2	+2.6
April 29 & 30	119 & 120	1.5-0.95	+8.8	+7.7
May 1 & 2	121 & 122	1.5-0.95	+7.1	+6.5
3-May	123	1.5-0.95	+13.9	+12.2
May 4 & 5	124 & 125	1.5-0.95	+6.8	
6-May	126	1.5-0.95	+12.8	+11.0
7-May	127	1.5-0.95	+5.5	-9.4
8-May	128	1.5-0.95		
9-May	129	1.5-0.95	+11.6	
10-May	130	1.5-0.95	+8.4	
11-May	131	1.5-0.95		
12-May	132	1.5-0.95	+11.5	
13-May	133	1.5-0.95	+7.4	
14-May	134	1.5-0.95	+7.5	
15-May	135	1.5-0.95	+9.8	+3.9
April 25 & 26	115 & 116	0.95-0.49	+7.3	D
April 27 & 28	117 & 118	0.95-0.49	+6.0	+3.6
April 29 & 30	119 & 120	0.95-0.49	+3.4	-4.1
May 1 & 2	121 & 122	0.95-0.49	+4.7	+4.6
3-May	123	0.95-0.49	+14.7	
May 4 & 5	124 & 125	0.95-0.49		
6-May	126	0.95-0.49	+9.4	
7-May	127	0.95-0.49	+3.9	-19.1
8-May	128	0.95-0.49	+20.3	
9-May	129	0.95-0.49		
10-May	130	0.95-0.49		
11-May	131	0.95-0.49		
12-May	132	0.95-0.49		
13-May	133	0.95-0.49	+4.3	
14-May	134	0.95-0.49	+5.6	+4.3
15-May	135	0.95-0.49	+5.5	+3.3

Note: D indicates the sample was discarded.

Table III-4 - $\delta^{34}S$ (‰) and $\delta^{34}S_{NSS}$ (‰) for <0.49μm daytime aerosols.

Date	Julian Day (2003)	Size (μm)	$\delta^{34}S$
April 25 & 26	115 & 116	<0.49	+2.7
April 27 & 28	117 & 118	<0.49	+6.5
April 29 & 30	119 & 120	<0.49	+4.2
May 1 & 2	121 & 122	<0.49	+4.7
3-May	123	<0.49	+8.7
May 4 & 5	124 & 125	<0.49	
6-May	126	<0.49	+4.3
7-May	127	<0.49	+3.2
8-May	128	<0.49	+8.1
9-May	129	<0.49	+5.4
10-May	130	<0.49	+4.6
11-May	131	<0.49	+5.1
12-May	132	<0.49	+10.9
13-May	133	<0.49	+3.6
14-May	134	<0.49	+5.2
15-May	135	<0.49	+4.8

Note: D indicates the sample was discarded.

Table III-5 - $\delta^{34}S$ (‰) and $\delta^{34}S_{NSS}$ (‰) for (<10 and <100μm) and 10-7.2μm night-time aerosols.

Date	Julian Day (2003)	Size (um)	$\delta^{34}S$	$\delta^{34}S_{NSS}$
April 26 & 27	116 & 117	<10	+4.0	+1.9
April 28 - 30	118 - 120	<10	+7.3	+2.2
May 1 & 2	121	<10	+20.8	
4-May	124	<10	+17.5	+16.7
5-May	125	<10	+10.3	
6-May	126	<10	ND	
7-May	127	<100	+17.7	+8.5
8-May	128	<100	+9.0	+3.1
9-May	129	<100	+13.4	+3.0
10-May	130	<100	+11.1	
11-May	131	<100		
12-May	132	<100	+17.0	
13-May	133	<100	+12.6	-10.6
14-May	134	<100	+4.4	+2.4
15-May	135	<100	+8.2	+5.6
April 26 & 27	116 & 117	10-7.2	+10.7	+0.2
April 28 - 30	118 - 120	10-7.2	+12.0	+7.8
May 1 & 2	121	10-7.2	+15.3	+11.4
4-May	124	10-7.2		
5-May	125	10-7.2	+19.7	+17.7
6-May	126	10-7.2	+20.6	+20.3
7-May	127	10-7.2	+21.2	+21.3
8-May	128	10-7.2		
9-May	129	10-7.2		
10-May	130	10-7.2	+16.5	+12.2
11-May	131	10-7.2	+18.5	
12-May	132	10-7.2	+21.5	
13-May	133	10-7.2	+18.5	
14-May	134	10-7.2	+12.1	
15-May	135	10-7.2	+11.9	+2.1

Note: ND indicates there was no sample.

Table III-6 - $\delta^{34}S$ (‰) and $\delta^{34}S_{NSS}$ (‰) for 7.2-3.0μm and 3.0-1.5μm night-time aerosols.

Date	Julian Day (2003)	Size (μm)	$\delta^{34}S$
April 26 & 27	116 & 117	7.2-3.0	+9.3
April 28 - 30	118 - 120	7.2-3.0	+15.7
May 1 & 2	121	7.2-3.0	+15.8
4-May	124	7.2-3.0	+21.5
5-May	125	7.2-3.0	+19.8
6-May	126	7.2-3.0	+21.7
7-May	127	7.2-3.0	+21.1
8-May	128	7.2-3.0	+19.8
9-May	129	7.2-3.0	+23.1
10-May	130	7.2-3.0	+18.9
11-May	131	7.2-3.0	+23.2
12-May	132	7.2-3.0	+21.1
13-May	133	7.2-3.0	+16.5
14-May	134	7.2-3.0	+3.8
15-May	135	7.2-3.0	+11.7
April 26 & 27	116 & 117	3.0-1.5	+9.8
April 28 - 30	118 - 120	3.0-1.5	+12.4
May 1 & 2	121	3.0-1.5	+11.8
4-May	124	3.0-1.5	+19.6
5-May	125	3.0-1.5	+17.1
6-May	126	3.0-1.5	+20.0
7-May	127	3.0-1.5	+19.0
8-May	128	3.0-1.5	+13.5
9-May	129	3.0-1.5	
10-May	130	3.0-1.5	+13.5
11-May	131	3.0-1.5	+19.8
12-May	132	3.0-1.5	+14.9
13-May	133	3.0-1.5	+10.4
14-May	134	3.0-1.5	+12.7
15-May	135	3.0-1.5	+6.9

Table III-7 - $\delta^{34}S$ (‰) and $\delta^{34}S_{NSS}$ (‰) for 1.5-0.95μm and 0.95-0.49μm night-time aerosols.

Date	Julian Day (2003)	Size (μm)	$\delta^{34}S$	$\delta^{34}S_{NSS}$
April 26 & 27	116 & 117	1.5-0.95	+6.9	+3.4
April 28 - 30	118 - 120	1.5-0.95	+7.2	+6.5
May 1 & 2	121	1.5-0.95	+6.2	+5.5
4-May	124	1.5-0.95	+20.8	+20.6
5-May	125	1.5-0.95	+15.9	
6-May	126	1.5-0.95	+13.4	
7-May	127	1.5-0.95	+14.4	+9.4
8-May	128	1.5-0.95	+17.5	
9-May	129	1.5-0.95	+13.7	+11.0
10-May	130	1.5-0.95	+11.0	+8.1
11-May	131	1.5-0.95	+13.6	+10.6
12-May	132	1.5-0.95	+8.3	+1.0
13-May	133	1.5-0.95	+8.1	+5.9
14-May	134	1.5-0.95	+6.0	+4.8
15-May	135	1.5-0.95	+7.8	+3.0
April 26 & 27	116 & 117	0.95-0.49		
April 28 - 30	118 - 120	0.95-0.49	+6.4	+4.9
May 1 & 2	121	0.95-0.49	+5.0	+4.8
4-May	124	0.95-0.49	+20.6	+17.9
5-May	125	0.95-0.49	+17.0	
6-May	126	0.95-0.49		
7-May	127	0.95-0.49	+13.1	
8-May	128	0.95-0.49	+8.4	-4.2
9-May	129	0.95-0.49	+7.3	-13.4
10-May	130	0.95-0.49	+7.4	+5.9
11-May	131	0.95-0.49		
12-May	132	0.95-0.49	+8.6	+6.6
13-May	133	0.95-0.49	+4.9	+4.5
14-May	134	0.95-0.49	+5.8	+4.0
15-May	135	0.95-0.49	+10.5	+7.6

Table III-8 - $\delta^{34}S$ (‰) and $\delta^{34}S_{NSS}$ (‰) for <0.49μm night-time aerosols.

Date	Julian Day (2003)	Size (μm)	$\delta^{34}S$
April 26 & 27	116 & 117	<0.49	+4.7
April 28 - 30	118 - 120	<0.49	+4.5
May 1 & 2	121	<0.49	+4.8
4-May	124	<0.49	+19.8
5-May	125	<0.49	+6.9
6-May	126	<0.49	+21.1
7-May	127	<0.49	+8.5
8-May	128	<0.49	+7.1
9-May	129	<0.49	+5.6
10-May	130	<0.49	+5.6
11-May	131	<0.49	
12-May	132	<0.49	+4.5
13-May	133	<0.49	+4.6
14-May	134	<0.49	+3.8
15-May	135	<0.49	

Table III-9 – Cation concentrations (ngm^{-3}) for total particulate (<100μm) and 100-7.2μm daytime aerosols.

Date	Size (um)	Na^+	NH_4^+	K^+	Mg^{2+}	Ca^{2+}
April 25 & 26	<100			13.8	35	139
April 27 & 28	<100	927		48.7	110	181
April 29 & 30	<100					
May 1 & 2	<100	5180	262	231	765	520
3-May	<100	51000		1760	6020	2180
May 4 & 5	<100	7890		336	1090	439
6-May	<100	14600	52.3	587	2111	861
7-May	<100	7240	32.6	1730	990	456
8-May	<100	1740		96.6	122	187
9-May	<100		82.1	66.5	40.5	
10-May	<100	2820	79.8	108	520	332
11-May	<100	2630		516	396	193
12-May	<100	1320		103	170	272
13-May	<100	1110	6.20	62.0	136	160
14-May	<100	304			76.9	
15-May	<100				47.1	
April 25 & 26	100-7.2	D	D	D	D	D
April 27 & 28	100-7.2	242		10.0	29.3	
April 29 & 30	100-7.2	696	60.9	64.1	35.1	
May 1 & 2	100-7.2	1260	20.6	660	153	47.8
3-May	100-7.2	2610		304	1220	391
May 4 & 5	100-7.2	1470	12.9	69.8	122	
6-May	100-7.2	1430		119	436	119
7-May	100-7.2	3340		108	354	89.4
8-May	100-7.2	613	17.8	32.7	12.9	
9-May	100-7.2	649	8.57	26.2		
10-May	100-7.2	436			32.2	80.1
11-May	100-7.2	434	2.97		28.6	84.1
12-May	100-7.2	549			40.0	
13-May	100-7.2	232			30.9	
14-May	100-7.2	744			59.0	158
15-May	100-7.2	222	10.4		63.5	181

Note: D indicates the sample was discarded.

Table III-10 – Cation concentrations (ngm^{-3}) for 7.2-3.0μm and 3.0-1.5μm daytime aerosols.

Date	Size (um)	Na^+	NH_4^+	K^+	Mg^{2+}	Ca^{2+}
April 25 & 26	7.2-3.0	D	D	D	D	D
April 27 & 28	7.2-3.0	460		10.3	51.2	46.6
April 29 & 30	7.2-3.0	935	6.90	58.2	68.9	
May 1 & 2	7.2-3.0	1120	3.26	45.0	120	
3-May	7.2-3.0	4510		1090	558	191
May 4 & 5	7.2-3.0	635	8.63	28.1	22.7	
6-May	7.2-3.0	2510	12.2	84.5	261	56
7-May	7.2-3.0	1480	8.83	55.6	143	
8-May	7.2-3.0	745	19.1	37.6	16	
9-May	7.2-3.0		8.31	61.9	7.92	
10-May	7.2-3.0	685		4.99	57.0	70.1
11-May	7.2-3.0	384			27.2	95.0
12-May	7.2-3.0	507	3.26		42.8	88.4
13-May	7.2-3.0	191			23.7	
14-May	7.2-3.0	285	3.45		38.3	
15-May	7.2-3.0	211	4.70		43.9	112
April 25 & 26	3.0-1.5	D	D	D	D	D
April 27 & 28	3.0-1.5			4.86	5.89	
April 29 & 30	3.0-1.5	170	10.3	11.9		
May 1 & 2	3.0-1.5	894	15.9		30.9	61.4
3-May	3.0-1.5	1640	30.8	72.0	75.6	
May 4 & 5	3.0-1.5	145	3.34	15.5		
6-May	3.0-1.5	792	14.5	48.3	42.0	
7-May	3.0-1.5	428	20.7	25.2		
8-May	3.0-1.5	376		10.8	10.1	
9-May	3.0-1.5	469	14.8	23.9		
10-May	3.0-1.5	278			18.3	66.7
11-May	3.0-1.5	387			31.8	94.3
12-May	3.0-1.5	385	6.73		29.5	82.2
13-May	3.0-1.5				12.2	
14-May	3.0-1.5	363			56.8	
15-May	3.0-1.5				45.4	155

Note: D indicates the sample was discarded.

Table III-11 – Cation concentrations (ngm^{-3}) for 1.5-0.95 μm and 0.95-0.49μm daytime aerosols.

Date	Size (um)	Na^+	NH_4^+	K^+	Mg^{2+}	Ca^{2+}
April 25 & 26	1.5-0.95	D	D	D	D	D
April 27 & 28	1.5-0.95	152		7.65	22.4	38.1
April 29 & 30	1.5-0.95	391	20.5	32.3	6.07	
May 1 & 2	1.5-0.95	566	3.73	25.6	6.53	
3-May	1.5-0.95	707	10.8	142	19.7	
May 4 & 5	1.5-0.95	145	18.0	15.7		
6-May	1.5-0.95	621	23.3	31.0	20.3	
7-May	1.5-0.95	350	13.3	18.7		
8-May	1.5-0.95	394	5.66	18.7		
9-May	1.5-0.95	486	20.8	21.8		
10-May	1.5-0.95			17.1	9.31	34.4
11-May	1.5-0.95	419			28.4	95.4
12-May	1.5-0.95	340			21.9	74.2
13-May	1.5-0.95				10.1	
14-May	1.5-0.95				8.71	
15-May	1.5-0.95				47.1	178
April 25 & 26	0.95-0.49	D	D	D	D	D
April 27 & 28	0.95-0.49			9.9	9.49	
April 29 & 30	0.95-0.49	368	15.7	25.8		
May 1 & 2	0.95-0.49	509	47.8	59.3	4.85	
3-May	0.95-0.49	2160		77.0	180	
May 4 & 5	0.95-0.49	217	22.5	16.2		
6-May	0.95-0.49	514	21.6	29.7		
7-May	0.95-0.49	360	12.4	14.3		
8-May	0.95-0.49	365	17.8	22.2		
9-May	0.95-0.49	417	20.6	17.7		
10-May	0.95-0.49				10.4	
11-May	0.95-0.49	483			28.4	106
12-May	0.95-0.49	305			16.1	73
13-May	0.95-0.49		14.9		9.87	
14-May	0.95-0.49	333	22.7		17.4	132
15-May	0.95-0.49		38.4		30.9	101

Note: D indicates the sample was discarded.

Table III-12 – Cation concentrations (ngm^{-3}) for <0.49μm daytime aerosols.

Date	Size (um)	Na^+	NH_4^+	K^+	Mg^{2+}	Ca^{2+}
April 25 & 26	<0.49	D	D	D	D	D
April 27 & 28	<0.49			14	10.8	
April 29 & 30	<0.49		198	12	19.4	201
May 1 & 2	<0.49	680	370		22.6	220
3-May	<0.49		75.4		46.7	
May 4 & 5	<0.49		23.0		17.5	
6-May	<0.49		50.2		48.8	172
7-May	<0.49	775	42.7		37.5	
8-May	<0.49	808	8.75		40.1	
9-May	<0.49	679		488	32.5	146
10-May	<0.49	434			20.5	
11-May	<0.49				41.1	161
12-May	<0.49	834			61.9	
13-May	<0.49		41.5	276	63.2	255
14-May	<0.49		87.1	70	100	507
15-May	<0.49		24.7	565	34.6	196

Note: D indicates the sample was discarded.

Table III-12 – Cation concentrations (ngm^{-3}) for total particulate (<10 and <100μm) and 10-7.2μm night-time aerosols.

Date	Size (um)	Na^+	NH_4^+	K^+	Mg^{2+}	Ca^{2+}
April 26 & 27	<10		37.1	43.7	47.2	142
April 28 - 30	<10	1650	82.9	324	280	371
May 1 & 2	<10	451000		17100	32600	15800
4-May	<10	538000		121000	2540	6000
5-May	<10	72400		28300	95.9	
6-May	ND	ND	ND	ND	ND	ND
7-May	<100	1130	165	173	184.4	318
8-May	<100	666	102	49.3	129.8	292
9-May	<100	1390		601	308.4	283
10-May	<100	1840		334	204.0	
11-May	<100	1930		66.9	186.0	184
12-May	<100			34.1	47.7	
13-May	<100	13500	328	620	2149	531
14-May	<100	1210	270	54.7	207	502
15-May	<100	1320		70.2	132	242
April 26 & 27	10-7.2		4.80		23.1	87
April 28 - 30	10-7.2	267	21.6	8.12	12.4	
May 1 & 2	10-7.2	1020	16.2	33.6	39.2	
4-May	10-7.2	1260		147	437	126
5-May	10-7.2	3220	15.9	125	201	113
6-May	10-7.2	896	25.9	45.2	28.3	
7-May	10-7.2	694	3.31	30.7	25.2	
8-May	10-7.2	452	22.2	26.0		
9-May	10-7.2	416		18.4		
10-May	10-7.2	466	8.53		32.5	
11-May	10-7.2	284		7.06	11.4	
12-May	10-7.2		30.7	10.4		
13-May	10-7.2		12.4		17.1	
14-May	10-7.2		3.31		13.6	
15-May	10-7.2	576			62.4	216

Note: ND indicates there was no sample.

Table III-13 – Cation concentrations (ngm^{-3}) for 7.2-3.0μm and 3.0-1.5μm night-time aerosols.

Date	Size (um)	Na^+	NH_4^+	K^+	Mg^{2+}	Ca^{2+}
April 26 & 27	7.2-3.0		8.73		25.5	88.2
April 28 - 30	7.2-3.0	426	15.1	17.8	21.1	
May 1 & 2	7.2-3.0	1360	20.9	44.1	73.3	52.6
4-May	7.2-3.0	2610	16.4	54.2	100	
5-May	7.2-3.0	4400		264	343.4	150
6-May	7.2-3.0	1130	5.66	49.6	48.7	
7-May	7.2-3.0	1150		45.4	65.3	
8-May	7.2-3.0	653	11.7	37.6	19.9	
9-May	7.2-3.0	811	3.09	37.7	31.1	
10-May	7.2-3.0	11200		32.5	115	49.9
11-May	7.2-3.0	437			26.7	
12-May	7.2-3.0				29.1	
13-May	7.2-3.0	305			50.6	
14-May	7.2-3.0	213			34.2	
15-May	7.2-3.0	1350		22.1	122	263
April 26 & 27	3.0-1.5		3.86		29.6	122
April 28 - 30	3.0-1.5	270	15.5	14.2	13.5	31.4
May 1 & 2	3.0-1.5	734	11.3	32.9	24.2	
4-May	3.0-1.5	1800	21.9	76.5	117.3	73.2
5-May	3.0-1.5	1670	30.9	68.6	62.5	
6-May	3.0-1.5	586	6.56	38.4	11.8	
7-May	3.0-1.5	630		42.6	16.4	
8-May	3.0-1.5	366	27.1	23.2	52.6	171
9-May	3.0-1.5	381	15.1	31.2		
10-May	3.0-1.5	378			21.0	
11-May	3.0-1.5	337			14.1	
12-May	3.0-1.5		7.28		16.6	
13-May	3.0-1.5		12.9		12.1	
14-May	3.0-1.5			79.5	34.3	
15-May	3.0-1.5	703			64.5	180

Table III-14 – Cation concentrations (ngm^{-3}) for 1.5-0.95μm and 0.95-0.49μm night-time aerosols.

Date	Size (um)	Na^+	NH_4^+	K^+	Mg^{2+}	Ca^{2+}
April 26 & 27	1.5-0.95		10.8		25.9	109
April 28 - 30	1.5-0.95	295	19.8	15.9	3.47	
May 1 & 2	1.5-0.95	582	25.5	36.0	14.1	
4-May	1.5-0.95	879		36.8	34.0	
5-May	1.5-0.95	1020	38.0	52.8		
6-May	1.5-0.95	470	29.3	29.1		
7-May	1.5-0.95	446	25.9	34.9	65.6	183
8-May	1.5-0.95	324	23.2	20.4		
9-May	1.5-0.95	372	6.84	27.4	11.6	
10-May	1.5-0.95	298	5.74		10.3	
11-May	1.5-0.95	256			7.32	
12-May	1.5-0.95		6.18		15.0	
13-May	1.5-0.95		19.1		29.1	70.0
14-May	1.5-0.95		9.93		10.7	
15-May	1.5-0.95	592			41.3	160
April 26 & 27	0.95-0.49		7.93	6.48	5.82	39.1
April 28 - 30	0.95-0.49	325	20	16.7	11.7	27.9
May 1 & 2	0.95-0.49	730	126124		12.8	42.8
4-May	0.95-0.49	4550		159	479.8	195
5-May	0.95-0.49	914	68.0	39.9		
6-May	0.95-0.49	363	42.7	19.8		
7-May	0.95-0.49	508	3.64	22.6		
8-May	0.95-0.49	460	30.8	32.8		
9-May	0.95-0.49	412	21.3	24.5		
10-May	0.95-0.49	332	7.36		13.2	
11-May	0.95-0.49	206		8.83	6.81	
12-May	0.95-0.49		11.7		14.3	
13-May	0.95-0.49		124		11.8	
14-May	0.95-0.49		74.4		44.0	194
15-May	0.95-0.49	396	18.9		46.1	216

Table III-15 – Cation concentrations (ngm^{-3}) for 1.5-0.95μm and 0.95-0.49μm night-time aerosols.

Date	Size (um)	Na^+	NH_4^+	K^+	Mg^{2+}	Ca^{2+}
April 26 & 27	<0.49		16.3		35.3	180
April 28 - 30	<0.49	349	23.7		23.4	82.1
May 1 & 2	<0.49		785	23.3	53.9	332
4-May	<0.49	462000		1540	5340	2183
5-May	<0.49	1400		400	122	199
6-May	<0.49	771	95.1		80.9	168
7-May	<0.49	675	28.0	1580	21.8	
8-May	<0.49		89.2		27.0	111
9-May	<0.49		107	28.0		
10-May	<0.49		91.4			
11-May	<0.49			357		
12-May	<0.49		15.3		35.9	
13-May	<0.49		25.1		44.4	
14-May	<0.49		122		78.2	330
15-May	<0.49		14.6		53.2	

Table III-16 – Anion concentrations (ngm^{-3}) for total particulate (<100μm) and 100-7.2μm daytime aerosols.

Date	Size	SO_4^{2-}	Cl^-	NO_3^-	PO_4^{3-}	MSA
April 25 & 26	<100	707	320	229		19.4
April 27 & 28	<100	737	1690	220		16.1
April 29 & 30	<100					
May 1 & 2	<100	3943	8480	1100		22.9
3-May	<100	14400	93100	794		28.3
May 4 & 5	<100	1440	3040	127		14.4
6-May	<100	4340	6630	399		31.9
7-May	<100	2130	3570	37		4.38
8-May	<100	466	2580			
9-May	<100		610			
10-May	<100	1660	4480	298		28.1
11-May	<100	1160	682			
12-May	<100	745	2560	239		51.3
13-May	<100	1430	1860	328		43.7
14-May	<100	436	1040			9.7
15-May	<100	473	728	106		15.9
April 25 & 26	100-7.2	D	D	D	D	D
April 27 & 28	100-7.2	129	412	11.1		
April 29 & 30	100-7.2	135	930	56.3		
May 1 & 2	100-7.2	573	4890	224		
3-May	100-7.2	1630	19600	63.0		
May 4 & 5	100-7.2	360	2430			
6-May	100-7.2	952	7370	16.9		
7-May	100-7.2	901	5930	115.0		
8-May	100-7.2	89.6	1060			
9-May	100-7.2	36.4	1037	27.3		
10-May	100-7.2	114	474		22.6	
11-May	100-7.2	73.8	404		9.7	
12-May	100-7.2	109	605	90.9	9.83	1.16
13-May	100-7.2	95.8	456	38.1		2.67
14-May	100-7.2	205	717	237	16.1	
15-May	100-7.2	230	501	58.2		

Table III-17 – Anion concentrations (ngm^{-3}) for 7.2-3.0μm and 3.0-1.5μm daytime aerosols.

Date	Size	SO_4^{2-}	Cl^-	NO_3^-	PO_4^{3-}	MSA
April 25 & 26	7.2-3.0	D	D	D	D	D
April 27 & 28	7.2-3.0	154	703	73.4		0.74
April 29 & 30	7.2-3.0	213	1590	273		0.92
May 1 & 2	7.2-3.0	333	2340	452		
3-May	7.2-3.0	1170	29600	244		
May 4 & 5	7.2-3.0	130	1060	11.6		
6-May	7.2-3.0	657	4640	107		1.08
7-May	7.2-3.0	469	2540	123		
8-May	7.2-3.0	105	1090	565		
9-May	7.2-3.0	37.8	540	77.4		
10-May	7.2-3.0	160	899	34.8	21.9	
11-May	7.2-3.0	55.0	347		10.7	
12-May	7.2-3.0	104	653	28.1	10.1	1.26
13-May	7.2-3.0	145	364	130		0.23
14-May	7.2-3.0	144	581	291		
15-May	7.2-3.0	192	391	219		0.28
April 25 & 26	3.0-1.5	D	D	D	D	D
April 27 & 28	3.0-1.5	18.8	18.5			
April 29 & 30	3.0-1.5		251			
May 1 & 2	3.0-1.5	234	1720	1500		0.75
3-May	3.0-1.5	314	2260	171		0.28
May 4 & 5	3.0-1.5	24.2	300			
6-May	3.0-1.5	246	1280	37.4		22.9
7-May	3.0-1.5	142	630	114		
8-May	3.0-1.5		625	42.7		12.2
9-May	3.0-1.5	41.3	666	50.0		
10-May	3.0-1.5	49.8	199	35.4	21.5	
11-May	3.0-1.5	34.2	302		10.4	
12-May	3.0-1.5	60.1	392	24.8	9.8	2.31
13-May	3.0-1.5	49.5	141	30.9		
14-May	3.0-1.5	224	712	393		
15-May	3.0-1.5	233	160	165		1.14

Note: D indicates the sample was discarded.

Table III-18 – Anion concentrations (ngm^{-3}) for 1.5-0.95μm and 0.95-0.49μm daytime aerosols.

Date	Size	SO_4^{2-}	Cl^-	NO_3^-	PO_4^{3-}	MSA
April 25 & 26	1.5-0.95	D	D	D	D	D
April 27 & 28	1.5-0.95	114	230	36.1		1.99
April 29 & 30	1.5-0.95	160	481	168		2.30
May 1 & 2	1.5-0.95	371	691	121		1.59
3-May	1.5-0.95	224	1190	60.8		
May 4 & 5	1.5-0.95	28.8	301			
6-May	1.5-0.95	244	865	17.3		0.86
7-May	1.5-0.95	178	476	85.9		
8-May	1.5-0.95		580	185		1.47
9-May	1.5-0.95	36.1	601	52.8		9.09
10-May	1.5-0.95	28.7	101	48.3		
11-May	1.5-0.95	29.7	301		11	
12-May	1.5-0.95	51.7	245	31.7	10	2.63
13-May	1.5-0.95	201	50.9	16.4		3.37
14-May	1.5-0.95	153	52.1	70.4		
15-May	1.5-0.95	288	120	127		2.99
April 25 & 26	0.95-0.49	D	D	D	D	D
April 27 & 28	0.95-0.49	144	43.0			5.89
April 29 & 30	0.95-0.49	307	338	54.0		2.94
May 1 & 2	0.95-0.49	1113	346	28.4		7.18
3-May	0.95-0.49	747	3720	110		4.69
May 4 & 5	0.95-0.49	24.0	313			
6-May	0.95-0.49	162	713			1.72
7-May	0.95-0.49	157	402	18.9		
8-May	0.95-0.49	25.9	479	833		3.96
9-May	0.95-0.49	100	527	19.9		1.69
10-May	0.95-0.49	88.5	49.7	25.4		0.19
11-May	0.95-0.49	35.5	366	34.7	12.5	
12-May	0.95-0.49	186	205	29.7	12.5	6.62
13-May	0.95-0.49	198	55.6			3.60
14-May	0.95-0.49	468	55.0	45.0	15.1	1.45
15-May	0.95-0.49	510	37.9	53.1		16.4

Note: D indicates the sample was discarded.

Table III-19 – Anion concentrations (ngm^{-3}) for <0.49μm daytime aerosols.

Date	Size	SO_4^{2-}	Cl^-	NO_3^-	PO_4^{3-}	MSA
April 25 & 26	<0.49	D	D	D	D	D
April 27 & 28	<0.49	336				16.3
April 29 & 30	<0.49	1300	71.9	68.9		30.2
May 1 & 2	<0.49	2500	470	121	627	23.4
3-May	<0.49	870	590			12.9
May 4 & 5	<0.49	288	131			
6-May	<0.49	481	549			11.5
7-May	<0.49	938	618	2640	9.17	
8-May	<0.49	376	560	906	28.4	2.41
9-May	<0.49	537	178		31.0	14.2
10-May	<0.49	520	123	39		7.17
11-May	<0.49	192	222	68		2.16
12-May	<0.49	487	1030	75		47.4
13-May	<0.49	1100	200	73		25.7
14-May	<0.49	2460	171	209		19.8
15-May	<0.49	1420	495	365		90.0

Note: D indicates the sample was discarded.

Table III-20 – Anion concentrations (ngm^{-3}) for total particulate (<10 and <100μm) and 10-7.2μm night-time aerosols.

Date	Size	SO_4^{2-}	Cl^-	NO_3^-	PO_4^{3-}	MSA
April 26 & 27	<10	908	294	264		22.7
April 28 - 30	<10	2160	2430	493		25.6
May 1 & 2	<10	53600	804000	700		
4-May	<10	24600	918000			
5-May	<10	4030	132000			
6-May	ND	ND	ND	ND	ND	ND
7-May	<100	382	2010	66.2		1.47
8-May	<100	832	1040	501		26.6
9-May	<100	600	3080	101		
10-May	<100	753	4490			
11-May	<100	921	3120	125		34.3
12-May	<100		1060			1.77
13-May	<100	6150	20100	3020		13.4
14-May	<100	4050	693	2170		47.9
15-May	<100	1660	1770	811		11.8
April 26 & 27	10-7.2	96.2	10.9	20		
April 28 - 30	10-7.2	81.7	363	20		
May 1 & 2	10-7.2	204	1240	92.4		3.7
4-May	10-7.2	939	7550	92.6		
5-May	10-7.2	711	5160	147		32.7
6-May	10-7.2	153	1300	65.6		
7-May	10-7.2	131	1900	15.7		7.95
8-May	10-7.2	110	582	33.5		
9-May	10-7.2		674	16.7		11.8
10-May	10-7.2	140	618	259	461	
11-May	10-7.2		234	479	400	
12-May	10-7.2		129	59.8		
13-May	10-7.2		127	119		
14-May	10-7.2		91.6	112		
15-May	10-7.2	253	460		634	

Note: ND indicates there was no sample.

Table III-21 – Anion concentrations (ngm^{-3}) for 7.2-3.0μm and 3.0-1.5μm night-time aerosols.

Date	Size	SO_4^{2-}	Cl^-	NO_3^-	PO_4^{3-}	MSA
April 26 & 27	7.2-3.0	178	106	118		0.87
April 28 - 30	7.2-3.0	138	549	75.7		1.24
May 1 & 2	7.2-3.0	350	1460	564		0.56
4-May	7.2-3.0	364	2690	204		3.92
5-May	7.2-3.0	889	7120	153		5.08
6-May	7.2-3.0	206	1810	60.7		13.7
7-May	7.2-3.0	230	1030	107		
8-May	7.2-3.0	192	888	205		9.41
9-May	7.2-3.0	129	1310	154		
10-May	7.2-3.0	298	2020	184	417	0.15
11-May	7.2-3.0	58.9	440	276	350	
12-May	7.2-3.0	54.7	390	86.3		0.66
13-May	7.2-3.0	163	423	664		
14-May	7.2-3.0	178	292	461		0.63
15-May	7.2-3.0	575	1500	226	809	8.07
April 26 & 27	3.0-1.5	190		32.8		0.87
April 28 - 30	3.0-1.5	141	304	58.9		1.41
May 1 & 2	3.0-1.5	286	771	330		0.56
4-May	3.0-1.5	399	2935	145		5.89
5-May	3.0-1.5	378	2270	149		9.27
6-May	3.0-1.5	84.2	836	22.6		19.1
7-May	3.0-1.5	114	903	105		1.43
8-May	3.0-1.5	299	557	130		
9-May	3.0-1.5	26.5	621	171		1.77
10-May	3.0-1.5	72.2	327	51.5	477	
11-May	3.0-1.5	37.6	246	468	404	
12-May	3.0-1.5		86	590		1.10
13-May	3.0-1.5	14548.	1	62.9		
14-May	3.0-1.5	121	271	339		
15-May	3.0-1.5	316	641	102	751	6.85

Table III-22 – Anion concentrations (ngm^{-3}) for 1.5-0.95μm and 0.95-0.49μm night-time aerosols.

Date	Size	SO_4^{2-}	Cl^-	NO_3^-	PO_4^{3-}	MSA
April 26 & 27	1.5-0.95	274		35.6		2.55
April 28 - 30	1.5-0.95	169	247	57.7		2.41
May 1 & 2	1.5-0.95	675	435145			1.69
4-May	1.5-0.95	161	1250	113		17.2
5-May	1.5-0.95	245	1550	62.5		10.8
6-May	1.5-0.95	52.7	626	15.5		
7-May	1.5-0.95	319	730	57.8		
8-May	1.5-0.95	87.9	431122			5.00
9-May	1.5-0.95	89.2	512299			6.18
10-May	1.5-0.95	98.3	198	1930	452	0.44
11-May	1.5-0.95	52.8	133207		375	3.66
12-May	1.5-0.95	86.1	31.8	391		7.73
13-May	1.5-0.95	415	69.0	283		
14-May	1.5-0.95	311	49.0	88.4		1.26
15-May	1.5-0.95	324	307	75.3	804	14.8
April 26 & 27	0.95-0.49	34.1		12.9		
April 28 - 30	0.95-0.49	253	342	71.8		3.83
May 1 & 2	0.95-0.49	2220	224	57.1		6.66
4-May	0.95-0.49	1170	8130	143		
5-May	0.95-0.49	81.0	1170	132		
6-May	0.95-0.49	60.1	401	20.9		0.91
7-May	0.95-0.49	171	641	26.7		1.55
8-May	0.95-0.49	229	546	20.6		6.16
9-May	0.95-0.49	171	47348			2.32
10-May	0.95-0.49	277	167642		620	5.74
11-May	0.95-0.49		14614		388	
12-May	0.95-0.49	219		57.6		19.4
13-May	0.95-0.49	1010	45.1	50.4		5.62
14-May	0.95-0.49	885	37.2	91.8		7.41
15-May	0.95-0.49	451	37.6	60.1	654	26.9

Table III-23 – Anion concentrations (ngm^{-3}) for <0.49μm night-time aerosols.

Date	Size	SO_4^{2-}	Cl^-	NO_3^-	PO_4^{3-}	MSA
April 26 & 27	<0.49	559		105		18.6
April 28 - 30	<0.49	565	52.3	74.6		8.32
May 1 & 2	<0.49	3000	340	227		15.6
4-May	<0.49	12200	93300	306		
5-May	<0.49	1110	1390	77.1		4.12
6-May	<0.49	110	1353	56.7		
7-May	<0.49	649	509	45.6		9.12
8-May	<0.49	367	164	52.0		10.8
9-May	<0.49	358	125	839		2.06
10-May	<0.49	220	142	1510		10.6
11-May	<0.49	364	290	648		24.2
12-May	<0.49	271	199	412		107
13-May	<0.49	1510	320	187		4.82
14-May	<0.49	2060	197	198		34.9
15-May	<0.49	427		556		19.1

Appendix III.2

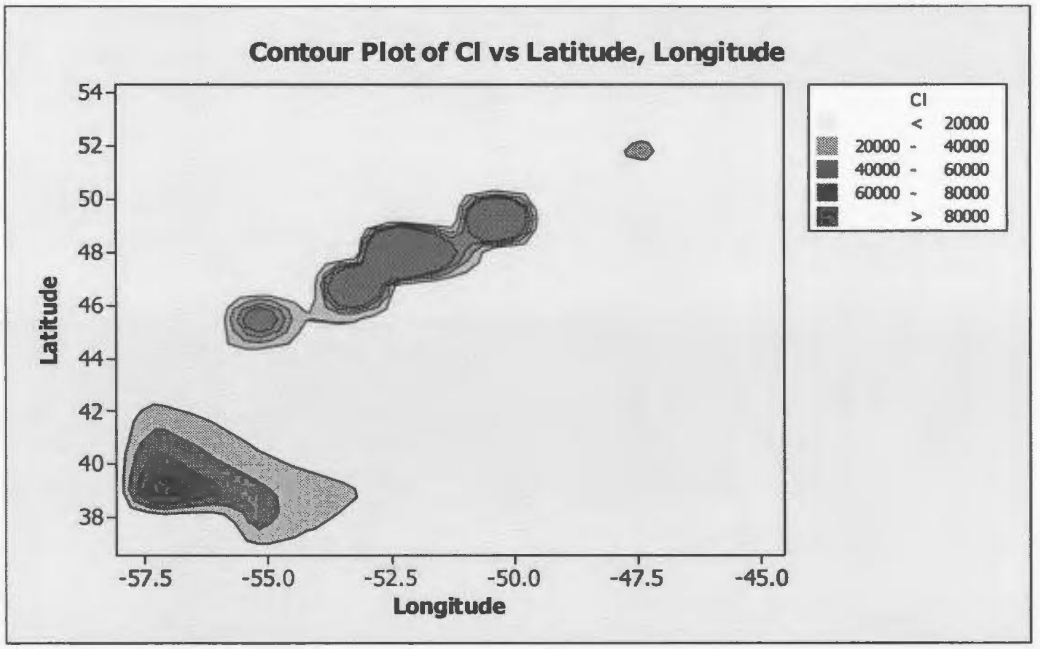

Figure III-1 – Contour plot of Cl^- concentrations (ngm^{-3}) for daytime total particulate (<100μm) Transect samples.

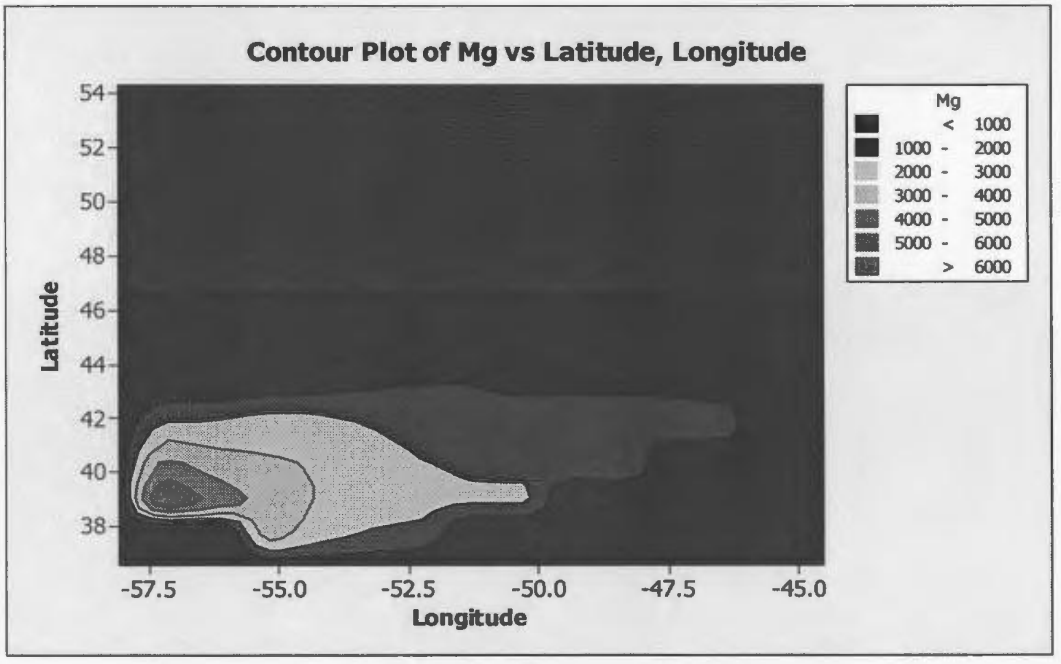

Figure III-2 – Contour plot of Mg^{2+} concentrations (ngm^{-3}) for daytime total particulate (<100μm) Transect samples.

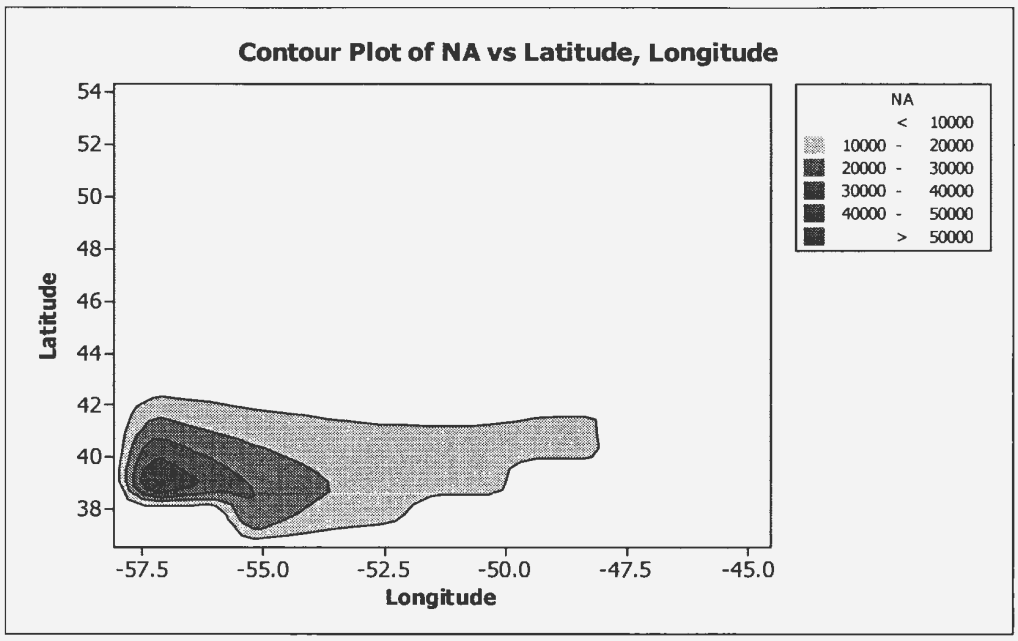

Figure III-3 – Contour plot of Na^{+} concentrations (ngm^{-3}) for daytime total particulate (<100μm) Transect samples.

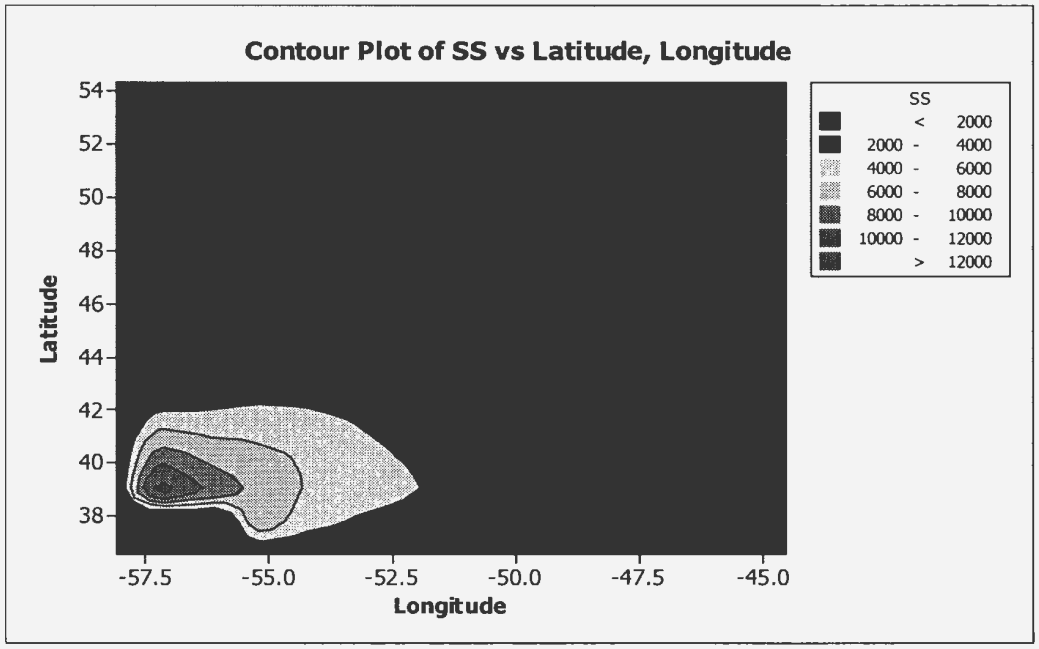

Figure III-4 – Contour plot of $SS\text{-}SO_4^{2-}$ concentrations (ngm^{-3}) for daytime total particulate (<100μm) Transect samples.

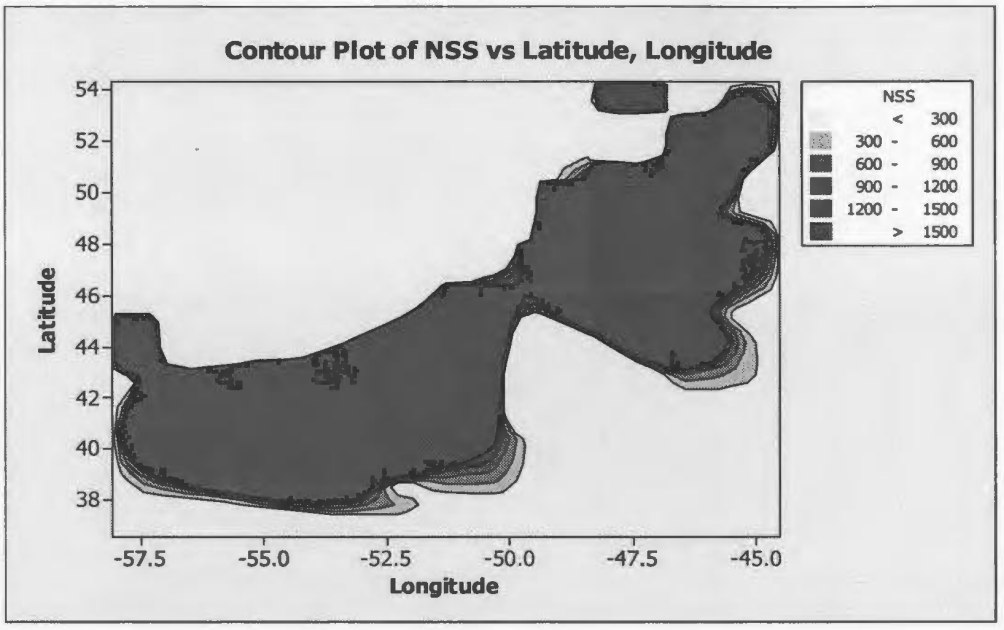

Figure III-5 – Contour plot of NSS-SO_4^{2-} concentrations (ngm^{-3}) for daytime total particulate (<100μm) Transect samples.

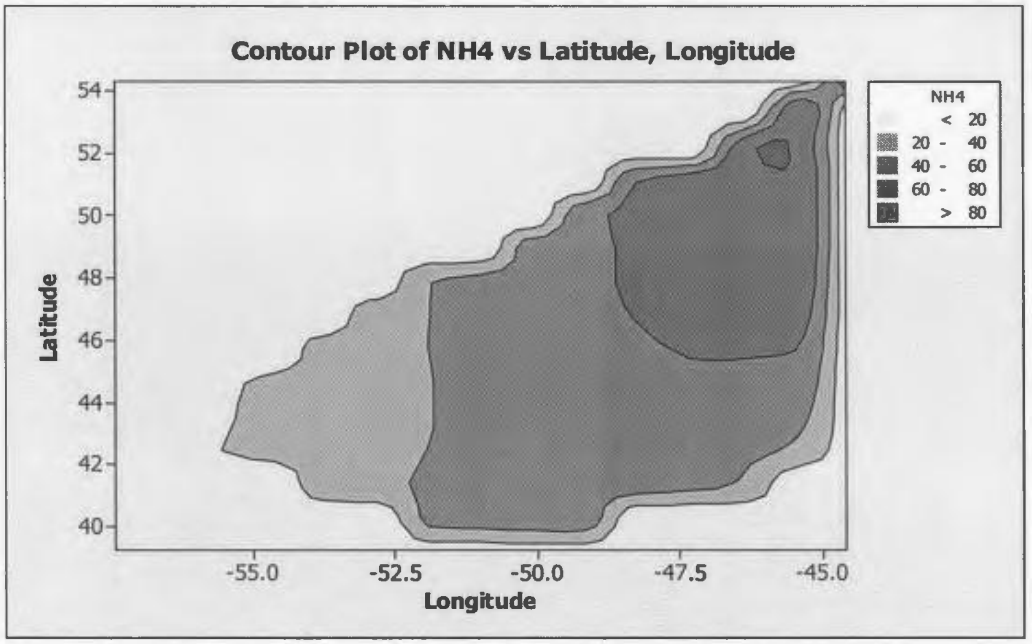

Figure III-6 – Contour plot of NH_4^+ concentrations (ngm^{-3}) for daytime total particulate (<100μm) Transect samples.

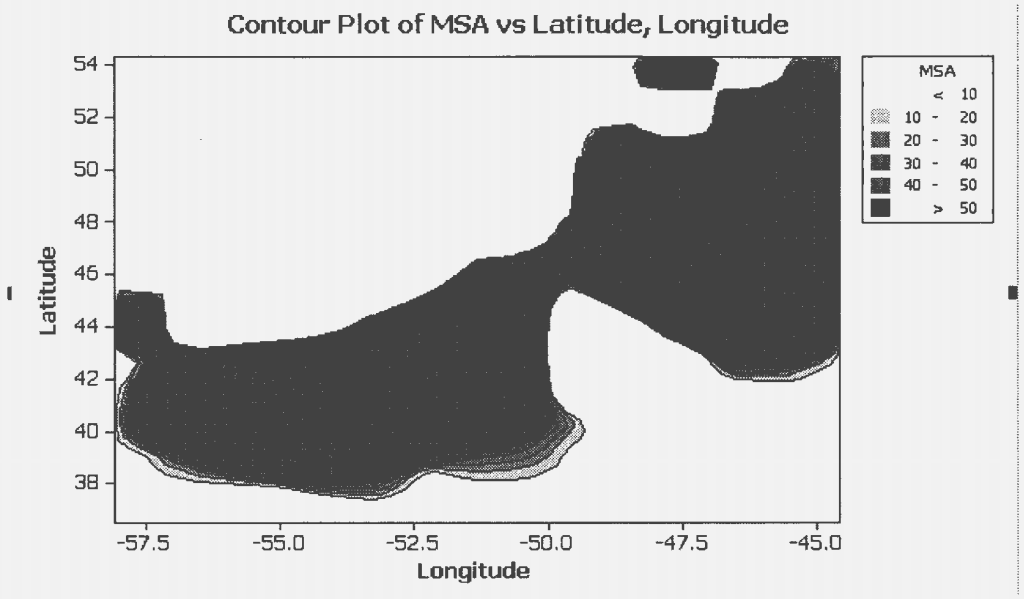

Figure III-7 – Contour plot of MSA concentrations (ngm^{-3}) for daytime total particulate (<100μm) Transect samples.

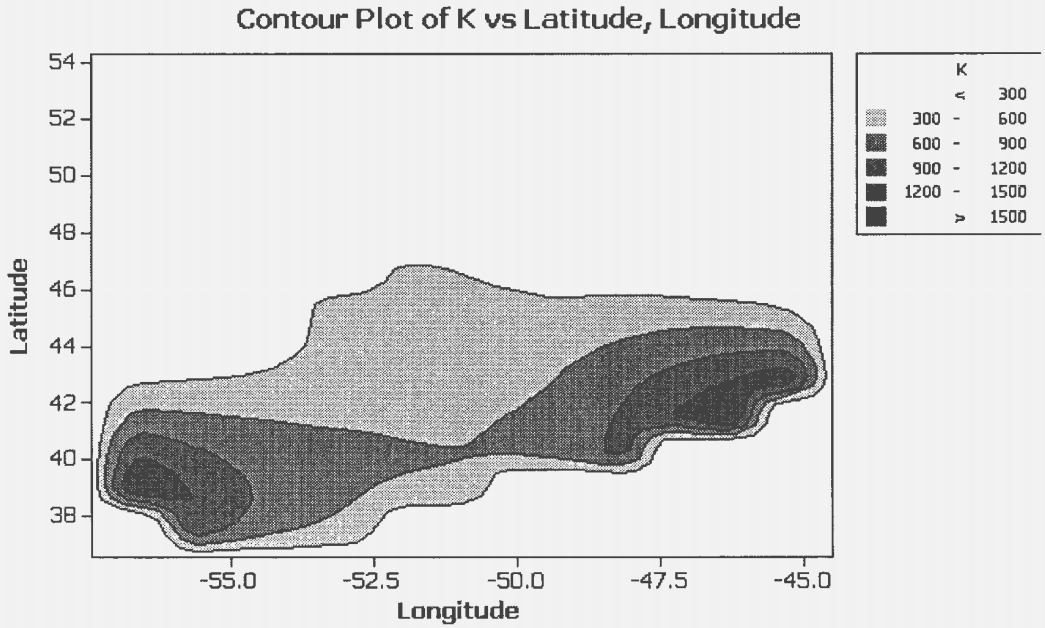

Figure III-8 – Contour plot of K^+ concentrations (ngm^{-3}) for daytime total particulate (<100μm) Transect samples.

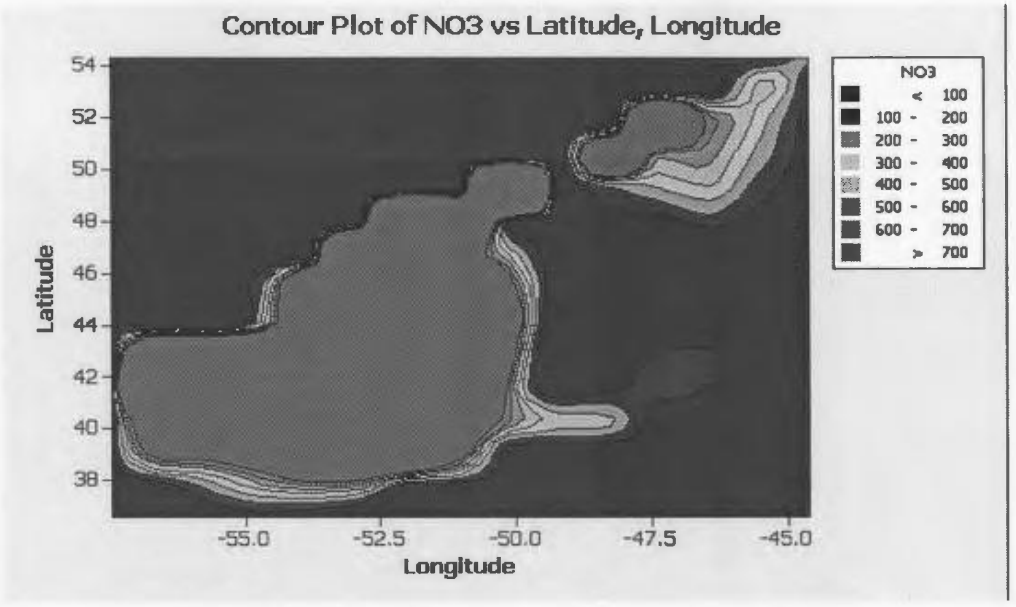

Figure III-9 – Contour plot of NO_3^- concentrations (ngm^{-3}) for daytime total particulate (<100μm) Transect samples.

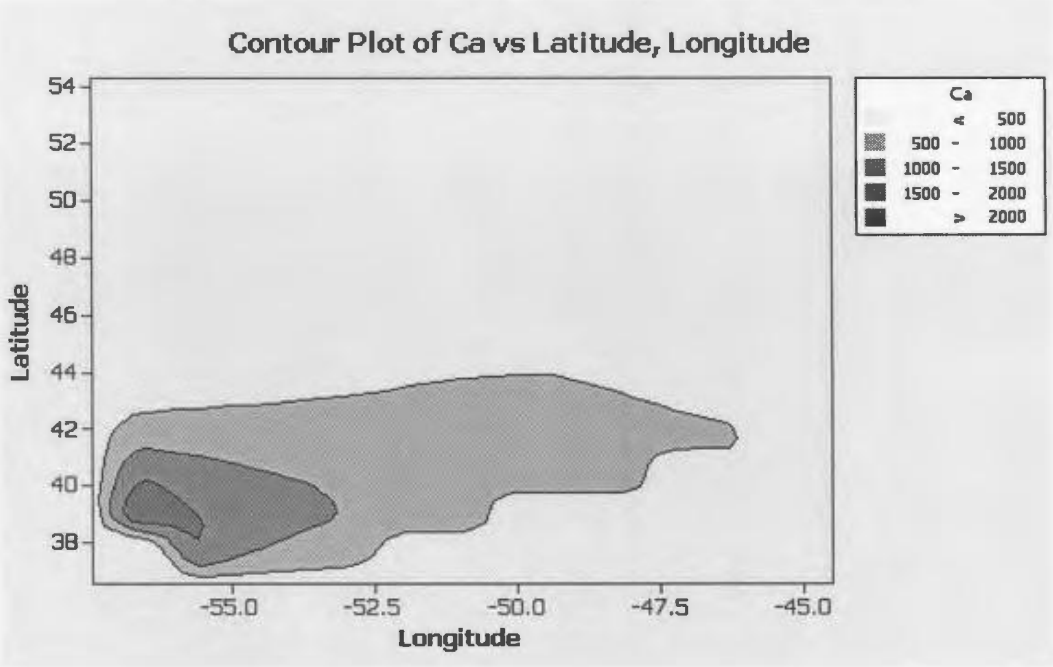

Figure III-10 – Contour plot of Ca^{2+} concentrations (ngm^{-3}) for daytime total particulate (<100μm) Transect samples.

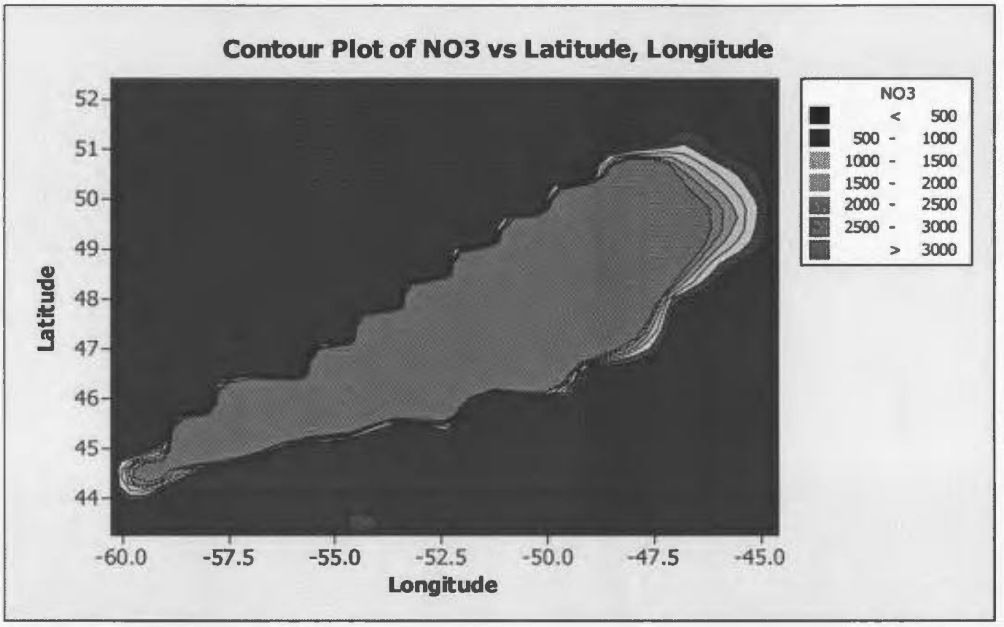

Figure III-11 – Contour plot of NO_3^{2-} concentrations (ngm^{-3}) for night-time total particulate (<100μm) Transect samples.

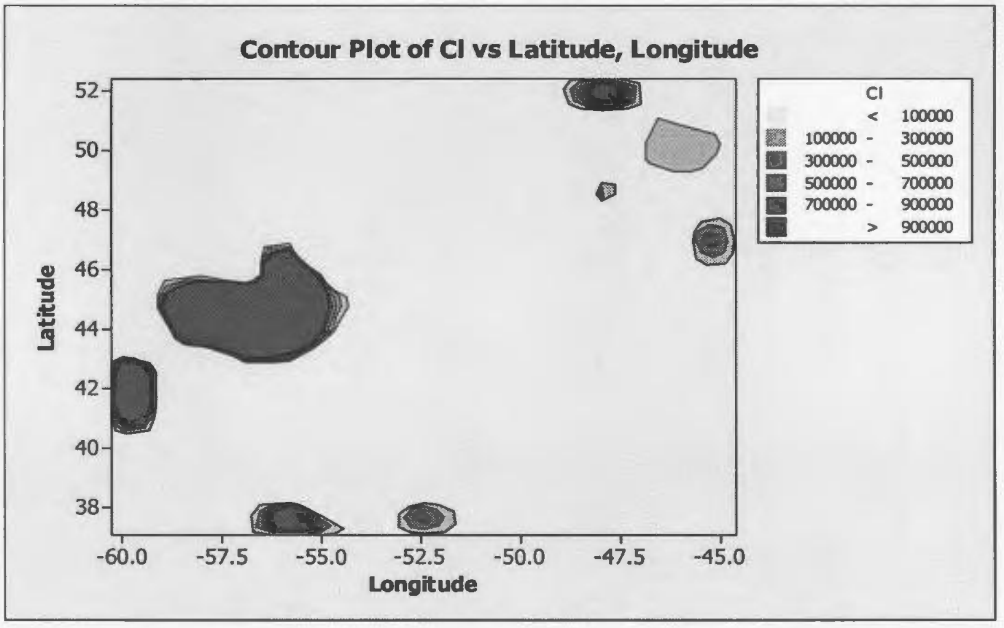

Figure III-12– Contour plot of Cl^- concentrations (ngm^{-3}) for night-time total particulate (<100μm) Transect samples.

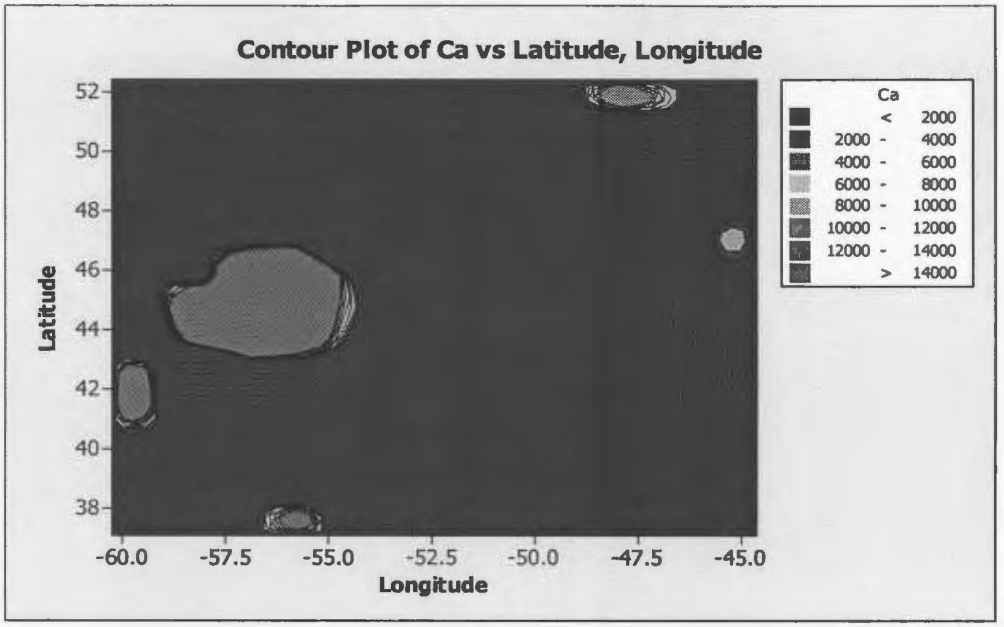

Figure III-13 – Contour plot of Ca^{2+} concentrations (ngm^{-3}) for night-time total particulate (<100μm) Transect samples.

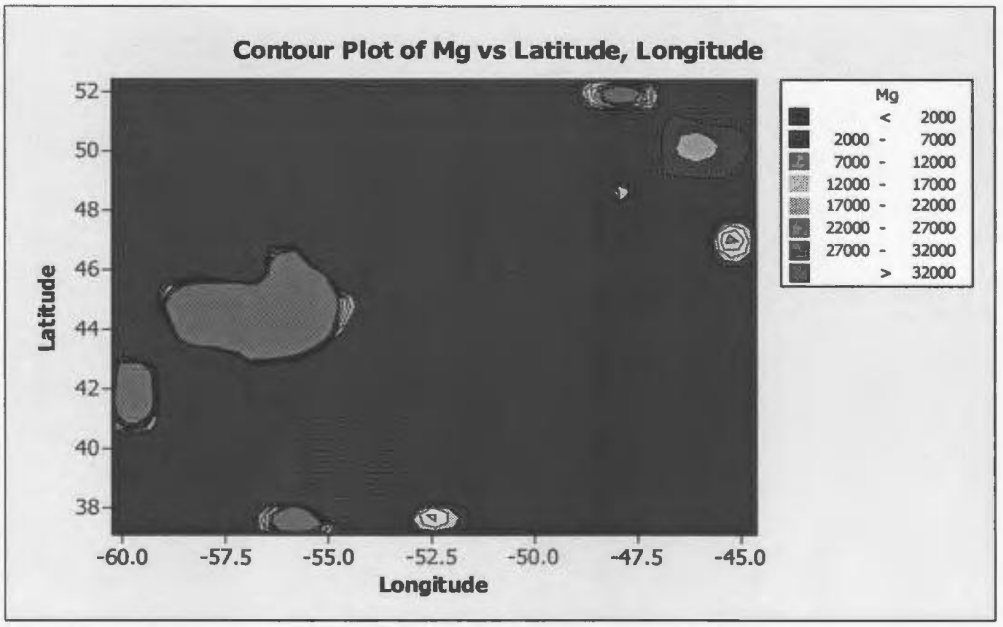

Figure III-14 – Contour plot of Mg^{2+} concentrations (ngm^{-3}) for night-time total particulate (<100μm) Transect samples.

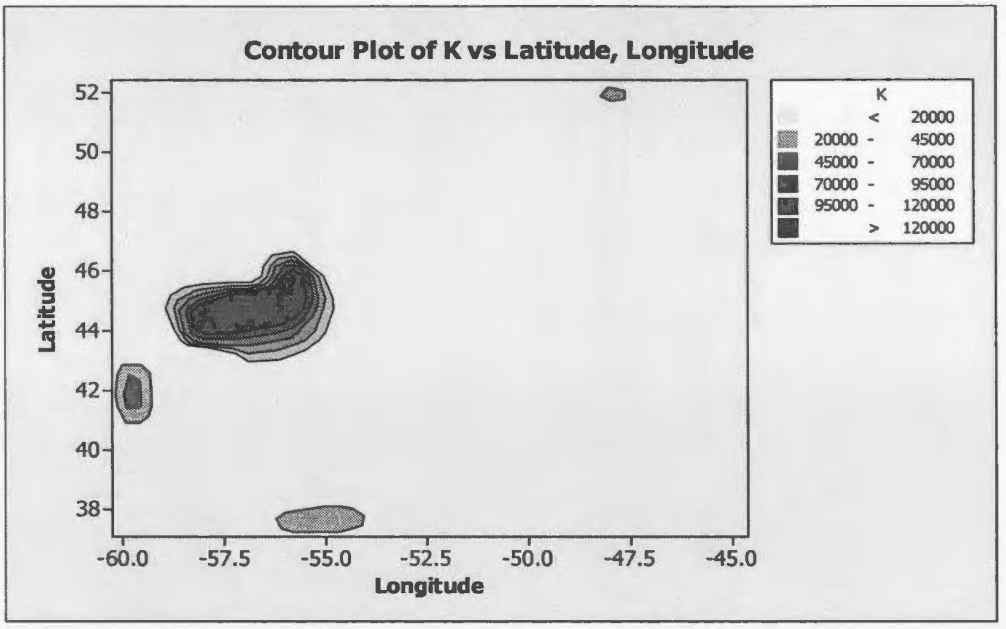

Figure III-15 – Contour plot of K^+ concentrations (ngm^{-3}) for night-time total particulate (<100μm) Transect samples.

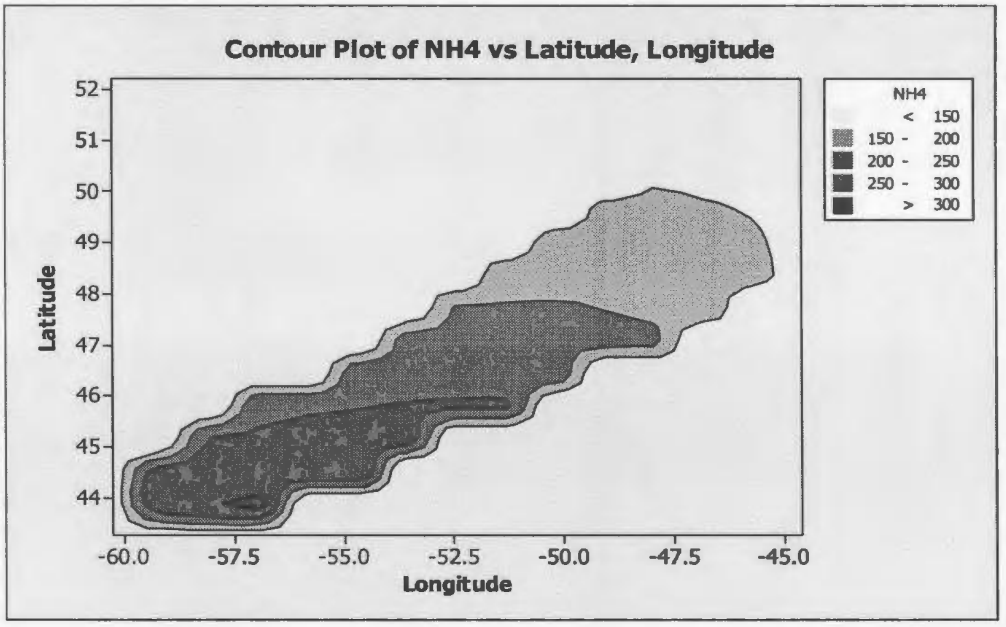

Figure III-16 – Contour plot of NH_4^+ concentrations (ngm^{-3}) for night-time total particulate (<100μm) Transect samples.

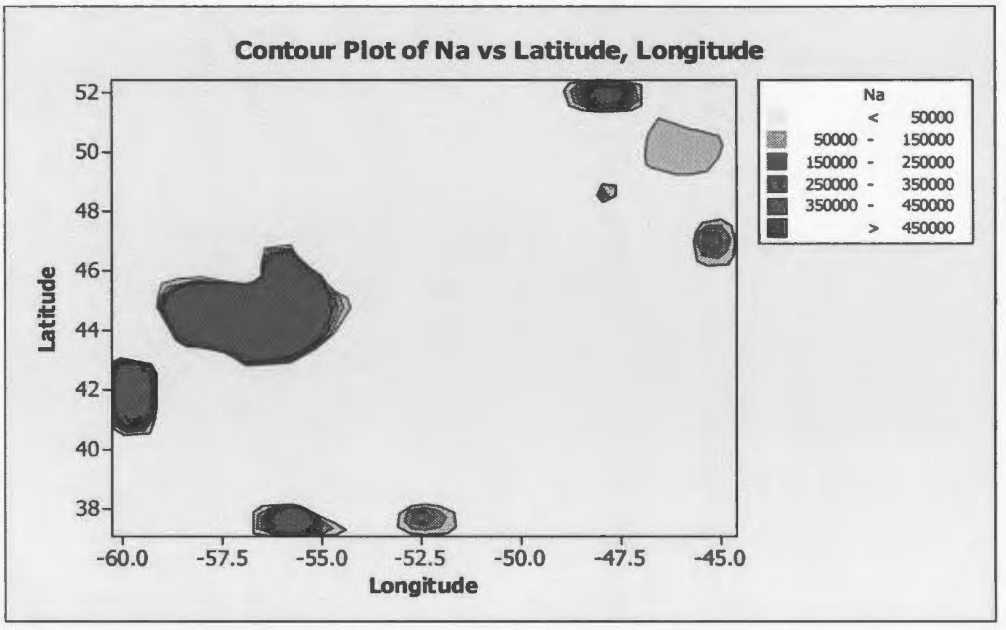

Figure III-17 – Contour plot of Na^+ concentrations (ngm^{-3}) for night-time total particulate (<100μm) Transect samples.

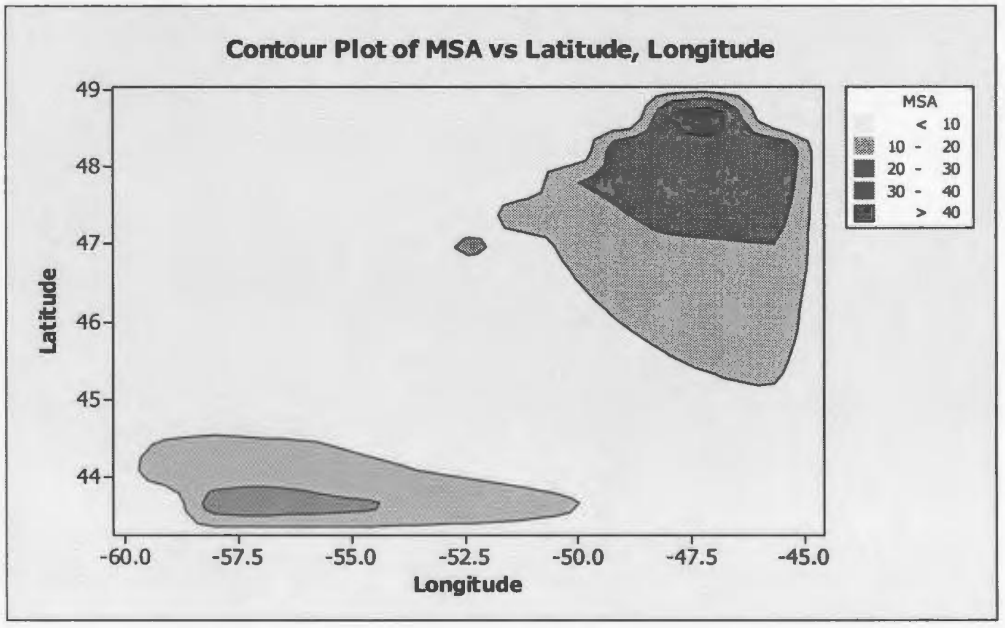

Figure III-18 – Contour plot of MSA concentrations (ngm^{-3}) for night-time total particulate (<100μm) Transect samples.

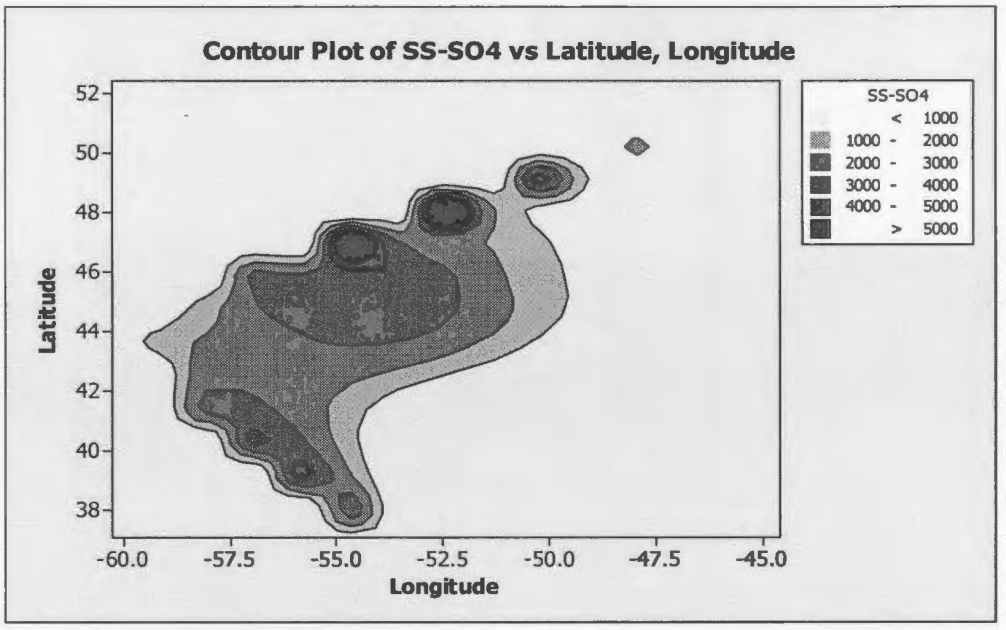

Figure III-19 – Contour plot of $SS\text{-}SO_4^{2-}$ concentrations (ngm^{-3}) for night-time total particulate (<100μm) Transect samples.

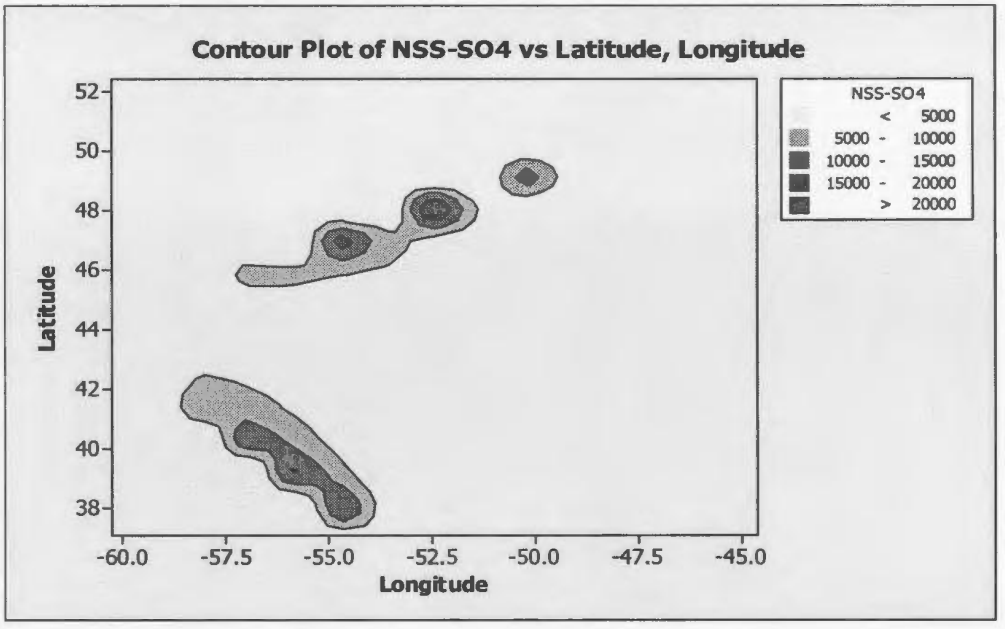

Figure III-20 – Contour plot of $NSS\text{-}SO_4^{2-}$ concentrations (ngm^{-3}) for night-time total particulate (<100μm) Transect samples.

Appendix IV

Calculation of SS-SO_4 (%):

$\%SS = \{0.25 / (SO_4/Na)_{sample}\} * 100$

$\%SS = \{2.10 / (SO_4/Mg)_{sample}\} * 100$

Calculation of Fraction SS and NSS:

$F_{SS} = \%SS/100$

$F_{NSS} = 1 - F_{SS}$

Calculation of NSS-SO_4 (%):

$\%NSS = 1 - \%SS$

Calculation of NSS-SO_4^{2-} (ngm^{-3}):

NSS-SO_4 (ngm^{-3}) = total SO_4^{2-} (ngm^{-3}) * f_{NSS}

Calculation of ng SS-SO_4^{2-}/m^3

SS-SO_4 (ngm^{-3}) = total SO_4^{2-} (ngm^{-3}) * f_{SS}

Calculation of ng Bio-SO_4^{2-}/m^3

Bio-SO_4^{2-} (ngm^{-3}) = total SO_4^{2-} (ngm^{-3}) * f_{bio}

Calculation of ng Anth-SO_4^{2-}/m^3

Anth-SO_4^{2-} (ngm^{-3}) = total SO_4^{2-} (ngm^{-3}) * f_{anth}

Appendix V

Calculation of anthropogenic and biogenic concentrations of SO_2:

$$\delta_{Total} = \delta_{Anthropogenic} * f_{Anthropogenic} + \delta_{Biogenic} * f_{Biogenic}$$

Where:

$f_{Anthropogenic} + f_{Biogenic} = 1$

$f_{Anthropogenic}$ = Anthropogenic SO_2 Concentration ÷ Total SO_2 Concentration

$f_{Biogenic}$ = Biogenic SO_2 Concentration ÷ Total SO_2 Concentration

Anthropogenic SO_2 = ~+3‰

Biogenic SO_2 = ~+18‰

$\delta_{Total} = \delta_{Anthropogenic} * f_{Anthropogenic} + \delta_{Biogenic} * f_{Biogenic}$

δ_{Total} = (+3‰ * [Anthropogenic ÷ Total]) + (+18‰* (1-[Anthropogenic ÷ Total]))

Anthropogenic $SO_2 = \{(-\delta_{Total} * Total) + (18 * Total)\} \div 15$

$\delta_{Total} = \delta_{Anthropogenic} * f_{Anthropogenic} + \delta_{Biogenic} * f_{Biogenic}$

δ_{Total} = (+3‰ * (1-[Biogenic ÷ Total]) + (+18‰* [Biogenic ÷ Total]))

Biogenic $SO_2 = \{(\delta_{Total} * Total) - (3 * Total)\} \div 15$